UNIVERSITÉ DE STRASBOURG

ÉCOLE DOCTORALE DES SCIENCES CHIMIQUES

Institut de Chimie, UMR 7177 CNRS

THÈSE présentée par :

Valentine CHARRA

Soutenue le : **05 septembre 2014**

Pour obtenir le grade de : **Docteur de l'université de Strasbourg**

Discipline / Spécialité : Chimie

Coordination de ligands carbène N-hétérocyclique multidentes sur le nickel.

THÈSE dirigée par :

M. BRAUNSTEIN Pierre	Directeur de recherche CNRS, Université de Strasbourg

RAPPORTEURS :

M. MARDER Todd	Professeur, Université de Würzburg
M. SÜSS-FINK Georg	Professeur, Université de Neuchâtel

AUTRES MEMBRES DU JURY :

M. CHETCUTI Michael	Professeur, Université de Strasbourg
Mme. OLIVIER-BOURBIGOU Hélène	Chef de département, IPF Energies nouvelles, Solaize
M. BRAUNSTEIN Pierre	Directeur de recherche CNRS, Université de Strasbourg

A mon père,

REMERCIEMENTS

En premier lieu, je tiens à remercier mon directeur de thèse, Dr. Pierre Braunstein pour son accueil au sein du Laboratoire de Chimie de Coordination à l'Université de Strasbourg. Je veux lui exprimer toute ma reconnaissance pour avoir valorisé au mieux le travail effectué, pour son soutien, pour sa disponibilité et pour ses précieux conseils.

Je souhaite remercier également le docteur Hélène Olivier-Bourbigou et les professeurs Michael Chetcuti, Todd Marder, Georg Süss-Fink de me faire l'honneur de juger mon travail.

Je souhaite remercier les docteurs Pierre-Alain Breuil et Hélène Olivier-Bourbigou pour leur implication et leur enthousiasme.

Je remercie le Centre National de la Recherche Scientifique (CNRS) et le Région Alsace pour leur soutien financier.

Parmi ces remerciements, un nom doit apparaître, Docteur Pierre de Frémont. Je tiens à le remercier tout particulièrement pour son encadrement, sa patience, ses encouragements, ses idées et les résolutions de structures par DRX. Je le remercie aussi pour nos nombreuses discussions chimiques et autres. Merci également de m'avoir fait découvrir le vaste monde de la junk-food.

Je tiens également à remercier les personnes qui ont pris le temps de m'aider dans mon travail : Messieurs Coppe et Sauer (Service RMN), Madame Heinrich (Service d'analyses, de mesures physiques et de spectroscopie optique), Mesdames Nierengarten et Lebreton (Service de spectroscopie de masse) et Madame Tortrotau (Magasin).

Je souhaite remercier également Marc Mermillon-Fournier et Mélanie Boucher pour leur aide technique durant ces années ainsi que Soumia Hnini and Sandrine Garcin pour avoir réglé au mieux tous les aspects administratifs qui ont jalonnés ces années de thèse. Je remercie chaleureusement tous les membres du laboratoire présents durant ces années : Mary, Caroline, Alexandre (Dr. C…), Alessio, Thomas, Martin, Sarah, Paulin, Minghui, Fan, Pengfei, Andreas, Sophie, Jacky, Marcel, Lucie, Béatrice…

Je souhaite remercier particulièrement Guillaume, JC (j'vous l'dis, merci !!!) et Houssein pour tous ces excellents moments passés au laboratoire et en dehors.

Fillette, Shaker (Chaker ou Shakir, comme tu sens !!!) et Gaëtan (you know !!), vous avez définitivement marqué ma vie. Merci d'avoir été là et de m'avoir soutenue.

Je tiens aussi à remercier grandement tous mes amis présents durant cette période : Cécilia (pour tous ses nouveaux mots d'anglais) Eloïse, Audren, Adèle, Célia, Mumu, Paul, Mansuy, Marine, Arnaud, Rabah, Margaux.

Enfin ces derniers mots sont dédiés à ma famille, particulièrement ceux sans qui je n'aurai jamais pu en arriver là : mes parents, mes frère et sœurs. Merci à eux pour leur soutien et leur confiance dans toutes les épreuves qui se sont imposées à nous mais aussi dans tous les moments de joie. Et désolé pour le harcèlement téléphonique.

Table des matières

Plan de la thèse

La thèse se compose d'une introduction et d'une conclusion générale. Chaque chapitre possède une bibliographie et une numérotation qui lui est propre.

Le chapitre 1 est rédigé sous forme d'une revue qui sera complétée par la suite en incluant les complexes tri-NHC et tétra-NHC de la première période des métaux de transitions ainsi que leurs applications en catalyse. Il s'agit du chapitre bibliographique.

Le chapitre 2 est rédigé sous forme de publication, les travaux décrits feront l'objet d'une publication.

Le chapitre 3 est rédigé sous la forme d'un rapport.

Liste des abréviations

δ	Chemical shift
1D	One dimension
2D	Two dimensions
Ac	Acetate
acac	Acetylacetonate
Ad	Adamantyl
anal. calcd.	Analysis calculated
Ar	Aryl
BARF	Tetrakis(3,5-di-trifluoromethylphenyl)borate)
bipy	2,2'-bipyridine
Bu	Butyl
br	Broad
Bn	Benzyl
CIF	Crystallographic information files
COD	Cyclooctadiene
COE	Cyclooctene
COESY	Correlation spectroscopy (NMR)
CNRS	Centre National de la Recherche Scientifique
Cp	Cyclopentadienyl
d	Doublet
DCM	Dichloromethane
dd	Doublet of doublets
DFT	Density functional theory
Dipp	2,6-diisopropylphenyl
dme	Dimethoxyethane
DMF	Dimethylformamide
DMSO	Dimethylsulfoxide
dt	Doublet of triplets
dq	Doublet of quartets
EADC	Ethylaluminium dichloride

EPR	Electron paramagnetic resonance
equiv.	Equivalent
ESI-MS	Electrospray ionization mass spectroscopy
Et	Ethyl
FIR	Far Infrared
FTIR	Fourier transform infrared spectroscopy
h	Hour
HBMC	Heteronuclear multiple bond correlation (RMM)
HDPE	High density polyethylene
HMF	Hydroxymethylfurfural
HSAB	Hard and soft acids and bases
Hz	Hertz
IFPEN	IPF Energies nouvelles
^{i}Me	1,3-dimethyl-2-imidazolylidene
^{i}Pr	Iso-propyl
IR	Infrared
J	Coupling constants
KHMDS	Potassium hexamethyldisilazide
LAO	Linear alpha olefin
LiHMDS	Lithium hexamethyldisilazide
LDA	Lithium diisopropylamide
LLDPE	Linear low density polyethylene
m	Multiplet
m-	Meta
MAO	Methylaluminoxane
Me	Methyl
Mer	Meridional
Mes	Mesityl
Min	Minutes
MMAO	Modified methylaluminoxane
MS	Mass spectroscopy
NaHMDS	Sodium hexamethyldisilazide

*n*BuLi	n-Butyl lithium
Nbd	Norbornadiene
NBu^t	*tert*-butylimido
NHC	N-heterocyclic carbene
NMO	*N*-methylmorpholine *N*-oxide
NMR	Nuclear magnetic resonance
o-	Ortho
ORTEP	Oak Ridge thermal ellipsoid plot
p-	Para
Ph	Phenyl
Ppm	Part per million
Py	Pyridine
q	Quartet
ROESY	Rotating-frame nuclear Overhausser effect correlation spectroscopy (NMR)
Rt	Room temperature
S	Singlet
SHOP	Shell higher olefin process
T	Triplet
^{t}Bu	Tertio butyl
Tf	Triflate
THF	Tetrahydrofuran
Tmeda	Tetramethylethylenediamine
TMS	Trimethylsilyl
TOF	Turnover frequency
TON	Turnover number
UV	Ultraviolet spectroscopy
Xyl	2,6-xylyl

Introduction générale

Introduction générale

Le sujet de cette thèse porte sur la synthèse de ligands de type bis-NHC (carbène *N*-hétérocyclique) et leur réactivité vis-à-vis de complexes d'argent, de cuivre et de nickel. Après avoir exploré les différentes méthodologies de synthèse des complexes NHC de nickel, le but était de tester leurs activités en catalyse d'oligomérisation de l'éthylène. Dans cette introduction, les propriétés des ligands NHC vont être définies ainsi que leurs voies de synthèse. Sera ensuite précisée l'utilité des ligands chélate. Un aperçu rapide de ce qui a été publié sur l'oligomérisation de l'éthylène catalysé par des complexes NHC de nickel suivra. La fin de l'introduction précisera les objectifs de la thèse.

1 Ligands NHCs

1.1 Définition générale

Les carbènes *N*-hétérocycliques (NHCs) sont des composés cycliques neutres comprenant un carbone divalent à six électrons de valence. Ce sont des carbènes singulets (ayant une orbitale moléculaire remplie et une autre vide) stabilisés par au moins un azote en position-α.

Avec les métaux de fin de transition, ils forment des liaisons robustes grâce à leur fort pouvoir σ-donneur. Ils stabilisent les complexes de métaux de transition aussi bien à haut qu'à bas degrés d'oxydation. Les NHCs sont souvent considérés comme des alternatives aux phosphines. Ils sont faiblement toxiques et peuvent permettre la formation de catalyseurs stables à l'air et thermiquement. Ils sont utilisés dans de nombreux domaines, allant de la biochimie à la catalyse.[1] Les NHCs libres font preuves d'excellentes aptitudes pour l'organocatalyse étant des bases fortes et nucléophiles.[1a,2]

1.2 Historique

En 1968, les groupes de Wanzlick et Öfele sont les premiers à synthétiser des complexes NHC.[3] La réaction d'un sel d'imidazolium avec $Hg(OAc)_2$ conduisant au complexe NHC de mercure(II) a été décrite par Wanzlick. La même année Öfele décrit la

réaction d'un sel d'imidazolium avec $HCr(CO)_5$ permettant le déprotonation du sel et la complexation du carbène (Schéma 1).

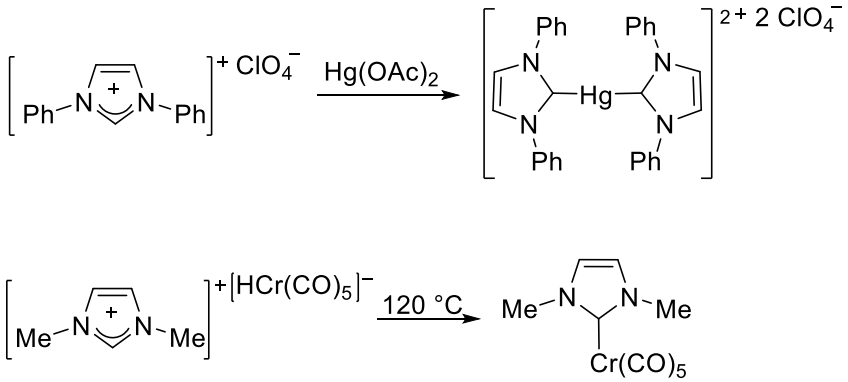

Schéma 1. Synthèses des premiers complexes NHC

Cependant, il faudra attendre 1991 pour obtenir l'isolement d'un NHC libre par Arduengo *et coll.* (Schéma 2).[4] Cette isolation a montré que les carbènes libres sont thermodynamiquement viables et de ce fait peuvent être utilisés comme intermédiaires réactionnels. C'est grâce à cet article que les NHCs ont suscité un nouvel engouement. Depuis, un grand nombre de NHCs libres ont pu être isolés. Ces ligands peuvent constituer une alternative aux phosphines. Les phosphines s'oxydent facilement contrairement aux sels d'imidazolium qui sont stables à l'air et qui peuvent être utilisés comme liquides ioniques.[5]

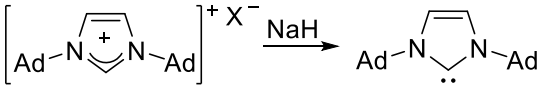

Schéma 2. Isolation du premier carbène libre

La Figure 1 présente les différentes familles de ligands NHCs. De nombreuses modifications du squelette sont possibles, cependant uniquement les imidazol-2-ylidenes sont concernés par ce travail.[5b,c,6]

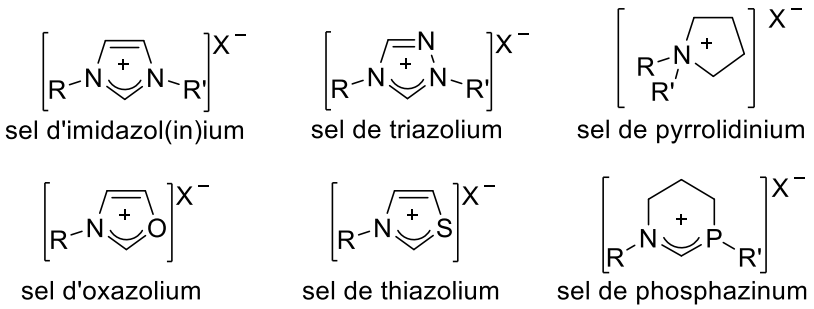

Figure 1. Différents types de pro-ligands

A ce jour, en plus de la réaction du carbène libre avec un précurseur métallique, plusieurs autres voies de synthèses donnant accès à des complexes NHC ont été répertoriées :[1b,6a,7]

- La déprotonation du sel d'imidazolium avec une base externe. Le carbène libre est formé comme intermédiaire avant de se coordiner à un centre métallique.
- La déprotonation du sel d'imidazolium avec un précurseur métallique ayant une base interne qui conduit à un complexe NHC sans passer par la formation du carbène libre.
- Le transfert du NHC avec un complexe NHC comme agent de transmétallation. Généralement, ce sont des complexes d'argent(I) qui servent d'agents car ils sont facilement synthétisés et stables à l'air.
- L'addition oxydante de sel d'imidazolium sur des métaux ayant un bas degré d'oxidation.

La chimie des composés NHC et de leurs complexes fait l'objet d'un grand nombre de revues et publications.

1.3 Propriétés électroniques

Les ligands NHCs sont considérés comme donneurs neutres de deux électrons, ayant un fort pouvoir σ-donneur. Les NHCs sont stabilisés par les effets push-pull des atomes d'azote. En effet, un atome d'azote a un effet inductif-accepteur et mésomère-donneur. Ainsi, l'orbitale σ du carbène est stabilisée par les effets inductifs attracteurs des atomes d'azote et l'orbitale π-liante du carbène est stabilisée par la donation des doublets non liants des atomes d'azote.[8] De plus, les substituants liés à ces atomes d'azote influencent aussi le caractère σ-donneur du carbone carbénique suivant leur effet donneur ou attracteur (voir propriétés stériques).

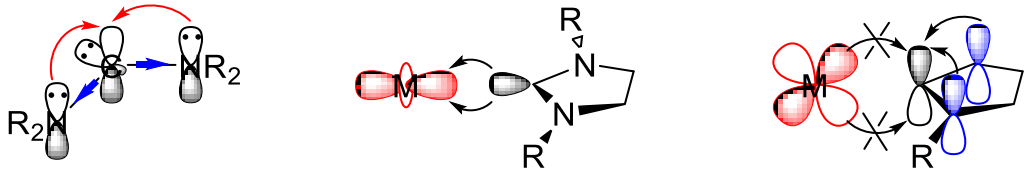

Schéma 3. Effets électrostatiques des atomes d'azote des NHC et leurs modes de coordination

La comparaison des fréquences de vibrations de ligands carbonyles (CO) coordinés à des métaux de transition portant soit un ligand NHC soit un ligand phosphine a permis de déterminer la force relative du pouvoir σ-donneur des ligands NHC ou phosphines.[1b,9] Plus la

σ-donation du ligand carbène ou phosphine vers le métal est forte, plus la π-rétrodonation du métal vers le ligand carbonyle est importante et plus les bandes de vibrations, correspondant aux carbonyles sur le spectre infrarouge sont décalées vers des nombres d'ondes plus petits.

Une conclusion s'est imposée, les ligands NHCs ont généralement un meilleur pouvoir σ-donneur que les phosphines.

1.4 Propriétés stériques

Il a été dit plus haut que les *N*-substituants influencent le pouvoir σ-donneur du carbène. En effet, des substituants volumineux induisent un encombrement stérique autour du métal. Les axes comprenant ces N-substituants sont orientés vers le métal alors que le plan contenant les atomes NCN est peu encombré.

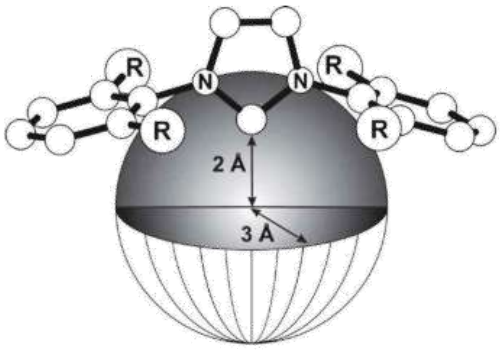

Figure 2. Représentation des dimensions de la sphère permettant la détermination du paramètre stérique des ligands NHCs : % $V_{occupé}$

Un modèle permettant de quantifier l'encombrement stérique des NHCs a été développé, où le pourcentage de volume occupé (% $V_{occupé}$) est considéré comme une sphère centrée sur le métal.[10] Cela a permis de comparer les volumes occupés par les phosphines tertiaires considérés comme des analogues avec les NHCs. Le pourcentage de volume occupé par les phosphines est basé sur l'angle solide qu'elles produisent (cône de Tolman).[11] Il a été montré que le ligand NHC portant des groupements tertio-butyle (^{t}Bu) est stériquement plus encombré que son analogue phosphine P(^{t}Bu)$_3$.

2 Ligands polyfonctionnels

Dans le cadre de la recherche fondamentale ou appliquée, la chimie organométallique représente un important champ d'investigation. L'interaction ligand-métal est le paramètre clé

Références p. 16

qu'il faut savoir contrôler et de ce fait comprendre. Plusieurs facteurs contrôlent cette interaction mais les plus importants sont les propriétés stériques et électroniques du ligand.

Les ligands polyfonctionnels sont le résultat de l'association d'au moins deux sites donneurs reliés par un espaceur. Un site donneur est une fonction classique en chimie de coordination qui peut interagir avec un centre métallique tel qu'un NHC ou une phosphine. Dans notre cas, les deux sites donneurs sont des NHCs. Trois différents modes de coordination sont possibles :

- La coordination d'une des deux fonctions par un centre métallique (monodente), la seconde restant libre (Figure 3 – cas 1).

- La coordination (chélation) des deux fonctions par le même centre métallique (Figure 3 – cas 2).

- La coordination des deux fonctions par deux centres métalliques différents. Le ligand est alors pontant et le complexe est polynucléaire (Figure 3 – cas 3).

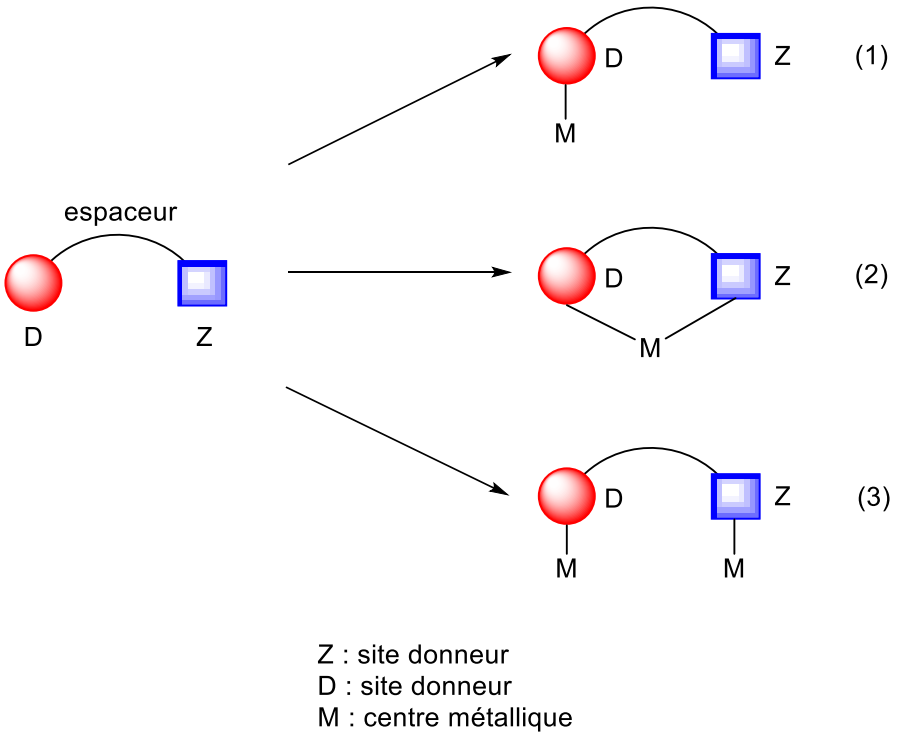

Figure 3. Type de coordination possible pour un ligand bi-fonctionnel

De nombreuses fonctions de chimie peuvent être associés à un NHC, telles que des phosphines, des alcools, des amines, etc...[12] Dans ce travail ne sont concernés que les ligands bidentes bis-NHC.

Références p. 16

3 Oligomérisation de l'éthylène

3.1 Aperçu général

Les alcènes comme l'éthylène (C_2H_4) sont obtenus durant les différentes étapes du raffinage du pétrole (craquage). L'éthylène est le plus souvent utilisé pour la synthèse de polymères ou d'oligomères. Les oléfines alpha-linéaires (LAO : linear alpha olefin) telles que le but-1-ène, l'hex-1-ène ou l'oct-1-ène sont les oligomères les plus recherchés. Selon la longueur de leurs chaînes, les industries les utilisent dans la production de lubrifiants synthétiques, de plastifiants ou encore de détergents. La copolymérisation des LAO avec l'éthylène permet la formation du polyéthylène de basse densité linéaire (LLDPE : linear low density polyehtylene).[13] En 2006, ce sont 4.6 Mt de LAO qui ont été produits dans le monde.[13f]

L'oligomérisation catalytique des oléfines, telles que l'éthylène, visant à produire des oléfines à chaînes courtes (C4 - C10) reste un enjeu académique et industriel de premier plan en raison des besoins économiques et de la difficulté à prévoir la sélectivité d'un catalyseur, et ce principalement en raison des faibles différences d'énergie qui distinguent les étapes critiques qui contrôlent cette oligomérisation. En outre la position de la double liaison C=C dans le produit est très importante car les α-oléfines sont clairement préférées aux oléfines internes.

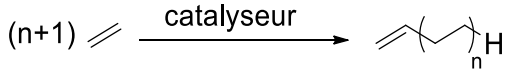

Schéma 4. Oligomérisation catalytique de l'éthylène en oléfines α avec $n \leq 10$

Depuis la découverte de « l'effet nickel »,[14] beaucoup de travaux se sont portés sur la synthèse de catalyseurs contenant du nickel(II). Les procédés Dimersol (IFP),[15] SHOP (Shell Oil Compagny)[13b,13i,16], Dupont (DuPont)[17] et Philips[18] sont les quatre grands procédés d'oligomérisation à base de complexes de nickel.

1 : Le procédé Dimersol, développé par Y. Chauvin et son équipe à l'Institut Français du Pétrole, utilise un catalyseur de type Ziegler-Natta formé *in-situ* par la réaction entre un alkyl aluminium et un sel de nickel(II). Il permet de dimériser le propylène en hexènes et le butène en octènes.

2- Le procédé SHOP, développé par la compagnie Shell, utilise comme catalyseur un complexe de nickel chélaté par un ligand bidente P, O. Il combine trois réactions catalytiques, l'oligomérisation, l'isomérisation et la métathèse. Ce procédé produit des oléfines linéaires interne à chaînes dont la longueur est principalement comprise entre C6 à C20. Des alcools linaires sont formés par hydroformylation après l'isomérisation et la métathèse des oléfines.

3- Le procédé Versipol, développé par DuPont, utilise comme catalyseur des complexes de nickel ou de palladium coordinés par des diimines qui activés par des alkyl aluminium (ex. MAO) présentent de fortes activités en polymérisation de l'éthylène.

4- Le procédé Philips utilise des composés de nickel, des phosphines pour transformer l'éthylène en hexène.

Grâce à une activité importante qui justifie son utilisation dans les procédés industriels décrits ci-dessus, le nickel est un métal de choix pour la réaction d'oligomérisation.

De nombreux types ligands sont utilisés dans les systèmes catalytiques permettant la formation d'oligomères d'éthylène tels que les phosphines, les diimines, phosphino-énolate, etc…[13e-g,17,19]

3.2 Utilisation des NHCs en oligomérisation

Les complexes NHCs sont populaires en catalyse, cependant, très peu sont utilisés comme catalyseurs en oligomérisation de l'éthylène. Il y a peu d'exemple de catalyseur d'oligomérisation d'alcynes ou d'alcènes portant un ligand NHC. Des complexes de chrome(III),[20] nickel(II),[21] palladium(II),[22] rhodium(I),[23] ruthénium(II)[24] et zirconium(IV)[25] ont été décrits dans la littérature. Les complexes de chrome(III) couplés avec du MAO sont très actifs en oligomérisation de l'éthylène. Le mécanisme mis en jeu durant la catalyse est de type métallacycle.[20a,20d]

Dans la plupart des cas, les complexes de nickel testés se sont avérés être sélectifs pour la dimérisation de l'éthylène et faiblement à moyennement actifs.[21b-e] L'élimination réductrice facile des ligands NHCs coordinés au nickel est, la plus part du temps, mis en cause.[26] Le complexe indényle de nickel représenté sur la figure **4** activé avec du MMAO présente une faible activité comme catalyseur pour l'oligomérisation de l'éthylène (260 g C_2H_4/g Ni) mais une forte sélectivité pour la dimérisation.[21e] L'allyle de nickel NHC est actif en oligomérisation de styrène et donne accès à un TOF de 748 mol styrène/(mol Ni·h) après 5 h de réaction.[27] Les iodures de nickel bis(NHC) après activation avec $AlEt_2Cl_2$ sont actifs en

dimérisation du 1-butène avec un TON de 50 mol C_4H_{10}/mol Ni.[21d] Finalement, les complexes de nickel(II) NHC sont aussi actifs en catalyse d'alcène autre que l'éthylène.[28]

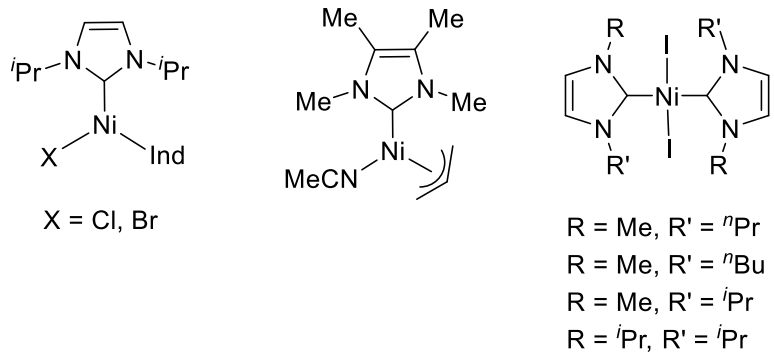

Figure 4. Complexes actif en oligomérisation d'alcène.

Deux alternatives permettent de contrecarrer les effets de l'élimination réductrice :

- L'utilisation de liquides ioniques comme solvant de réactions, permettant de régénérer l'espèce active (acide de Lewis), s'oppose aux effets de l'élimination réductrice.[21d] Dans le toluène, aucune réaction ne fut observée entre l'éthylène et les complexes iodures de nickel bis (NHC). Cependant dans un milieu liquide ionique, la catalyse a eu lieu avec un TON maximum de 3510 mol C_4H_{10}/mol Ni.

- L'utilisation d'un ligand bidente afin d'ancrer le site NHC sur le métal peut permettre d'éviter sa décoordination définitive et d'être plus actif en catalyse. Des ligands NHC possédant une fonctionnalisation pyridine, énolate, phénolate ou salicylaldiminato ont été testés en polymérisation ou oligomérisation de différents alcènes ou alcynes (éthylène, propylène, styrène, norbornène…) en présence d'un co-catalyseur.[29] Les résultats ont été très variables allant de complexes inactifs à de bonnes activités.

4 Objectifs de la thèse

L'objectif de cette thèse était de synthétiser des complexes de nickel(II) portant des ligands bidente bis-NHC et de les tester comme catalyseur en oligomérisation de l'éthylène.

La thèse de Matthieu Raynal faite dans notre Laboratoire (2005-2009)[30] a permis de mettre en évidence une grande diversité de modes de coordination des ligands bis-carbènes N-hétérocycliques (NHC) sur l'iridium. Il est apparu que cette chimie s'annonçait encore plus riche que prévue. Le fait de pouvoir contrôler les séquences de réaction et de réaliser les métallations par étapes ajoutait une dimension importante à la modularité du système. Ce fut

le point de départ d'études portant cette fois sur le nickel, connu pour la capacité de certains de ses complexes à catalyser l'oligomérisation de l'éthylène.

Références p. 16

Références :

(1) (a) Cazin, C. S. J. *N-Heterocyclic Carbenes in Transition Metal Catalysis and Organocatalysis*; 1st ed.; Springer, 2011 (b) de Frémont, P.; Marion, N.; Nolan, S. P. *Coord. Chem. Rev.* **2009**, *253*, 862 (c) Diez-Gonzalez, S.; Marion, N.; Nolan, S. P. *Chem. Rev.* **2009**, *109*, 3612 (d) Garrison, J. C.; Youngs, W. J. *Chem. Rev.* **2005**, *105*, 3978.

(2) (a) Enders, D.; Niemeier, O.; Henseler, A. *Chem. Rev.* **2007**, *107*, 5606 (b) Marion, N.; Díez-González, S.; Nolan, S. P. *Angew. Chem. Int. Ed.* **2007**, *46*, 2988.

(3) (a) Öfele, K. *J. Organomet. Chem.* **1968**, *12*, P42 (b) Wanzlick, H. W.; Schönherr, H. J. *Angew. Chem. Int. Ed.* **1968**, *7*, 141.

(4) Arduengo, A. J.; Harlow, R. L.; Kline, M. *J. Am. Chem. Soc.* **1991**, *113*, 361.

(5) (a) Fei, Z.; Geldbach, T. J.; Zhao, D.; Dyson, P. J. *Chem. - Eur. J.* **2006**, *12*, 2122 (b) Olivier-Bourbigou, H.; Magna, L. *J. Mol. Catal. A: Chem.* **2002**, *182–183*, 419 (c) Olivier-Bourbigou, H.; Magna, L.; Morvan, D. *Appl. Catal., A* **2010**, *373*, 1 (d) Welton, T. *Chem. Rev.* **1999**, *99*, 2071.

(6) (a) Hahn, F. E. *Angew. Chem. Int. Ed.* **2006**, *45*, 1348 (b) Schuster, O.; Yang, L.; Raubenheimer, H. G.; Albrecht, M. *Chem. Rev.* **2009**, *109*, 3445.

(7) (a) Crudden, C. M.; Allen, D. P. *Coord. Chem. Rev.* **2004**, *248*, 2247 (b) Hahn, F. E.; Jahnke, M. *Angew. Chem. Int. Ed.* **2008**, *47*, 3122 (c) Herrmann, W. A.; Köcher, C. *Angew. Chem. Int. Ed.* **1997**, *36*, 2162.

(8) (a) Gusev, D. G. *Organometallics* **2009**, *28*, 763 (b) Jacobsen, H.; Correa, A.; Poater, A.; Costabile, C.; Cavallo, L. *Coord. Chem. Rev.* **2009**, *253*, 687 (c) Radius, U.; Bickelhaupt, F. M. *Coord. Chem. Rev.* **2009**, *253*, 678.

(9) (a) Crabtree, R. H. *J. Organomet. Chem.* **2005**, *690*, 5451 (b) Dorta, R.; Stevens, E. D.; Scott, N. M.; Costabile, C.; Cavallo, L.; Hoff, C. D.; Nolan, S. P. *J. Am. Chem. Soc.* **2005**, *127*, 2485.

(10) (a) Cavallo, L.; Correa, A.; Costabile, C.; Jacobsen, H. *J. Organomet. Chem.* **2005**, *690*, 5407 (b) Díez-González, S.; Nolan, S. P. *Coord. Chem. Rev.* **2007**, *251*, 874.

(11) Brown, T. L.; Lee, K. J. *Coord. Chem. Rev.* **1993**, *128*, 89.

(12) (a) Kuhl, O. *Chem. Soc. Rev.* **2007**, *36*, 592 (b) Normand, A. T.; Cavell, K. J. *Eur. J. Inorg. Chem.* **2008**, *2008*, 2781 (c) Pugh, D.; Danopoulos, A. A. *Coord. Chem. Rev.* **2007**, *251*, 610 (d) Braunstein, P.; Naud, F. *Angew. Chem. Int. Ed.* **2001**, *40*, 680.

(13) (a) Lutz, E. F. *J. Chem. Educ.* **1986**, *63*, 202 (b) Skupinska, J. *Chem. Rev.* **1991**, *91*, 613 (c) Al-Jarallah, A. M.; Anabtawi, J. A.; Siddiqui, M. A. B.; Aitani, A. M.; Al-Sa'doun, A. W. *Catal. Today* **1992**, *14*, whole issue (d) Britovsek, G. J.; Mastroianni, S.; Solan, G. A.; Baugh, S. P. D.; Redshaw, C.; Gibson, V. C.; White, A. J. P.; Williams, D. J.; Elsegood, M. R. J. *Chem. - Eur. J.* **2000**, *6*, 2221 (e) Bianchini, C.; Giambastiani, G.; Rios, I. G.; Mantovani, G.; Meli, A.; Segarra, A. M. *Coord. Chem. Rev.* **2006**, *250*, 1391 (f) Forestière, A.; Olivier-Bourbigou, H.; Saussine, L. *Oil & Gas Science and Technology - Rev. IFP* **2009**, *64*, 649 (g) Bianchini, C.; Giambastiani, G.; Luconi, L.; Meli, A. *Coord. Chem. Rev.* **2010**, *254*, 431 (h) Agapie, T. *Coord. Chem. Rev.* **2011**, *255*, 861 (i) Keim, W. *Angew. Chem. Int. Ed.* **2013**, *52*, 12492 (j) Wang, S.; Sun, W.-H.; Redshaw, C. *J. Organomet. Chem.* **2014**, *751*, 717.

(14) Fischer, K.; Jonas, K.; Misbach, P.; Stabba, R.; Wilke, G. *Angew. Chem. Int. Ed.* **1973**, *12*, 943.

(15) (a) Keim, W. *Angew. Chem. Int. Ed.* **1990**, *29*, 235 (b) Chauvin, Y.; Olivier-Bourbigou, H. In *Applied homogeneous catalysis with organometallic compounds*; Cornils, B., Herrmann, W. A., Eds.; Wiley-VCH: Weiheim, 1996; Vol. 1 (c)

Commereuc, D.; Chauvin, Y.; Leger, G.; Gaillard, J. *Oil & Gas Science and Technology - Rev. IFP* **1982**, *37*, 639.
(16) Lappin, G. R.; Nemec, L. H.; Sauer, J. D.; Wagner, J. D. *Higher Olefin, Kirk-Othmer Encyclopdia of Chemical Technology*, 2005.
(17) (a) Gibson, V. C.; Spitzmesser, S. K. *Chem. Rev.* **2003**, *103*, 283 (b) Ittel, S. D.; Johnson, L. K.; Brookhart, M. *Chem. Rev.* **2000**, *100*, 1169.
(18) Freeman, J. W.; Buster, J. L.; Knudsen, R. D. *Preparation of homogeous catalysts for olefin oligomerization*: USA, 1999.
(19) (a) Rhinehart, J. L.; Brown, L. A.; Long, B. K. *J. Am. Chem. Soc.* **2013**, *135*, 16316 (b) Mecking, S. *Angew. Chem. Int. Ed.* **2001**, *40*, 534 (c) Killian, C. M.; Johnson, L. K.; Brookhart, M. *Organometallics* **1997**, *16*, 2005 (d) Dixon, J. T.; Green, M. J.; Hess, F. M.; Morgan, D. H. *J. Organomet. Chem.* **2004**, *689*, 3641 (e) Boudier, A.; Breuil, P.-A. R.; Magna, L.; Olivier-Bourbigou, H.; Braunstein, P. *Chem. Commun.* **2014**, *50*, 1398.
(20) (a) McGuinness, D. *Dalton Trans.* **2009**, 6915 (b) McGuinness, D. S. *Organometallics* **2009**, *28*, 244 (c) McGuinness, D. S.; Gibson, V. C.; Wass, D. F.; Steed, J. W. *J. Am. Chem. Soc.* **2003**, *125*, 12716 (d) McGuinness, D. S.; Suttil, J. A.; Gardiner, M. G.; Davies, N. W. *Organometallics* **2008**, *27*, 4238.
(21) (a) Benítez Junquera, L.; Puerta, M. C.; Valerga, P. *Organometallics* **2012**, *31*, 2175 (b) Li, W.-F.; Sun, H.-M.; Chen, M.-Z.; Shen, Q.; Zhang, Y. *J. Organomet. Chem.* **2008**, *693*, 2047 (c) MacKinnon, A. L.; Baird, M. C. *J. Organomet. Chem.* **2003**, *683*, 114 (d) McGuinness, D. S.; Mueller, W.; Wasserscheid, P.; Cavell, K. J.; Skelton, B. W.; White, A. H.; Englert, U. *Organometallics* **2002**, *21*, 175 (e) Sun, H. M.; Shao, Q.; Hu, D. M.; Li, W. F.; Shen, Q.; Zhang, Y. *Organometallics* **2005**, *24*, 331.
(22) Khlebnikov, V.; Meduri, A.; Mueller-Bunz, H.; Montini, T.; Fornasiero, P.; Zangrando, E.; Milani, B.; Albrecht, M. *Organometallics* **2012**, *31*, 976.
(23) Gil, W.; Lis, T.; Trzeciak, A. M.; Ziolkowski, J. J. *Inorg. Chim. Acta* **2006**, *359*, 2835.
(24) (a) Csabai, P.; Joo, F.; Trzeciak, A. M.; Ziolkowski, J. J. *J. Organomet. Chem.* **2006**, *691*, 3371 (b) Diver, S. T.; Kulkarni, A. A.; Clark, D. A.; Peppers, B. P. *J. Am. Chem. Soc.* **2007**, *129*, 5832.
(25) Dagorne, S.; Bellemin-Laponnaz, S.; Romain, C. *Organometallics* **2013**, *32*, 2736.
(26) Cavell, K. J.; McGuinness, D. S. *Coord. Chem. Rev.* **2004**, *248*, 671.
(27) Càmpora, J.; Ortiz de la Tabla, L.; Palma, P.; Alvarez, E.; Lahoz, F.; Mereiter, K. *Organometallics* **2006**, *25*, 3314.
(28) (a) Berding, J.; Lutz, M.; Spek, A. L.; Bouwman, E. *Appl. Organomet. Chem.* **2011**, *25*, 76 (b) Buchowicz, W.; Conder, J.; Hryciuk, D.; Zachara, J. *J. Mol. Catal. A: Chem.* **2014**, *381*, 16 (c) Buchowicz, W.; Kozioł, A.; Jerzykiewicz, L. B.; Lis, T.; Pasynkiewicz, S.; Pęcherzewska, A.; Pietrzykowski, A. *J. Mol. Catal. A: Chem.* **2006**, *257*, 118 (d) Buchowicz, W.; Wojtczak, W.; Pietrzykowski, A.; Lupa, A.; Jerzykiewicz, L. B.; Makal, A.; Wozniak, K. *Eur. J. Inorg. Chem.* **2010**, 648.
(29) (a) Benson, S.; Payne, B.; Waymouth, R. M. *J. Polym. Sci., Part A: Polym. Chem.* **2007**, *45*, 3637 (b) Ketz, B. E.; Ottenwaelder, X. G.; Waymouth, R. M. *Chem. Commun.* **2005**, 5693 (c) Kong, G.-Q.; Xu, X.; Zou, C.; Wu, C.-D. *Chem. Commun.* **2011**, *47*, 11005 (d) Li, W.; Sun, H.; Chen, M.; Wang, Z.; Hu, D.; Shen, Q.; Zhang, Y. *Organometallics* **2005**, *24*, 5925 (e) Zhang, D.; Zhou, S.; Li, Z.; Wang, Q.; Weng, L. *Dalton Trans.* **2013**, *42*, 12020.
(30) (a) Raynal, M.; Cazin, C. S. J.; Vallée, C.; Olivier-Bourbigou, H.; Braunstein, P. *Chem. Commun.* **2008**, 3983 (b) Raynal, M.; Cazin, C. S. J.; Vallée, C.; Olivier-Bourbigou, H.; Braunstein, P. *Dalton Trans.* **2009**, 3824 (c) Raynal, M.; Cazin, C. S. J.; Vallée, C.; Olivier-Bourbigou, H.; Braunstein, P. *Organometallics* **2009**, *28*, 2460

(d) Raynal, M.; Pattacini, R.; Cazin, C. S. J.; Vallée, C.; Olivier-Bourbigou, H.; Braunstein, P. *Organometallics* **2009**, *28*, 4028.

Références p. 16

Résumé de la thèse

Résumé du chapitre 1

Ce chapitre est rédigé sous la forme d'une revue. Nous avons référencé les complexes comprenant au moins un ligand ayant au minimum deux fonctions NHC. Nous avons limité la portée des métaux de transition à ceux de la quatrième période du tableau périodique en raison du grand nombre de publications traitant de complexes de métaux de transition portant les ligands NHC.

Le chapitre est divisé en trois parties selon le mode de coordination des ligands (chélatant, pontant et chélatant/pontant). A l'intérieur de chaque partie, le critère de classement porte sur le métal.

Il ressort de ce travail bibliographique que le fer et le nickel sont les métaux les plus utilisés avec les ligands NHC polyfonctionnels.

Après incorporation de deux parties supplémentaires dédiées à la chimie des ligands NHC tripodes et tétrapodes et aux différentes applications en catalyse homogène de tous les complexes présentement référencés, ce chapitre devrait être soumis pour publication en tant que revue.

Ma contribution a porté sur la recherche bibliographique, ainsi que l'écriture complète de cette revue.

Résumé du chapitre 2

Les sels d'imidazolium **1a-1d** ont été préparés par quaternisation de composés bis-imidazole N-monosubstitués ou par métathèse entre un sel d'imidazolium (**1a-c**) et $NaBF_4$ ou HBF_4 (Schéma 1).

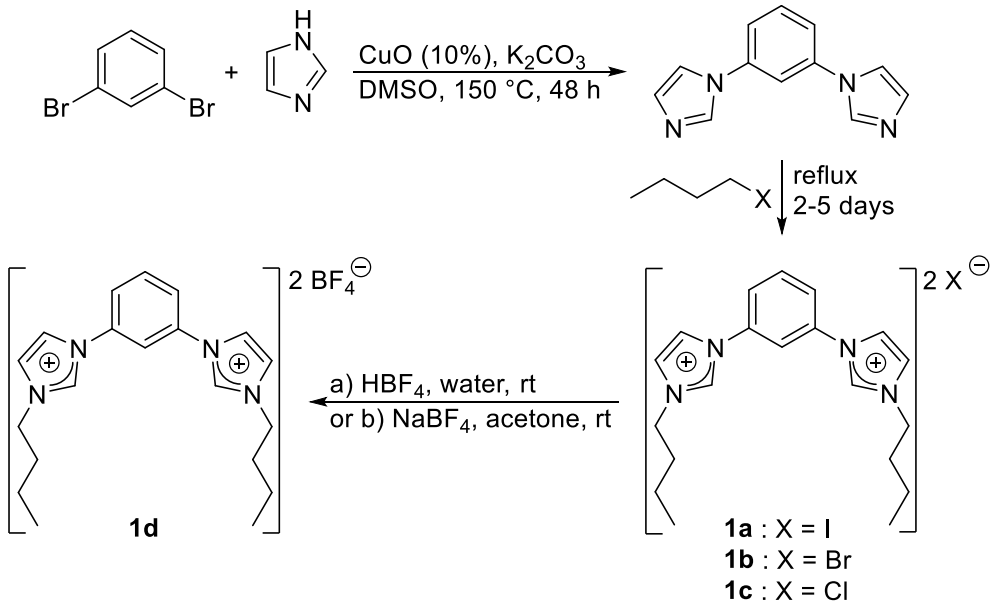

Schéma 1

Dans le but de réaliser une transmétallation des ligands NHCs de l'argent ou du cuivre au nickel, les complexes d'argent **2a-d** et les complexes de cuivre **3a-c** ont été synthétisés par réaction des sels d'imidazolium **1a-d** avec Ag_2O et $Cu(N(SiMe_3)_2)$ (Schéma 2-3).

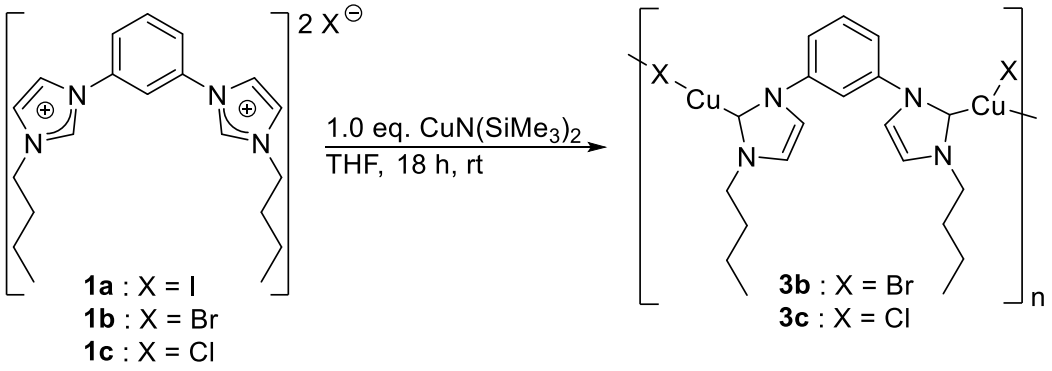

Schéma 2

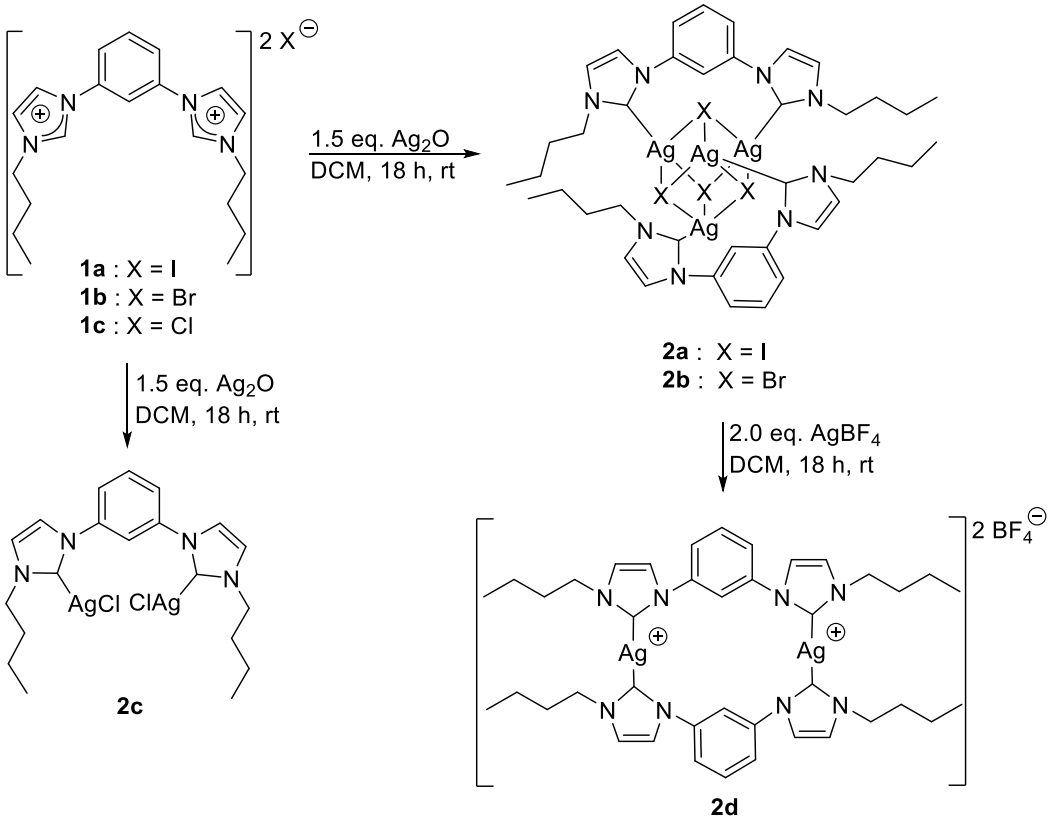

Schéma 3

Plusieurs analyses des complexes ont été réalisées : RMN du proton et du carbone, IR IR lointain, MS, analyses élémentaires et diffraction de rayon-X sur monocristal.

Ma contribution a porté sur la recherche bibliographique et l'ensemble du travail expérimental qui y est décrit, ainsi que l'écriture de la publication qui est en cours de soumission.

Résumé du chapitre 3

Pour synthétiser un complexe de nickel(II) comprenant un ligand de type NHC, plusieurs voies sont possibles :

- L'utilisation de précurseurs de nickel contenant une base interne, en présence de sels de bis-imidazolium

- L'utilisation de précurseurs de nickel en présence de bases externes et de sels de bis-imidazolium

- L'utilisation de nickel pulvérulent, tel que le nickel de Raney ou du nickel(0) en poudre, en présence de sels de bis-imidazolium

- L'utilisation de complexes NHC de zirconium(IV), d'argent(I) ou de cuivre(I) comme agents de transfert des ligands NHCs au nickel.

- L'utilisation des carbènes libres isolés en présence de précurseurs de nickel(II).

Ces 5 voies de synthèse ont été explorées dans le but d'obtenir des complexes de nickel(II) bis-NHC. Les transmétallations à partir des complexes de bromure ou d'iodure d'argent(I) représentent les résultats les plus probants. Cependant, aucun composé n'a été obtenu propre.

Chapitre 1

Bibliogaphy

1 Introduction

In 1968, Öfele and Wanzlick independently reported the first *N*-heterocyclic carbene (NHC) complexes.[1] In 1991, Arguendo *et al.* established that NHCs were stable enough to be isolated, launching a new era of intense research on carbene chemistry. Nowadays, NHCs are more popular than ever in coordination and organometallic chemistry and in organic catalysis. These heterocycles contain a divalent carbon with six electrons and at least one α-amino substituent. NHCs are singlet carbenes (of the Fischer type), meaning that their divalent carbon atom has an empty and a full p orbital. Such electronic configuration is possible due to the π-donor and σ-acceptor α-amino groups(s) (+M/-I push-pull effect). Usually, NHCs are strong nucleophilic bases, but they really stand out as ligands in transition metal coordination chemistry. They display strong σ-donor ability with little or no π-back donation from the metal center, and have become highly desired surrogates to the ubiquitous phosphine ligands because most of the NHC complexes of the late transition metals (in usual oxidation states) are air- and moisture- stable. They also tend to display a good thermal stability, which is favorable for a broad range of applications in catalysis.

Multidentate ligands contain at least two donor sites held by a linker (or spacer). Common donors include non-metallic elements such as chalcogens (e.g. alcoholates, thioethers…), pnictogens (e.g. phosphines, amines...), and group 14 elements (carbenes). Less common donor groups include semi-metallic elements such as boron or silicium (e.g. borylenes, silylenes…), or even more scarcely, low oxidation state metals (metallo-ligands, e.g. bis-NHC platinum(0)complexes and Ga(I)Cp*).[2]

Multidentate ligands bind one or more metal center(s) with the following coordination modes:

- Chelating mode: At least two donor sites from the same ligand bind the same metal center.
- Bridging mode: At least two donor sites from the same ligand bind different metal centers.
- Dangling mode: At least one donor site from the ligand is non-coordinated.

It is important to note that depending on the number of available coordination sites and the geometry of the coordination sphere around the metals, multidentate ligands can feature

multiple coordination modes at the same time. In general, the formation of chelates is thermodynamically favored, defining the so-called "chelate effect". Finally, multidentate ligands can give rise to mono- or poly-nuclear complexes featuring appealing chemical or physical properties, with applications ranging from homogeneous / heterogeneous catalysis, luminescence, to magnetism…

In this chapter, we will focus on recent advances in the chemistry of pincer bis-NHC (bidentate) ligands. We have narrowed the scope to the transition metals to those of fourth row of the Periodic Table because of the plethora of publications dealing with pincer NHC transition metals complexes. After inclusion of two additional parts dedicated to the chemistry of tripodal and tetrapodal NHC ligands and to the various catalytic applications of the pincer complexes under consideration, this chapter should be submitted to publication as a review.

2 Syntheses and reactivity of chelating bis-NHC ligands

2.1 Scandium

Only two bis-NHC scandium(III) complexes are known, they were described in 2009 by Lv and Cui,[3] To a THF suspension of the imidazolium bromide salts **L1** or **L2,** 1 equiv of $ScCl_3$ and 3.0 equiv of *n*BuLi were added dropwise under vigorous stirring. The complexes **1** and **2** were obtained in 71 and 45% yields, respectively.

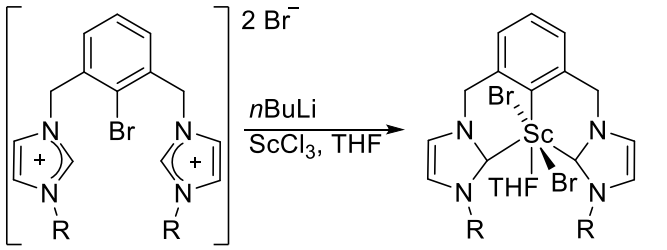

Scheme 1. Sc(III) complexes bearing chelating bis-NHC ligands.[3-4]

Surprisingly, the addition of $ScCl_3$ to **L1** or **L2** salts with *n*BuLi, failed. The quantitative formation of **1** was confirmed by ^{1}H NMR spectroscopy with the absence of the azolium proton from **L1**. In the $^{13}C\{^1H\}$ NMR spectrum, the signal of the scandium-bound carbene is visible at 193.2 ppm. The solid-state structure of **1** unveils a THF-solvated mononuclear NHC scandium(III) dibromide complex. The Sc center is in a square-bipyramidal coordination environment with the bis-NHC ligand adopting a pseudo-meridional conformation in a $\kappa C{:}\kappa C{:}\kappa C'$ tridentate mode. Two bromide ligands and a THF molecule

complete the coordination sphere of the scandium cation. The two NHC moieties are in *trans*-arranged positions whereas the two bromides are in mutual *trans*-positions. The N-aryl rings and the coordinated THF molecule lie almost parallel to each other. The average Sc–Br bond distance is equal to 2.5879(18) Å, the $C_{carbene}$–Sc–$C_{carbene}$ and the Br–Sc–Br angles are equal to 163.9(3) and 171.17(7)°. These complexes are convenient precursors to alkyl, amido derivatives. They are also active homogeneous catalysts for the polymerization of diolefins.[4a]

Complex **2**, structurally similar to **1**, was theoretically investigated at the DFT level.[4b] The coordination of the NHC ligands is dominated by ligand → metal σ-donation and no π-donation from the ligand to metal was found. From an energetic perspective, the more electron-poor the metal fragment is, the higher the coordination energy is.

2.2 Titanium

The free bis-NHC arising from the 1,1'-bis(3-borane-4,5-dimethylimidazolyl)methane zwitterion (**L3**) decomposing at 20 °C, a fresh solution of **L3** was treated with two equiv of *n*BuLi in presence of titanocene dichloride at -78 °C to afford the extremely air and moisture sensitive NHC Ti(IV) complex **3** (75%).[5]

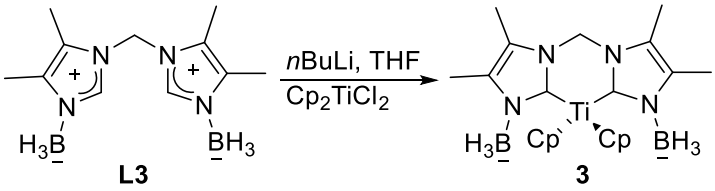

Scheme 2. Ti(IV) complexes bearing bis-NHC ligands.[5-6]

^{1}H NMR spectroscopy reveals two signals at 6.45 and 6.53 ppm for the Cp rings of **3** and two signals at 6.08 and 6.31 ppm for the methylene bridge. The $^{13}C\{^{1}H\}$ NMR spectrum contains two signals at 109.9 and 110.8 ppm assigned for the Cp rings while the carbene signal was not detected. The borane groups give rise to a ^{11}B NMR signal at -22.3 ppm. Two Cp ligands and the bis-NHC ligand complete the titanium coordination sphere. The methylene bridge points out of the plane formed by the two NHC rings and the metal center, which results in two magnetically non-equivalent protons in axial and equatorial positions. Hermann *et al*. also reported this behavior with different metals (e.g. palladium).[7] The Ti–$C_{carbene}$ bond distances are in the range of 2.202(5)-2.215(5) Å.

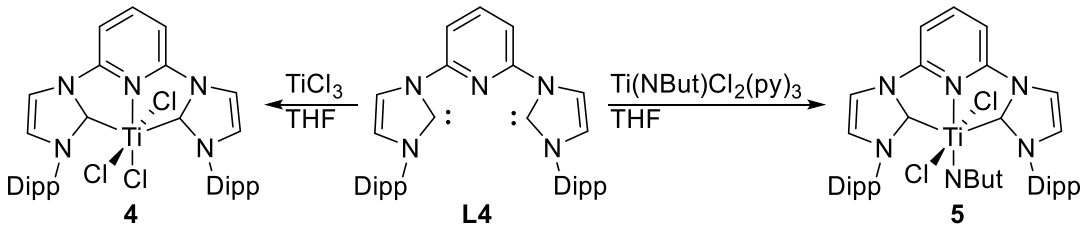

Scheme 3. Ti(III) and Ti(IV) complexes bearing a (bis-NHC)-pyridine ligand.[6a]

The titanium(III) complex **4** was prepared in quantitative yield by reaction of the free bis-carbene **L4** (obtained by deprotonation of the corresponding bis-imidazolium bromide salt using $KN(SiMe_3)_2$) with $TiCl_3(THF)_3$ in THF.[6a] Complex **4** was analyzed by ^1H NMR spectroscopy but no $^{13}C\{^1H\}$ NMR data were reported. It exhibits a titanium cation in a distorted octahedral coordination environment. The meridional sites are occupied by the 'pincer' NHC ligand and one chloride while the other two chlorides are in apical positions, Like other known metal(III) trihalide pincer complexes, the metal-halide bond *trans* to the pyridine is significantly shorter than those in *cis*-positions.[6b] The Ti–$C_{carbene}$ bond distances (2.211(5) and 2.215(5) Å) are similar to those in complex **3**. The highly air- and moisture-sensitive complex **4** was tested as catalyst for ethylene polymerization.

The free bis-carbene **L4** substituted the pyridine ligands in $Ti(NBu^t)Cl_2(py)_3$ to form complex **5** in excellent yield (95%).[6b] It was analyzed by ^1H and $^{13}C\{^1H\}$ NMR spectroscopy. The octahedral environment around the titanium(IV) center, similar to that in **4**, was established by X-ray diffraction and the pincer and the *tert*-butylimido group form the equatorial plane. The two axial chlorides are mutually *trans*. The Ti–$C_{carbene}$ bond distances (2.281(6) and 2.286(6) Å) are much longer than those for **3** and **4**, but the reasons for this elongation were not discussed. These bonds were found to be relatively inert in presence of tmed or PMe_3. Like **3** and **4**, **5** is moisture-sensitive.

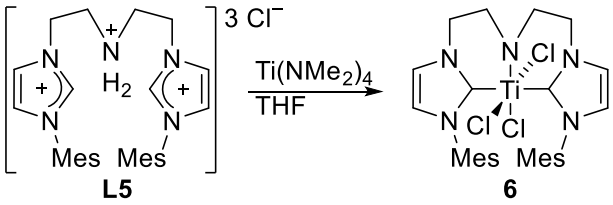

Scheme 4. Ti(III) complex bearing a (bis-NHC)amino ligand.[6c]

The titanium(III) complex **6** was obtained in very low yield (16%) by trans-amination reaction between the bis-imidazolium chloride salt **L5** and $Ti(NEt_2)_4$.[6c] It was characterized by NMR spectroscopy, but its poor solubility in all common aprotic solvents, except pyridine, prevented the observation of the carbene carbon resonance. It should be noted that the

reaction between the lithium adduct of **L5** and $TiCl_3(NMe_2)$, in THF at room temperature for 24 h, yielded a brown solid that could not be identified by NMR spectroscopy.

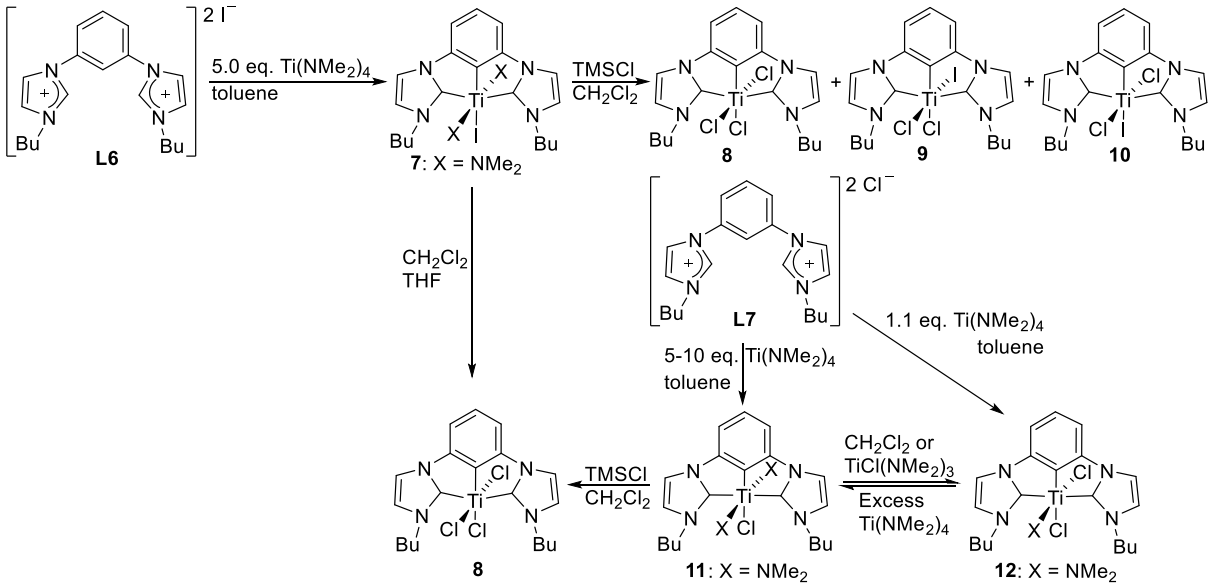

Scheme 5. Reactivity of the complexes **7** and **11**.[8]

The titanium(IV) complexes **7** to **12** were described by Hollis *et al.*[8] Reacting the bis-imidazolium iodide salt (**L6**) with an excess of $Ti(NMe_2)_4$ yielded complex **7** (94%). ^{1}H NMR analysis reveals a triplet accounting for the methylene protons belonging to the *n*-Bu arms, in α-position to the nitrogen atoms. Such a pattern is consistent with either a symmetric complex with amido groups in *trans*-positions from the imidazole rings, or a rapid inter-conversion within the *cis*-amido coordination sphere. Crystallizing **7** from a dichloromethane/THF solution led to the unexpected formation of **8,** even though dimethylamido/halide exchange due to the presence of dichloromethane has been previously reported for zirconium complexes. In an attempt to rationalize the formation of **8**, **7** was reacted with TMSCl in dichloromethane, yielding a mixture of **8** and two geometric isomers **9** and **10** (97%, with **9**:**10** ratio equal to 3:1 after 1 h). The reaction of the imidazolium chloride salt **L7** with 5-10 equiv of freshly distilled $Ti(NMe_2)_4$ in toluene gave, in 70% NMR yield, the complex **11** which is the chlorinated version of the iodo-complex **7**. This complex was not isolated as it converted to the complex **12** and $TiCl(NMe_2)_3$ during the reaction work up. Complexes **11** and **12** are in equilibrium in solution and in the presence of a large excess of $Ti(NMe_2)_4$, the equilibrium is completely shifted toward the formation of **11** and no trace of **12** is visible. As the excess of $Ti(NMe_2)_4$ is removed during reaction work-up, the equilibrium is displaced toward the formation of **12**. The direct synthesis of **12**, in moderate yield (48%), was also possible by reacting **L7** with 1.1 equiv of $Ti(NMe_2)_4$. The reaction of **11** with TMSCl in

dichloromethane produced cleanly **8**, but in low yield (19%). From these studies, it appears that the high yield synthesis of **8** and **11** is somewhat challenging.

The $^{13}C\{^{1}H\}$ NMR spectra of **7-12** display the characteristic resonances of titanium-bound carbenes, between 185.9 and 201.8 ppm. Furthermore, the signals corresponding to the carbon atoms of the titanium-bound aryl fall between 161.2 and 181.8 ppm. The molecular structures of **8** and **12** show that the titanium center is in a distorted-octahedral coordination environment, owing to the geometric constraints of the C,C,C-NHC pincer ligand. The Ti–$C_{carbene}$ bond distances are similar to those in **4** and **5**. The NHC ligands are in *trans*-positions. The $C_{carbene}$–Ti–$C_{carbene}$ angles (143.01 and 142.98°) of **8** and **12** are about 3° larger than those calculated for **4** or **5**[6a,b] likely due to differences in Ti–C_{aryl} and Ti–$N_{pyridine}$ bond lengths.

2.3 Vanadium

Similarly to **7**, the (bis-NHC)-pyridine ligand **L4** was prepared by deprotonation of the parent imidazolium salt using $KN(SiMe_3)_2$. It was then reacted with $VCl_3(THF)_3$ to produce the highly air- and moisture-sensitive vanadium(III) complex **13** (100%).[6a] This complex, as well as **7**, promotes ethylene polymerization.

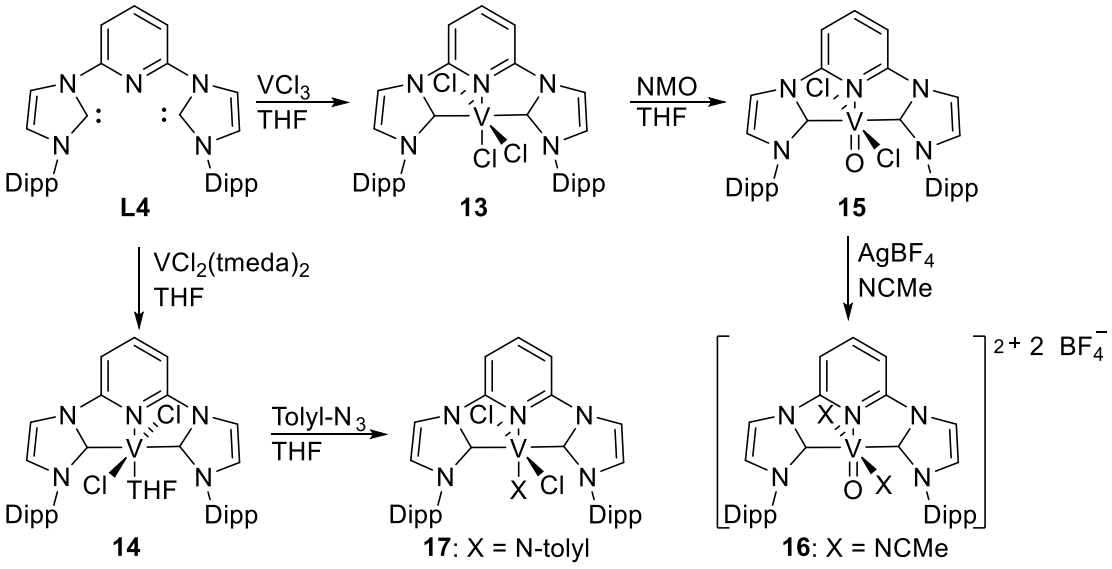

Scheme 6. V complexes bearing bis-NHCpyridine ligands.[6a,b]

Danopoulos *et al.* reported four vanadium complexes **14-17**.[6b] The vanadium(II) complex **14** was formed in excellent yield (98%) by reaction between the free bis-carbene **L4** and $VCl_2(tmeda)_2$. Most high oxidation state NHC complexes are prepared by reaction of free NHCs with high oxidation state metal sources. Generally, this approach affords moderate yields due to side reactions. The Danopoulos *et al.* proposed an alternative pathway based on

the oxidation of low oxidation state vanadium NHC complexes. With this aim, the reaction of the vanadium(III) complex **13** with *N*-methylmorpholine *N*-oxide yielded the paramagnetic vanadium(IV) complex **15**, in very good yield (90%) (or in lower yield starting from complex **14**). The IR spectrum indicates a ν(V=O) absorption band at 974 cm^{-1}. This value is at the lower end of the range observed for other vanadium(IV)-oxo complexes, in agreement with strongly σ-donating NHC ligands.

$AgBF_4$ easily abstracted the chloride ligands of complex **15** in acetonitrile to generate the complex **16** in excellent yield (97%). The V=O bond distance of the dicationic vanadium(IV) complex **16** is comparable to that in **15**. A bis-NHC vanadium(IV)-tolylimido complex **17** was prepared by the reaction of **14** with *p*-tolylazide in 72% yield. The V=N(*o*-tolyl) bond stretch at 974 cm^{-1} and the magnetic susceptibility (1.66 μ_B) are similar to those of complexes **15** and **16**. These data point to a monomeric six coordinate complex **17**. However, no XRD study was possible owing to extremely fragile crystals decomposing by solvent loss. No ^1H NMR and $^{13}C\{^1H\}$ NMR spectroscopic data are available for complexes **13-17**, due to their paramagnetic nature. The structures of **13-16** were determined by XRD. All of them exhibit a vanadium center situated in a distorted octahedral coordination environment. The pincer ligand is bound to the vanadium in equatorial positions. In **13-16**, chlorides or acetonitrile ligands occupy mutually *trans*-positions. A third chloride (**13**), a THF molecule (**14**) and an oxo group (**15-16**) complete the metal coordination sphere in each complex. The chlorides are pointing away from the pyridine ring (**14**) or from the oxo ligand (**15**). Moreover, in **14**, there is no sign of interaction between the formally vacant molecular orbitals of the carbenes and the chloride lone-pairs while such a $Cl–C_{carbene}$ bonding interaction was reported in a trichloro-oxo-vanadium(V) mono-NHC complex.[9] All the $V–C_{carbene}$ bond distances are in the range of 2.129(3) - 2.209(9) Å with that of **16** being the shortest, likely because of a more pronounced ionic interaction between vanadium and the NHC ligand. The V=O bond lengths of **15-16** are in the range reported for similar complexes.[10] Finally, for **16**, the *trans*-influence of the oxo ligand lengthens the $V–N_{pyridine}$ bond compared to the $V–N_{acetonitrile}$ bonds.

2.4 Chromium

Herrmann *et al.* published two protocols to synthetize the chromium(0) complex **18** (Scheme 7).[7,11] First, a one-pot reaction between the imidazolium iodide salt **L7**, chromium hexacarbonyl, sodium hydride and potassium *tert*-butoxide yielded **18** in very low yield

(10%).[11] Second, a reaction using **L7** with $K_4[Cr_4(\mu_3\text{-}OCH_3)_4(CO)_{12}]$ afforded **18** in moderate yield (45%).[7]

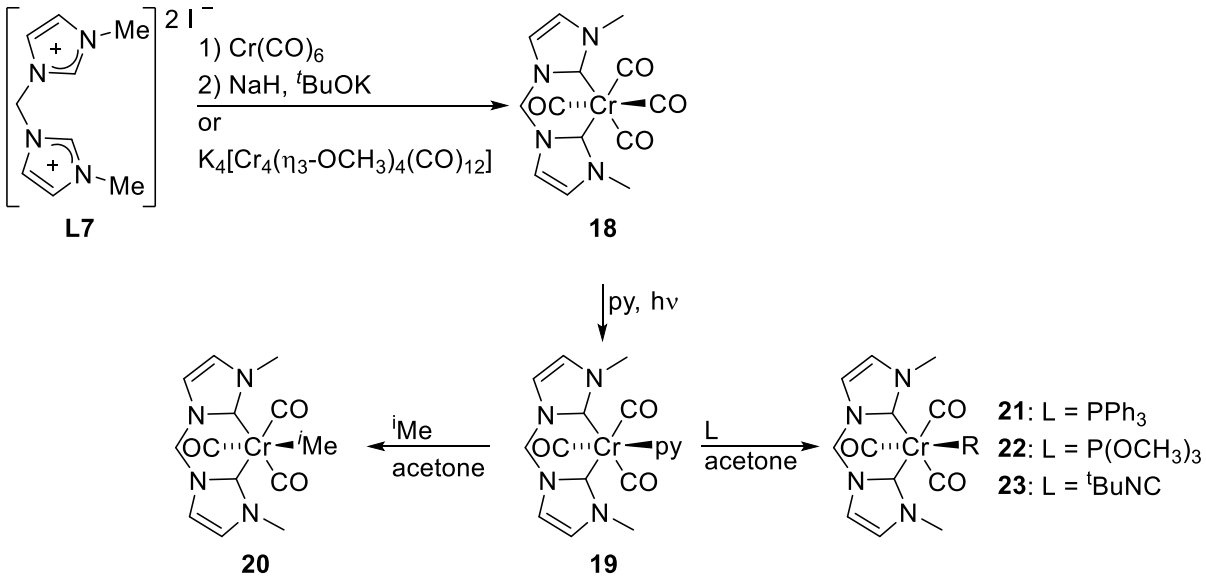

Scheme 7. Bis-NHC Cr complexes.[7,11]

Complex **18** was characterized by elemental analysis, ^{1}H NMR and infrared spectroscopy. No crystal structure was reported.

Under irradiation in pyridine, a carbonyl ligand of **18** was displaced to generate the pyridine complex **19** (90%) which underwent further pyridine substitution with ^{i}Me, PPh_3, $P(OCH_3)_3$ or ^{t}BuNC to afford the complexes **20** (75%), **21** (no yield given), **22** (no yield given) and **23** (82%), respectively. The characteristic $^{13}C\{^1H\}$ NMR signals of the carbenes of **20** are observed at 197.95 and 201.87 ppm. Complexes **19** and **21** to **23** were solely characterized by infrared spectroscopy and elemental analysis.

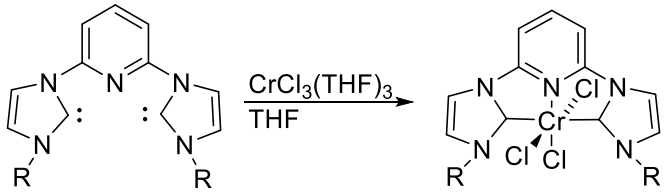

Scheme 8. Cr(III) bis-NHC pincer complexes.[6a,12]

McGuinness *et al.* reported a series of chromium bis-NHC complexes **24-28**.[6a,12-13] The chromium(III) complexes **24-27**, bearing NHCs of different sizes, were prepared in good

yield (> 80%), by reaction of the free carbenes **L4** and **L8**-**L10** with $CrCl_3(THF)_3$.[6a,12] The crystalline structure of **24** reveals a chromium(III) center in a slightly distorted octahedral coordination environment. The apical and equatorial positions are occupied by **L8** and a chloride anion and two chloride anions, respectively. The $Cr–C_{carbene}$ bonds distances (2.087(6) and 2.120(6) Å) are similar to those reported for chromium(II)-NHC complexes.[14] The chelate bite angles of the (bis-NHC)-pyridine and bis(imino)pyridine ligands are similar for bis(imido)pyridyl Cr(III) complexes.[15]

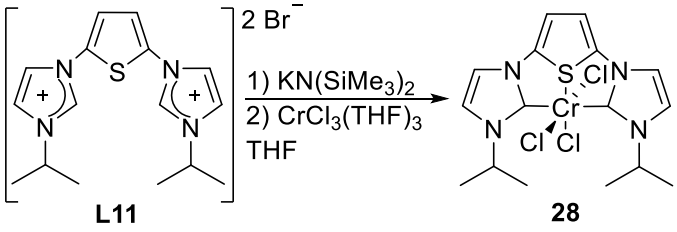

Scheme 9. Cr(III) bis-NHC pincer complex.[13b]

The complex **28** was synthesized from **L11** in excellent yield (92%), following the same procedure as for **24**-**27**. The thiophene-functionalized free NHC, too unstable to be isolated, was prepared *in situ*. Complex **28** was not characterized by NMR spectroscopy. Elemental analysis was performed. Its solid-state structure, determined by crystallography, exhibits a chromium(III) center in a distorted octahedral environment. The equatorial and apical positions are occupied by **L11** and a chloride anion and two chloride anions, respectively. The complexes **24**-**28** were designed for ethylene or α-olefin oligomerization.[6a,13a]

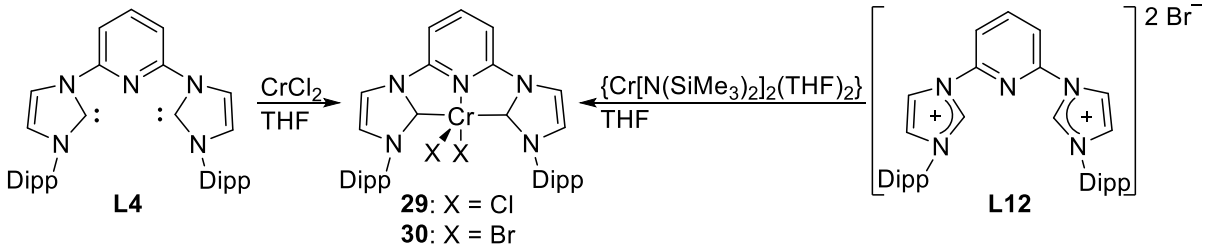

Scheme 10. Cr(II) bis-NHC pincer complexes.[6b]

The free carbene **L4** was added to a solution of $CrCl_2$ to yield the chromium(II) complex **29** (92%).[6b] The analogous bromo complex **30** was prepared by aminolysis of $\{Cr[N(SiMe_3)_2]_2(THF)_2\}$ (no yield provided). Both complexes are paramagnetic. The five-coordinate chromium(II) center of **30** exhibits a distorted square pyramidal coordination environment. **L4** and a bromide ligand occupy the equatorial positions. The second bromide

occupies the apical position. There is an approximate C_s symmetry defined by the plane containing the chromium, bromine, and pyridine nitrogen atoms. The Cr–$C_{carbene}$ bond lengths (2.122(10) and 2.125(10) Å) are slightly longer than those reported for **24**. However, they are slightly shorter than those of tetrahedral bis-NHC chromium(II) complexes.[6a,13a]

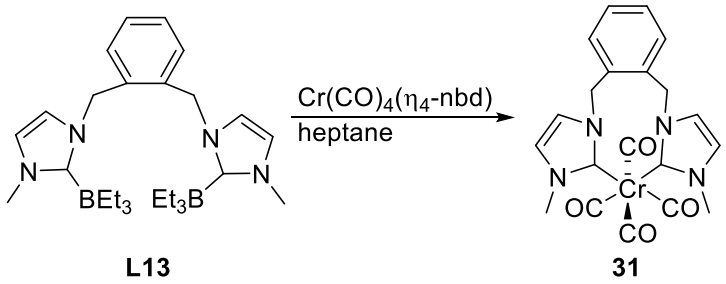

Scheme 11. Cr(0) bis-NHC complex.[16]

Refluxing the pro-ligand **L13** (BEt_3-adduct of bis-NHC) with $Cr(CO)_6$ led to the chromium(IV) complex **31** in low yield (no values given), whereas using $Cr(CO)_4(\eta^4$-nbd) afforded a better yield (57%).[16] **13** was characterized by ^{1}H and $^{13}C\{^1H\}$ NMR spectroscopy. The carbene signal resonates at 196.4 ppm. No crystalline structure was determined. However, a bis-NHC ligand with *o*-xylylene as linker was coordinated to molybdenum in a twisted mode forming a C_2-symmetric structure in the solid state. This complex and **31**, featuring similar spectroscopic data (IR, ^{1}H and $^{13}C\{^1H\}$ NMR), might be structurally close.

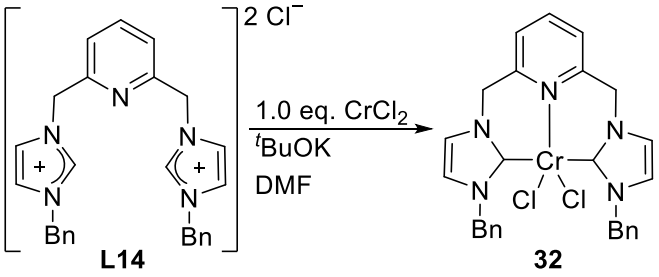

Scheme 12. Cr(II) bis-NHC pincer complex.[17]

The imidazolium chloride salt **L14** was mixed with ^{t}BuOK and $CrCl_2$ in DMF to form the complex **32** that was used to catalyze the transformation of sugars into HMF without any spectroscopic characterization.[17]

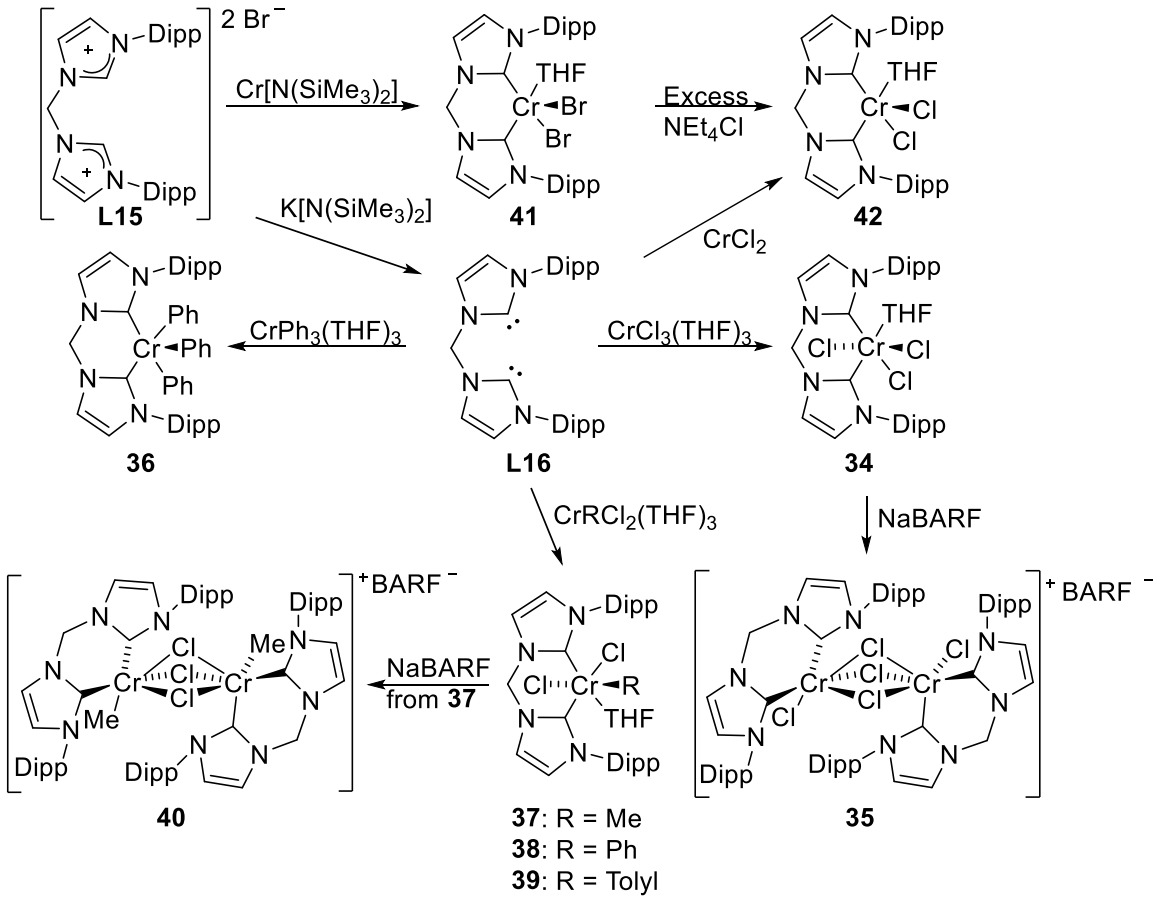

Scheme 13. Reactivity of the free bis(carbene) **L16**.[18]

Theopold *et al*. reported the complexes **34 - 42**. The free carbene **L16** was added to a suspension of $CrCl_3(THF)_3$ in THF yielding, in excellent yield (89%), the chromium(III) complex **34** that was characterized by elemental analysis, X-ray diffraction studies, infrared, mass and ^1H NMR spectroscopic methods. This complex contains a Cr center with a quasi-octahedral coordination sphere. The bis-NHC ligand, a chloride and the THF ligand occupy the equatorial positions whereas the other two chlorides occupy the apical positions. The Cr–Cl and Cr–$C_{carbene}$ bond distances are in agreement with other reported chromium complexes except for the carbene in *trans* position to a chloride ligand (2.134(5) Å), which exhibits a metal–NHC bond slightly longer than usual (av: 2.073 Å).[19] The lability of the THF ligand results in an increased reactivity for **34**. The bridged, dinuclear cationic complex **35** (74%) was obtained by mixing **34** with NaBARF to assess the reactivity of the chloride ligand toward substitution. Complexes **35-36**, **39-42** were only characterized by infrared and mass spectroscopy.

$CrPh_3(THF)_3$ was reacted with the free carbene **L16** to generate the chromium(III) complex **36** in moderate yield (57%). However, it decomposed over a few hours under

ambient light in solution or in the solid state. The geometry of the coordination environment around the chromium center is square pyramidal, with a phenyl ligand occupying the apical position. The bis-carbene and two other phenyl ligands occupy the equatorial positions. Complex **36** is a rare example of low 5-coordinated chromium(III) cation. Here the "folding" of the bis-NHC ligand at the bridging methylene position pushes the Dipp substituents into the potential sixth site of coordination. According to Theopold *et al.*, the $Cr–C_{carbene}$ bond distances (2.228(4) and 2.244(4) Å) are much longer than in the aforementioned complexes **24**, **29** and **30** as well as in most other carbene complexes with aryl substituents. This indicates a substantial amount of electron density placed on chromium by the three phenyl ligands as well as the carbene's inability to accept back donation from the metal.[20]

For the purpose of having more stable chloride alkyl and aryl compounds, $CrMeCl_2(THF)_3$, $CrPhCl_2(THF)_3$ and $Cr(tolyl)Cl_2(THF)_3$ were used to generate the chromium(III) complexes **37** (79%), **38** (78%) and **39** (71%). **37** and **38** were characterized by ^1H NMR, infrared and mass spectroscopy. Due to solubility problems with **37** and **38**, complex **39** was the only one structurally characterized by single crystal X-ray diffraction. Its structure shows a chromium cation with an octahedral environment. The planes formed by the tolyl and chloride ligands and the bis-NHC ligand, respectively, are orthogonal. A coordinated THF molecule and a second chloride complete the chromium coordination sphere. The $Cr–C_{carbene}$ bond distances (2.128(3) and 2.151(3)) are slightly longer than in **34**.

To gain more insight into the reactivity of **37**, a chloride abstraction reaction was attempted. Reaction with NaBARF led to the triply Cl-bridged di-nuclear complex **40** (71%) suggesting that similarly to **34**, complex **37** possesses a quite labile ligand THF.

The coordination geometry around the two chromium(III) centers in **35** and **40** forms a distorted octahedron. The cations are coordinated to the bis-NHC ligand **L16** and a chloride (**35**) or methyl (**40**) ligand. Three bridging chlorides complete the coordination spheres. The $[(CrCl)_2(\mu\text{-}Cl)_3]$ or $((CrMe)_2(\mu\text{-}Cl)_3]$ core is not familiar with chromium(III). Since Cr(III) is not known to form Cr–Cr bonds easily, the driving force giving **35** and **40** is likely to be the formation of an octahedral coordination sphere.[21] The $Cr–C_{carbene}$ bond lengths (range: 2.094(5)-2.120(2) Å) of **35** and **40** and the $Cr–Cl_{terminal}$ bond distances (2.2433(16) and 2.2419(15) Å) of **35** are similar to those of **34**. The Cr–Cl bond distances involving the bridging chlorides of **35** and **40** are longer (range: 2.3636(15) - 2.5000(6) Å) than those involving terminal chlorides.[18] In **40**, the chlorides in *trans* position to the methyl groups

show some sign of *trans* influence; their Cr–Cl bond distances increase to 2.5000(6) Å. In contrast, the Me–Cr bond distances are in agreement with those in other reported chromium (NHC) alkyl complexes.[20b,22]

To determine a correlation between oxidation state and catalyst activity, the Cr(III) complexes **34** - **40** were tested in ethylene polymerization, as well as the Cr(II) complex **42**. The reaction of **L15** with $Cr[N(SiMe_3)_2]$ led to the Cr(II) complex **41** in high yield (79%). The analogue **42**, which contains chlorides instead of bromides, was prepared from the free carbene **L16** and $CrCl_2$ (90%). Halide exchange between **41** and NEt_4Cl gave also **42**. Due to its poor solubility, complex **42** was not structurally characterized by single crystal X-ray diffraction.

In the solid state, **41** exhibits a chromium center in a square pyramidal environment similarly to **36**. The bis-NHC ligand, a THF molecule and a bromide occupy the equatorial positions whereas the second bromide occupies the apical position. The $Cr–C_{carbene}$ distances (for **41**) are longer than those of the Cr(III) complexes **34**,**35**-**36**,**39** and **40**. The Cr–Br bond distances are in agreement with the values found in the literature.[19] Complex **41** was characterized by ^1H NMR, infrared and mass spectroscopy whereas complex **42** was only characterized by infrared and mass spectroscopy.

2.5 Manganese

The free pyridine-bis(carbene) **L4** was added to $MnBr_2$ to form the Mn(II) complex **43** in excellent yield (92%),[6b] which was characterized by X-ray diffraction and elemental analysis.

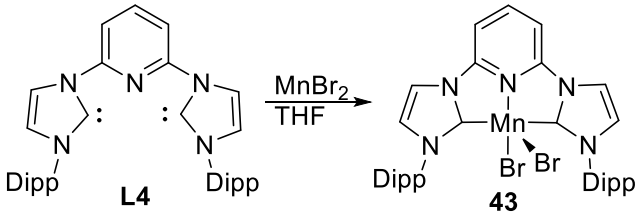

Scheme 14. Mn(II) complex bearing a bis-NHC pincer.[6b]

Its structure exhibits a five-coordinate metal center with a distorted square pyramidal geometry. The ligand **L4** and a bromide occupy equatorial positions. The second bromide is in apical position. As for **30**, the plane containing the manganese (II), the bromine and the pyridine nitrogen atom define an approximate C_s symmetry. **43** is a rare example of structurally characterized Mn–NHC complex.[23] The apical Mn–Br bond (2.210(2) Å) is

longer than the basal one (2.206(2) Å). The Mn–$C_{carbene}$ bond distances (2.206(2) and 2.210(2) Å) are in agreement with those previously reported, and longer than Mn–C σ(sp^3) bonds.[24]

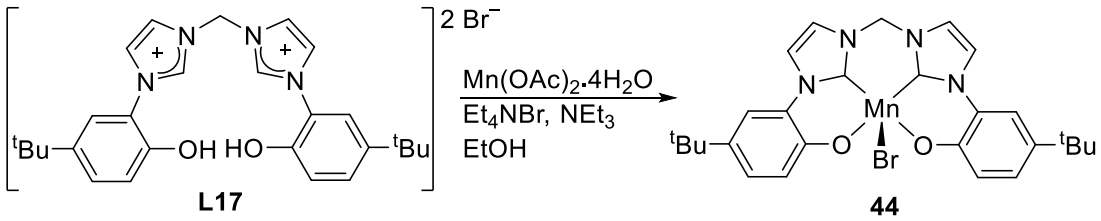

Scheme 15. Mn(III) complex bearing a bis-NHC tetradentate ligand.[25]

The phenolimidazolium bromide salt **L17** and $Mn(OAc)_2$•$4H_2O$ were mixed in the presence of Et_4NBr and NEt_3 to afford the complex **44** in moderate yield (47%).[25] The manganese cation is in a distorted square pyramidal coordination geometry. The bromide is in the apical position and the tetradentate bis-NHC ligand **L17** occupies the equatorial positions. Compared to salen complexes with Mn(III) cations in a square pyramidal coordination geometry with a chloride in the apical position (0.12-0.344 Å), the deviation of the metal center from the basal plane is larger in pincer-type Mn(III) NHC complexes (0.342(4) *versus* (0.27(2) Å). The Mn(III)–$C_{carbene}$ bond distances (1.983(9) and 2.014(9) Å) are shorter than those of NHC Mn(I), Mn(II) or Mn(IV) complexes but similar to those of a bis-(phenolate)NHC pincer Mn(III) complex.[6b,23,26] The Mn–O bond distances in **44** (1.894(6) and (1.905(6) Å) are similar to those of salen complexes, indicating that the binding of the aryloxy group to Mn is similar in both families of complexes. The chelate bite angle $C_{carbene}$–Mn–$C_{carbene}$ (83.9(4)°) is similar to those of various bis-NHC complexes such as **16**-**23**, **34**-**42**. Under air, **44** is stable for months in the solid state and several weeks in solution (DCM-acetone or DCM-methanol). This enhanced stability might result from the rigid structure of the tetradentate bis-NHC ligand **L17**.

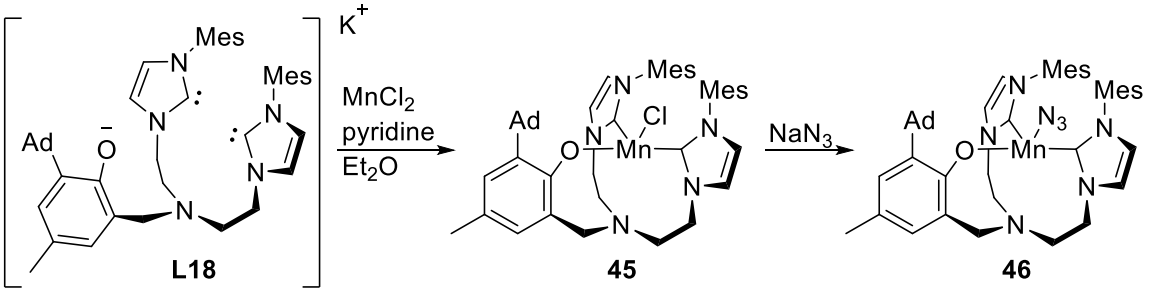

Scheme 16. Mn(II) complex bearing a (bis-NHC)phenolate ligand.[27]

The reaction of **L18** with $MnCl_2$ led to the Mn(II) complex **45** in moderate yield (55%).[27a] Salt metathesis between **45** and NaN_3 afforded **46** in good yield (63%). The Mn(II)

complex **46** was identified by the intense infrared vibration bands of N_3 at 2077 and 2056 cm^{-1} in KBr. Both **45** and **46** are NMR-silent. They feature two UV bands at 257 and 309 nm (with similar intensity) tentatively assigned to a ligand π-π* transition (phenolate), and a charge transfer from phenolate to the Mn(II) center.[28] In the solid state, the geometry around the metal is distorted trigonal pyramidal. The chloride ligand occupies the apical position and the NHC and the phenolate donors occupy the equatorial positions. The manganese cation is situated 0.362(2) Å above the plane formed by the NHC and phenolate donors. The Mn–Cl bond distances (2.227(3) and 2.230(3) Å) are in agreement with those of **43**. The molecular structure of **46** exhibits a Mn(II) center in a distorted trigonal pyramidal coordination geometry. The NHC moieties and the phenolate occupy equatorial positions. The azide ligand occupies the apical position in a bent coordination mode. Variable-temperature SQUID experiments confirmed that **45** and **46** have a high spin ground state with a magnetic moment of 5.82 and 5.78 μ_B, respectively. Complex **45** is paramagnetic and only infrared and mass spectroscopy data are available. A patent described **45** as an agent to improve the oxidizing and bleaching action of peroxygen compounds at low temperatures in laundry detergents.[27b]

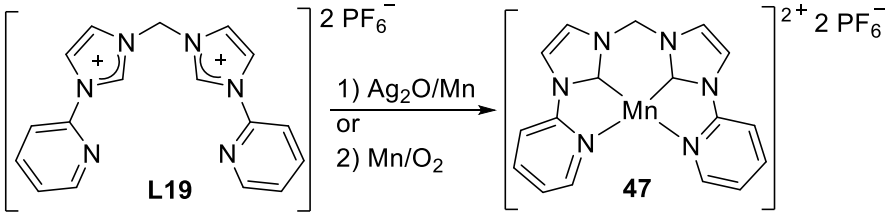

Scheme 17. Mn(II) complex bearing a bis-NHC tetradentate ligand.[29]

Another patent described two syntheses of **47**.[29] The first one dealt with the *in situ* generation of the silver NHC complex arising from the imidazolium hexafluorophosphate **L19**, under exclusion of light and under inert atmosphere, followed by the addition of manganese metal. The second one dealt with the reaction of **L19** with manganese metal under air. Both routes provide **47** in moderate yields (respectively 68 and 53%), which was only characterized by elemental analysis.

2.6 Iron

The bis-NHC iron(II) complexes **48**-**57** and **59**-**62** were reported by Meyer *et al.* in 2011.[30] Ingleson's group described five other complexes with similar or longer alkyl linkers (**58**, **63**-**66**).[31]

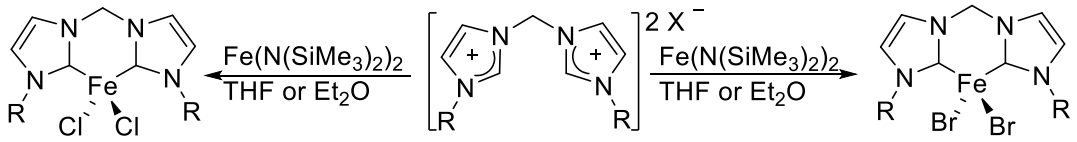

48: R = Bn
49: R = ^{t}Bu
50: R = Mes
51: R = Ad

X = Cl
L20: R = Bn
L21: R = ^{t}Bu
L22: R = Mes
L23: R = Ad

X = Br
L24: R = Me
L25: R = Et
L26: R = Bn
L27: R = ^{t}Bu
L28: R = Mes
L29: R = Ad
L15: R = Dipp

52: R = Me
53: R = Et
54: R = Bn
55: R = ^{t}Bu
56: R = Mes
57: R = Ad
58: R = Dipp

Scheme 18. Fe(II) complexes bearing a methylene bridge bis-NHC ligand.[30-31]

Aminolysis of $Fe(N(SiMe_3)_2)_2$, overnight, with the imidazolium chloride or bromide salts (**L20**-**L32**) afforded the complexes **48**-**62** in moderate to excellent yields (44%-90%). The yields of **53**, **59** and **63** were lower due to the formation of tetracarbene complexes as by-products (refer to the complex **87**). All these complexes quickly decomposed in solution under air conditions. However, their stability in the solid-state ranged from a few minutes to hours for the most sterically demanding substituents (Ad and Mes). The poor solubility of the complexes **48**-**57** in nonpolar solvents hampered their purification and characterization by XRD.

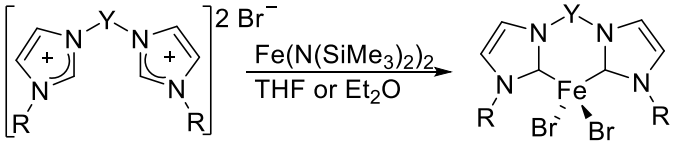

L30: Y = $(CH_2)_2$; R = Me
L31: Y = $(CH_2)_2$; R = Mes
L32: Y = $(CH_2)_3$; R = Me
L33: Y = CHPh; R = Me

59: Y = $(CH_2)_2$; R = Me
60: Y = $(CH_2)_2$; R = Mes
61: Y = $(CH_2)_3$; R = Me
62: Y = CHPh; R = Me

Scheme 19. Fe(II) bromide complexes bearing a bis-NHC ligand.[30]

Complexes **48**, **54**, **56**, **57**, **60** and **62** were characterized by single crystal X-ray diffraction. They all present an iron(II) center in a distorted tetrahedral geometry formed by the bis-NHC ligand and two halides. The Fe–$C_{carbene}$ bond distances are close to 2.10 Å and in agreement with those found in other tetrahedral bis-NHC iron complexes.[32] The 6-membered rings formed by the ligands and the iron cation adopt a distorted boat-like conformation. ^{57}Fe Mössbauer spectroscopy of **48**-**50** and **59**-**61** showed a large quadrupole splitting at the upper range of 3-4 $mm.s^{-1}$ typical of high-spin iron(II) (S = 2) in a tetrahedral environment. Complexes **51** and **62** could not be separated from tetra-NHC iron complexes formed as by-

products (see complexes **84** and **86**, vide infra). Most of these complexes were tested for aryl Grignard–alkyl halide cross coupling.

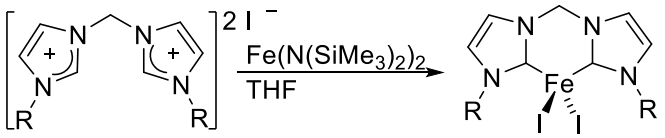

L34: R = ^{i}Pr
L35: R = Dipp

63: R = ^{i}Pr
64: R = Dipp

Scheme 20. Fe(II) iodide complexes bearing a bis-NHC ligand.[31]

Using the procedure described above, complexes **63** and **64** were synthesized by reaction between the imidazolium iodide salts **L34** or **L35** and $Fe(N(SiMe_3)_2)_2$ in 57% and 97% yield, respectively.[31] The deprotonation of the imidazolium bromide salt **L15** with KH and addition of the resulting free carbene to $FeBr_2$ led to complex **58** in moderate yield (40%). Complexes **58**, **63** and **64** were characterized by elemental analysis, ^{1}H NMR spectroscopy and single crystal X-ray diffraction. The molecular structures of **58**, **63** and **64** are similar to those reported above for **47**-**49** and **60**-**62** (i.e. tetrahedral geometry). Two halides (bromides for **58** and iodides for **63**-**64**) and the bis-NHC ligands are coordinated to the iron(II) cation. For **63** and **64** the halides are classified as pseudo-apical or pseudo-equatorial due to a highly distorted tetrahedral geometry. The Fe–$C_{carbene}$ bond distances fall in the range of 2.08 to 2.11 Å. The ^{57}Fe Mössbauer spectrum of **64** displays isomer shifts and quadrupole splitting parameters comparable to those of a FeI_2(bis-phosphine) complex with similarly distorted geometry.[33]

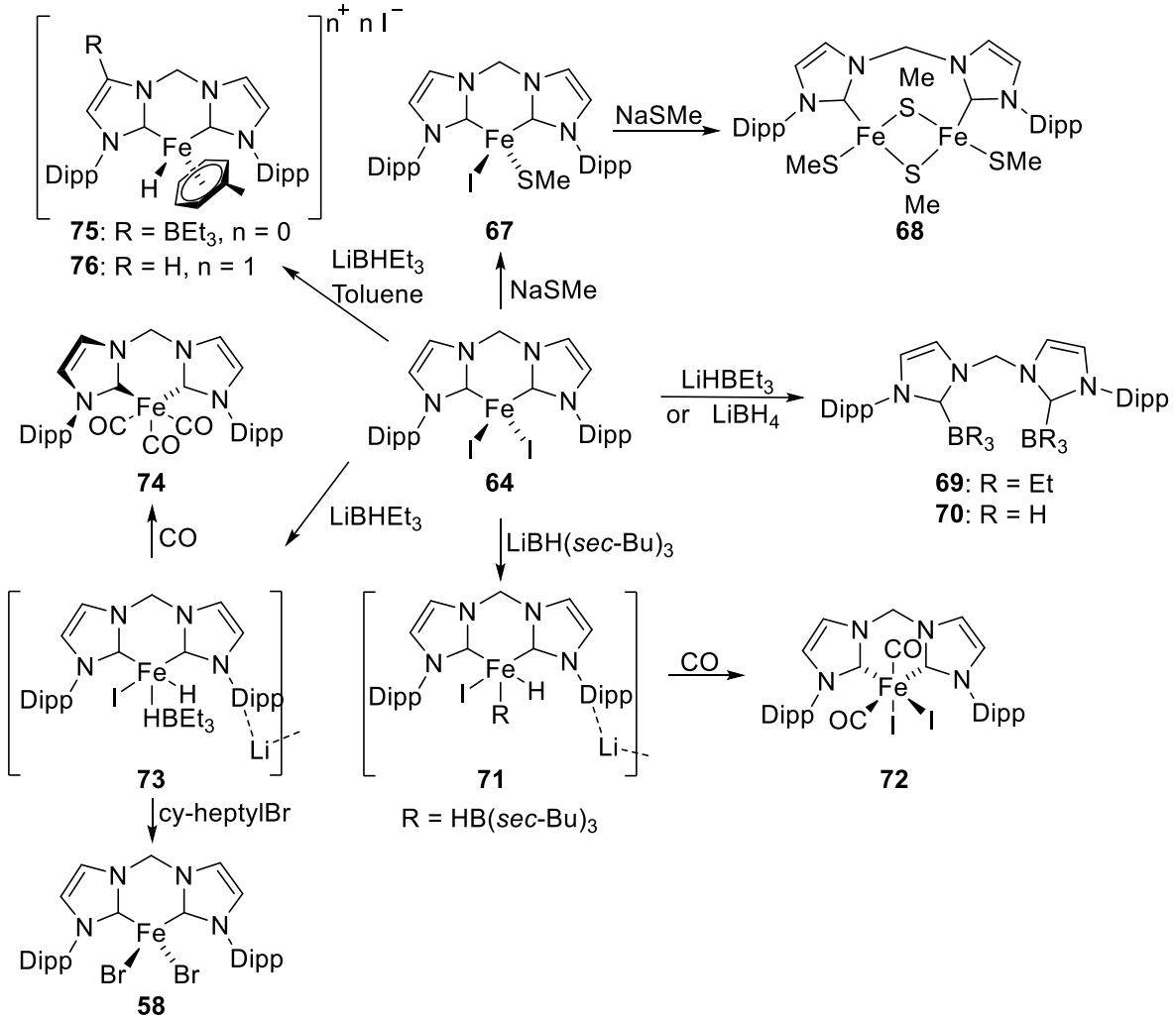

Scheme 21. Reactivity of the complex **64**.[31,34]

Ingleson's group studied the reactivity of **64** and therefore reported the synthesis of **67**-**76**.[31,34] The reaction of **64** with one equivalent of NaSMe yielded the complex **67** (34%) which was then characterized by ^{1}H NMR spectroscopy, elemental analysis and X-ray diffraction. Its solid-state structure reveals an Fe(II) center with a distorted tetrahedral coordination geometry completed by the bis-NHC-, iodide-, and SMe- ligands. The Fe–$C_{carbene}$ bond distances (2.112(13) and 2.103(14) Å) are in agreement with those in **63**-**64** described above. The thiomethoxide ligand occupies the less sterically hindered pseudo-equatorial position and the bulky Dipp groups prevent any dimerization through μ-SMe bridges.[34] The addition of an additional equivalent of NaSMe to **67** led to a new paramagnetic compound in good yield (81%). The ratio bis-NHC/Fe/SMe equal to 1:2:4, and the analogy with the methylation of **37** leading to **40**[35] suggested the formation of the complex **68**. However, the structure was not confirmed by X-ray diffraction studies. The reaction of **64** with $LiBHEt_3$ or $NaBH_4$ in THF or acetonitrile led to the bis-NHC borane adducts **69**-**70** (no

yield value given). **70** was characterized by ^{1}H, $^{13}C\{^{1}H\}$ NMR spectroscopy and X-ray diffraction studies whereas **69** was only characterized by crystallography.

Moreover, the reaction of **64** with 1 equiv. of $LiBHEt_3$ (or $LiBH(sec\text{-}Bu)_3$) in Et_2O yielded the paramagnetic complex **73** (or **71**). **73** proved to be extremely prompt to undergo carbene dissociation. In contrast, **71** was stable in Et_2O for several days. Complex **71** reacted with CO to afford the paramagnetic complex **72**. The observation of two ν(CO) bands at 2024 and 1974 cm^{-1} indicates a *cis*-CO arrangement. No crystal structure was described. Addition of *cyclo*-heptylbromide to a solution of **73** led to the complex **58** (no yield provided).

The reaction of **64** with $LiBHEt_3$ under 1 atmosphere of CO led quantitatively to the Fe(0) complex **74**. The latter was characterized by infrared spectroscopy and the ν(CO) bands (1968, 1891 and 1864 cm^{-1}) are at lower wawenumbers than those of analogous phosphine complexes.[36] The geometry around the iron center is trigonal-bipyramidal with an equatorial and two axial sites occupied by CO ligands. The bis-NHC ligand occupies the two remaining equatorial sites. The two Fe–CO bond distances are identical. The reaction of **64** with $LiBHEt_3$ in toluene produced the complex **75**, in low yield (no given value), which contains coordinated hydride, η^6-toluene, and deprotonated anionic borane-carbene ligands, forming an octahedral environment around the iron center. X-ray diffraction studies were performed. The $Fe–C_{carbene}$ bond lengths (1.966(5) and 1.970(5) Å) are usual while the B–C bond (1.647(10) Å) appears elongated. In the electron density difference map (generated from crystallographic data), the hydride was not located. In order to trap an hydride iron(II) complex, 12-crown-4 ether or 12-crown-4 ether/cyclooctene or 12-crown-4 ether/PMe_3 was added to **64** producing the complex **76** in low yield (16% maximum). It was characterized by ^{1}H NMR spectroscopy and X-ray diffraction. The geometry around the iron center and the $Fe–C_{carbene}$ bond distances are similar to those in **75**.

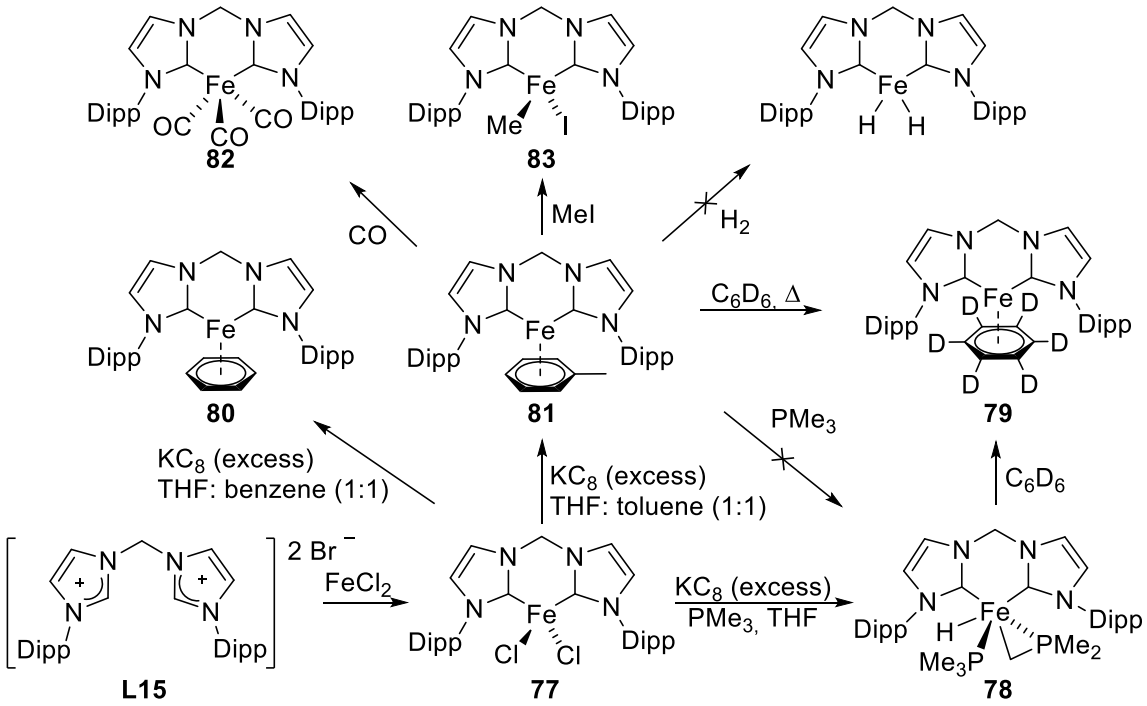

Scheme 22. Reactivity of complex **77**.[37]

Driess *et al.* described the synthesis of the complexes **77**-**83** in 2013.[37] The reaction of the free carbene **L15** with anhydrous $FeCl_2$ led to the complex **77** in high yield (81%). This pathway was an alternative to a synthetic protocol described by Meyer and Ingleson[30-31]. The complex **77** being analogous to **48**-**58**, its solubility in hydrocarbon solvents was very poor, precluding any crystallization. However, ^{1}H NMR, EIMS, and HMRS analyses confirmed its composition. Furthermore, ^{57}Fe Mössbauer analysis displayed values typical of a tetrahedral high-spin iron(II) complex.

The reduction of **77** with an excess of KC_8, in THF, in the presence of PMe_3 led to the 18 electron hydride iron(0) complex **78** (24%) rather than the expected 16 electron bis-NHC bis-(triphenyl)phosphine iron (II) complex via intra-molecular C-H activation of P-Me bond. A close look at the ^{1}H and $^{31}P\{^{1}H\}$ NMR spectra reveals the coexistence of three stereoisomers of **78** with a static distribution. In contrast, $^{13}C\{^{1}H\}$ NMR measurements reveal a highly symmetric spectrum featuring sharp signals assignable to a unique isomer. In the solid state, the Fe(II) center exhibits a distorted octahedral environment with two mutually *trans* phosphine groups in axial positions. The bis-NHC, the hydride and the methyl ligands occupy the equatorial positions. The Fe–$C_{carbene}$ bond distances (1.915(3) and 1.919(3) Å) are shorter than those reported by Meyer,[30,34] which suggests an increased π-back donation from iron(II) cation to carbene, facilitated by the presence of electron-donating alkyl phosphane

ligands in the coordination sphere. Complex **78** is unstable for prolonged periods in deuterated benzene and affords the arene iron(0) complex **79** by spontaneous loss of PMe_3 ligands. Calculations at the DFT level conclude that the transformation of **78** into **79** is an exergonic process. The complex **79** was characterized by ^1H, $^{13}C\{^1H\}$ NMR spectroscopy. Its $^{13}C\{^1H\}$ NMR spectrum exhibits a characteristic carbene signal at 198.4 ppm.

The reduction of **77** with excess KC_8 in a 1:1 THF/arene (toluene or benzene) mixture led to the complexes **80** (75%) and **81** (61%), which have a very similar structure to **79**. In these protocols, THF was used to solubilize the starting material **77**. The ^1H NMR spectra of **80** and **81** are similar to that of **79** and exhibit a highly symmetrical pattern. The $^{13}C\{^1H\}$ NMR spectra of both complexes feature sharp peaks indicating free rotation of the arene ligands. The carbene signals are observed at 197.8 and 197.5 ppm, respectively. In the solid state, both complexes **80** and **81** exhibit an iron(0) center with a pseudo-trigonal bipyramidal environment. The arenes occupy two equatorial sites and an apical one. The bis-NHC ligand occupies the last basal site and the second apical site. The Fe–$C_{carbene}$ bond distances of **80** and **81** are similar (1.921(3); 1.9190(19), 1.9212(19) Å) and in the range of those of complex **78**. However, they are shorter than those reported by Meyer's group.[30] These bond distances suggest some π-back donation from the iron(0) center to the carbene, in contrast to analogous imine or phosphine complexes.

The reaction of **81** with MeI afforded the paramagnetic complex **83** characterized by NMR and ESI-MS analyses but its structure could not be confirmed by X-ray diffraction. Complex **81** was unreactive under H_2 atmosphere, or in presence of an excess of PMe_3. It reacted with deuterated benzene at 70 °C, or with CO to yield **79** (100%) or **82** (91%), respectively. Contrary to Ingelson's group,[34] Driess *et al.* found no decomposition of **82** under vacuum or under N_2 atmosphere in solution.[37] This complex was also characterized by ^1H and $^{13}C\{^1H\}$ NMR and ESI-MS spectroscopy.

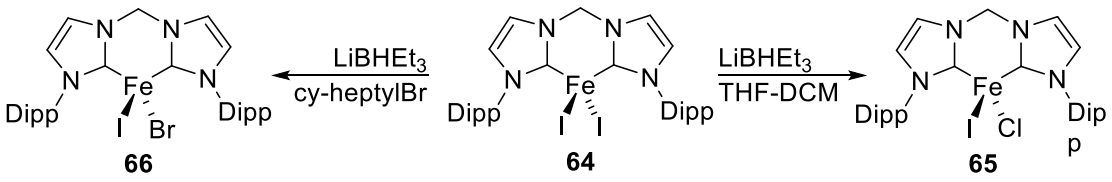

Scheme 23. Fe complexes bearing chelating bis-NHC ligands.[34]

The synthesis of **65** was attempted, starting from **64**, following three different routes: a) Addition of benzyl bromide; b) Addition of 2 equiv. of $LiBHEt_3$ and *cyclo*-heptylbromide;

c) Addition of **58** (halide exchange). The three methods failed to convert cleanly and completely **64** into **65**. As the crystallization of **66** from the crude reaction mixtures failed, no further characterization or isolation was undertaken.

The reaction of **64** with $LiBHEt_3$ in THF-DCM yielded complex **66** (34%) similarly to the synthesis of **65**.[34] A two-step mechanism was proposed: the hydride bis-NHC iron ($[(({}^{Dipp}C)_2CH_2)FeI_2(H)]^-$) complex (signal at -7.6 ppm in ^1H NMR) was first formed which then reacted slowly, within three days, with an excess of DCM. The complex **66** was characterized by elemental analysis and single crystal X-ray diffraction. Its structure, close to that of **58**, exhibits an iron(II) center with a distorted tetrahedral coordination geometry. The $Fe–C_{carbene}$ bond distances (2.095(14) and 2.105(11) °) are similar to those in complexes **48**, **54**, **56**, **57**, **60**, and **62**.

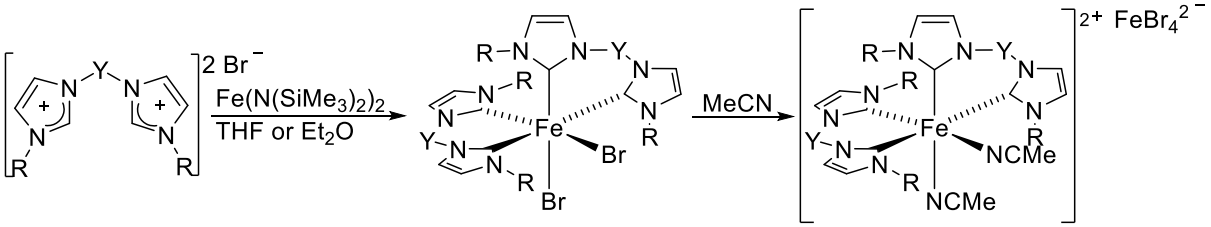

L24: Y = CH_2; R = Me
L25: Y = CH_2; R = Et
L33: Y = CHPh; R = Me

84: Y = CH_2, R = Me
85: Y = CH_2, R = Et
86: Y = CHPh, R = Me

87: Y = CH_2, R = Me
88: Y = CH_2, R = Et
89: Y = CHPh, R = Me

Scheme 24. Tetra(NHC) iron(II) complexes bearing two bis-NHC ligands.[30]

We have previously described iron complexes with only one chelating bis-NHC ligand. Now, we are going to describe iron complexes with two bis-NHC ligands. They are all by-products from the syntheses of **52, 53** and **62**.

The formation of the tetra-NHC iron(II) complexes **84**-**86** was observed during the syntheses of the bis-NHC complexes **52**, **53** and **62**. Their very similar solubility rendered their separation from the reaction crude mixtures very tricky. In acetonitrile, **84**-**86** underwent bromide exchange with the solvent leading to the complexes **87**-**89** with $[FeBr_4]^{2-}$ (no yield provided) as counter-anion. The complexes **87**-**89** were characterized by single crystal X-ray diffraction as well as by elemental analysis for **87**. All of them exhibit very similar molecular structures. The environments around the iron centers are octahedral with two bis-NHC ligands occupying the equatorial positions, and two acetonitrile molecules occupying the apical positions. The two $Fe–C_{carbene}$ bonds distances *trans* to the MeCN ligands are between 1.92 and 1.95 Å. The other two $Fe–C_{carbene}$ bonds distances mutually *trans* are slightly longer

(1.96-1.99 Å) than the Fe–$C_{carbene}$ bond distances in other reported octahedral tetra-NHC iron complexes.[6a,22b]

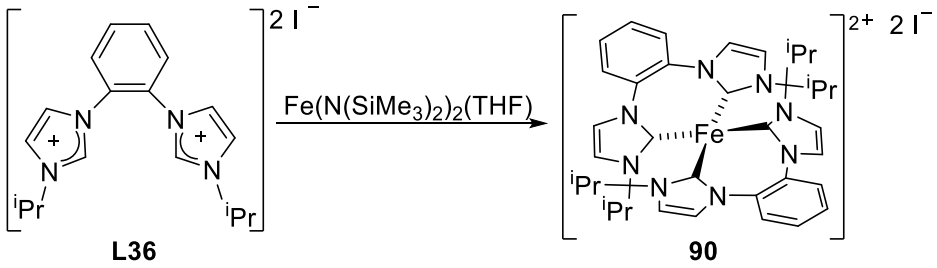

Scheme 25. Tetra(NHC) iron(II) complexes bearing two bis-NHC ligands [31]

Similarly to complexes **48**-**58**, **63** and **64**, the complex **90** was obtained by aminolysis of $Fe(N(SiMe_3)_2)_2(THF)$ in presence of the imidazolium iodide salt **L36** in 60% yield. A side product, likely a second iron complex, was detected during the course of the reaction, but not characterized. The complex **90** was characterized by single crystal X-ray diffraction and elemental analysis. Surprisingly, the geometry around the iron center is square planar with two bis-NHC ligands coordinated to the iron(II) center. The Fe–$C_{carbene}$ distances (1.920(10) and 2.010(9) Å) are longer than those of the diamagnetic square planar complex **114** (vide infra).[38] The two bis-NHC linkers adopt a *trans* arrangement with their phenylene groups oriented either above or below the square plane. The steric hindrance of the bis-NHC ligands blocks any further coordination of potential incoming ligands.

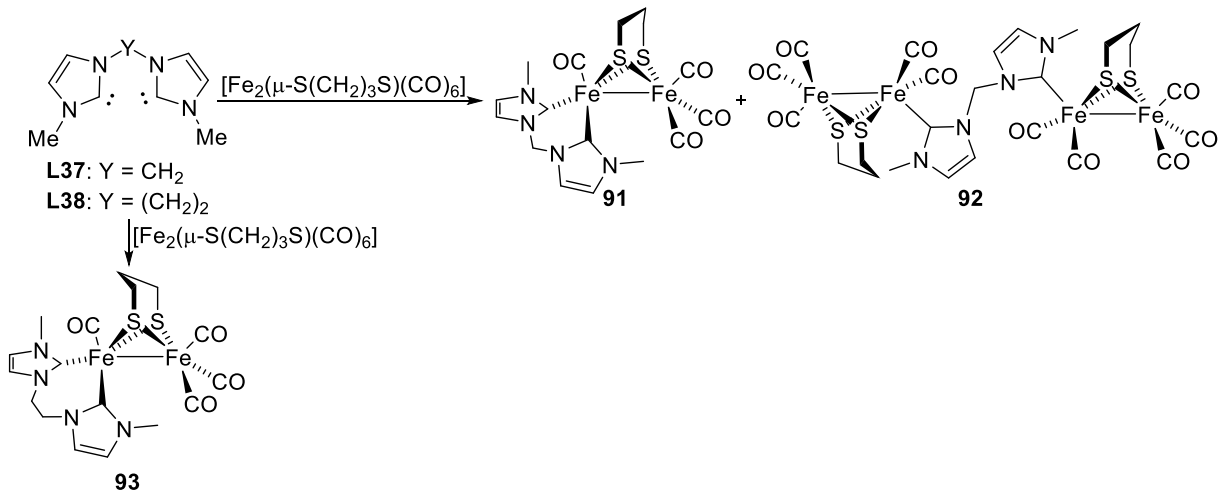

Scheme 26. Fe-S complexes bearing bis-NHC ligands.[39]

A solution of the free carbene **L37** was transferred to a THF solution of $[Fe_2(\mu\text{-}S(CH_2)_3S)(CO)_6]$ producing a mixture of the dinuclear iron(I) complexes **91** and **92**.[39] Complex **92** will be described in section 3.2. The ratio of **91**:**92** depends on the reaction

conditions. Employing one or two equivalents of **L37** led mainly to the recovery of the starting material with small amounts of **91** and **92**. To consume completely the metal source, three equivalents of **L37** were necessary. Besides, the addition of **L37** to a solution of [Fe_2(μ-$S(CH_2)_3S$)$(CO)_6$] led, after treatment on a silica gel column, to the complexes **91** (15%) as a major product and **92** as a minor product (7%). Surprisingly, slow addition of the iron source to **L37** (the addition order of the reagents was reversed) gave essentially **92** with a small amount of **91**. The ^{1}H NMR spectrum of **91** features a singlet for the two equivalent *N*-methyl groups and an AB system for the methylene bridge, which is consistent with a basal/basal (on two of the four square-based positions) coordination mode of the bis-NHC ligand in a distorted octahedral geometry around the iron(I) centers. $^{13}C\{^1H\}$ NMR spectroscopy reveals a carbene signal at 197.8 ppm, in agreement with the literature.[32b,40] The octahedral geometry around the iron centers was further confirmed by single crystal X-ray diffraction. The two iron centers are held together by two thiolate ligands and the Fe–Fe bond distance is equal to 2.5774(6) Å. Only one (over two) iron cation is coordinated by the NHC ligand, the CO ligands completing the coordination sphere. The Fe–$C_{carbene}$ bond distances (1.935(3) and 1.921(3) Å) are typical of bonds having a strong σ-character.[40] The three ν(CO) bands (1996, 1920, 1872 cm^{-1}) of **91** are shifted to lower wavenumbers compared to those of the iron precursor [Fe_2(μ-$S(CH_2)_3S$)$(CO)_6$], with respect to those of **92** (2039, 1974, 1913 cm^{-1}), indicating the substitution of two carbonyl ligands. Moreover, the NHC ligand increases the π-back donation from iron to the carbonyls. In this case, the Fe–C_{CO} bond distances become significantly shorter (1.737(3) Å) than in $Fe(CO)_3$ subunit or [Fe_2{μ-$S(CH_2)_3S$}$(CO)_6$].[41] Following a protocol described for **91**, the iron(I) complex **93** was synthetized in low yield (11%). Its ^{1}H NMR spectrum displays two AB systems accounting for the ethylene bridge, and indicating that the coordination geometry around the iron cations is similar to that in **91**. The $^{13}C\{^1H\}$ NMR carbene signal was found at 192.4 ppm. The IR spectra of **91** and **93** in the ν(CO) region are similar. The solid-state structure of **93** displays, as anticipated by NMR spectroscopy, the same spatial organization as for **91** for the diverse ligands around the iron centers. The Fe–$C_{carbene}$ bond distances (1.950(2) and 1.985(2) Å) are slightly longer than those of **91**.

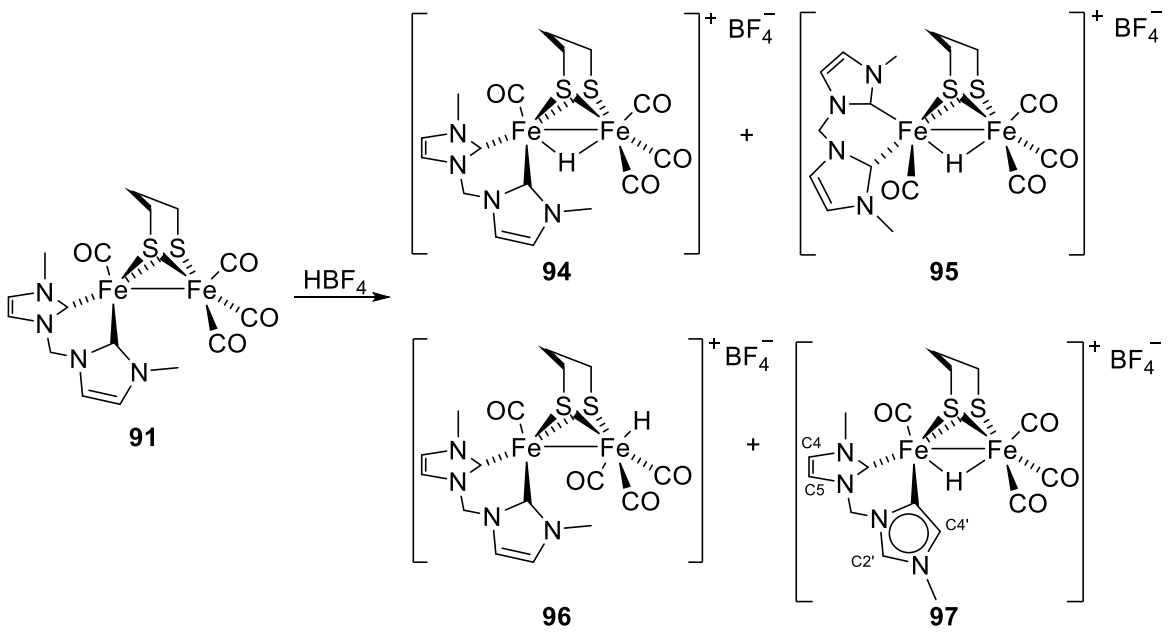

Scheme 27. Reactivity of complex **71**.[39,42]

The protonation of **91** by HBF_4 at -25 °C led to a 90:10 mixture of the isomeric complexes **94** and **95**. After two hours in solution, ^{1}H NMR spectroscopy evidenced the slow conversion of **94** to **95**. After 7 days, **95** has become the major product (60%). Both complexes display a hydride signal at -12.16 (**94**) and -15.10 ppm (**95**). The $^{13}C\{^1H\}$ NMR spectra of **94** and **95** display respectively a carbene signal at 182.89 ppm and three signals for the CO ligands, and two carbene signals at 183.7 and 182.2 ppm and four signals for the CO ligands. Complexes **94** and **95** are stable in presence of HBF_4 or CF_3CO_2H. The authors suggest that during the conversion of **94** to **95**, the bis-NHC ligand moved from basal/basal positions (magnetically equivalent carbenes) to basal/apical positions (magnetically non-equivalent carbenes). Crystals of **95** were grown from the mixture of isomers in CH_2Cl_2. The two iron(II) centers bridged by the hydride and the di-thiolate ligands are in a distorted octahedral coordination geometry. For the first one, the bis-NHC, the hydride ligands and a sulfur atom are in equatorial positions. The CO ligand and the second sulfur atom are in apical positions. For the second one, two CO, the hydride ligands, and a sulfur atom are in the equatorial positions. The last CO ligand and the second sulfur atom are in the apical positions. The second iron cation is not bound to any NHC ligand. Compared to **91**, the Fe–Fe bond distance (2.6054(6) Å) is elongated by 0.03 Å. The Fe–H bond distances (1.710 and 1.562 Å) are in agreement with the literature. By monitoring the protonation of **91** with HBF_4 at -90 °C, two additional complexes **96**-**97** were observed, by ^{1}H NMR, with hydride signals at -12.06 ppm (**96**) and -6.26 ppm (**97**). No further characterization was made with **96**, due to its extreme instability. At -80 °C, the hydride signal of **96** fades to be replaced by the signals of

94 and **97**. ^{1}H-$^{13}C\{^{1}H\}$ HBMC 2D measurements of **97** unveil two signals at 184.0 and 155.0 ppm characteristic respectively of normal and abnormal carbenes bound to iron (see Scheme **26**). The coexistence of these different NHC types was also confirmed by ^{1}H NMR spectroscopy with two sets of signals for the imidazole protons at 8.63 and 6.36 ppm (protons on carbon atoms C4 and C5) and 7.45 and 6.95 ppm (protons of carbon atoms C2' and C4'). At room temperature, **97** is fully converted to the more thermodynamically stable complex **94**.

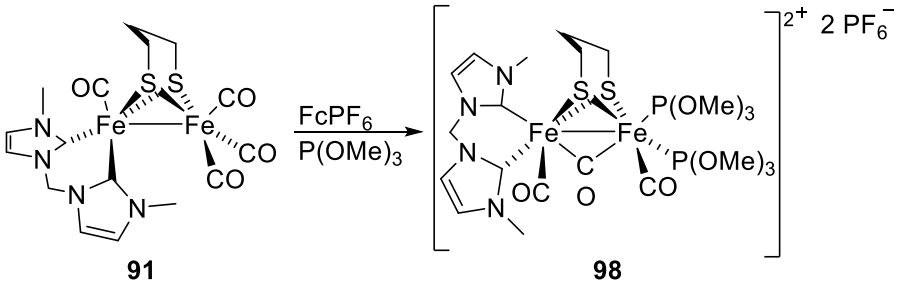

Scheme 28. Oxidation of complex **91**.[42]

The oxidation of **91** with ferricenium hexafluorophosphate and $P(OMe)_3$ led to the iron(II) complex **98** in good yield (76%).[42] Its IR spectrum displays three ν(CO) bands at 2036, 2021 and 1912 cm^{-1}. $^{31}P\{^{1}H\}$ NMR spectroscopy confirms the presence of two coordinated phosphite-ester ligands with signals at 140.5 and 156.3 ($^{2}J_{PP}$ = 129 Hz). $^{13}C\{^{1}H\}$ NMR spectroscopy displays the carbenes signals at 171.9 and 177.3 ppm. There are also a doublet of doublets at 227.8 ppm ($^{2}J_{PC}$ = 19 and 9 Hz), a singlet at 205.9 ppm and a doublet of doublets at 206.3 ppm ($^{2}J_{PC}$ = 25 and 46 Hz) attributable to the bridging and two terminal carbonyls, respectively. The solid-state structure of **98** features two iron(I) centers in a distorted octahedral geometry, and bridged by CO and di-thiolate ligands. For the first one, the bis-NHC and a CO ligand and a sulfur atom occupy equatorial positions. A CO ligand and the second sulfur atom are in apical positions. For the second one, two $P(OMe)_3$ and a CO ligand, and a sulfur atom are in equatorial positions. A further CO ligand and the second sulfur atom are in apical positions. The second iron cation is not bound to any NHC ligand.

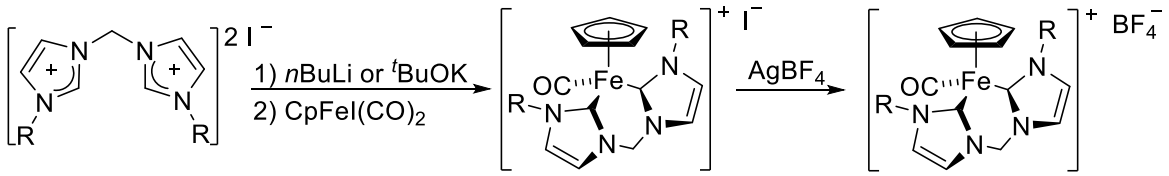

L39: R = Me
L34: R = ^{i}Pr
L40: R = Mes
L41: R = ^{t}Bu

99: R = Me
100: R = ^{i}Pr
101: R = Mes
102: R = ^{t}Bu

103: R = Me
104: R = ^{i}Pr
105: R = Mes

Scheme 29. Piano-stool Fe complexes bearing chelate bis-NHC ligands.[32b,43]

Piano-stool complexes result from the presence in a tetra-coordinated metal complex of an aryl group representing the "seat" of the stool. Albrecht and Tapish reported the piano-stool bis-NHC iron(II) complexes **99-103**.[32b,43] The deprotonation, *in situ*, of the imidazolium iodide salts **34**, **39-41** with *n*BuLi (or *t*BuOK) and reaction with $CpFeI(CO)_2$ afforded the complexes **99** (64%), **100** (55%), **101** (54%), and **102** (73%) in good yields. In the solid-state, the complexes **99-102** are air stable for several weeks. The ratio imidazolium/Cp protons (measured by NMR) indicates the formation of the expected bis-NHC iron complexes The two AX doublets for the methylene bridge confirm the chelation of both NHC donors. The $^{13}C\{^{1}H\}$ NMR carbene signals of **99**, **100** and **101** occur at 182.9, 180.3 and 186.2 pm. The *ν*(CO) band of **102**, having the lowest wavenumber value compared to that of **100** and **101**, implies that the NHC ligand arising from the salts **L41** is the strongest donor. The complexes **101** and **102** were characterized by single crystal X-ray diffraction, and display iron centers in an octahedral environment. Three sites are occupied by the Cp ligand (η^5-coordination) and the coordination sphere is completed by the bis-NHC and carbonyl ligands. The $Fe–C_{carbene}$ bond distances of **101** (1.952(5) and 1.955(5) Å) and **102** (1.982(3) and 1.984(3) Å) are similar to those of other reported bis-NHC iron(II) complexes.[30-31,34,39] The central metallacycle adopts a boat-like conformation explaining the magnetic non-equivalence of the methylene bridge protons. In this regard, the crystal structure of **101** displays an interesting hydrogen bonding interaction between a methylene bridge proton and the iodide anion. Metathesis of anions between **99-101** and $AgBF_4$ afforded the complexes **103-105** in good yield (no values given).[32b] The reactions were monitored by ^{1}H NMR spectroscopy, via the signals of a heterocyclic or a methylene bridge proton. The complex **105** was characterized by $^{13}C\{^{1}H\}$ NMR spectroscopy by a carbene signal at 186.3 ppm. The IR spectra of **99-101, 105** display identical signals for the CO ligands, indicating that changing the non-coordinating anion did not affect much the electronic density at the iron center. Electrochemical analyses of

the redox potential of complexes **103**-**105** exhibited some reversible Fe^{II}/Fe^{III} oxidation waves for **104**-**105** (E_{obs} = +1.36 V) whereas **77** was irreversibly oxidized (E_{obs} = +1.36 V).

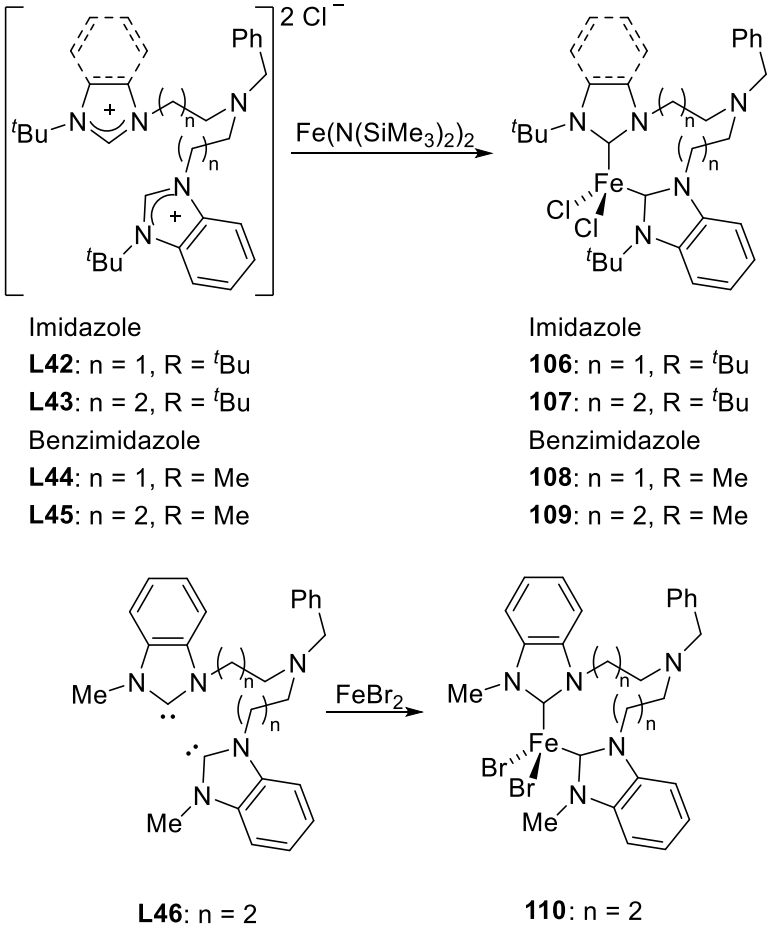

Scheme 30. Fe complexes bearing bis-NHC complexes.[44]

Hazari *et al.* published the synthesis of bis-NHC iron(II) halide with flexible amine-spacers.[44] The complexes **106**-**109** were synthetized in high yields (> 86%) by reaction of the imidazolium chloride salts (**L42**-**L45**) with $Fe(N(SiMe_3)_2)_2$. No side reactions were observed as reported in previous cases (complexes **68**-**70**).[30] The reactions of the free carbenes arising from **L42**-**L45** with $FeCl_2$, $FeBr_2$ or $FeBr_2(THF)_2$ in coordinating or non-coordinating solvents were unsuccessful. In contrast, a similar reaction between the free carbene **L46**, generated *in situ*, and $FeBr_2$ led to the complex **110** in moderate yield (52%). The Evans' method indicates that the magnetic moments of **108**-**110** are equal to 4.77, 4.84 and 4.79 μ_B, suggesting a S = 2 ground state. The complexes **106**-**110** were characterized by infrared, mass spectroscopy and single crystal X-ray diffraction. The complex **110** was also characterized by ^{1}H NMR spectroscopy. The different iron centers are in a distorted tetrahedral coordination environment (**107**-**110**). The Fe–$C_{carbene}$ bond distances range from 2.090(5) to 2.166(4) Å and

are similar to those reported in the literature.[30] Apart from the different types of halides present, the structures of **109**-**110** are virtually identical; there is no noticeable change for the different Fe–$C_{carbene}$ bond lengths. For **107**, there is a slight twist of the nitrogen linker compared to **109** and **110**. The ^{57}Fe Mössbauer spectrum of **109** displays values in agreement with other high-spin tetrahedral iron(II) complexes reported by Ingleson.[31]

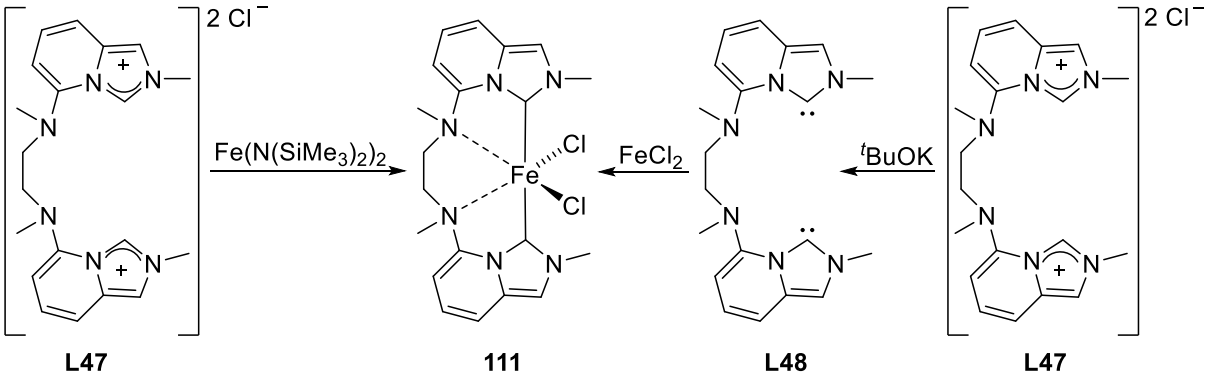

Scheme 31. Fe(II) complex bearing a bis-NHC ligand with a nitrogen linker.[45]

Ohki, Tatsumi and Glorius reported the iron(II) complex **111** with a new linker based on ethylenediamine.[45] It was obtained by reaction between the precursor imidazolium chloride salt (**L47**) and $Fe(N(SiMe_3)_2)_2$ (44%) or between the free carbene (**L48**) and $FeCl_2$ (19.6%). The magnetic moment of **111** (5.39-5.65 μ_B) is slightly larger than the value (4.90 μ_B) for complexes with a S = 2 ground state. The complex **111** was characterized by mass spectroscopy and single crystal X-ray diffraction. The iron cation is in a highly distorted tetrahedral coordination environment. Moreover, the Fe–N_{amine} bond distances (2.5591(14) and 2.5803(15) Å) are characteristic of weak interactions suggesting a pseudo-octahedral geometry. Overall, the iron(II) center of **111** exhibits an intriguing geometry intermediate between octahedral and tetrahedral. The triflate version of the salt **L40** mixed with $Fe(N(SiMe_3)_2)_2$ led to the triflate version of **95.** This complex was characterized by ESI-MS analysis from the crude reaction mixture, but was not further isolated.

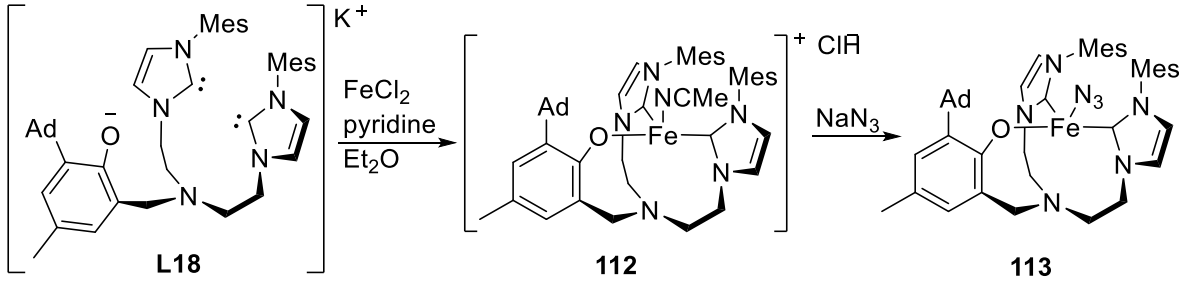

Scheme 32. (Bis-NHC)phenolate Fe(II) complex.[27a]

Similarly to **45**, **L18** reacted with $FeCl_2$ to afford complex **112** in very good yield (80%). The paramagnetic ^1H NMR spectra in DMSO-d_6, MeCN-d_3, $CDCl_3$ or THF-d_8 display signals from 55 to -10 ppm. Assignment and integration are difficult due to broad and overlapping resonances. However, the structure of **112** in solution was found to depend on the solvent ability to coordinate the metal and solvate the chloride.

Salt metathesis between NaN_3 and **112** led to the complex **113** in excellent yield (93%). Infrared spectroscopy confirmed the formation of **113** by the strong absorption bands of the azide group at 2086, 2054 and 2001 cm^{-1} in KBr. Interestingly, the ^1H NMR spectra of **113** in DMSO-d_6, MeCN-d_3, $CDCl_3$ are identical to those of **112**, except in THF-d_8. Thus, azide and chloride might coordinate the iron only in THF. The molecular structures of **112** and **113** obtained respectively in acetonitrile and DMF confirm this statement. The iron(II) centers exhibit a distorted trigonal pyramidal environment, with the NHC- and phenolate-ligands occupying the equatorial positions. In **112**, a molecule of acetonitrile occupies the apical position. The iron is situated 0.113(1) Å above the plane formed by the carbenes and the phenolate function. The Fe–N_{anchor} distance (2.462(2) Å) indicates a weak interaction between the iron(II) center and the anchoring nitrogen. The Fe–$C_{carbene}$ bond distances (2.100(2) and 1.122(2) Å) are similar to those in the iron(II) bis-NHC complexes **48**, **54**, **56** and **57**.[22b,30-31,46] In **113**, the azide ligand occupies the apical position in a bent coordination mode, as in **46**. Finally, the ^{57}Fe Mössbauer spectra show doublets with isomer shifts of 0.68(1) (**112**) and 0.83(1) $mm.s^{-1}$ (**113**) in agreement with high spin iron(II) complexes.

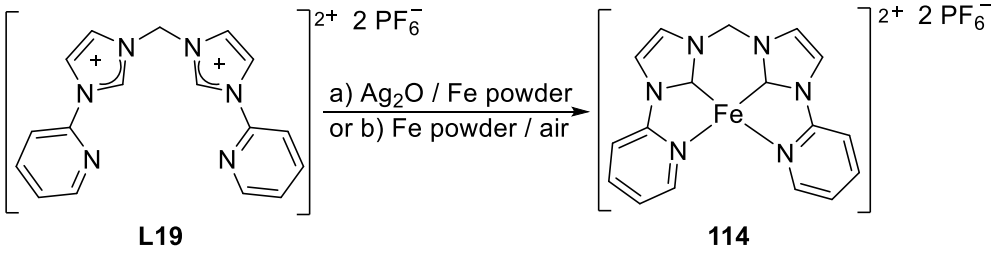

L19 **114**

Scheme 33. Fe(II) complex bearing a tetradentate bis-NHC ligand.[29,38]

Chen *et al.* reported the synthesis of the pyridine-bis-NHC iron(II) complex **114** through two routes:[29,38] i) by reaction of Fe(0) powder with a silver complex generated *in situ* (from the corresponding imidazolium hexafluorophosphate salt in presence of Ag_2O); ii) by direct treatment of **L19** with Fe(0) powder under air conditions. Both methods gave moderate yields (respectively 57.1%, 30-50%). The complex **114** was characterized by elemental analysis, mass or ^1H, $^{13}C\{^1H\}$ NMR spectroscopy, and X-ray diffraction. Its $^{13}C\{^1H\}$ NMR

spectrum displays the iron bound carbene signal at 159.1 ppm. The coordinated tetradentate bis-NHC ligand forms a square planar environment around a 14-electron iron(II) center. Compared to other reported tetrahedral 14-electron iron complexes, **114** is air and moisture stable.[47] However, Hermann, Kühn *et al.* who also investigated the syntheses of tetradentate bis-NHC iron complexes with *N*-donor groups (**115-120**), questioned the existence of **114**.[48] Indeed, it exhibits nearly the same bond distances (Fe–$C_{carbene}$ = 1.801(6) Å) and angles ($C_{carbene}$–Fe–$C_{carbene}$ = 84.9(4)°) as the isostructural cobalt complex reported in the same paper. This is quite striking given the different ionic radii between Fe(II) and Co(II). Moreover, Hermann, Kühn *et al.* were unable to synthetize **114** according to the published route starting from Fe powder. Finally, numerous attempts on re-crystallizing **114** to access **115** via removal of the *trans*-coordinated nitrile ligands failed. Overall, it was concluded that **114** was likely not stable as a 14 valence electron complex without solvent ligands, and Hermann, Kühn *et al.* suggested that the reported complex **114** was in fact **115**. The Fe–$C_{carbene}$ bond distances (1.801(6) Å) are considerably shorter than those of 16 (or 18) electron-iron(II) complexes.

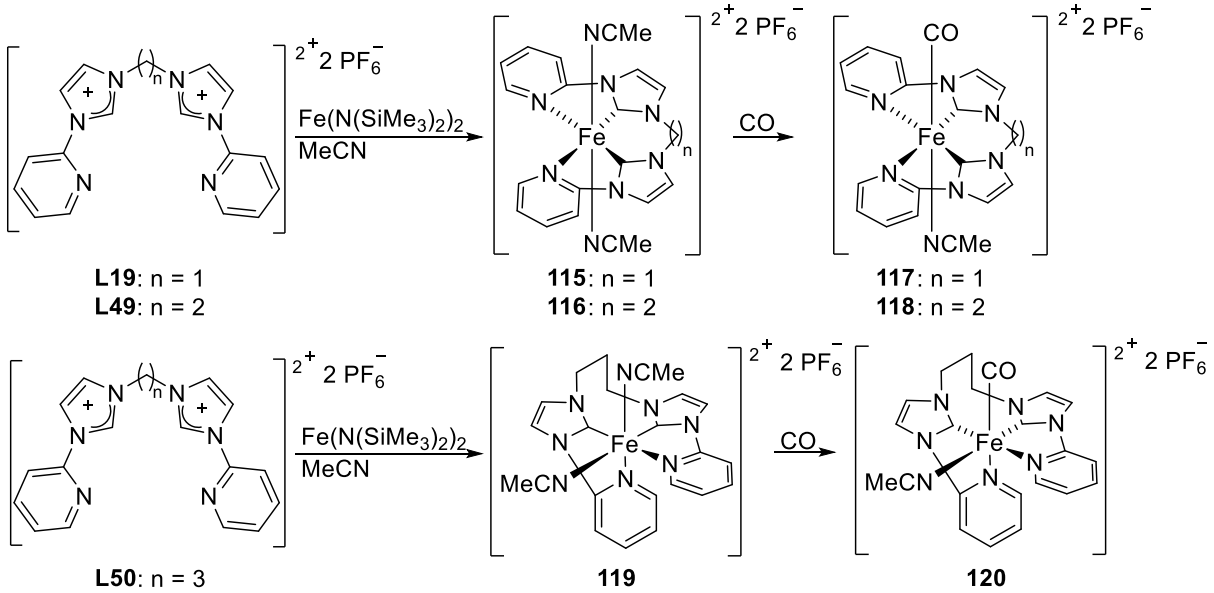

Scheme 34. Reactivity of complexes 115-116 and 119 toward CO.[48]

The reaction of $Fe(N(SiMe_3)_2)_2$ with different imidazolium hexafluorophosphate salts (**L19** and **L49-L50**) led to the iron(II) complexes **115-116** and **119** in excellent yields (90-93%). The ^{1}H NMR spectrum of **115** displays a clear singlet for the protons of the methylene bridge and that of complex **116** displays a broad doublet for the protons of the ethylene bridge, suggesting two inter-converting enantiomers on the NMR time scale. This assumption was further confirmed by variable-temperature ^{1}H NMR experiments, with a clear singlet at 35 °C and two doublets at low temperature (< -5°C). Compared to **115** and **116**, the complex

119 has a pyridine group with an *ortho*-proton upfield shifted ($\Delta\delta$ = -2.35 ppm compared to the other one) owing to the magnetic anisotropy of the ring current caused by the π system of another vicinal pyridine group. The $^{13}C\{^{1}H\}$ NMR carbene signals were found at 216.2 (**115**), 208.3 (**116**), 213.7 (**119**) and 206.6 ppm (**119**). So far, the signal at 216.2 ppm is the most downfield one observed for an iron(II)-NHC complex. The stretching vibrations bands of **115-116** and **119**, observed by IR at 2256, 2283, 2320 and 2287 cm^{-1}, confirm the coordination of acetonitrile. In the solid-state, the iron(II) centers of **115-116** are in a distorted octahedral environment. The tetradentate ligands form the equatorial plane, and two acetonitrile molecules are in the apical positions. In contrast, for **119**, the tetradentate ligand has a sawhorse type of coordination mode with two *cis*-oriented acetonitrile ligands. The $Fe–C_{carbene}$ bond distances determined for **115-116** (1.837(2) and 1.905(2) Å) are longer than those in **114**. In **119**, two different $Fe–C_{carbene}$ bond distances (1.897(2) and 1.913(2) Å) are found due to different *trans*-influence of the nitrile and pyridine donor ligands. The $Fe–N_{pyridine}$ bond distances in **115-116, 119** (2.096(2), 2.099(2), 1.993(2) and 2.037(2) Å) are similar to those found in **114**. However, they are remarkably long compared to those in the complexes **147**, **148** described by Danopoulos[22b] and Hahn.[49] Moreover, the Fe–N–C angle (166.9(2) °) for an acetonitrile ligand deviates substantially from 180° likely due to steric interaction with the bridge. The complexes **115-116** and **119** do not exhibit any reactivity under pressure of dihydrogen or propylene. In the presence of CO, they were quantitatively converted to the complexes **117-118, 120** by substitution of one acetonitrile ligand. These complexes were characterized by ^{1}H and $^{13}C\{^{1}H\}$ NMR spectroscopy. A solid-state structure was determined for **120** by X-ray diffraction, confirming the substitution of the acetonitrile ligand in *trans*-position to the pyridine ring. Contrary to **117-118,** the complex **120** has two possible substitution sites, leading to isomers with different ground-state free energy. The difference between both states being equal to 19.7 kJ/mol, a unique isomer is formed. The $Fe–C_{CO}$ bond distance (1.771(2) Å) is in agreement with the literature and the $Fe–N_{pyridine}$ bond distance (2.042(2) Å) is similar to that determined for **119**. Moreover, the Fe–C–O angle (172.4 °) deviates from 180° likely due to the close presence of the propylene bridge.

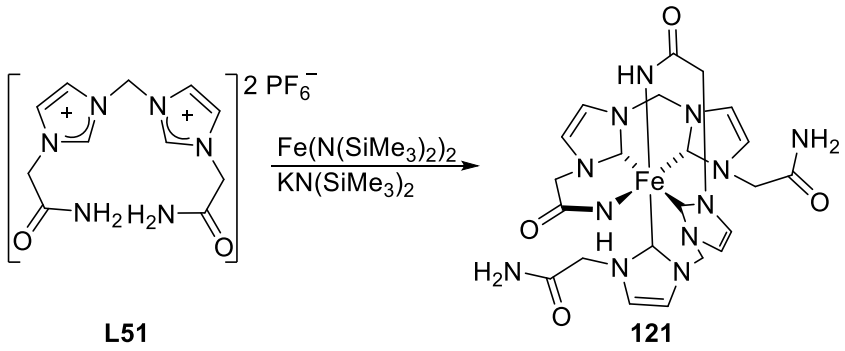

Scheme 35. Fe(II) complex bearing two (bis-NHC)amido ligands.[50]

Meyer *et al.* reported the first six-coordinate neutral NHC iron(II) complex **121** with two amido groups[50] (42%) made by reaction between the amido-imidazolium hexafluorophosphate salt (**L51**) with 2 equivalents of KHMDS and $Fe(N(SiMe_3)_2)_2$. Its formation was independent from the ratio salt/metal precursor used. It was characterized by infrared, mass spectroscopy, elemental analysis and X-ray diffraction analysis. The octahedral geometry around the iron(II) center is completed by two ligands. The four NHC sites form the equatorial plane. Two amido groups belonging to different ligands occupy the *cis*-positions, leaving also two dangling non-coordinated amido groups. The $Fe–C_{carbene}$ bond distances (between 1.917 and 1.929 Å) are in the range observed for six-coordinated ferrous NHC complexes,[6a,49] but slightly shorter than those of complex **131**. The ^{57}Fe Mössbauer spectrum of **121** shows a reversible one-electron redox process at - 0.96 V assigned to the couple $[Fe(II)/Fe(III)]^+$ hinting at a very strong σ-donation from the NHC and amido-ligands. The complex **121** was oxidized chemically by addition of an excess of $AgBF_4$ in acetonitrile. A zero-field ^{57}Fe Mössbauer spectrum of the crude mixture confirmed the presence of a low spin iron(III) center. Other redox processes were observed but not explained in detail.

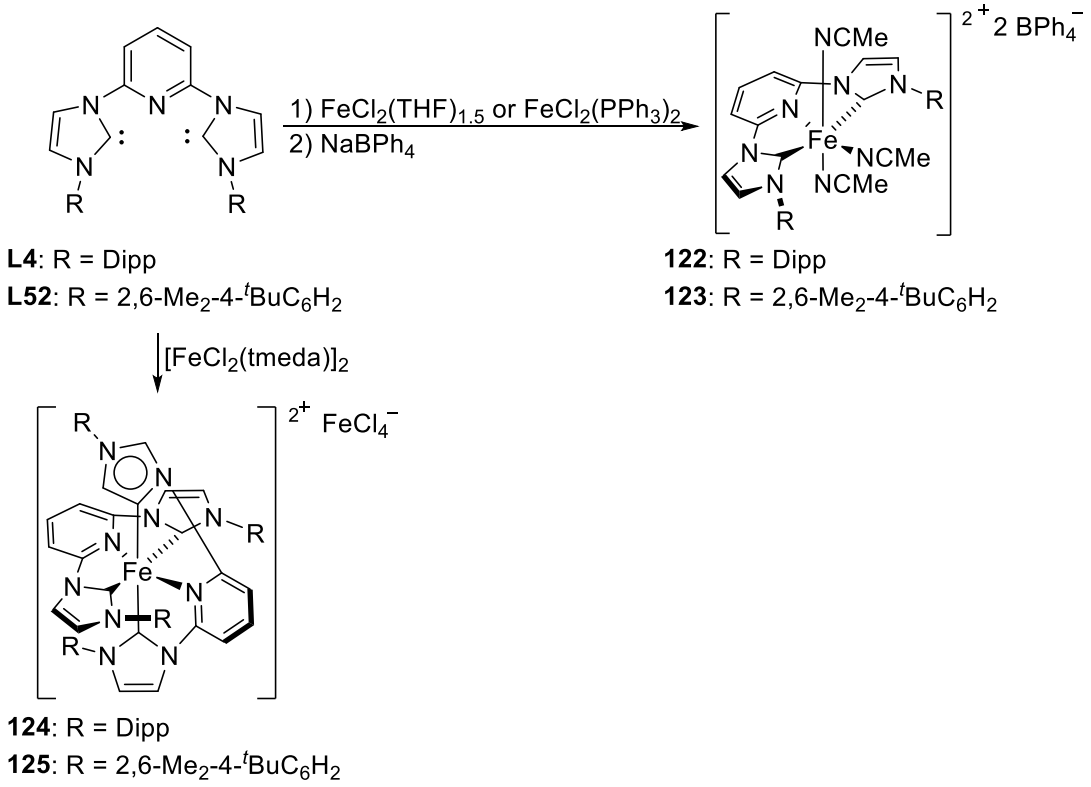

Scheme 33. Fe(II) complexes bearing (bis-NHC)-pyridine ligands.[22b]

Danopoulos *et al.* reacted the free carbenes **L4**, **L52** with $FeCl_2(THF)_{1.5}$ or $FeCl_2(PPh_3)_2$ to afford the air- and moisture-sensitive iron (II) complexes poorly soluble in organic solvents.[22b] Anion exchange reactions were possible between these complexes and $NaBPh_4$ forming the air-stable diamagnetic complexes **122**-**123** in moderate yield (35-40%). They were characterized by ^1H NMR spectroscopy and X-ray diffraction. The iron center of **122** exhibits a distorted octahedral geometry with the ligand **122** and an acetonitrile molecule occupying the equatorial positions. Two acetonitrile molecules occupy the apical positions. The Fe–$C_{carbene}$ bond distances (1.994(5) and 1.947(5) Å) are similar to those of octahedral iron complexes reported above.[2b,38,30,44] Changing the iron source for $[FeCl_2(tmeda)]_2$ led to the complexes **124** and **125** in moderate yields (40-45%). Due to their paramagnetic nature, these complexes were not characterized by NMR spectroscopy. However, the structure of **125** was solved by X-ray diffraction of single crystal, and features an iron(II) center with a distorted octahedral geometry, surrounded by two **L52** ligands. The first ligand adopts a symmetrical binding mode with two C-2 metalated NHC rings while the second ligand adopts a non-symmetrical binding mode with C-2 metalated- and C-5 metalated- NHC rings (abnormal). The Fe–$C_{carbene}$ bond distances (1.933(8) – 1.938(8) Å) are in agreement with the literature.[2b,38,30,44]

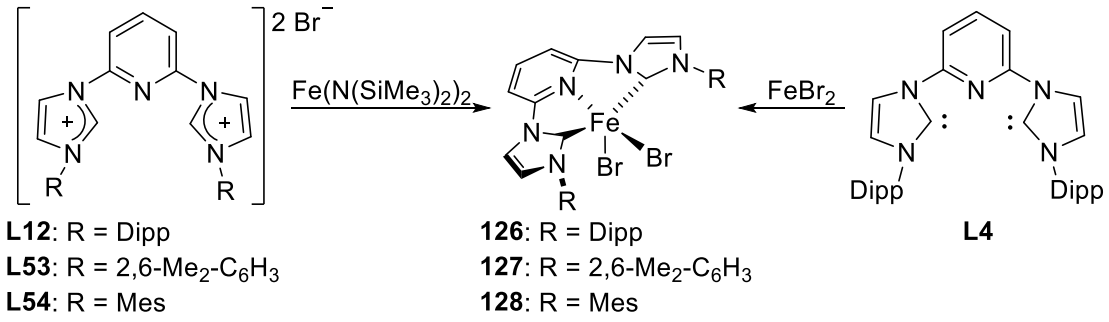

Scheme 34. Fe(II) complexes bearing a bis(NHC)pyridine ligand.[6a,22b]

Using $Fe(N(SiMe_3)_2)_2$ with the imidazolium bromide salt **L12** led to the iron(II) complex **126** in good yield (80%). It decomposed within 5 minutes in chlorinated solvents. Acetonitrile, displaced the bromide ligands giving rise to $[(C–N–C)Fe(MeCN)_3]^{2+}$ species. During the same year, Gibson *et al.* reported the reaction of the free carbene **L4** with $FeBr_2$ to form **126** in lower yield (62%).[6a] The complex was tested for catalytic activities.[51] Due to its paramagnetic nature, exploitable ^1H NMR spectra were impossible to obtain. X-ray diffraction studies unveiled a metal center exhibiting a distorted square pyramidal geometry with a bromide ligand in the apical position. The second bromide- and the bis(NHC)pyridine pincer- ligands are in the equatorial positions. The $Fe–C_{carbene}$ and $Fe–N_{pyridine}$ bond distances (2.145(11) – 2.193(10) and 2.211(8) – 2.241(8) Å) are longer than those measured with **122**. Using the same procedure as for **125**, Chirik *et al.* reported the iron(II) complexes **126**-**177** in moderate yields (34-64%).[52] They were characterized by elemental analysis.

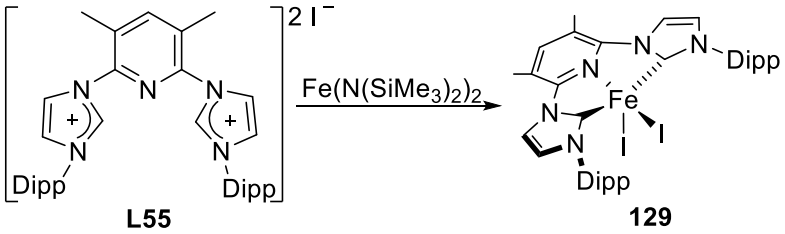

Scheme 38. Fe(II) (bis-NHC)-pyridine complex.[46]

Danopoulos *et al.* reported the paramagnetic iron(II) complex **129** in excellent yield (96%), still following the synthetic approach used for **125**.[46] It was characterized by elemental analysis and single crystal X-ray diffraction. The iron center exhibits a severely distorted square pyramidal geometry (τ = 0.34, quantifying the distortion of a square pyramidal structure) with an iodide ligand in the apical position. The second iodide- and the (bis-NHC)-pyridine pincer- ligands occupy the equatorial positions. The $Fe–C_{carbene}$ bond distances

(2.164(11) and 2.134(11) Å) are similar to those of complex **125** but the Fe–$N_{pyridine}$ bond distance (2.279(8) Å) is longer than for the complex **125**.

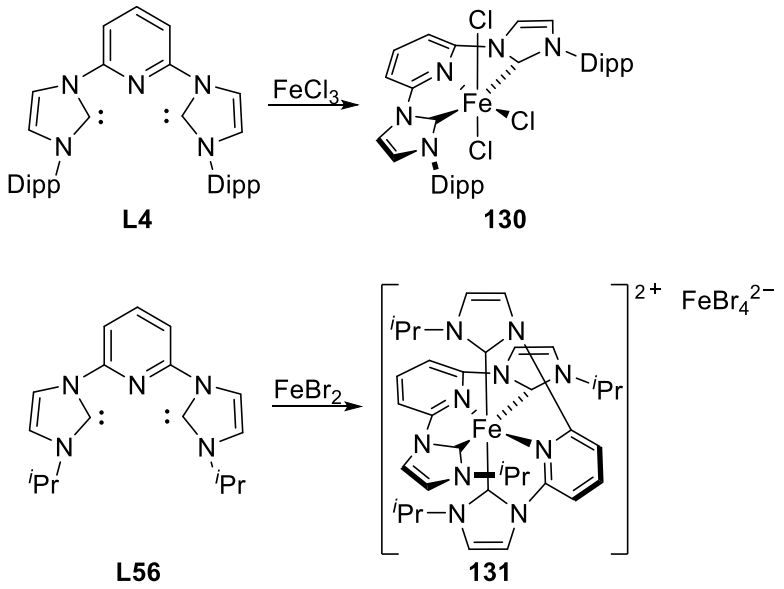

Scheme 35. Fe(II) and Fe(III) complexes bearing a one or two (bis-NHC)-pyridine.[6a]

The iron(III) complex **130** (97%) and iron(II) complex **131** (98%) were synthetized, by Gibson *et al.*,[6a] by coordination of the free carbenes **L4** and **L56** with $FeCl_3$ and $FeBr_2$. They were characterized by elemental analysis and mass spectroscopy, but only **131** was crystallized. The geometry around the iron(II) center is octahedral with the two (bis-NHC)-pyridine pincer **L56** coordinated. The Fe–$C_{carbene}$ bond distances (1.959(2) and 1.952(2) Å) of complex **131** are similar to those of the octahedral iron complexes **122**, **123**, **124** and **131**, described above. The Fe–$N_{pyridine}$ bond distance is equal to 1.9235(17) Å.

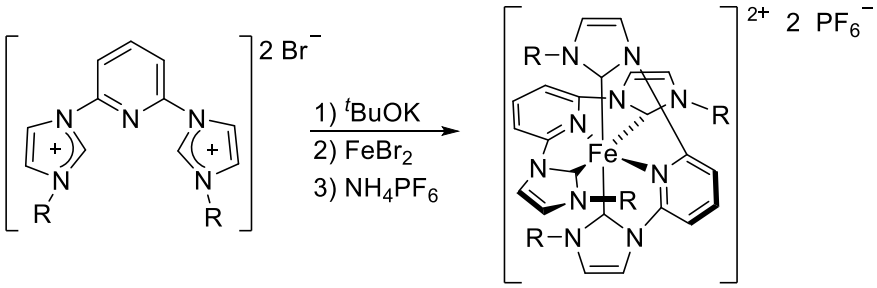

Scheme 40. Fe(II) complexes bearing two (bis-NHC)-pyridine ligand.[53]

The deprotonation, *in situ*, of the imidazolium bromide salts **L57-L58** followed by the addition of $FeBr_2$ and anion metathesis with NH_4PF_6, led to the complexes **132** (53%) and **133** (55%).[53] They were characterized by ^1H, $^{13}C\{^1H\}$ NMR spectroscopy and X-ray diffraction

studies. Both complexes adopt a distorted octahedral geometry. The two planes, each comprised of a ligand, are orthogonal. The Fe–$C_{carbene}$ bond distances (1.966(3), 1.965(3) and 1.970(3) Å) measured for **133** are longer than those of **132** (2.104(3), 2.083(3), 2.088(3) and 2.108(2) Å). This is due to the repulsion between the ^{t}Bu- and pyridine- groups from different ligands causing an expansion of the coordination sphere. The shorter Fe–$C_{carbene}$ bond enhances considerably the σ-donation of the NHC ligand. It is consistent with the $^{13}C\{^{1}H\}$ NMR carbene signal of **132** (201.2 ppm) being shifted downfield compared to that of **133** (190.7 ppm).

These strongly σ-donating ligands prolong the ^{3}MLCT state of the Fe(II) complexes compared to common $[FeN_6]^{2+}$. With an extension of almost two orders of magnitude, the ^{3}MLCT state lifetime (9 ps) for **132** is the longest ever reported. In this regard, **133** might replace the expensive Ru(II) complexes commonly used for photovoltaics or artificial photosynthesis applications.

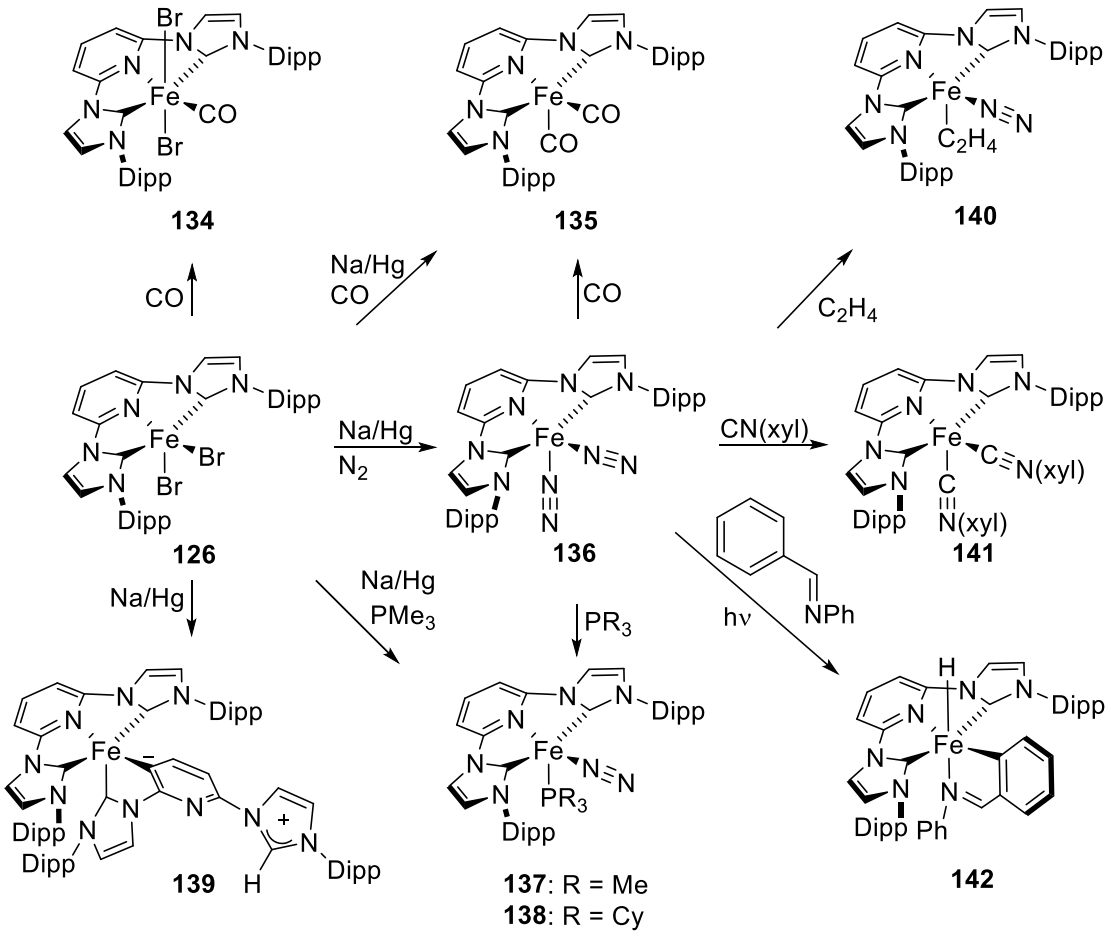

Scheme 41. Reactivity of the complex **126**.[46,54]

Danopoulos *et al.* investigated the reduction of **126** with an excess of Na/Hg under N_2 atmosphere, and isolated the iron(0) complex **136** with 36% yield.[46,54a] Its ^{1}H NMR spectrum was consistent with a C_{2V} symmetric structure. The iron bound carbene was visible at 203.9 ppm, by $^{13}C\{^1H\}$ spectroscopy. In the solid-state, the iron center owns a distorted pyramidal geometry with a dinitrogen ligand in the apical position. The second dinitrogen- and the pincer- ligand are in the equatorial positions. The N≡N (1.113(3) and 1.115(3) Å) and the Fe–N bond distances (1.847(2) and 1.820(2) Å) are similar to those of other mono-N_2 iron(0) complexes. The free N≡N bond distances (1.0968 Å) is slightly shorter than those of **136**, so only weak interactions between the metal center and the end-on N_2 ligands seem present. Zhang published a DFT study on the N_2 elimination mechanism occurring with **136**.[54b]

Chirik and Obligacion used **136** as a catalyst in hydroboration reactions.[54c] Having on hands the complexes **126** and **136**, ligand exchange reactions were easily set. Reduction of **126** or **136** with CO afforded the complex **135** (11%). Zhang *et al.* reported their theoretical investigation to the reaction mechanism involving **136**. The S_N1 pathway was evidenced for the substitution of both N_2 ligands by CO.[54d] The complex **136** exhibits a distorted square pyramidal geometry around the iron cation similarly to **136**. The ligand **L4** and a CO group are in the equatorial positions whereas the second CO group occupies the apical position. The Fe–$C_{carbene}$ bond distances are similar to those of complex **136**.

The reduction of **126** by Na/Hg in presence of phosphine under N_2 atmosphere yielded to the complexes **137** and **138**. These complexes were also obtained by substituting a dinitrogen ligand of **126** in presence of PR_3 (R = Me, Cy) (no yield value given). **137** and **138** were characterized by ^{1}H, ^{31}P NMR spectroscopy. The characterization of **137** was pushed further with $^{13}C\{^1H\}$ NMR and X-ray diffraction studies (the signal of the carbene is visible at 208.6 ppm). In the solid-state, the iron center exhibits a distorted square pyramidal geometry with a phosphine in the apical position. The N≡N bond distance is similar to that observed for **136**. Exposure of **126** under CO led to the carbonyl bromide complex **134** (80%).[46] It was characterized by elemental analysis and X-ray diffraction studies. The iron cation adopts a distorted octahedral geometry with the ligand **L4** and the carbonyl monoxide in the equatorial positions. The bromides ligands are in the apical positions. The Fe–$C_{carbene}$ bond distances (1.958(2) and 1.955(2) Å) are in agreement with the literature.[22b,48]

A last attempt on reducing **126** with Na/Hg under argon yielded to the zwitterionic iron(0) complex **139** (43%). The geometry around the iron(0) center forms a trigonal bi-

pyramid made with two NHC pincers ligands. The first one is chelating, as expected, in a tridentate (C-N-C) mode while the second one is chelating in a bidentate (C-C) mode through an NHC site and a *meta*-metalated pyridine. The non-coordinated carbene site is reprotonated. The Fe–$C_{carbene}$ bond distances are within the range of those previously observed for analogous species (**137**, **138** and **141**).[48] The Fe–$C_{carbene}$ bond distances (1.908(4) and 1.906(5) Å) arising from the tridentate ligand are shorter than that from the bidentate ligand (1.966(5) Å). The complex **139** being isolated from different reaction mixtures, a decomposition pathway might explain its formation.[37]

More substitutions of N_2 ligands were reported with the complex **126**.[45,47a,42,50a] Reaction of **126** with ethylene led to the complex **140** (77%) which was characterized by ^{1}H, $^{13}C\{^{1}H\}$ NMR spectroscopy (carbene signal at 210.8 ppm) and X-ray diffraction studies.[54a] The iron center adopts a distorted square pyramidal geometry with the ethylene group in the apical position. The nitrogen and the ligand **L4** are in the equatorial positions. The Fe–$C_{carbene}$ (1.927(6) and 1.933(6) Å) and N≡N (1.121(5) Å) bond distances are longer than those of **136**.

Moreover, reaction of **136** with 2 equivalents of 2,6-xylyl isocyanide resulted in the substitution of both N_2 groups forming the iron(0) complex **141** in moderate yield (56%). It was characterized by ^{1}H and $^{13}C\{^{1}H\}$ NMR spectroscopy (carbene signal at 208.6 ppm) and X-ray diffraction. There is a symmetry plane orthogonal to the pincer plane as for **135**. The iron center exhibits a square pyramidal geometry with an isocyanide group in the apical position. The ligand **L4** and the second isocyanide group are in the equatorial positions. The Fe–$C_{carbene}$ bond distances (1.918(3) Å) fall in the range of previously described Fe(0)–$C_{carbene}$ bond distances.[37,54a] The Fe–$C_{isocyanide}$ bond distances (1.798(3) and 1.796(3) Å) are in agreement with the literature.[55]

Finally, under UV-irradiation, **136** and N-benzylideneaniline reacted to afford the hydride iron(II) complex **142** in moderate yield (58%). Its ^{1}H NMR spectrum is difficult to assign due to a structure lacking symmetry. Its $^{13}C\{^{1}H\}$ NMR spectrum displays two signals for the iron bound carbenes at 203.9 and 214.5 ppm. X-ray diffraction studies reveal an iron center with a distorted octahedral environment. The hydride- and the imino- ligands occupy the axial positions. The phenyl ring- and **L4**- ligands occupy the equatorial positions. The hydride is placed in *cis*-position from the phenyl ring (concerted C–H oxidative addition reaction). The Fe–$C_{carbene}$ bond distances (1.890(3) and 1.907(3) Å) are among the shortest

observed for iron(II) NHC complexes.[48,50] The Fe–$N_{pyridine}$ bond distance (1.903(2) Å) is shorter than the Fe–N_{imine} bond distances by ≈ 0.1 Å.

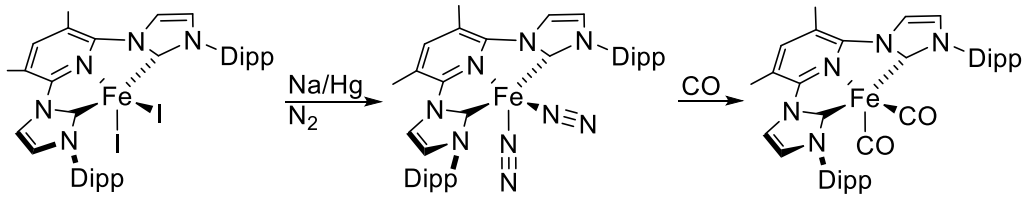

129 **143** **144**

Scheme 42. Reactivity of complexes **129**.[46]

The reactivity of **129**, an analogous of **126**, was also investigated.[46] By a similar procedure used with **136**, the reduction of **129** by an excess of Na/Hg under N_2 atmosphere led to the complex **143** in excellent yield (96%) (see scheme **33**). Its ^{1}H NMR spectrum indicates a plane of symmetry passing through the iron(0) center (a singlet for the pyridine methyl; two doublets and a septet for the ^{i}Pr groups). Its $^{13}C\{^1H\}$ NMR spectrum displays a carbene signal at 204.6 ppm. The crystalline structure exhibits an iron center with a slightly distorted square pyramidal geometry. The (bis-NHC)-pyridine pincer- and a nitrogen- ligands occupy the equatorial positions. The second nitrogen ligand occupies the apical position. The Fe–$C_{carbene}$ bond distances (1.9063(16) and 1.9057(16) Å) are in agreement with the literature for Fe(0)–$C_{carbene}$ bonds.[46,54a] The N≡N bond distances are equal to 0.966(2) and 1.124(2) Å; they suggest some π-back donation from the coordinated basic iron(0) center to N≡N. The N≡N_{apical} bond distance in **143** is shorter than that measured for **126**.

Substitution of both N_2 groups, by CO, afforded the formation of **144** in excellent yield (92%). Its ^{1}H NMR spectrum is consistent with the presence of two symmetry planes: the first one coinciding with the pincer plane, and the second one orthogonal passing through the iron(0) center, the pyridine nitrogen atom and the two carbonyl ligands. On the $^{13}C\{^1H\}$ NMR spectrum, the peak at 210.8 ppm accounts for the carbene. The crystal structure of **144** exhibits an iron center with a square pyramidal environment. A carbonyl ligand occupies the apical position. The second CO- and the (bis-NHC)-pyridine pincer- ligands occupy the equatorial positions. The Fe–$C_{carbene}$ bond distances (1.904(3) and 1.901(3) Å) are identical to those of complex **135**. The C≡O_{basal} and C≡O_{apical} bond distances (1.154(4) Å and 1.111(4) Å) are respectively longer and shorter than the free C≡O bond distance (1.128 Å). DFT calculations were performed with the complexes **135**, **136**, **143** and [Fe(P-N-P)$(CO)_2$] to have a better understanding of their bonding situations with N_2 and CO groups. The two methyl

groups on the pyridine ring have a marginal effect on the iron electronic environment and so on the N_2 bonding. Back-bonding from iron to pyridine decreases the back-bonding from iron to N_2 and CO ligands.

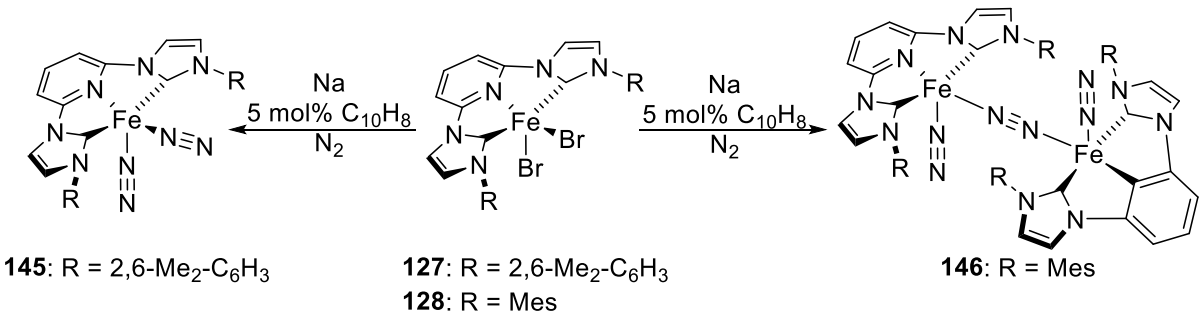

Scheme 43. Reduction of complexes **127-128**. [52]

Chirik *et al.* reported the formation of the complexes **145-146** by the reduction of **127-128** with sodium in presence of naphthalene under N_2 atmosphere with 34 and 66% yields. The complexes **145-146** were characterized by ^{1}H, $^{13}C\{^{1}H\}$ NMR spectroscopy. Their carbene signals are visible at 204.8 and 230.7 ppm. X-ray diffraction studies unveiled a mononuclear complex (**145**) and a N_2 bridged dinuclear complex (**146**). Yet, infrared data indicate that both monomers and dimers are present in the solid state, while in toluene at 23 °C, only the monomer is present. These complexes were used in catalytic hydrogenation.[52]

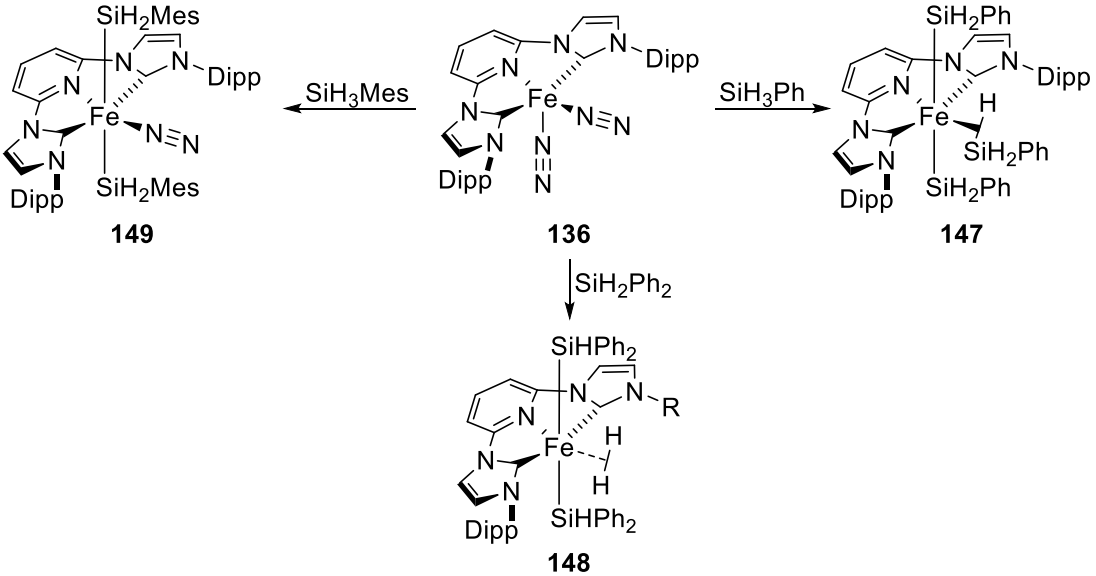

Scheme 44. Reactivity of complex **136**.[56]

Danopoulos *et al.* investigated the reactivity of the complexes **136** and **143** towards silanes.[56] The reaction of **136** with 5 equivalents of $SiPhH_3$, $SiPh_2H_2$ or SiH_3Mes led to the iron(II) complexes **147** (85%), **148** (64%) or **149** (64%), respectively. The different ^{1}H NMR

spectra reveal some silyl protons coordinated to the iron with signals at - 12.13 (**147**) and - 12.63 ppm (**148**). On the $^{13}C\{^{1}H\}$ NMR spectra, the carbene resonance signal of **147** appears at 211.9 ppm whereas the carbene resonance of **148** was not observed. For **147**, the relaxation time T_1 measured in the ^{1}H NMR and the ^{57}Fe Mössbauer data were consistent with a low spin Fe(II) species. The molecular structures of all complexes **147**-**149** exhibit an iron center with a distorted octahedral geometry. Two phenylsilyl, the (bis-NHC)-pyridine and a η^2-phenylsilane group ligands coordinates the iron(II) center. The complexes **148** and **149** contain a H_2 or a N_2 ligand *trans* to the pyridine moiety of the pincer and two silyl ligands coordinated to the iron(II) cation. The diphenylsilyl group being bulkier than the phenylsilyl group, promotes a π-stacking with diphenylsilyl- (A) and Dipp- (B) aromatic rings forming an A-B layer blocking the way to the iron(II) center. According to the authors, it might explain the presence of iron bound di-hydrogen in **148**. Moreover, it is unclear why N_2 was coordinated in **149** instead of H_2. The $Fe–C_{carbene}$ (range: 1.9160(19)-1.9650(5) Å), Fe–H (1.29(5) and 1.616(15) Å) and $Fe–N_{dinitrogen}$ (1.827(7) Å) bond distances of **147**-**149** are in agreements with the literature.[46,54a] The Si–H bond distance, which is *trans* to the pyridine ring in **147** (1.92(5) Å) is longer than the range of the Si–H bond distances in the complex (1.38(4)–1.49(4) Å) . However, lengthening of the Si–H bond upon η^2-coordination to a metal center is common.[57]

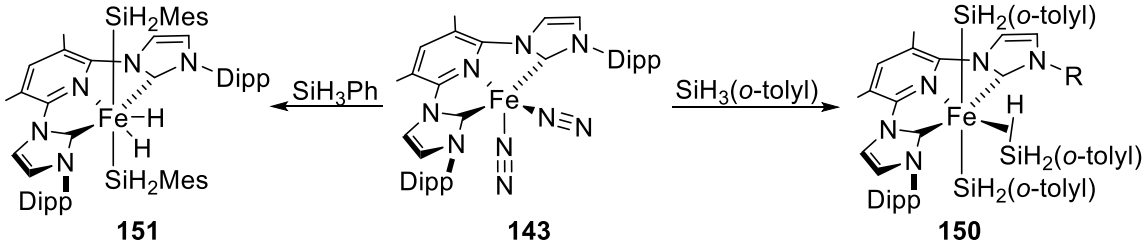

Scheme 45. Reactivity of **143** towards silanes. [56]

Similarly to **136**, **143** reacted with 5 equiv. of SiH_3(*o*-tolyl) to give the complex **150** with 85% yield. Its ^{1}H NMR analysis indicated the presence of a hydride (- 13.62 ppm). Its molecular structure presents a distorted octahedral iron center with metric data similar to **147**. There are two mutually *trans* phenylsilyl groups. The (bis-NHC)-pyridine- and a η^2-phenylsilane- ligands occupy the equatorial positions completing the coordination sphere. The reaction of **143** with 14 equiv. of SiH_3Ph led to the complex **151** in excellent yield (92%). Its ^{1}H NMR spectrum reveals an iron hydride complex with a specific signal at -12.92 ppm. Its $^{13}C\{^{1}H\}$ NMR features a carbene signal at 218.8 ppm. By the same analytical techniques used for **147** and **150**, **151** was proven to be the first Fe(IV)-NHC complex. Its exhibits a severely

distorted pentagonal bipyramidal geometry around the iron(IV) center. The two NHC moieties occupy the apical positions. Two hydride-, the pyridine- and two silyl- ligands are in the equatorial positions and complete the coordination sphere. The Fe–H bond distances (1.53(4) and 1.57(3) Å) are consistent with values reported for other hydride iron complexes.[31b,34a] The $Fe–C_{carbene}$ bond distances (1.883(3) and 1.887(7) Å) are shorter than those of complexes **147**-**150**.

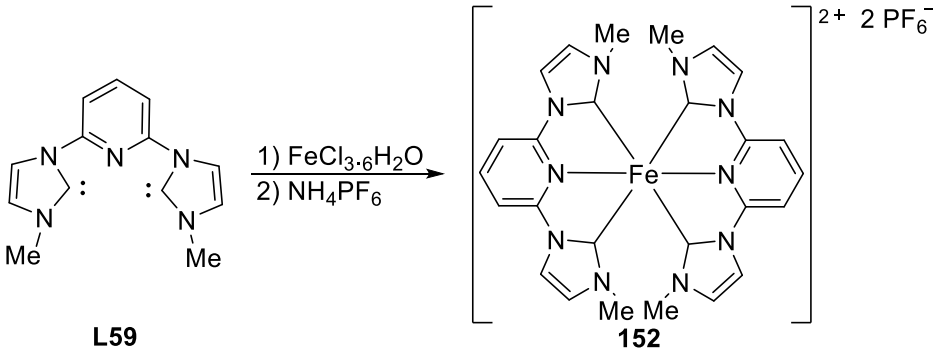

Scheme 46. Fe(II) complex bearing two ligand (bis-NHC)-pyridine.[58]

The reaction between the ligand **L59** and $FeCl_3•6H_2O$ followed by the addition of NH_4PF_6 led to the complex **152** (71.3%).[58] It was described in a patent as suitable electrolyte for redox flow battery. However, no spectroscopic, analytical, or crystallographic data were given.

2.7 Cobalt

After having demonstrated the efficiency of the aminolysis methodology for the synthesis of bis(carbene)pyridine pincer iron complexes, **153** was made following this way.[59] The imidazolium bromide salt **L12** was reacted with $Co(N(SiMe_3)_2)_2$ to afford the paramagnetic cobalt(II) complex **153** in excellent yield (90%). It was only characterized by elemental analysis.

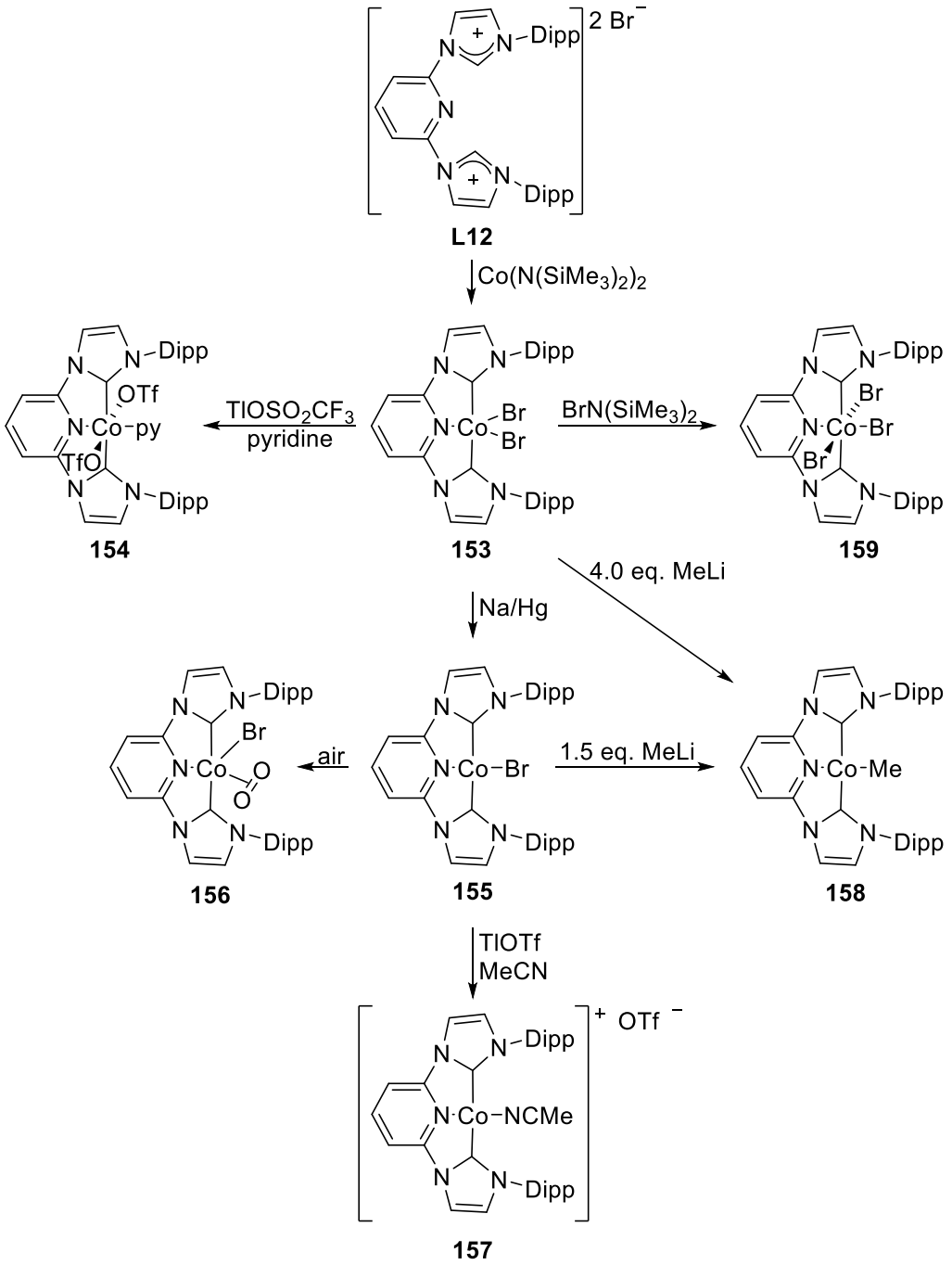

Scheme 47. Reactivity of complex **153**.[59]

The reaction of **153** with TlOTf in pyridine led to the air-stable paramagnetic complex **154** with 80% yields. The molecular structure of **154** exhibits a cobalt center with a distorted octahedral environment. The trifluoromethanesulfonate groups occupy the apical positions. The ligand **L4** and the pyridine occupy the equatorial positions. The Co–$C_{carbene}$ bond distances are practically identical (1.941 Å) and the Co–N_{pincer} bond distance (1.890(5) Å) is shorter than the Co–$N_{pyridine}$ bond distance (1.936(5) Å). The Co–$O_{triflate}$ bond distances (2.358(4) and 2.396(4) Å) are in the range of those of reported Co(II) triflate complexes.[60]

The reduction of complex **153** by Na/Hg in toluene led to the cobalt(I) complex **155** with a very good yield (86%). The complex is unstable in chlorinated and protic solvents. Its ^{1}H NMR spectrum reveals a pyridine ring with *para*-hydrogen unusually shifted downfield (9.5 ppm). Its carbene signal was not observed by $^{13}C\{^{1}H\}$ NMR spectroscopy. X-ray diffraction studies unveiled a Co(I) center with a square planar geometry. The $Co–C_{carbene}$ (1.917(5) and 1.909(5) Å) and $Co–N_{pincer}$ (1.839(4) Å) bond distances are shorter than those of the Co(II) complex **154**. Alkylation attempts **153** with RLi or R_2Mg (R = CH_2SiMe_3, CH_2CMe_3 or $CH_2(Ph)Me_2$) led only to the cobalt(I) complex **155**. In contact with air, **155** reacted immediately to form **156** whereas with $TlOSO_2CF_3$ it forms **157**. No characterization was reported for these two complexes.

The methylation of **155** with 1 equiv. of MeLi led to the complex **158** with better yield (68%) than the methylation of **153** with an excess of MeLi. By NMR spectroscopy, the peak of the methyl group is observed at -0.8 ppm, while the carbene signal is not visible. As for **155**, the geometry around the Co(I) center of **158** is square planar. The $Co–C_{carbene}$ (1.914(4) and 1.898(4) Å) and $Co–N_{pincer}$ (1.865(3) Å) bond distances are similar to those of complex **155** and so shorter than those of the Co(II) complex **154**.

Preliminary reactivity data on **158** with H_2, MeLi, CH_3OTf or Brookhardt's acid gave products that are still currently under investigation. However, **158** was inert towards ethylene, CO or aliphatic aldehydes.

We have seen that **153** could be reduced, but it could also be also oxidized by $BrN(SiMe_3)_2$ in excellent yield (94%) leading to the air-stable diamagnetic complex **159**. This complex was characterized by ^{1}H NMR spectroscopy but, due to its poor solubility, no $^{13}C\{^{1}H\}$ NMR data were obtained. The Co(III) center of **159** exhibits an octahedral geometry with two bromide ligands in the apical positions. The pincer **L4-** and the third bromide-ligands occupy the equatorial positions. The $Co–C_{carbene}$ (1.962(7) Å) bond distances are longer than those of complex **154** and so than those of complex **154**. The $Co–N_{pincer}$ bond distance (1.894(5) Å) is similar to that of complex **154** and longer than that of complexes **155** and **158**.

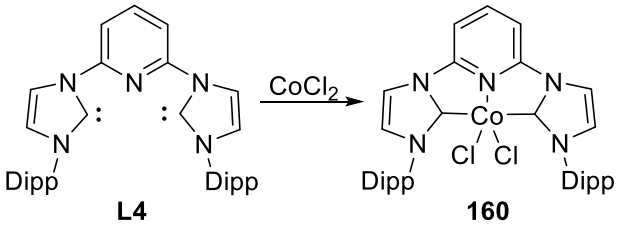

Scheme 48. A Co complex bearing bis-NHC ligands.[6a,6c,11,61]

The same year, McGuinness *et al.* published the synthesis of and catalytic activity of the complex **160**.[6a] Reaction of the free carbene **L4** with $CoCl_2$ led to the cobalt(II) complex **160** in moderate yield (62%). **160** was characterized by elemental analysis and mass spectroscopy.

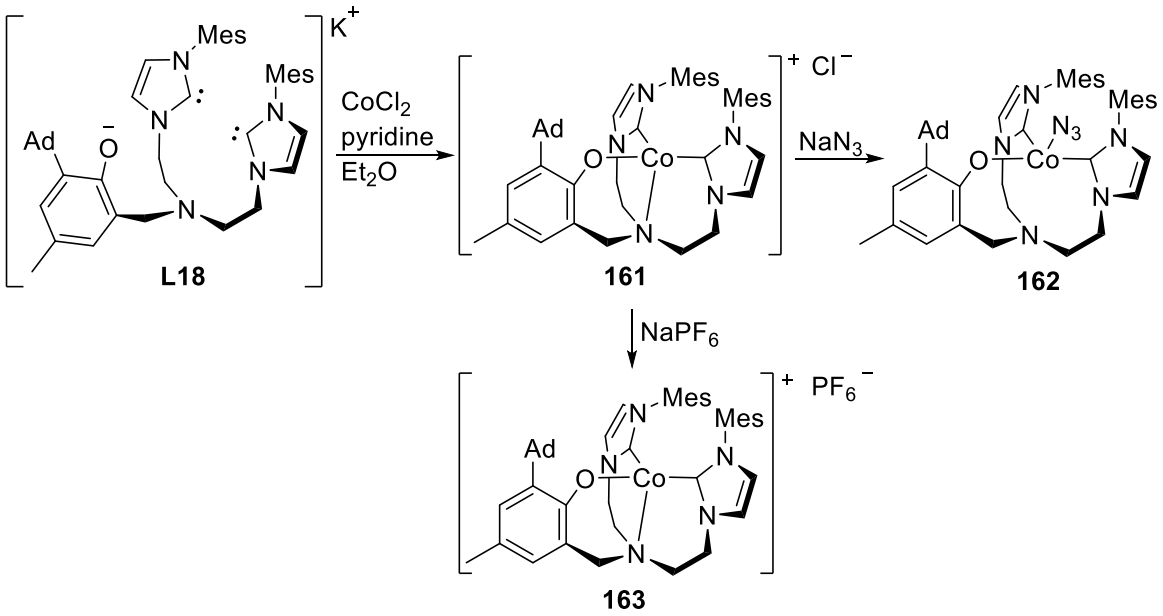

Scheme 36. (bis-NHC)phenolate Co(II) complex.[27a]

Similarly to the synthesis of **45** and **46**, **L18** reacted with $CoCl_2$ and gave the complex **161** in good yield (76% if **161** is considered pure or 67% if 1.0 equiv. of KCl per ligand molecule is accounted). The difficulty to remove the salt KCl formed during the reaction suggests an interaction between K^+ and the phenolate site. Anions metathesis with **161** and $NaPF_6$ (or NaN_3) led to the complexes **162** (or **163**) with 91% or (74%) yields. These complexes are identifiable by infrared spectroscopy with strong bands at 843 cm^{-1} (or 2081, 2044 and 1999 cm^{-1}) in KBr. The ^1H NMR spectra of complexes **161**, **162** and **163** in MeCN-d_3 and $CDCl_3$ exhibit the same signals. However in THF-d_8, the spectrum of **163** remains the same whereas, that of **162** differs completely. These observations suggest that in complex **161**, as for **163**, contrary to the azide moiety, the chloride does not bind the cobalt cation but

remains solvated. In the solid state, the complexes **161** and **162** have similar structures. The geometry around the cobalt(II) centers is distorted triangular pyramidal with the NHC moieties and the phenolate in the equatorial positions. The Co–$C_{carbene}$ bond distances are equal to 2.021(2), 2.023(3) Å for **161** and 2.009(3) and 2.023(3) Å for **162**. In **161**, the cobalt center is underneath the plane passing through the carbene sites and the oxygen atoms by 0.621 Å. Notably, from the complex **45** (Mn) to **112** (Fe) to **161** (Co), the distance of the metal center above the basal plane decreases from 0.632(2) Å to 0.113(1) Å to finish below the plane by -0.621 Å. Consequently, the distances between the N_{anchor} and the metal center (Mn to Fe to Co) decrease from 2.695(2) Å (no interaction) to 2.461(2) Å (weak interaction) to 2.141(2) Å (covalent interaction). The magnetic moments of **162** (4.28 μ_B) is larger than the spin only value for an S = 3/2 system, confirming that there is a spin-orbit coupling contribution.

The molecular structure of **162** exhibits a distorted trigonal pyramidal geometry around the cobalt(II) center. The NHC moieties and the phenolate are in the equatorial positions and the azide is in the apical position. The azide is coordinated in a bent mode. The Co–$C_{carbene}$ bond distances (2.081(2) and 2.060(2) Å) are slightly longer than those in **161** and **162**. Variable temperature SQUID experiment indicates that the magnetic moment (4.42 μ_B) of **163** is similar to that of **162** or **161**. Nevertheless, the magnetic moment remains high for a large temperature range indicating a smaller zero-field splitting.

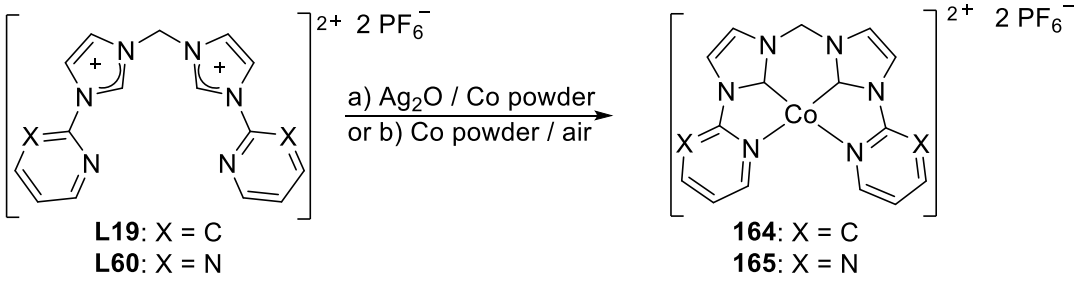

Scheme 37. Co(II) complexes bearing a tetradentate bis-NHC ligand.[29,38]

The cobalt(II) complexes **164** and **165** were made in good yields (66.8 and 74.6%, respectively) by reaction of an excess cobalt powder with the corresponding silver complexes, generated *in situ*, from the imidazolium hexafluorophosphate salts (**L19** and **L60**) and silver oxide.[29,38] A second pathway consisted in reacting **L19** or **L60** with cobalt powder to give the desired complexes (**164** and **165**) in lower yields (30-50%). Finally, mixing **L19** and **L60**, silver oxide and cobalt powder together also led to the complexes **164** and **165** (no yield value given). The complexes **164** and **165** were characterized by ^{1}H and $^{13}C\{^{1}H\}$ NMR

spectroscopy. Their $^{13}C\{^1H\}$ NMR spectra reveal a cobalt bound carbene signal at 159.1 and 161.4 ppm. The crystalline structure of complex **164** and **165** are very similar. Both complexes **164**-**165** have a cobalt center coordinated to the tetradentate bis-NHC ligand with a square planar geometry. These complexes were the first example of 15 valence electron cobalt(II) complexes with NHC ligands. The $Co–C_{carbene}$ (1.803(3) Å) and Co–N (1.985(2) Å) bond distances of **164** are very close to the $Co–C_{carbene}$ (1.800(3) Å) and Co–N (1.979(2) Å) bond distances of **165**. Their $Co–C_{carbene}$ bond distances are shorter than those of other cobalt complexes reported above.[59]

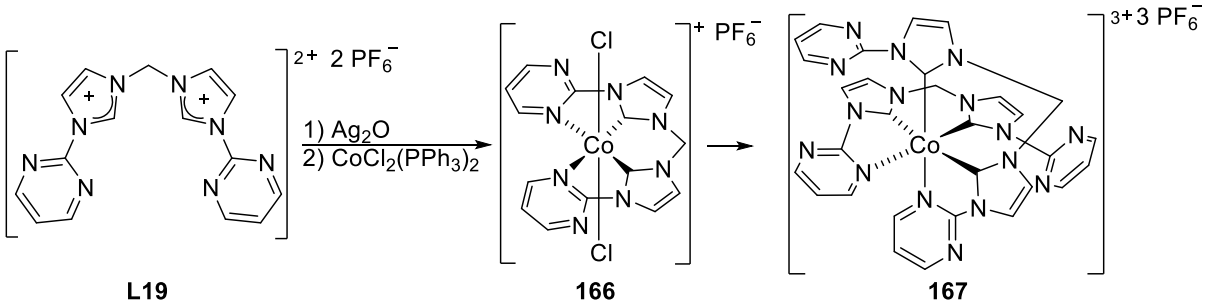

Scheme 38. Co(III) complexes bearing a tetradentate bis-NHC ligand.[61]

The addition of $Co(PPh_3)_2Cl_2$ to a silver-NHC complex, generated from **L19** with Ag_2O without isolation, led to the cobalt(III) complexes **166** (minor product) and **167** (45%). No cobalt(II) complexes were detected due to their spontaneous oxidation under air.[61] Complex **166** was not stable in solution, transforming into **167**. In the ^1H NMR spectrum of **167**, the doublets at 6.70 and 6.40 ppm correspond to the methylene linker. The protons are magnetically non-equivalent due a restricted rotation of the linker upon complexation. On the $^{13}C\{^1H\}$ NMR, the carbene signal is not observed. The solid-state structure of **166**, determined by X-ray diffraction studies, exhibits a Co center with an octahedral geometry. The tetradentate- and two chloride- ligands occupy, respectively, the equatorial plane and the axial positions. The $Co–C_{carbene}$ bond distances (1.823(5) and 1.828(4) Å) are shorter than those of **158**. The Co–Cl and $Co–N_{pyrimidine}$ bond distances are roughly equal to 2.22 and 2.06 Å. A preliminary structure of **167** was solved but not refined, due too poor quality crystals. It exhibits two ligands coordinated to the cobalt center by two NHC- and a pyrimidine- sites. The other nitrogen group from pyrimidine is free. Two carbenes are mutually in *trans*-positions whereas the others are in *trans* to two pyrimidines.

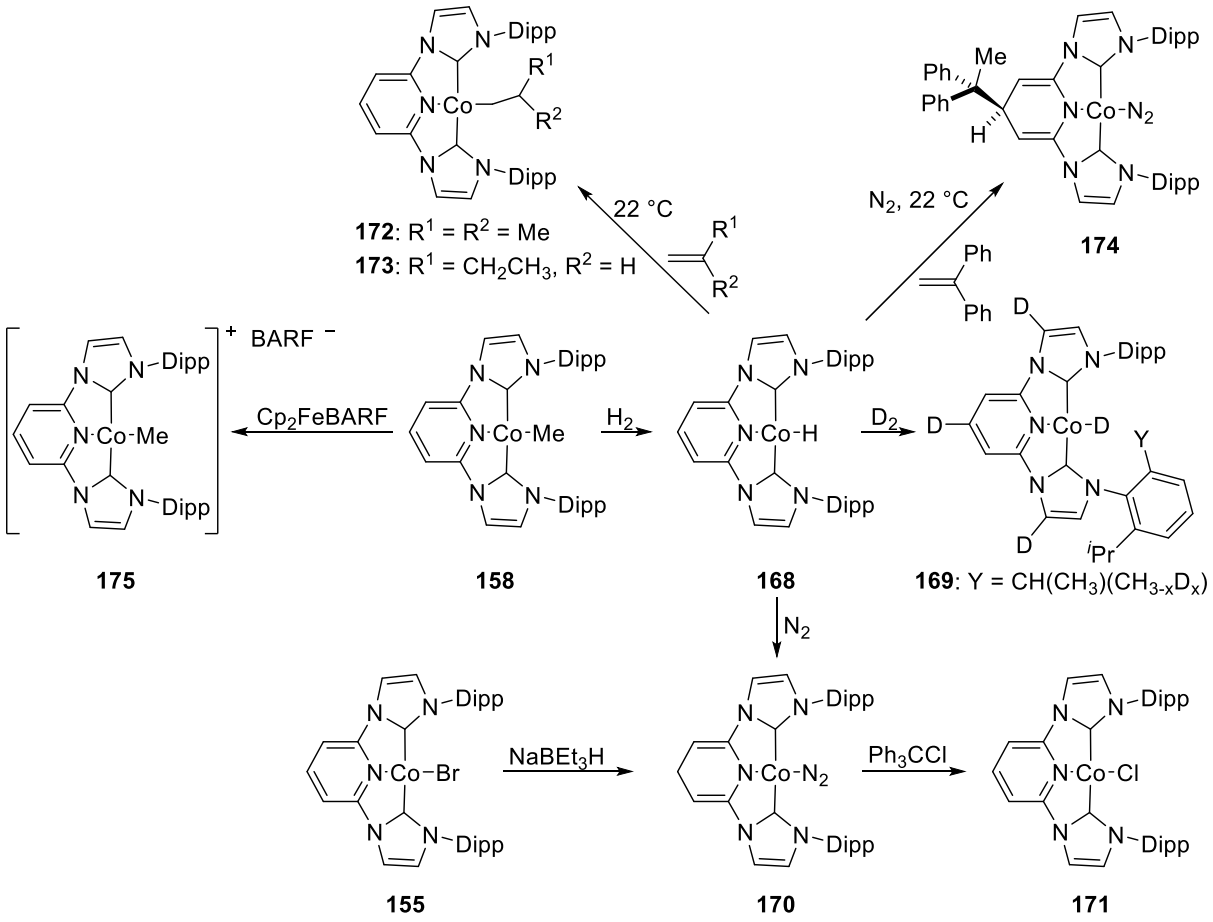

Scheme 39. (bis-NHC)-pyridine pincer cobalt hydride and alkyl complexes.[62]

Chirik *et al.* reported some hydride and alkyl cobalt complexes.[62] Exposure of the complex **158** to a H_2 atmosphere led to the cobalt(I) complex **168** (no yield value given) and CH_4. In the ^{1}H NMR spectrum, the signal of the hydride is very broad and dependent of the amount of H_2 present. In degassed samples, the signal appears at -27.0 ppm and under 1 atmosphere of H_2, it shifts to -18 ppm. Moreover, signals of the 4-pyridine- and imidazole-moieties are broad due to a rapid exchange with free H_2. On the ^{13}H NMR spectrum, the signal of the carbene is visible at 187.6 ppm. The rapid exchange between **169** and free H_2 was confirmed by the addition of D_2 to a solution of **158**, thus yielding to **169** with formation of CH_3D and CH_4 in a 87:13 ratio. After several hours, the deuteration of the 4-pyridine-, imidazolylidene- and isopropyl methyl- positions was complete and the hydride signal in ^{1}H the NMR disappeared.

The exposure of **168** to an N_2 atmosphere resulted in the formation of the cobalt(I) complex **170** (74%). The infrared spectrum reveals a strong band at 2048 cm^{-1} corresponding to the cobalt bound N_2 group. Remarkably, in the ^{1}H NMR spectrum, two triplets at 3.57 and

4.31 ppm, suggest the presence of allylic and vinylic protons possibly due to modification of the pyridine ring. The assignment of the allylic resonances was confirmed by isotopic labeling. Moreover, an excess of H_2 or D_2 suppressed the migration of the cobalt hydride to the 4-pyridine position of the pyridine. In the $^{13}C\{^1H\}$ NMR spectrum, the signal of the carbene is visible at 194.4 ppm. At the same time, a second pathway (treatment of **155** by $NaBEt_3H$) was found to produce **170** in lower yield (32%).

Addition of Ph_3CCl to **170** yielded the cobalt(I) complex **171** (74%). It was characterized by X-ray diffraction studies, and ^1H and $^{13}C\{^1H\}$ NMR spectroscopy. The signal of the carbene is visible at 178.2 ppm. The molecular structure of **171** exhibits a cobalt(I) center with a square planar environment. The metric data are similar to those of complex **155** (e. g. $Co–C_{carbene}$ = 1.918(6) and 1.909(6) Å).[59] This reaction proved the ability of the ligand to participate in cooperative metal-ligand reactivity to form Co–Cl bonds, or cleave C–H bonds.

The reactivity of the hydride complex **168** towards alkenes was investigated. The complex **168** was totally converted in the presence of a slight excess of 1-butene or isobutene to the complexes **172** or **173**.[62] Both complexes decomposed in solution over 48 h under an N_2 atmosphere and even quicker under vacuum. The complexes **172** and **173** were characterized by ^1H and $^{13}C\{^1H\}$ NMR spectroscopy. The signal of the carbene is visible at 179.7 (**172**) and 179.9 (**173**) ppm. In these reactions, there is no sign of modification of the pyridine ring as observed with **170**.

Nevertheless, the reaction of **168** with a more hindered olefin afforded the complex **174** (62%). The infrared spectrum confirms that the N_2 group is coordinated to the cobalt (strong band at 2050 cm^{-1}). In the ^1H NMR spectrum, signals between 4 and 5 ppm indicate a modification of the pyridine ring. In the $^{13}C\{^1H\}$ NMR spectrum, the carbene signal is visible at 178.2 ppm. Infrared and NMR spectroscopic data support the formation of complex **174**, arising from the migration of the cobalt bound alkyl to the 4-position of the pyridine ring. X ray diffraction studies confirmed this hypothesis. The geometry of the cobalt(0) center is square planar. The (bis-NHC)-pyridine pincer- and the dinitrogen- ligands are coordinated to the cobalt(I) center. The Dipp groups are almost orthogonal to the plane of the ligands-cobalt. Two pathways are possible for the formation of **174**: i) a 2,1 insertion of the alkene into the Co–H bond followed by the migration of the alkyl group or ii) a H-atom transfer. The

reactivity of the (bis-NHC)-pyridine ligand suggests its likely radical character in the structures of **132**, **133**, **140** and **143-145.**

Oxidation of **158** with $Cp_2FeBARF$ gave the cobalt(II) complex **175** in low yield (15%). It was characterized by ^1H NMR spectroscopy. The crystal structure data indicates a square planar geometry around the cobalt center and no contact between the cation / anion pairs. The ligand **L4** and the methyl ligand are coordinated to the cobalt. The $Co–C_{carbene}$ bond distances (1.913(3) and 1.903(3) Å) are similar to those of the complexes **155**, **164** and **165** reported before.[29,38,59]

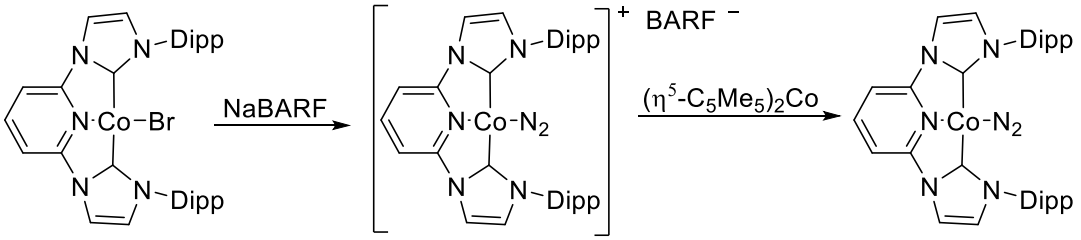

Scheme 40. Reactivity of complex **155**.[62]

Furthermore, addition of NaBARF to **155** under N_2 atmosphere led to **176** in excellent yield (92%). The strong band at 2141 cm^{-1} in infrared spectrum confirms the coordination of the N_2 group. The ^1H NMR and $^{13}C\{^1H\}$ NMR spectra are consistent with a C_{2v} symmetric molecule. The signal of the carbene is visible at 188.3 ppm. The metal center exhibits a square planar geometry with no contact between the cation / anion pair. Attempts to prepare complex **177** by reduction of **155** with a sodium amalgam failed. In place, it gave a mixture of products including **176**. Moreover, performing the reduction of **155** with sodium metal in the presence of naphthalene (5 mol %) led also a mixture of products including **170** and [L4]Na. However, the reaction of **176** with $(\eta^5\text{-}C_5Me_5)_2Co$ led quantitatively to **177**. The $Co–C_{carbene}$ bond distances of **177** (1.904(3) and 1.907(6) Å) are in the same range of those of **176** and **177**. The spectroscopic, structural and computational studies conclude that the bis(carbene)pyridine ligand is redox active in one electron reduction processes in cobalt chemistry. Moreover, the ligand-centered radical in the bis(carbene)pyridine is basically pyridine localized. This ligand is an excellent support for metal base catalysis.

2.8 Nickel

Green *et al.* reported two cationic bis-NHC nickel(II) complexes. The free carbenes **L61** and **L62** reacted with $NiCl_2(PMe_3)_2$ to afford the mononuclear nickel(II) complexes **178** and **179** with 95 and 85% yields.[63]

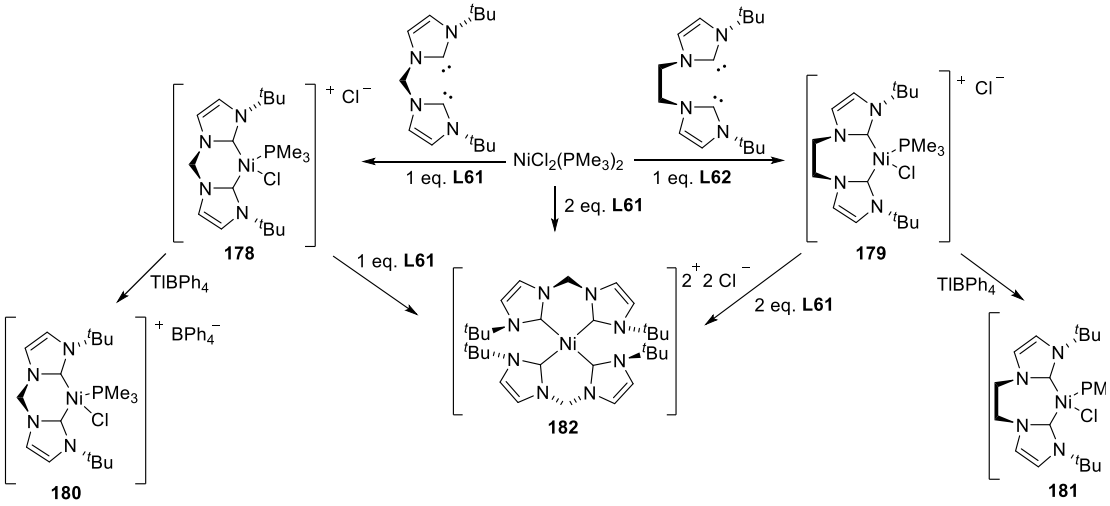

Scheme 41. Substitution of the bis-NHC ligand in Ni(II) complexes.[63]

Both complexes are stable under air in polar aprotic solvents, or in the solid state. In protic solvents, they degrade within a few minutes. Their ^{1}H NMR spectra indicate that **L61** and **L62** are chelating (the protons of the methylene bridges are diastereotopic). In their $^{13}C\{^{1}H\}$ NMR spectra, the carbene resonances are non-equivalent and observed at 161.6, 165.8 ppm and 155.0, 162.6 ppm for **178** and **179**. These values are characteristic of cationic nickel NHC complexes. They are shift upfield by 10 to 30 ppm compared to neutral nickel complexes.[64]

Anions exchange between **178-179** and $TlBPh_4$ led to the mononuclear nickel(II) complex **180-181** with 51% (or 78%) yields. Their ^{1}H and $^{13}C\{^{1}H\}$ spectra are similar to those of **178** and **179**, except for the additional signals of the BPh_4 anion. The complexes **178** and **181** are chiral and crystallized as racemic mixtures. The geometry around the nickel(II) centers is distorted square planar. The phosphorus atoms are displaced perpendicularly (by 0.903(2) Å for **178** and 0.477(1) Å for **181**) from the plane passing through the nickel(II) center, the bis(NHC)-, and the chloride-ligands due to the interactions between the ^{t}Bu and the PMe_3 groups. The six- and seven-membered rings containing the chelated nickel, in complexes **178** and **181,** adopt a boatlike conformation. The Ni–$C_{carbene}$ bond distances in

trans position to the PMe_3 groups (1.942(4) and 1.915(8) Å) are longer than those in *trans* position to the chloride due to the electronic *trans* influence of the phosphine. The difference of bite angle between **178** (84.92(18)°) and **181** (88.4(4)°) is smaller than expected compared to other bis(phosphine) nickel complexes (an increase of 8-10° per CH_2 unit).[65] The ethylene bridged bis-NHC ligand is under a higher degree of steric strain and is more demanding than the methylene bridge bis-NHC ligand. The fact that **182** was obtained but not the analogous ethylene bridge complex illustrates this statement.

The reaction of $NiCl_2(PMe_3)_2$ with 2 equiv. of free carbene **L61** led to the mononuclear nickel(II) complex **182** in excellent yield (92%) as well as the reaction of **178** or (**179**) with 1 (or 2) equiv. of **L61**. This is the first example of transition metal NHC substitution chemistry but its mechanism is unclear. The ^1H NMR spectroscopy of **182** is consistent with a (bis-NHC)$_2$Ni(II) complex with two ligands **L61** in a *trans* double-boat conformation (a single resonance for the four ^{t}Bu groups and two resonances for the diastereotopic protons of each methylene bridge). The $^{13}C\{^1H\}$ NMR spectrum exhibits a signal at 170.3 ppm attributable to four equivalent carbenes.

The reaction of 2 equiv. of **L62** with $NiCl_2(PMe_3)_2$ did not lead to the tetra-NHC nickel(II) complex analogue of **182** but rather to a mixture of **179** and **L62** with a ratio of 1:1 Furthermore, the reaction between 1**78** and **L62** did not occur. Finally, reduction of **182**using zinc, Na/Hg or potassium failed.

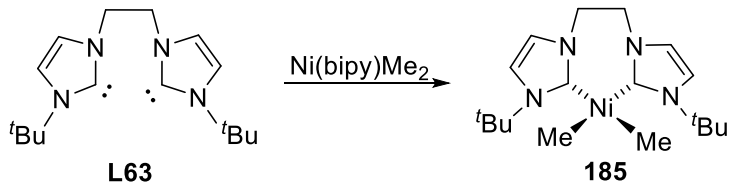

Scheme 42. Methyl Ni(II) complex.[22c]

The reaction of the free carbene **L63** with NiX_2 (X = Cl, Br, I), $NiBr_2$(dme) or $NiBr_2(PPh_3)_2$ led to intractable mixtures. A different pathway using Ni(bipy)Me_2 gave the mononuclear nickel(II) complex **185** in good yield (73%).[22c] This complex is sensitive towards air. It is soluble in toluene and common polar solvents, but decomposes within minutes in CH_2Cl_2. Its ^1H NMR spectrum exhibits an AA'XX' pattern at 3.29 and 5.87 ppm for the ethylene bridge. The $^{13}C\{^1H\}$ NMR spectrum displays a carbene signal at 197.6 ppm. There is a C_s symmetry attributed to the back-and-forth motion of the ethylene bridge. The geometry around the nickel(II) center is square planar with the ligand **L85** and two methyl

ligand coordinated. The Ni–$C_{carbene}$ bond distances (1.907(5) and 1.911(6) Å) are in the same range as those in **178** and **181**.

Nonetheless, any attempts on isolating the analogous methylene bridge complex of **185** using Ni(bipy)Me_2 failed. The reaction was monitoring by ^{1}H NMR spectroscopy over 10 h from - 75 °C to room temperature. Above - 50 °C, the signals assigned to the expected complex were observed with low intensity compared to those of the free carbene and other decomposition products. After 24 h at room temperature, the expected complex was not detected anymore. The thermal decomposition of **185** was studied because of the difference of thermal stability between complexes **185** and its methylene bridge analogue. Above 50 °C, the decomposition of **185** follows a unimolecular thermal decomposition with concomitant formation of methane. The decomposition displays a first order kinetics. Unfortunately the difference of the decomposition rate between **185** and its analogous methylene bridge complex stay unclear.

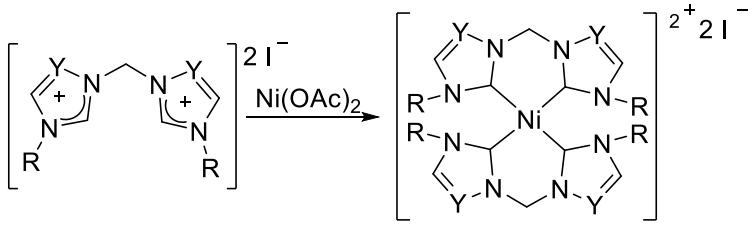

L64: Y = CH; R = Me
L34: Y = CH; R = ^{i}Pr
L65: Y = CH; R = Cy
L66: Y = NH; R = Me

186: Y = CH; R = Me
187: Y = CH; R = ^{i}Pr
188: Y = CH; R = Cy
189: Y = NH; R = Me

Scheme 43. Tetra-NHC Ni(II) complexes.[64b]

Herrmann *et al.* reported four tetracarbene nickel(II) complexes in 1999.[64b] The reaction of the pro-ligands **L34** and **L64-L566** with anhydrous Ni$(OAc)_2$ in DMSO led to the mononuclear nickel(II) complexes **186-189** in excellent yield (>90%) and NiI_2 as byproduct. No neutral *cis*-dihalide nickel(II) complexes were observed. No reaction occurred with the bulkier *N*-^{t}Bu-imidazolium iodide pro-ligand. On the ^{1}H NMR spectra, the signals of the methylene bridges and the imidazoline-2-ylidene ring protons of **189** are downfield by approximately 1 ppm compared to those of **186-188**. A 150°C, the non-equivalent methylene bridges protons indicate the retention of the boat shape conformation of the 6-membered rings comprised of the chelated nickel(II) center. The $^{13}C\{^1H\}$ NMR spectrum of **188** exhibits six signals for the cyclohexyl-group suggesting a hindered rotation around the N–CH bond. In the $^{13}C\{^1H\}$ NMR spectra of **186-189**, the nickel bound carbene signals are visible at 171.1 (**186**),

171.3 (**187**), 173.1 (**188**) and 173.8 (**189**) ppm. Only the complex **186** was characterized by single crystal X-ray diffraction. Its owns a nickel center with a square planar geometry completed by two ligands **L64**. The Ni–$C_{carbene}$ bond distances (1.909(2) Å) are in agreement with the literature.[66]

Olivier-Bourbigou *et al.* reported a second pathway to obtain the complex **186**. The nickel precursor used was still $Ni(OAc)_2$. However, the reaction was carried in nitromethane for 1 h under vacuum at 150 °C. The conversion was not complete (no yield provided). The complex **186** is active for 1-butene dimerization.[67]

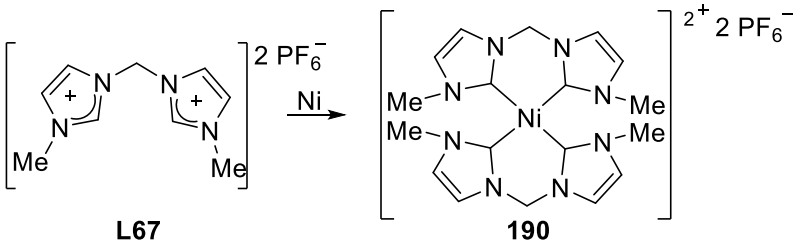

L67 **190**

Scheme 44. Tetra-NHC Ni(II) complexes. [68]

The mononuclear nickel(II) complex **190** was accessible by electrochemical oxidation of nickel plates in presence of the salt **L67** (43.1%).[68] This complex was characterized by elemental analysis and ^{1}H NMR analysis.

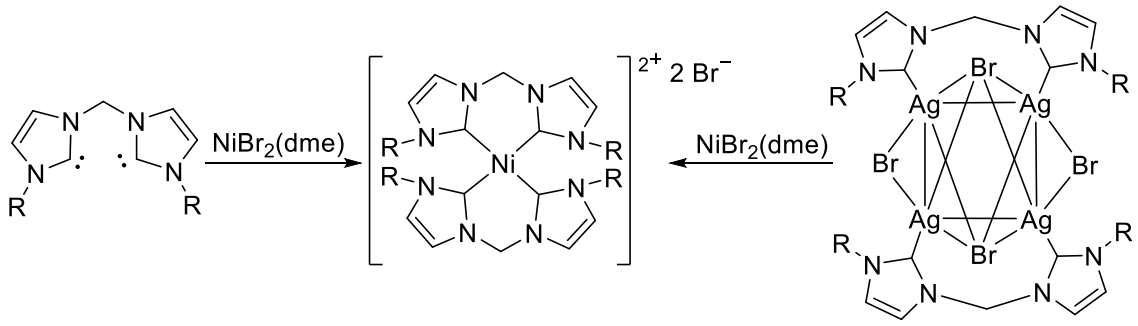

L61 R = ^{t}Bu
L68: R = Bn
L69: R = ^{t}Bu-C6H4-CH2

191: R = ^{t}Bu
192: R = Bn
193: R = ^{t}Bu-C_6H_4-CH_2

L70: R = Bn
L71: R = ^{t}Bu-C_6H_4-CH_2

Scheme 45. Two different pathways leading to Ni(II) complexes. [63,69]

The complex **191**, analogous of **184**, was made by reaction of $NiBr_2$(dme) with the free carbene **L61**.[63] In the final mixture, 20% of impurities were present and not removable. The ^{1}H and ^{13}C{^{1}H} NMR spectra of **191** are identical to those of **184**. The crystalline structure of **191** exhibits a nickel center with a square planar geometry. The di-cation adopts a

trans double boatlike conformation. The Ni–$C_{carbene}$ bond distances (1.936(4) and 1.928(4) Å) are similar to those in *trans* from the PMe_3 groups in complexes 1**78** and **181**.

Foley *et al.* reported the reaction of the free carbenes **L68** and **L69** with $NiBr_2$(dme) to afford the complexes **192-193** in moderate yields (60 and 40%).[69] Regardless the stoichiometries of carbenes used, only **192-193** were formed. Besides, the bis-NHC tetranuclear silver(I) complexes **L70** and **L71**, underwent transmetalation with $NiBr_2$(dme) to produce **192-193** in lower yields (45 and 35%, respectively). **192-193** are stable towards air and moisture. The non-equivalent resonances of the methylene bridges on the ^1H NMR spectra suggest a retention of conformation for the chelating boat-shaped six-membered rings containing the nickel atom. On the $^{13}C\{^1H\}$ NMR spectra, the nickel bound carbenes are visible at 171.3 and 171.2 ppm, respectively. The crystalline structures exhibit a distorted square planar geometry around the nickel(II) centers. Two bis-NHC ligands are coordinated to the nickel(II) atoms. The two planes, each defined by the nickel cation and a bis-NHC ligand, are coplanar. The Ni–$C_{carbene}$ bond distances (1.897(2) and 1.906(2) Å) are in agreement with the literature.[63,64b] Complex **192** catalyzed Suzuki-Miyaura reactions.

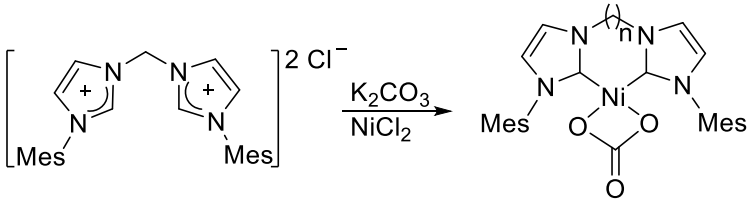

L22: n = 1
L72: n = 2
L73: n = 3

194: n = 1
195: n = 2
196: n = 3

Scheme 46. Carbonate Ni(II) complexes.[70]

Cao, Shi *et al.* reported a series of carbonate nickel(II) complexes.[70] The reaction of the imidazolium chloride salts **L22**, **L72** or **L73** with $NiCl_2$ and K_2CO_3 led to the formation of the complexes **194-196** in moderate yields (56, 65 and 68%). The preparation of a similar complex with a butylene bridge under the same conditions failed. Mixing at least 4.0 equiv. of nickel precursor with the base is essential to avoid any side reaction. Traces of water in the mixture were not detrimental for the synthesis. However, the reaction using $NiCl_2 \cdot 6H_2O$ as nickel precursor failed. The complexes **194-196** were characterized by NMR spectroscopy. Unfortunately, their $^{13}C\{^1H\}$ NMR spectra did not unveil the carbene- and carbonate-signatures. The infrared spectra show some strong bands between 1657 and 1604 cm^{-1} corresponding to the carbonate ligand. For each complex, X-ray diffraction studies reveal a

nickel center with a slightly distorted square planar geometry. The coordination spheres are completed by a carbonate ligand and **L22**, **L72** or **L73**. The two carbene sites are in *cis*-position. Due to conformational constraints, the μ-O bonds are out of the plane containing the bis-NHC ligands and the nickel atom. The Ni–$C_{carbene}$ bond distances fall in the range of 1.853(5)-1.885(4) Å. The O–Ni–O bite angles (**194**: 69.33(12)°, **195**: 69.87(10)° and **196**: 69.99(12)°) remain almost the same despite the increasing of the $C_{carbene}$–Ni–$C_{carbene}$ bite angles (**194**: 88.71(19)°, **195**: 94.49(15)° and **196**: 99.27(17)°). The complexes **194**-**196** catalyze the Kumada reaction.

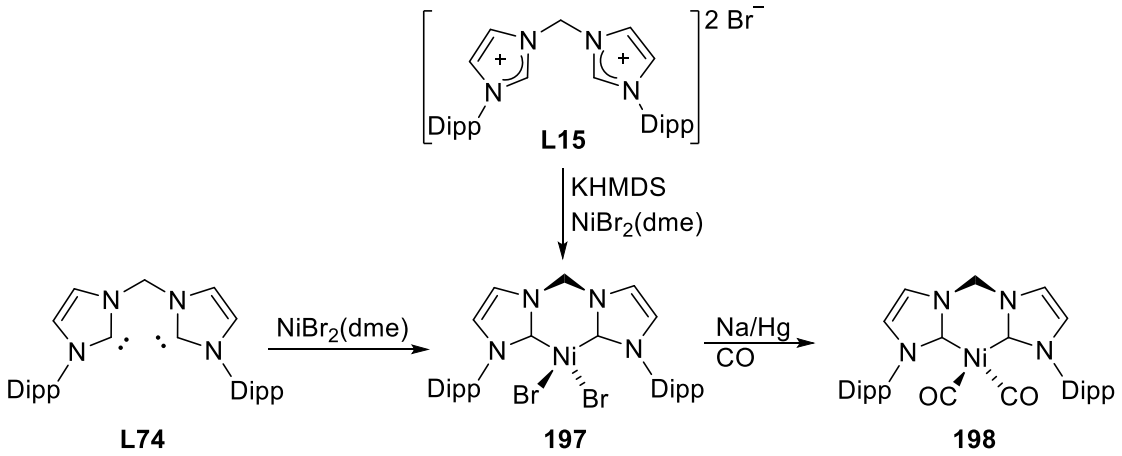

Scheme 47. Reduction of Ni(II) complex to Ni(0).[71]

Two reactions are possible for the formation of the complex **197**: a) the isolation of the free carbene followed by its complexation to nickel or b) deprotonation *in situ* of **L15** with KHMDS followed by the addition of $NiBr_2$dme.[71] The reaction of the free carbene **L74** with $NiBr_2$(dme) yielded the paramagnetic complex **197** (75%). Due to the sensitivity of free carbenes towards temperature and air, the addition of the nickel precursor to **L74**, freshly prepared by deprotonation *in situ* of the imidazolium bromide salt with KHMDS, was attempted. The complex **197** was quickly washed with degassed water to remove the KBr formed during the reaction. Elemental analysis supports a ratio of ligand-to-metal of 1: 1. In the presence of CO, Na/Hg reduced **197** to form **198** (no yield value given). The complex **198** is paramagnetic and **198** was only characterized by single crystal X-ray diffraction. In the solid state, both complexes **197** and **198** exhibit a tetrahedral geometry around the nickel centers. The ratios metal-to-ligand 1:1 differ from the nickel(II) complexes described above (**186**-**193**) (ratio 1:2) likely due to the higher steric bulk of the carbene substituents (Dipp). The Ni–$C_{carbene}$ bond distances of **197** (1.976(7) and 1.975(6) Å) are longer than those of the complex **198** (1.955(2) and 1.957(2) Å).

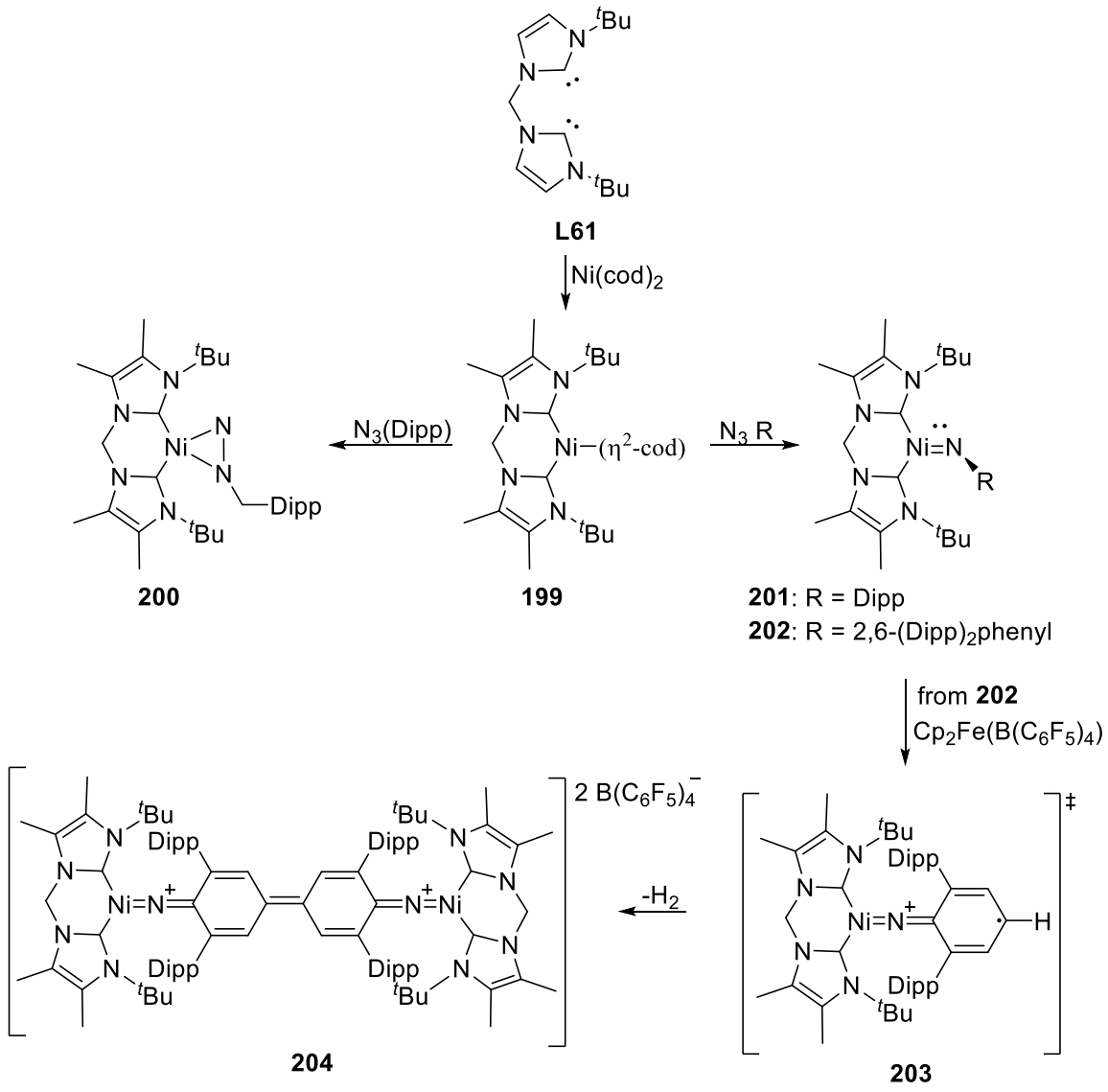

Scheme 48. Synthesis and reactivity of arylimido Ni(II) complexes.[72]

The free carbene **L61** reacted with $Ni(COD)_2$ to form the nickel(0) complex **199** in excellent yield (94%).[72] The ^{1}H and $^{13}C\{^{1}H\}$ NMR analysis suggests that the ligand COD is coordinated by a single olefin bond. The molecular structure of **199** reveals a trigonal planar geometry around the nickel(0) center and confirms the coordination of the ligand COD, in chair conformation, by a single olefin bond.

The reaction of **199** with $(Dipp)N_3$ led, in excellent yield (94%), to the nickel(0) complex **200** which was quite inert (only mild decomposition) under thermal (80 °C for days) and photolytic conditions (253 nm). It was characterized by ^{1}H and $^{13}C\{^{1}H\}$ NMR spectroscopy. The geometry around the nickel center is distorted square planar with delocalized π-bonding in the N_3 framework, which has been seen in other nickel organoazide complexes,[73] and the ligand **L61** in cis-position.

The reaction of **199** with bulky terphenylazides led to **201**-**202** in excellent yields (86 and 89%). Both complexes were analyzed by infrared, ^{1}H and $^{13}C\{^{1}H\}$ NMR spectroscopy, elemental analysis and single crystal X-ray diffraction. In the solid state, the three-coordinated nickels adopt a Y-shaped geometry. The Ni=N bond distances (1.732(3) – 1.718(2) Å) are shorter than those found for terminal bis(trialkylphosphine) nickel (II) imides.[74] The Ni–$C_{carbene}$ bond distances are in the range of 1.882(2)-1.902(2) Å.

The reaction of **202** with $Cp_2Fe(B(C_6F_5)_4$ was thought to form the nickel(II) complex **203** (not observed) by a 1-electron oxidation process. However, a supplementary bimolecular *para*-C,C coupling step generated a linked-quinoneimine intermediate which after dehydrogenation, gave the complex **204** in excellent yield (89%).

The complex **204** was characterized by ^{1}H and $^{13}C\{^{1}H\}$ NMR spectroscopy and X-ray diffraction. In the solid state, like **201** and **202**, the nickel centers adopt Y-shaped geometry. They are chelated by **L61** and held together by an arylimido linker. The Ni=N (1.725(8) Å) and N=C (1.297(12) Å) bond distances are typical to double bonds. The angle Ni–N–C is almost linear (163.7(9) Å). The Ni–$C_{carbene}$ bond distances of complex **204** are equal to 1.880(10) and 1.914(10) Å.

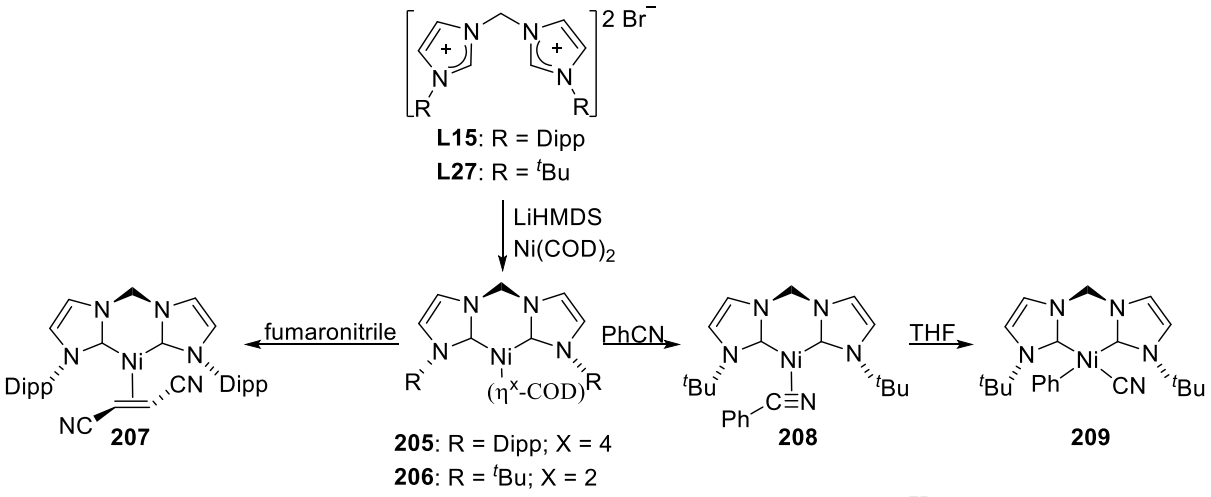

Scheme 49. C–C bond activation of benzonitrile.[75]

Hofmann reported bis-NHC nickel(0) complexes.[75] The isolated free carbenes arising from the imidazolium bromide salts **L15** and **L27** are not stable at room temperature. Thus, the imidazolium bromide salts **L15** and **L27** were deprotonated *in situ* by LiHMDS. The formed lithium NHC adducts reacted with $Ni(COD)_2$ to form the complexes **205**-**206** in moderate yields (50 and 34%). At room temperature, the ^{1}H NMR spectrum of complex **205** reveals two singlets at 3.66 and 5.53 ppm for the COD- and the methylene bridge- protons,

indicating the η^4-coordination of the COD ligand, and the fast inter-conversion between both conformations of the six-member ring comprised of the chelated nickel center. In the $^{13}C\{^1H\}$ NMR spectrum of **205**, the nickel bound carbene signal appears at 206.1 ppm. In the solid state, **205** exhibits a Ni(0) center with a distorted tetrahedral geometry. The Ni–$C_{carbene}$ bond distances (1.938(3) and 1.953(3) Å) are similar to those of the complexes **188**-**191** described above.[63,71]

The ^1H NMR spectrum of complex **206** is significantly different from that of **205**. The two doublets characterizing the methylene bridge indicates that the central metallacyle retains a boat conformation at room temperature due to the steric effect of the ^{t}Bu groups. Moreover, two multiplets at 2.92 and 6.08 ppm indicate an uncommon η^2-coordination of the COD ligand. On the $^{13}C\{^1H\}$ NMR spectrum, the nickel bound carbene signal is visible at 203.8 ppm. X-ray diffraction studies confirm the structure of **205** based on NMR data. The Ni–$C_{carbene}$ bond distances (1.905(3) and 1.921(4) Å) are slightly shorter than for **205**. DFT calculations confirm that the steric encumbrance of the ^{t}Bu substituents forced the η^2-coordination of the COD ligand.

Addition of fumaronitrile to **205** produced **207** in excellent yield (90%). The ^1H NMR spectrum confirmed the substitution of the COD ligand by an electron-deficient olefin. On the $^{13}C\{^1H\}$ NMR spectrum, the signal of the carbene is at 190.9 ppm. The complex **207** was not characterized by single crystal X-ray diffraction.

In presence of benzonitrile, **206** was converted to **208** in very good yield (82%), thus corroborating the nickel(0) complexes reactivity as 14 valence electron fragments. ^1H NMR spectroscopy confirms that the nitrile group replaced the COD ligand in the coordination sphere of the nickel(0) center. The $^{13}C\{^1H\}$ NMR spectrum displays the signals of the carbenes are at 200.8 and 201.3 ppm. A large difference is visible between the chemical shifts of free and bound nickel acetonitrile molecules (119 ppm *vs* 173 ppm for CN). In the solid state, the nickel(0) center owns a distorted square planar geometry with the bis-NHC ligand and the benzonitrile coordinated. The Ni–$C_{carbene}$ bond distances (1.932(5) and 1.893(5) Å) are similar to those of **205**-**206**.

Finally, an irreversible oxidative addition took place slowly on **208** at room temperature in THF, Heating the solution for 5 hours at 65 °C allowed the complete conversion in **209**. The new complex was characterized by X-ray diffraction, NMR and IR spectroscopy. The carbene signals are visible at 184.9 and 186.1 ppm. The cyano-ligand has a

stretching band at 2101 cm^{-1}. The Ni–$C_{carbene}$ bond distances (1.896(6) and 1.937(6) Å) are in the range of those of **205**-**206** and **208**.

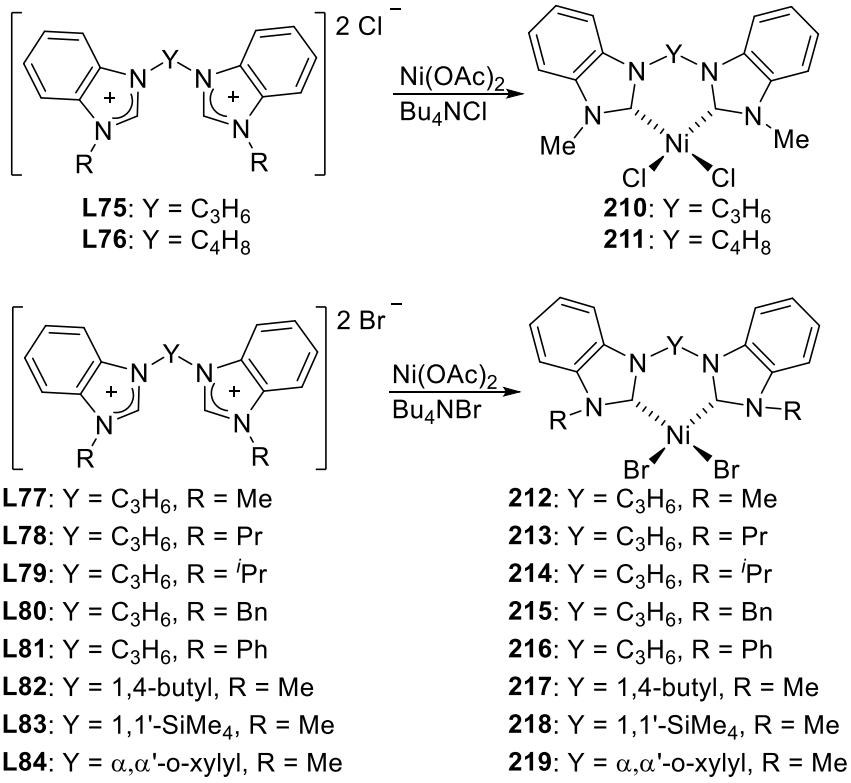

L75: Y = C_3H_6
L76: Y = C_4H_8

210: Y = C_3H_6
211: Y = C_4H_8

L77: Y = C_3H_6, R = Me
L78: Y = C_3H_6, R = Pr
L79: Y = C_3H_6, R = ^{i}Pr
L80: Y = C_3H_6, R = Bn
L81: Y = C_3H_6, R = Ph
L82: Y = 1,4-butyl, R = Me
L83: Y = 1,1'-$SiMe_4$, R = Me
L84: Y = α,α'-o-xylyl, R = Me

212: Y = C_3H_6, R = Me
213: Y = C_3H_6, R = Pr
214: Y = C_3H_6, R = ^{i}Pr
215: Y = C_3H_6, R = Bn
216: Y = C_3H_6, R = Ph
217: Y = 1,4-butyl, R = Me
218: Y = 1,1'-$SiMe_4$, R = Me
219: Y = α,α'-o-xylyl, R = Me

Scheme 50. Benzimidazol-based NHC Ni(II) complexes.[76]

We have seen that bis(NHC)Ni(halide)$_2$ are difficult to obtain whereas [(bis(NHC))$_2$Ni]$^{2+}$ complexes are not (page 56-58 and 67). A different methodology using some benzimidazolium salts allowed the formation of neutral halide nickel(II) complexes. Bouwman *et al.*[76a] reported the synthesis of the complexes **210**-**219**, in good yields (41%-77%), by reaction between Ni(OAc)$_2$ and the imidazolium halide salts **L75**-**L84**, in molten tetrabutylammonium halides. These complexes are stable towards moisture and air. They were characterized by NMR spectroscopy. The ^{1}H NMR spectra of **210**-**219** and **L75**-**L84** are very similar except for the bridging moieties. The carbene signals were not observed. The complexes **212, 215**, **217** and **218** were characterized by X-ray diffractions; they own a nickel(II) center with a slightly distorted square planar geometry. The bis-NHC ligand and the bromides complete de coordination sphere. The Ni–$C_{carbene}$ bond distances range from between 1.859(6) to 1.872(2) Å). For **217**, there is a weak agostic interaction between the nickel and the hydrogens of NCH_2 due to the difference of torsion angles of the bridge (eclipsed, -124.0(5)° and staggered, 51.6(7)°) . The complexes **210**-**219** catalyze the Kumada reaction[76a,b] and the addition polymerization of norbornene.[76c] Huynh and Jothibasu reported

the complex **212** by modifying the stoichiometry,[76b] and the temperature of the reaction described by Bouwman. Overall, both methods gave similar yields. In solution after several days (~40 days), **212** became a dicationic tetracarbene nickel(II) complex. Mass spectroscopy confirms the formation of a bis-chelate NHC complex.

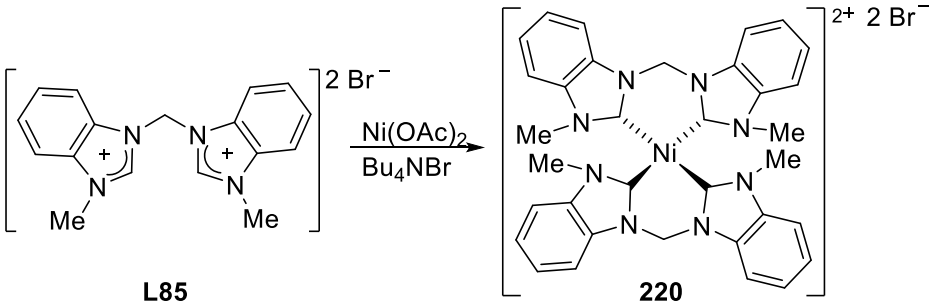

Scheme 51. Benzimidizol-2-ylidene Ni(II) complex.[76b]

Reacting the methylene-bridged bis-benzimidazolium dibromide salt **L85** with anhydrous $Ni(OAc)_2$ led to the cationic complex **220** in excellent yield (89%).[**76b**] The ethylene-bridged version of **L85** was not reacting with anhydrous $Ni(OAc)_2$. Its reaction with Ag_2O was possible, but the resulting silver(I) complex was inefficient toward transmetalation with nickel. On the ^1H NMR spectrum of **220**, the ethylene bridge protons appear diastereotopic. The $^{13}C\{^1H\}$ NMR spectrum exhibits the carbene signals at 183.0 ppm. X-ray diffraction studies unveiled an nickel(II) center with a quasi square planar geometry. The sphere of coordination is completed by two bis-NHC ligands. The two resulting 6-membered rings, sharing the doubly chelated nickel cation, adopt a *trans* boat conformation. The Ni–$C_{carbene}$ bond distances (1.891(6) and 1.906(6) Å) are longer than for the neutral complexes **212**, **215**, **217** and **218**. The complex **220** catalyzes the Kumada reaction.

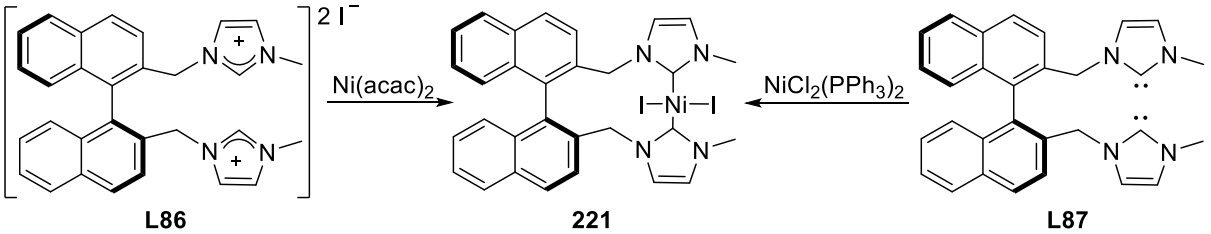

Scheme 52. Chelated bis-NHC Ni(II) complexes.[77]

RajanBabu *et al.* reported the chiral bis(NHC) chelate nickel(II) complex **221**.[77] The first attempts on making **221** by reaction between the imidazolium iodide salt **L86** and $Ni(acac)_2$ or $NiCl_2(PPh_3)_2$ in hot DMSO, failed. No reaction occurred or **L87** decomposed. At higher temperature (200 °C in NMP), a second attempt led to **221** in low yield (26%). Finally,

the free carbene **L87** was reacted with $NiCl_2(PPh_3)_2$ to form **221** in better yield (45%). The complex was studies by ^1H, $^{13}C\{^1H\}$ NMR spectroscopy and X-ray diffraction. The bridging methylene protons give rise to an AX system of doublets. The carbene signals are visible at 176.4 ppm. The solid-state structure exhibits a nickel(II) center owning a distorted square planar geometry with the NHC ligands in *trans* configuration. The Ni–$C_{carbene}$ bond distances (1.889 and 1.901 Å) are similar to those of the nickel complexes quoted above.[63-64,70-71,75-76]

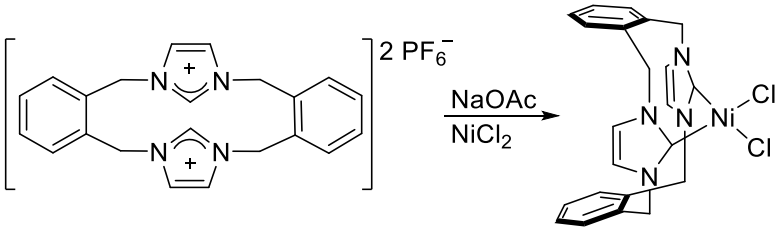

L88 **222**

Scheme 53. Bis-NHC cyclophane Ni(II) complex.[78]

Baker *et al.* reported a bis(NHC) cyclophane nickel(II) complex with structural constraints and rigidity enforced by the cyclophane ligand.[78] The reaction between **L88** and anhydrous $NiCl_2$ in presence of NaOAc allowed the formation of complex **222** in moderate yield (41%). The complex was characterized by ^1H, $^{13}C\{^1H\}$ NMR spectroscopy and X-ray diffraction. The benzylic protons, close to the nickel cation, are unusually shifted a low field (7.89 ppm in an AX system), hinting at a possible agostic interaction. The carbene signals appear at 162.1 ppm. The solid-state structure unveiled a nickel cation with a distorted square planar environment. Two carbene sites, in *cis* configuration, and two chlorides complete the coordination sphere. The Ni–$C_{carbene}$ bond distances (1.862(2) and 1.863(2) Å) are in agreement with the literature.[55-56,60-61,65-66]

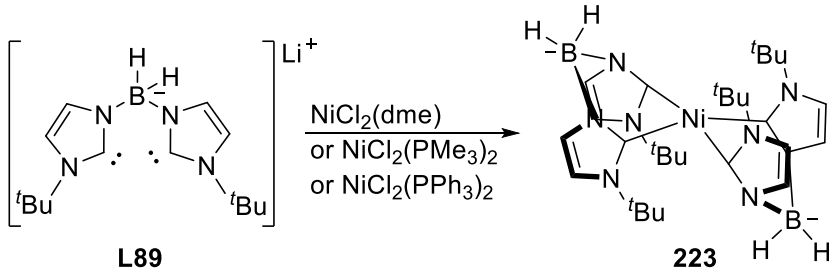

L89 **223**

Scheme 54. (Bis-NHC)borate Ni(II) complex.[79]

Smith *et al.* reported a (tetra-carbene)borate nickel(II) complex.[79] The lithium complex **L89** reacted with $NiCl_2$(dme), $NiCl_2(PMe_3)_2$ or $NiCl_2(PPh_3)_2$ to form the complex **223** in excellent yield (> 90%). The ^1H NMR spectrum of **223** displays a set of signals

corresponding to the bis(NHC) ligands. No $^{13}C\{^1H\}$ NMR spectroscopy data are available. X-ray diffraction studies unveiled a nickel center with a square planar environment. As we have seen previously, the six-membered rings containing the nickel adopt a boat conformation. The structure of **223** and **191** are similar; the ligands **L89** and **L61** bring equivalent steric bulk around the nickel cation. The Ni–$C_{carbene}$ bond distances and the $C_{carbene}$–Ni–$C_{carbene}$ angles are similar (**223**: 1.940(3) and 1.949(3) Å, **191**: (85(5) and 94.5(2)°). The short C···C distance (3.62 Å) between the ^{t}Bu groups reflects the steric pressure created by the rigid NHC rings and the short Ni–$C_{carbene}$ bond. DFT calculations provide evidences that an octahedral geometry has a higher free energy than a square planar geometry in the case of **223**. Moreover, the ΔH values (20 kcal/mol) indicate that the bis(NHC) ligands stabilize the square planar geometry by forming strong bonds to nickel center. Therefore, the strongly donating property of the bis(NHC)borate ligand overcome the unfavorable steric interactions between the ^{t}Bu substituents of each **L89** in the square planar geometry.

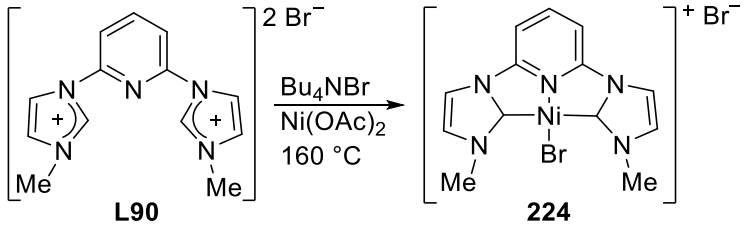

Scheme 55. Ni(II) complexes bearing pincer (bis-NHC)-pyridine.[80]

We have seen the coordination of different bidentate bis-NHC ligands to a nickel center. From this point, we report tripodal bis-NHC ligands coordinated to a nickel.

The cyclometalation of the bis(imidazolium)pyridine bromide salt **L90** with $Ni(OAc)_2$ in presence of Bu_4NBr led to the complex **224** in good yield (63%).[80b] It was characterized by ^1H NMR spectroscopy and X-ray diffraction studies. ^1H NMR spectroscopy indicates the presence of planes of symmetry. The nickel owns a distorted square planar geometry. The Ni–$C_{carbene}$ bond distances (1.862(3) and 1.920(5) Å) are in agreement with other Ni(II) complexes.[76b,77-78]

Anion exchange between **224** and $AgNO_3$ led to a NHC supported Ag_7 cluster, with a $[Ag_6]$ core in a twisted bowtie geometry, rather than the expected (bis-NHC)-pyridine nickel(II) nitro complex. Only two articles described the successful transmetalation of (bis-NHC)-pyridine ligand from silver to nickel cations (see complex **235**).[81] The complex **224** catalyzed Heck, Kumada and Suzuki reactions.[80]

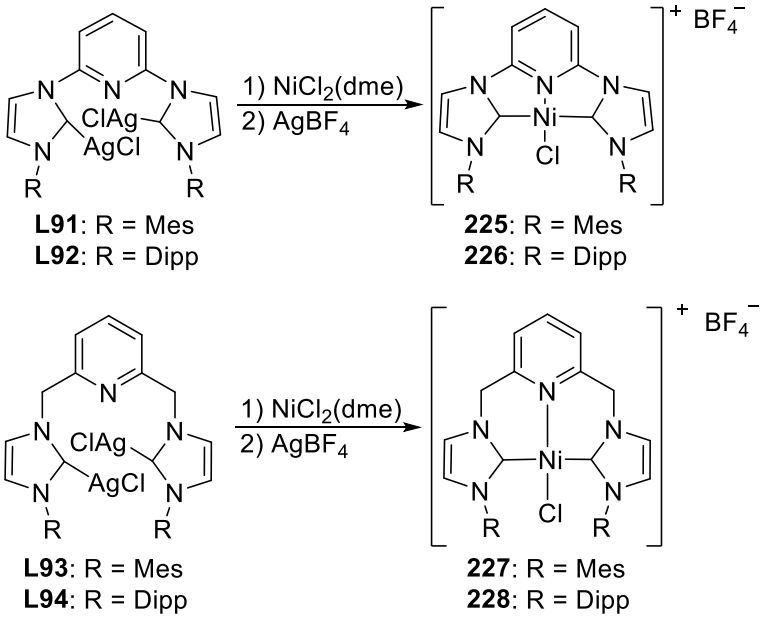

Scheme 56. (bis-NHC)-pyridine Ni(II) complexes.[82]

The protocol used for **199** did not work for the syntheses of the complexes **225**-**226**. Reaction of silver bis(NHC)-pyridine chloride complexes **L91**-**L94** with $NiCl_2$(dme), followed by counter anion exchange with $AgBF_4$, led to the complexes **225** (99%), **226**(88%), **227** (>99%) and **228** (78%).[82] They were characterized by NMR spectroscopy and X-ray diffraction studies. For **225-226**, the protons signals of Mes or Diip groups indicate a symmetry plane by opposition with **227-228**. The $^{13}C\{^1H\}$ NMR spectra were recorded but the signals were not assigned. All nickel centers exhibit a slightly distorted square planar geometry. For **225**-**226**, the plane comprised of the pyridine ring is nearly coplanar with the $C_{carbene}$–$N_{pyridine}$–$C_{carbene}$–Cl plane whereas for **227**-**228**, the same planes present a tilt angle of 46.60 (**227**) and 46.73° (**228**). The Ni–$C_{carbene}$ bond distances of **225**-**228** are between 1.891(3) and 1.932(4) Å. These complexes catalyze the Suzuki reaction.[80d,82]

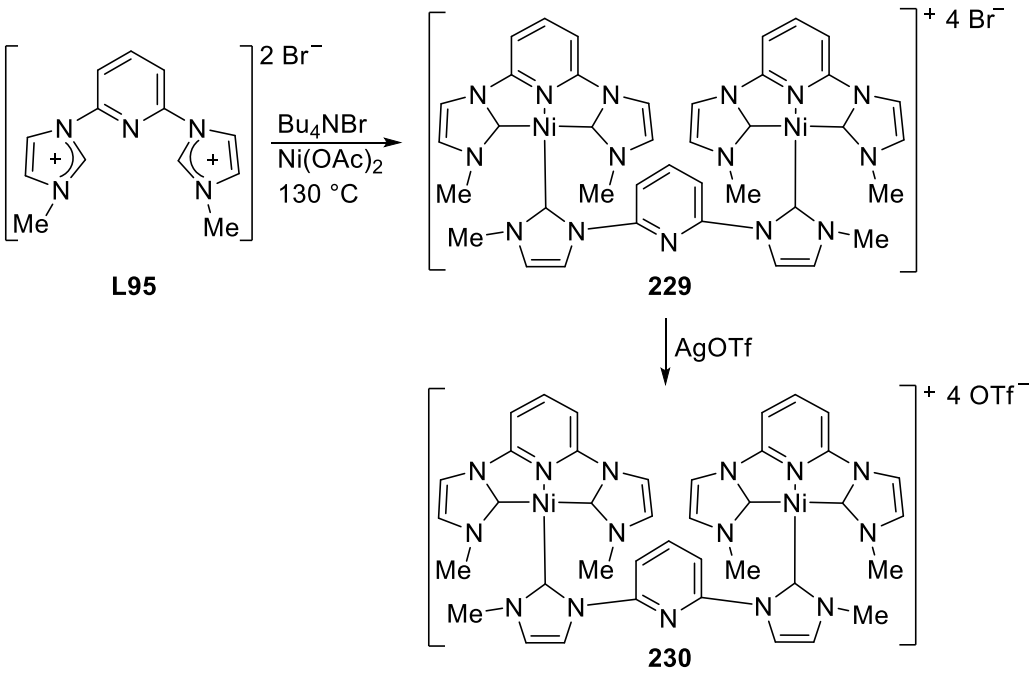

Scheme 57. Dinuclear bis-NHC Ni(II) complexes.[83]

Using the same starting materials (**L95**) and decreasing the reaction temperature from 160 to 130 °C allowed the formation of the new complex **229** (32%).[83] Its ^{1}H NMR spectrum reveals the presence of two types of ligand bis(NHC) pyridine in a ratio 2:1. However, due to a lack of solubility, no $^{13}C\{^{1}H\}$ NMR or X-ray diffraction studies were made. The complex **230** was synthetized by anions exchange between the dinuclear nickel(II) complex **229** and AgOTf (80%) in order to have a soluble version of **229** more prompt to crystallize. The ^{1}H NMR spectrum of **229** and **230** are practically identical. The $^{13}C\{^{1}H\}$ NMR spectrum of **230** exhibits two carbene resonances at 165.6 and 166.8 ppm. In the solid state, the nickel(II) centers exhibit a distorted square planar geometry. Two (bis-NHC)-pyridine pincer nickel(II) fragments are bridged by a third bis(NHC)pyridine ligand. The mutually *trans* Ni–$C_{carbene}$ bond distances (1.915(3) and 1.916(3) Å) are similar to those of **229**. The third Ni–$C_{carbene}$ bond distance is shorter (1.870(2) Å) due to a weaker *trans* influence of the pyridine compared to the *trans* influence of the carbenes. The combination of (bis-NHC)-pyridine ligands exhibiting both chelating and bridging modes in the same molecule in a ratio metal-to-ligand 2:3 is unique.

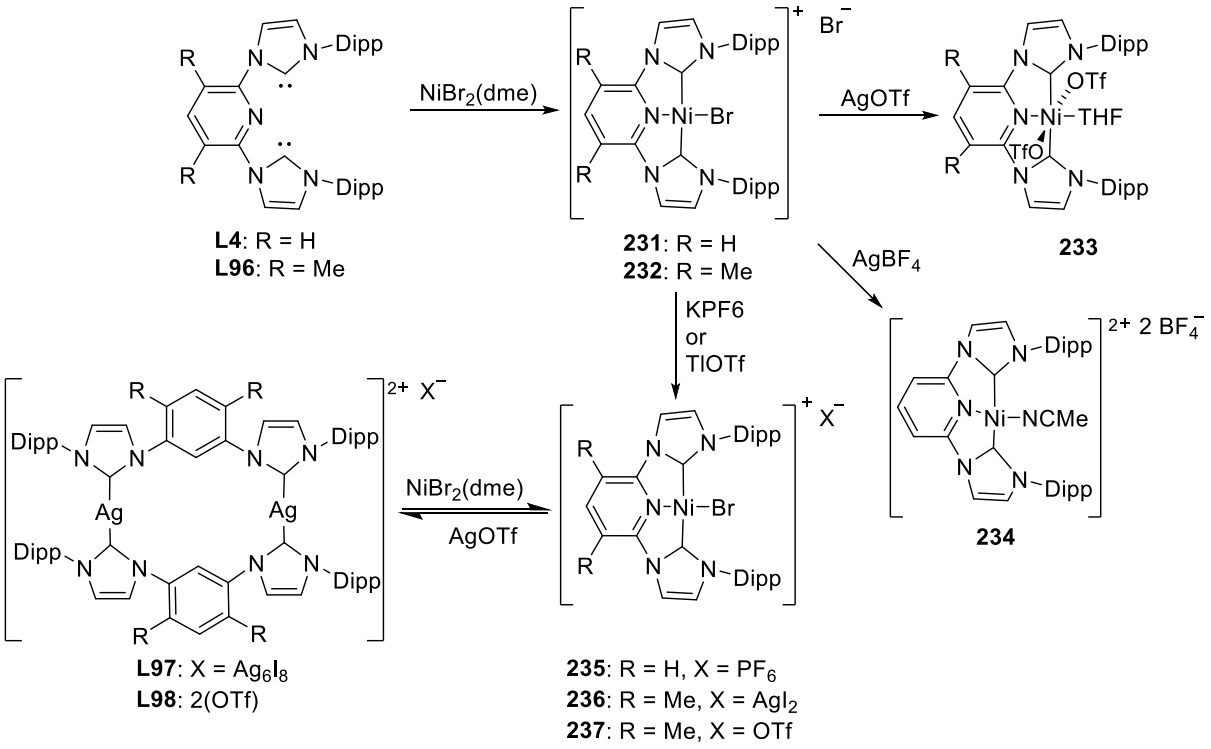

Scheme 58. Reactivities of pincer (bis-NHC)-pyridine nickel complexes.[81b]

The free (bis-NHC)-pyridine **L4** and **L96** reacted with $NiBr_2$(dme) to afford the complexes **231-232** in good yields (74 and 94%).[81b] They were characterized by ^1H spectroscopy and X-ray diffraction studies. The proton signals of **231** features a high symmetric complex whereas those of **232** are unusually broad. The $^{13}C\{^1H\}$ NMR spectra were recorded, but signals were only assigned for **231**. Its carbene resonance is visible at 182.2 ppm. The nickel center of **232** exhibits a distorted square planar geometry with metrical data (e.g. Ni–$C_{carbene}$: 1.920(7) and 1.914(7) Å) similar to the previously reported nickel(II) complexes **262-266**.

The reaction of **231** with AgOTf in THF gave the complex **233** in excellent yield (94%). The paramagnetic complex **233** was characterized by elemental analysis and X-ray diffraction studies. The nickel center owns an octahedral coordination sphere completed by the tridentate (bis-NHC)-pyridine ligand, a molecule of THF and two mutually *trans* triflate ligands. The Ni–$C_{carbene}$ bond distances (2.103(4) Å) is longer than the previous Ni–$C_{carbene}$ bond distances. The octahedral geometry contributes to the lengthening of the Ni–$C_{carbene}$ bond distances.

The reaction of **231** with another silver precursor ($AgBF_4$) in acetonitrile led, by substitution of both bromides, to the complex **234** (92%). Poor quality single crystal data

suggests a square planar geometry around the nickel(II) center, which is constituent with ^{1}H and $^{13}C\{^{1}H\}$ NMR spectroscopy and elemental analysis data.

Finally, the reaction of **231** with KPF_6 in THF led, by substitution of a bromide, to the complex **235** (92%). It was characterized by ^{1}H, $^{13}C\{^{1}H\}$ NMR spectroscopy and X-ray diffraction studies. The nickel bound carbenes signal appears at 165.2 ppm. The structure of **235** is very similar to that in **231**.

The free (bis-NHC)-pyridine **L84** being difficult to isolate, a transmetalation via the dinuclear silver complex **L85** was carried out. The reaction between $NiBr_2$(dme) **L85** allowed the formation of the complex **236** (no yield value given). Its ^{1}H NMR spectrum suggested a species with high symmetry. Its $^{13}C\{^{1}H\}$ NMR spectrum was partially assigned. X-ray diffraction unveiled a nickel center with a square planar geometry similarly to **231, 232** and **230.** The $Ni–C_{carbene}$ bond distances are equal to 1.911(8) and 1.895(8) Å.

The complex **236** reacted with AgOTf to obtain a dimeric silver complex with OTf as counter ions. This carbene transfer from nickel to silver complexes is scarce. The formed Ni(II) stayed in solution, presumably under the NiI_2 form. This transmetalation implies some degree of lability of the pincer ligand in the complex **236**. Furthermore, it underlines the importance of the anions and the strength of the $M–C_{carbene}$ bonds that were broken and reformed during transmetalation process.

To prevent the transmetalation from nickel to silver, TlOTf was used. The reaction between **232** and TlOTf led to the complex **237** (94%). The complex **237** was characterized by ^{1}H and $^{13}C\{^{1}H\}$ NMR spectroscopy. Its $^{13}C\{^{1}H\}$ NMR spectrum was partially assigned.

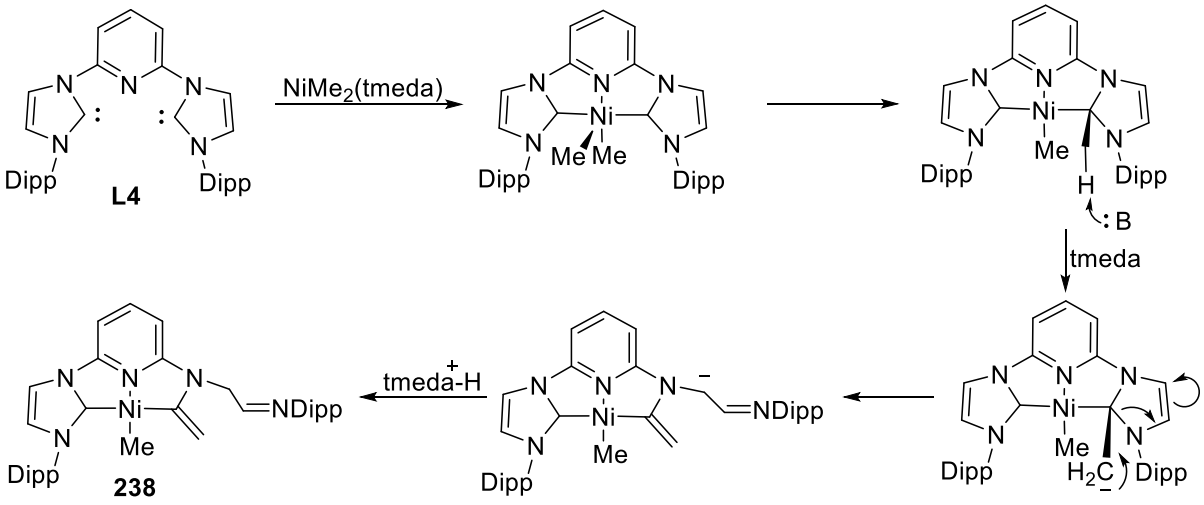

Scheme 59. Mechanism of NHC-opening.[81b]

The alkylation of complexes **231**-**232** by MeLi, $AlMe_3$ or PhMgCl led to intractable reaction mixtures. In order to obtain a nickel methyl complex, **L4** was mixed with $NiMe_2$(tmeda) producing the complex **238** in moderate yield (45%).[81b] Its ^1H NMR spectrum was complicated with broad resonances instead of the usual sharp signals. Several resonances in the olefinic region suggested a possible decomposition of the ligand **L4**. Its $^{13}C\{^1H\}$ NMR spectrum displayed a nickel bound carbene signal at 186.9 ppm. Single crystal X-ray diffraction established clearly the identity of the complex **238**. The geometry around the nickel(II) center is square planar. The molecular structure revealed an unexpected ring opening of the NHC moiety accompanied by the migration of the methyl group from nickel- to carbene- sites. The nickel(II) center coordinates a methyl-, an imine-, a NHC- and a pyridine- ligands. Surprisingly, the Ni–$C_{carbene}$ bond distance (1.912(2) Å) is shorter than the Ni–C_{vinyl} one (1.930(2). The N_1–C_1 (1.259(3) Å) and C_2–C_3 (1.337(3) Å) bond distances are consistent with an imine group and a C=C bond. Similar methyl migration has been observed with other late transition metal complexes[84] (e.g. palladium[85]) thus questioned the view that the NHCs are ideal "innocent" ligand in organometallic chemistry.

The authors proposed a plausible mechanism: i) coordination of the ligand **L4**, ii) methyl migration to the $C_{carbene}$, iii) β-hydrogen elimination from a methyl group triggered by tmeda, iv) ring opening of the imidazole ring, v) finally, reprotonation of the carbanion by the ammonium cation tmeda·H^+.

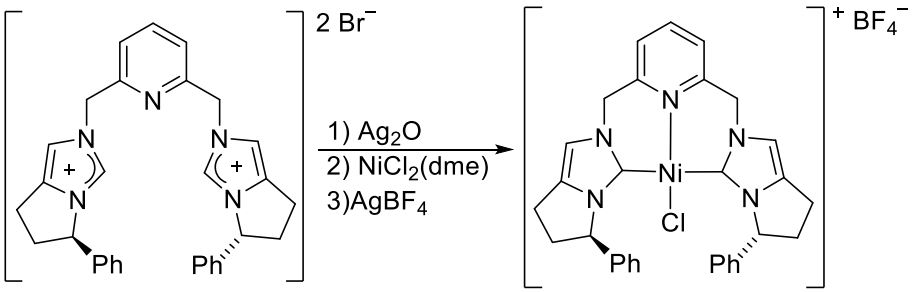

L99 **239**

Scheme 60. (bis-NHC)-pyridine Ni(II) complex.[86]

The complex **239** was obtained by the reaction of $NiCl_2$(dme) with the silver complex, prepared from **L99** and Ag_2O, followed by counter anion exchange with $AgBF_4$ in moderate yield (45%).[**86**] ^1H and $^{13}C\{^1H\}$ NMR spectra were recorded without any assignation for the carbon resonances. X-ray diffraction studies unveiled a Ni(II) center with a square planar geometry. The structure displays a C_2-symmetric environment. The Ni–$C_{carbene}$ (1.893(4) Å) bond distances are in agreement with the literature.[55-56,61-62,66-67]

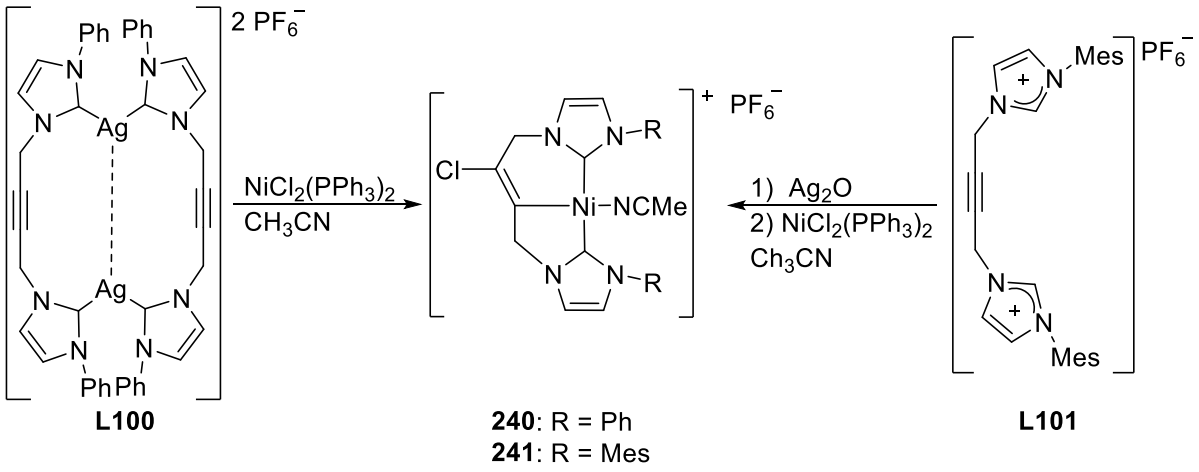

Scheme 61. Chloronickelation reaction.[87]

Chen *et al.* reported in 2009, two nickel(II) complexes formed by chloronickelation.[87] The treatment of the silver(I) complex **L100** with $NiCl_2(PPh_3)_2$ led to the unexpected nickel(II) complex **240** in very good yield (83%). Similarly, the reaction of the silver(I) complex, formed *in situ* from **L101**, with $NiCl_2(PPh_3)_2$ allowed the formation of the nickel(II) complex **241** in excellent yield (92%). The ^{1}H NMR spectra of complexes **240**-**241** display four singlets for the imidazole rings protons (7.17, 7.35, 7.90 and 7.92 ppm). On the $^{13}C\{^{1}H\}$ NMR spectra, two singlets for each complex (**240**: 173.1 and 169.7 ppm; **241**: 172.2 and 169.7 ppm) are assignable to non-equivalent carbene sites. The two signals of the non-aromatic C=C bond observed at 140.0 and 115.0 ppm, are characteristic of sp^2 carbons bound to nickel or chloride atoms. The molecular structure of complexes **240**-**241** exhibits a distorted square planar geometry around the nickel(II) atoms. The six- and five- membered rings, comprised of the chelated nickel, adopt respectively boat- and planar- conformations. The $Ni–C_{carbene}$ bond distances (ca. 1.90 Å) are in the range of those of **235** and **238**. The chloronickelation was unprecedented contrary to analogous known *trans*-chloropalladation.[88] The authors suggested a chloronickelation reaction with the following mechanism: i) coordination of the first NHC moiety, ii) coordination of the triple bond, iii) chloride nucleophilic addition on the triple bond, and iv) coordination of the second NHC moiety. The complexes **240** and **241** are active catalysts for Kumada coupling.

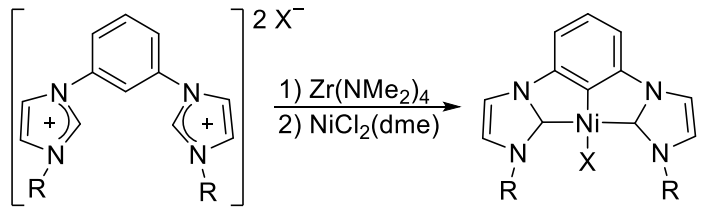

L102: X = Br, R = Bu
L103: X = Cl, R = Bu
L104: X = Cl, R = Bn

242: X = Br, R = Bu
243: X = Cl, R = Bu
244: X = Cl, R = Bn

Scheme 62. Pincer Ni(II) complexes.[89]

Hollis *et al.* patented the nickel(II) complexes **242-244**.[89] The imidazolium salts **L102-L104** reacted with $Zr(NMe_2)_4$ to form *in situ* some zirconium complexes, which were used as transmetalating agents with $NiCl_2$(dme) (or $NiBr_2$(dme) for **242**) to form the complexes **242-244** in good to excellent yields (63, 84 and 98%). The complexes were characterized by ^{1}H and $^{13}C\{^{1}H\}$ NMR spectroscopy, elemental analysis and mass spectroscopy.

The resonances observed for the α-N_{NHC} protons of the butyl chain are downfield (4.66 ppm) compare to those of the Zr pincer complex (4.44 and 4.32 ppm). Only the carbenic carbon signal of the complex **244** was assigned at 174.5 ppm. The complex **243** was also characterized by single crystal X-ray diffraction. The geometry around the nickel(II) center is distorted square planar. The pincer and a halide complete the coordination sphere.

The Ni–$C_{carbene}$ bond distances are longer than those of complexes reported by Inamoto *et al.*[80b,82] Preliminary studies on fluorescence, in the solid-state, were made for **242** and **243**. They exhibit a maximum emission at λ_{max} = 440 and 420 nm.

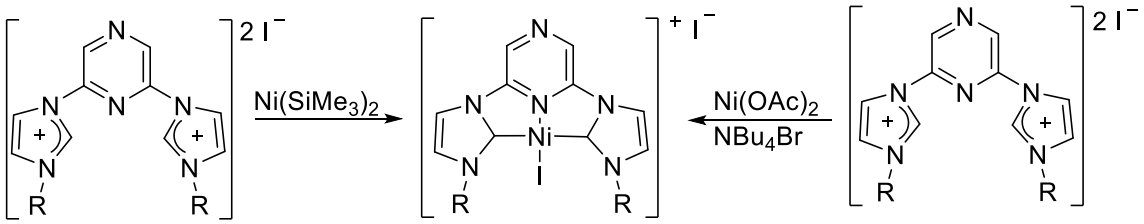

L105: R = Me

245: R = Me
246: R = iPr
247: R = tBu
248: R = Mes

L106: R = iPr
L107: R = tBu
L108: R = Mes

Scheme 63. Pincer bis-NHC Ni(II) complexes.[90]

In 2012, Mueller *et al.* patented the complexes **245-250** for the catalytic oxidation of hydrocarbons (see section 7).[90] The reaction between the imidazolium salt **L105** and $Ni(SiMe_3)_2$ led to the nickel(II) complex **245** in good yield (71%). No spectroscopic, analytic

or crystallographic data were available for this complex. The complexes **246**-**250** were made by reaction between the imidazolium salts **L106**-**L110**, NBu_4Br and $Ni(OAc)_2$ in good yields (63-85%).

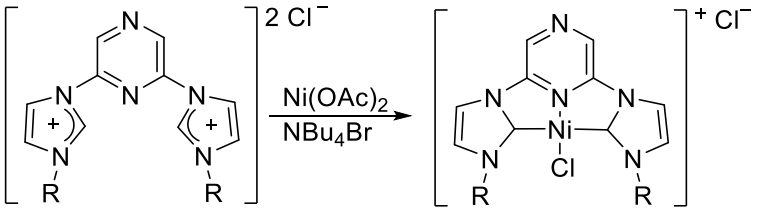

Scheme 64. Ni(II) pincer complexes.[90]

The complexes **246**-**250** were characterized by ^1H, $^{13}C\{^1H\}$ NMR and mass spectroscopy. The signals of the nickel bound carbene appear between 152.0 and 171.2 ppm, except for complex **249** for which no signal is observable.

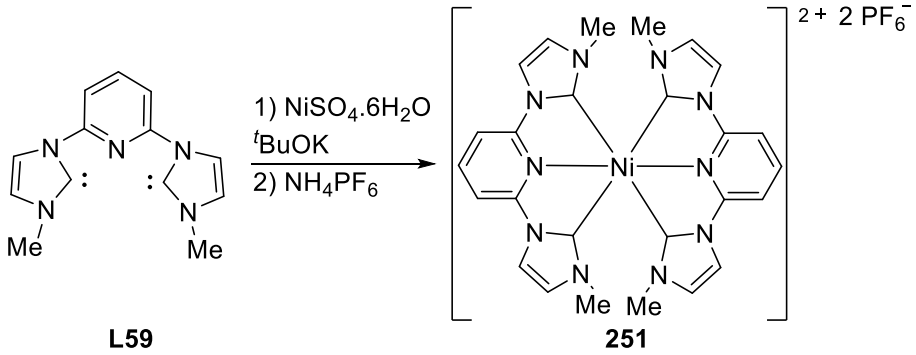

Scheme 65. Pincer (bis-NHC)-pyridine Ni(II) complex.[58]

The reaction between the ligand **L59** and $NiSO_4•6H_2O$ followed by addition of NH_4PF_6 led to the complex **251** (59%).[58] No spectroscopic, analytic or crystallographic data were reported. The complex **251** was patented for its use as electrolyte in redox flow batteries.

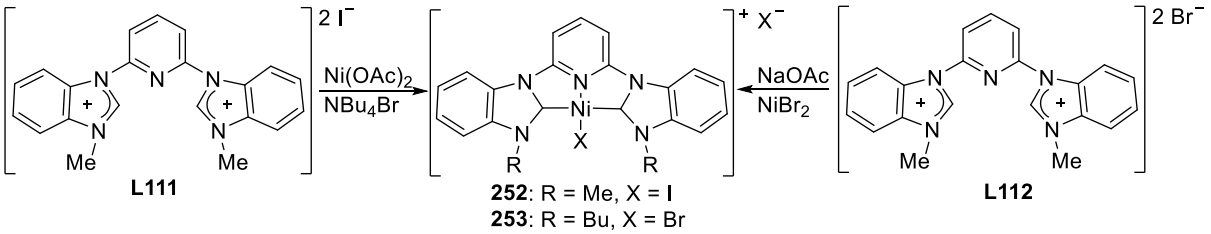

Scheme 66. Pincer Ni(II) complexes.[90-91]

The complex **252** was reported by Mueller *et al.*, as well as **246**-**250**.[90] Similarly, the reaction of the imidazolium iodide salt **L111** with $Ni(OAc)_2$ and NBu_4Br led to the complex

252 in good yield (71%). The complex was characterized by ^{1}H, $^{13}C\{^{1}H\}$ NMR and mass spectroscopy. On the $^{13}C\{^{1}H\}$ NMR spectrum, the nickel bound carbene signal is visible at 165.4 ppm.

The treatment of the imidazolium bromide salt **L115** by NaOAc and $NiBr_2$ led to the nickel(II) complex **253** in good yield (80%).[91] The complex was characterized by ^{1}H NMR, mass spectroscopy and elemental analysis. The literature protocols for the synthesis of **224-228** were ineffective in the **253** case.[38,80b,82,92] This complex was tested for Suzuki reaction.

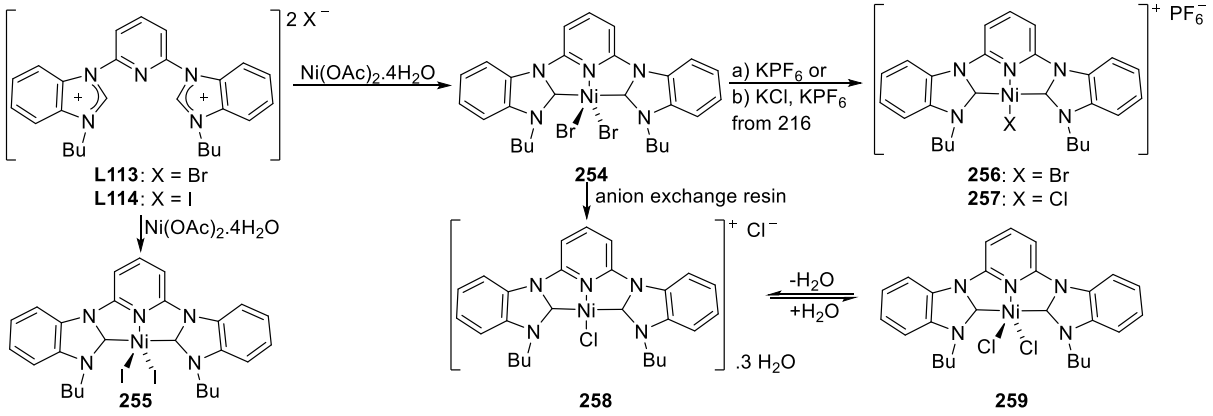

Scheme 67. Reactivity of pincer bis-NHC pyridine Ni(II) complexes.[93]

Brown and Skelton reported the nickel(II) bis-NHC complexes **254-265**.[93-94] The reaction of the benzimidazolium bromide salt **L113** with $Ni(OAc)_2 \bullet 4H_2O$ led to the nickel(II) complex **254** in high yield (71%).[93] The complex **254** exhibited low solubility in pure solvents whereas it was more soluble in mixed solvent systems. For this reason, no NMR spectroscopy study was made. Single crystal X-ray diffraction study revealed a nickel(II) center with trigonal bipyramidal geometry, surrounded by two bromide- and a pincer- ligands. Due to the poor quality of the crystals, only the geometry of the complex was determined. The treatment of **254** by KPF_6 in hot methanol, followed by the addition of water, led to a new nickel(II) four-coordinated complex **256** in excellent yield (93%). This complex was more soluble than **254** rendering possible its full characterization by ^{1}H, $^{13}C\{^{1}H\}$ NMR spectroscopy and single crystal X-ray diffraction. On the $^{13}C\{^{1}H\}$ NMR spectrum, the nickel bound carbene signal is visible at 170.4 ppm. The molecular structure confirms a four-coordinated nickel(II) atom with a square planar geometry. The pincer- and a bromide ligand- complete the coordination sphere. The Ni–$C_{carbene}$ bond distances are equal to 1.924(4) and 1.932(4) Å. The comparison of the UV-visible spectra between solutions of **254** and **256** indicates that the major absorption bands are similar (339-440 nm) suggesting that both complexes own the same

coordination geometries in solution. When **254** is solubilized, the nickel center likely loses a bromide ligand, adopting a square planar geometry.

Similarly to **256**, the reaction of the benzimidazolium iodide salt **L114** with $Ni(OAc)_2•4H_2O$ allowed the formation of the nickel(II) complex **255** in good yield (65%). It was only characterized by mass spectroscopy and elemental analysis. The complex **255** displayed even lower solubility behavior than **254**. Its conversion into **256**, as described above, failed.

The treatment of complex **256** by a large excess of KCl, followed by the addition of KPF_6, allowed the formation of the nickel(II) complex **257** in excellent yield (91%). Its solubility is similar to that of **256**. It was characterized by ^{1}H, $^{13}C\{^{1}H\}$ NMR spectroscopy and X-ray diffraction studies. The nickel bound carbene signal is visible at 169.8 ppm. The nickel center exhibits a square planar geometry. A chloride- and the pincer- ligands complete the coordination sphere. The $Ni–C_{carbene}$ bond distances (1.911(2) and 1.917(2) Å) are shorter than those of **256**.

To obtain the complex **258**, **254** was passed through a DOWEX®-Cl resin (no yield's value given). It was characterized by ^{1}H $^{13}C\{^{1}H\}$ NMR spectroscopy and X-ray diffraction studies. The nickel bound carbene signal is visible at 170.2 ppm.

Depending on the amount of water present in the solvents used for the crystallizations of complex **258**, the molecular structure obtained changes. Crystallizations in dry ethanol allowed the formation of the complex **259**. Aqueous ethanol (5% water) permitted the formation of **258**. The molecular structure of **258** exhibits a nickel center(II) with a square planar geometry. The NHC pincer- and a chloride-ligand complete the coordination sphere. A second non-coordinating chloride ensures the complex electronegativity. The $Ni–C_{carbene}$ bond distances (1.913(4) and 1.922(4) Å) are slightly shorter than those of **256**. The molecular structure of **259** exhibits a nickel(II) center with a trigonal bipyramidal geometry. The NHC pincer ligand in the equatorial positions and two chlorides in the apical positions complete the coordination sphere. The $Ni–C_{carbene}$ bond distances (1.897(6) and 1.900(7) Å) are shorter than those of **254**.

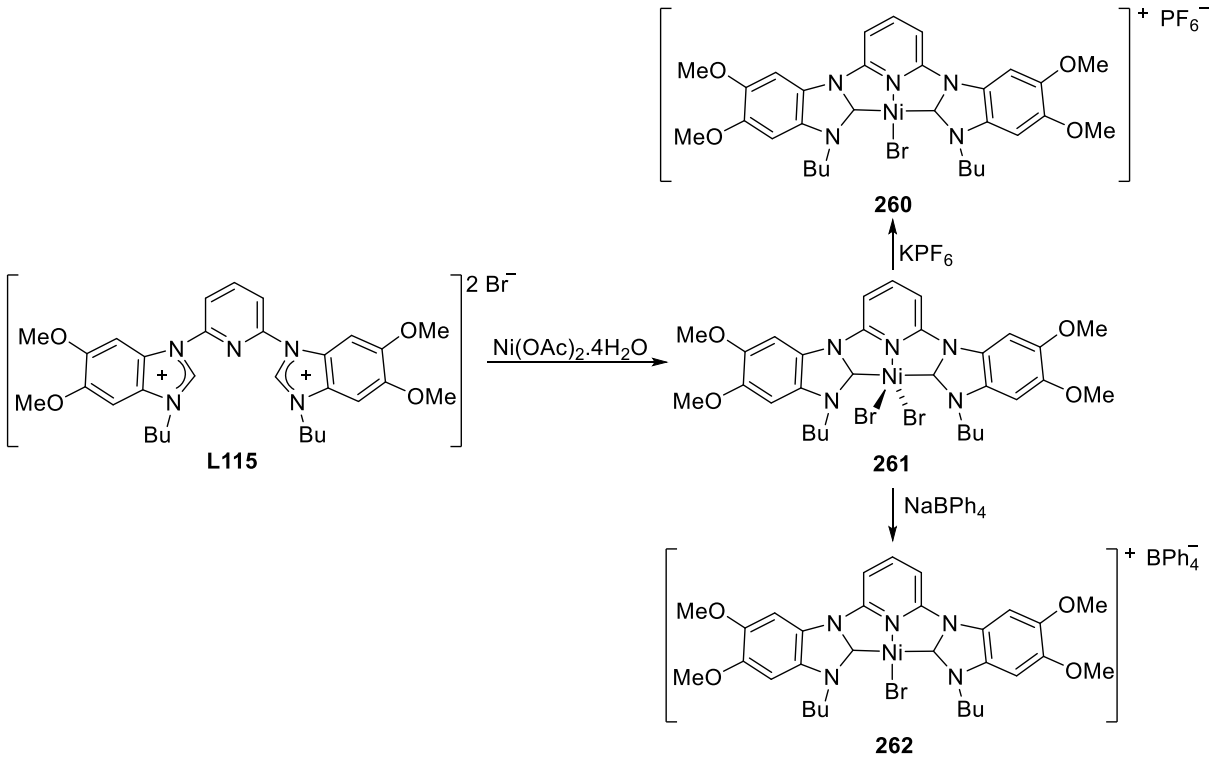

Scheme 68. Pincer bis-NHC pyridine Ni(II) complexes. [94]

The reaction of the imidazolium bromide salt **L115** with $Ni(OAc)_2 \bullet 4H_2O$ led to the nickel(II) complex **260** in moderate yield (54%). Treatment of the **260** with KPF_6 allowed the formation of the nickel(II) complex **261** in very good yield (85%). Similarly to **261**, the complex **262** was obtained (71%) by treatment of the complex **260** with $NaBPh_4$. All three complexes were characterized by ^1H, $^{13}C\{^1H\}$ NMR spectroscopy. The nickel bound carbene signal are visible at 166.4 (**260**), 156.6 (**261**) and 166.6 ppm (**262**). Attempts at growing X-ray diffraction quality crystals of **260** and **261** were unsuccessful. However, the structure of **262** was solved by X-Ray diffraction. The nickel center(II) owns a quasi-square planar geometry. The pincer NHC- and a bromide- ligands complete the coordination sphere. The UV-visible spectra of complexes **260** and **261** in solution are similar.

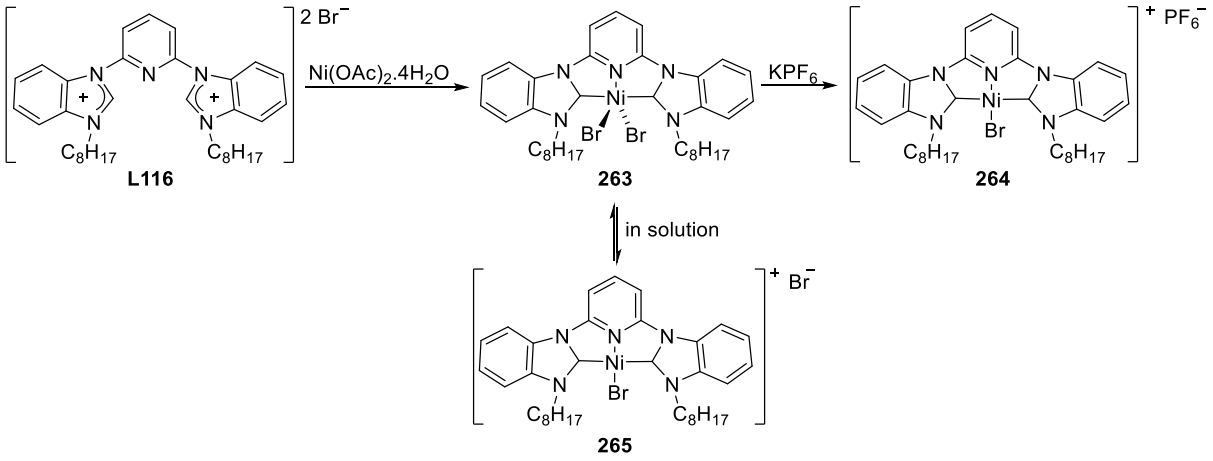

Scheme 69. Pincer bis-NHC pyridine Ni(II) complexes.[94]

As the lack of solubility of **254**-**255** was an issue, similar complexes with longer alkyl chains **263**-**265** were made. The reaction between the imidazolium salt **L116** and $Ni(OAc)_2•4H_2O$ led to the complex **263** in good yield (81%). Treatment of **263** by KPF_6 led to the complex **264** in moderate yield (43%). The complexes **263** and **264** were characterized by ^1H, $^{13}C\{^1H\}$ NMR spectroscopy. The nickel bound carbene signals are visible at 172.0 (**263**) and 169.8 ppm (**264**). X-ray diffraction studies unveiled a nickel center with trigonal bipyramidal geometry for **263**. The two bromide ligands in the apical positions and the NHC pincer ligand in the equatorial positions complete the coordination sphere. The $Ni–C_{carbene}$ bond distances (1.891(2) and 1.890(2) Å) are shorter than those reported by Danopoulos for **178** and **181**.[63] Interestingly, the structure of **254** and **263** were the first examples of five-coordinated nickel complexes characterized by crystallography with this class of pincer. Usually, this scarce geometry is observed with benzimidazolin-2-ylidene pincers rather than with imidazolin-2-ylidene pincers.

The UV-visible spectrum of **263** in methanol was similar to that of **264** in methanol or dichloromethane. However, the UV-visible spectrum of **263** in dichloromethane was quite different. These data corroborates the fact that dissolving **264** in methanol or dichloromethane, and dissolving **263** in methanol form the same four-coordinated species. The spectrum of **263** recorded in dichloromethane relates likely to a five-coordinated species. The addition of Bu_4NBr to a solution of **264** in dichloromethane changed significantly the feature of the spectrum and made it suitable for a five-coordinated species, while no change occurred in methanol. This behavior is consistent with equilibrium between the five-coordinated complex **263** and the four-coordinated complex **265**. When water was added to

263 in dichloromethane (in the miscible limits), the equilibrium shifted toward **265**. The complexes **254** and **260** were tested for Kumada reaction.

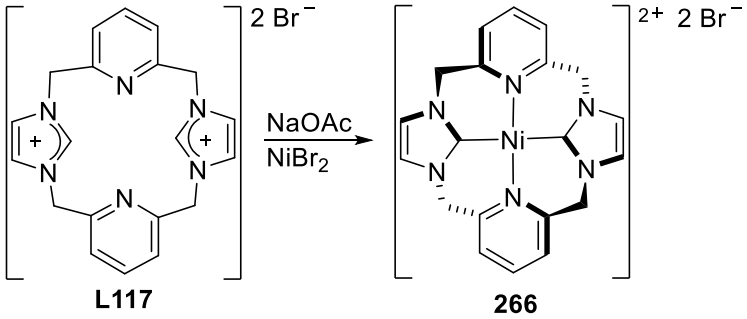

Scheme 70. Cyclic bis-NHC complex.[95]

Baker *et al.* reported the only known nickel(II) bis-NHC cyclic complex in 2002.[95] The reaction of the imidazolium bromide salt **L117** with NaOAc and $NiBr_2$ for 3 days at 85 °C led to the nickel(II) complex **266** in moderate yield (52%). Its ^{1}H NMR spectrum displays an AB pattern for the benzylic protons, indicating a restriction of the conformational mobility of the cyclophane scaffold. Its $^{13}C\{^{1}H\}$ NMR spectrum displays a nickel bound carbene signal at 165.3 ppm. The simplicity of both spectra suggests a puckered conformation of the nickel cation with C_2 axes defined by the two carbene sites or pyridine nitrogen atoms. The ^{1}H NMR spectrum of **266** did not change upon addition of 2 equiv. of $AgNO_3$ while a colored and light sensitive precipitate was appearing (possibly AgBr), consistently with the presence of similar nickel cationic cores ($[Ni(bis\text{-}NHC)\text{-}pyr]^{2+}$) with non-coordinating bromide or PF_6^- anions. Single crystal X-ray diffraction study confirmed this hypothesis. The nickel(II) center owns a square planar geometry. Two NHC- and two pyridine- ligands complete the coordination sphere. The bromides anions are of each side of the four-coordinated plane, creating a pseudo-octahedral geometry. The $Ni–C_{carbene}$ bond distances (1.870(8) and 1.834(9) Å) are shorter than those of **178** and **181**.

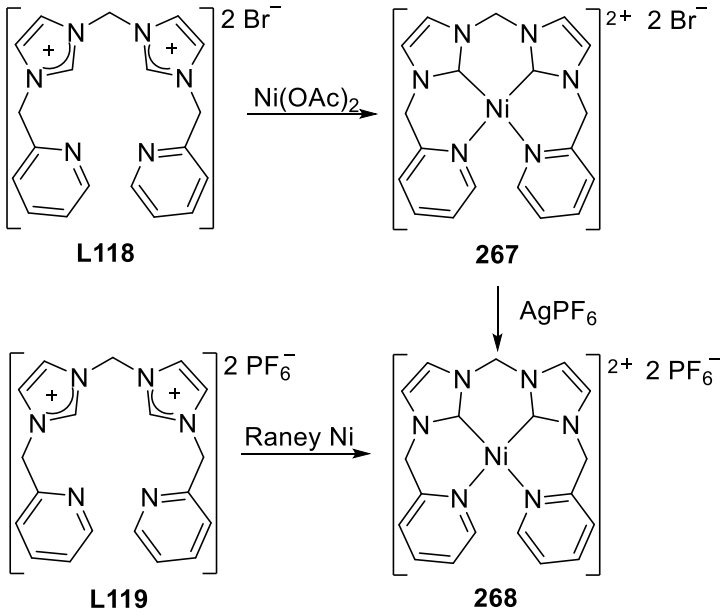

Scheme 71. Tetrapodal bis-NHC Ni(II) complexes.[96]

The reaction of the imidazolium bromide salt **L118** with $Ni(OAc)_2$ in DMSO for 2-5 at 50 °C allowed the formation of the C,C,N,N-nickel(II) complex **267** quantitatively.[96a] The reaction time is considerably shorter than that employed by Baker *et al.* for the C,N,C-cyclophane complex **266** synthesis. The complex **267** is only soluble in DMF and DMSO. It should be quoted that attempts on making **266** via transmetalation from NHC silver(I) complexes were unsuccessful. The ^{1}H NMR spectrum of **266** displays two sharp singlets at 6.32 and 5.83 ppm assignable to the methylene bridges protons. The magnetic equivalence of these protons can be due to fast changes of conformations in solution. Moreover, the addition of 10 equiv. of Bu_4NBr or Bu_4NI or a trace of trifluoroacetic acid did not affect the 1H NMR spectrum of **267**. $AgPF_6$ was attempted. Reaction of **267** with $AgPF_6$ afforded the complex **268** in good yield (77%). DFT calculations demonstrates that in solution the tetradentate ligand chelates the nickel center Low temperature ^{1}H NMR analyses of **229** and **230** display some overlapping broad signals indicating rapid twist-motions of the ligands, on the NMR time scale. The $^{13}C\{^{1}H\}$ NMR spectrum displays a carbene signal at 149.6 ppm. X-ray diffraction studies unveiled a nickel center with a tetrahedral geometry rather than a square planar due to a lack of space to accommodate two incoming *cis*-pyridine rings. As expected the tetradentate pincer-ligand helically completes the coordination sphere. A bromide anion has a short contact distance with the nickel center (3.006 Å). The $Ni–C_{carbene}$ bond distances (1.862(5) Å) are similar to those of **268**.

Seven years later, Chen *et al.* reported a second protocol to synthesize the complex **268**.[96c] The nickel(II) complex **268** was easily synthesized, under air conditions, by reaction of the imidazolium hexafluorophosphate salt **L119** with freshly prepared Raney nickel powder (80%). Using the Raney nickel method led to a better yield because the one step reaction does not require any bis-NHC nickel intermediate. The complex **268** was used as carbene transfer reagent for palladium chemistry.[96b,c] It was also tested for Negishi and Kumada reactions.[97]

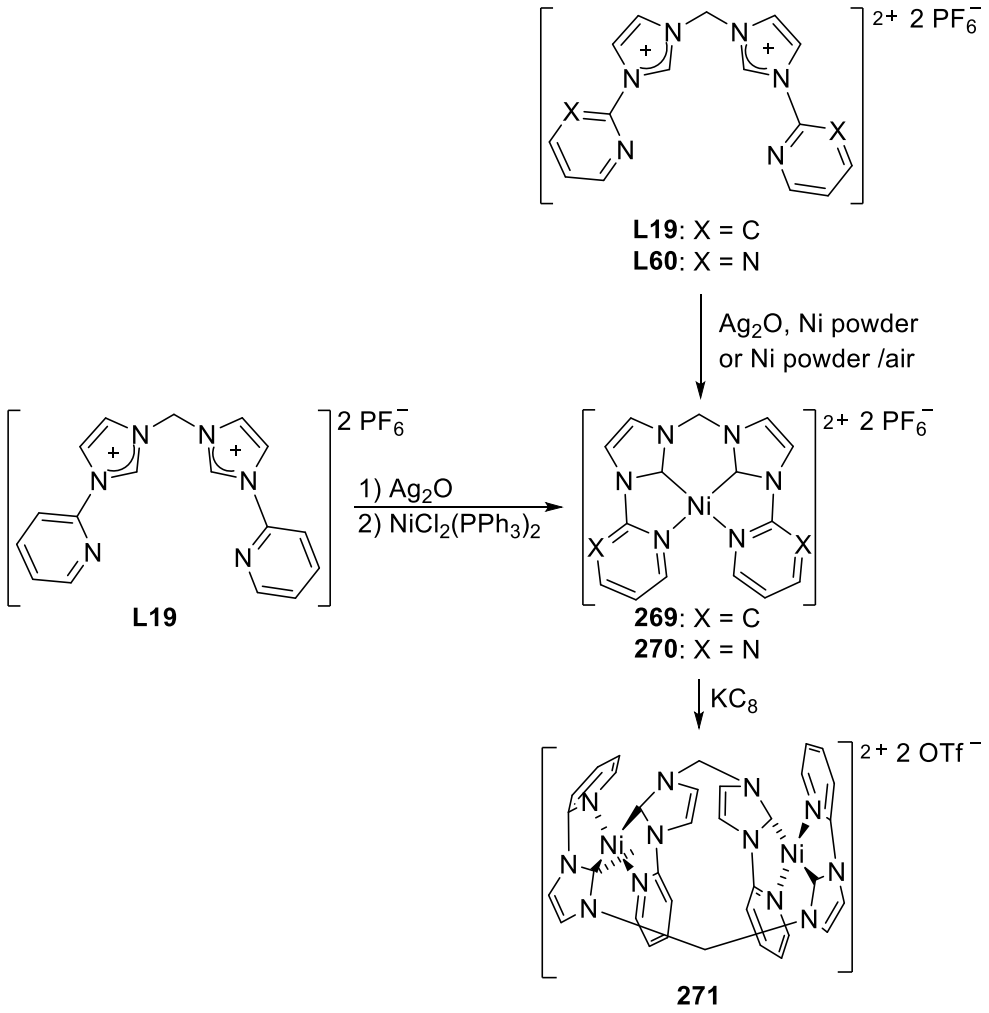

Scheme 72. Formation of dinuclear Ni(II) complexes.[29,38,97-98]

Chen *et al.* reported the complex **269** using four different pathways.[29,38,68b,98a] The first pathway (73%) consisted in carbene transfer reaction between $NiCl_2(PPh_3)_2$ and the silver(I) complex generated *in situ* from the salt **L19** and Ag_2O.[98a] The second pathway (43%) relied on the electrochemical oxidation of nickel(0) plate and imidazolium hexafluorophosphate salt **L19**.[68] The third pathway (94%) was based on the reaction of nickel(0) powder with the parent silver(I) complex generated *in situ* from **L19** and silver oxide. Finally, the fourth

pathway (30-50%) consisted in reacting **L19** directly with nickel(0) powder without using any silver intermediates.[29,38] The complex **269** was characterized by ^{1}H, $^{13}C\{^{1}H\}$ NMR spectroscopy and X-ray diffraction studies. The nickel bound carbene signal is visible at 158.9 ppm. The nickel center exhibits a square planar geometry. The tetradentate ligand completes the coordination sphere. The Ni–$C_{carbene}$ bond distances are equal to 1.809(3) Å.

Similarly to **269**, **270** was accessible through the second (76%), third (75%) and fourth pathways (30-50%). It was characterized by ^{1}H, $^{13}C\{^{1}H\}$ NMR spectroscopy and elemental analysis. The nickel bound carbene signal is visible at 161.3 ppm. As for the complex **268**, the complex **269** was tested for Kumada and Negishi reactions.[97]

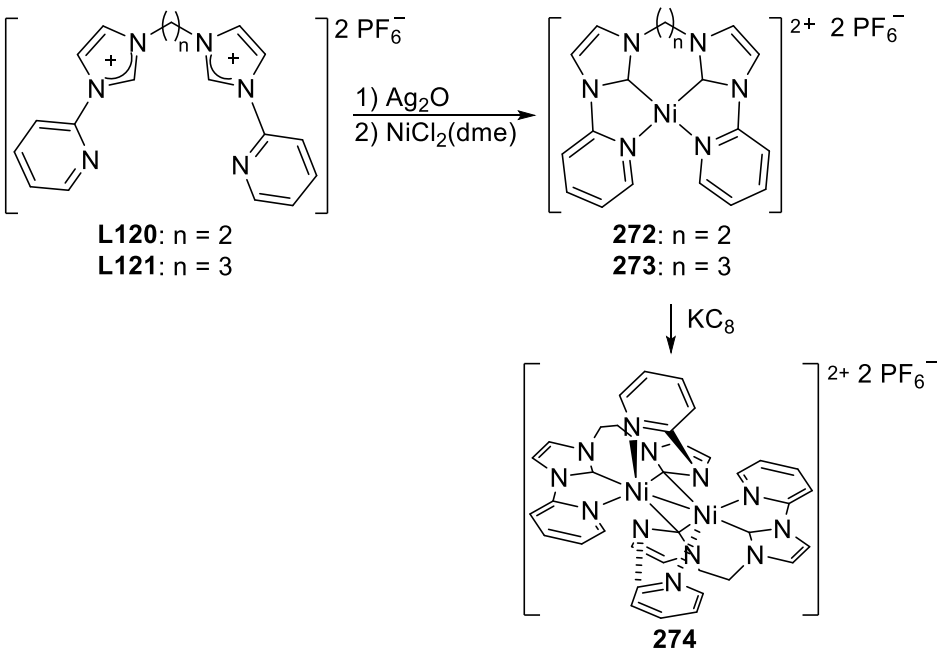

Scheme 73. Formation of dinuclear Ni(II) complexes.[98b]

Chang *et al.* reported two analogous complexes to **269** with ethylene or propylene linkers.[98b] Similarly to **269**, the silver(I) complexes, generated *in situ* by mixing the imidazolium salts **L120** or **L121** with Ag_2O, reacted with $NiCl_2$(dme) to afford the the nickel(II) complexes **272** or **273** in 40% yield or quantitatively. $TlPF_6$ was added at the end of the synthesis from **L121** in order to obtain the complex **273** quantitatively. The complexes **272** and **273** were characterized by ^{1}H, $^{13}C\{^{1}H\}$ NMR spectroscopy and X-ray diffraction studies. However, the $^{13}C\{^{1}H\}$ NMR spectra were not assigned. For both complexes, the nickel(II) centers exhibit a distorted square planar environment. The distortion becomes more important as the pincers length increases, rendering the geometry more tetrahedral-like, with higher dihedral angles between the planes formed by each half of the ligand: **269** (2.2 °C) to

272 (19.4 °C) to **273** (31.0 °C). The Ni–$C_{carbene}$ bond distances in **272** (1.8473(15) Å) are almost the same as those of **273** (1.854(3) and 1.856(3) Å).

The cyclic voltammogram of **269** exhibits an irreversible oxidation at - 0.29 V, an irreversible reduction at - 0.84 V and a reversible reduction at 1.69 V, relative to SCE. However, for **272** and **273**, two reversible reductions are observed respectively at - 0.86 , - 1.54 and - 0.80, - 1.46 V. The potential of the second reduction shifts into potentials that are more positive as the length of the linker increases.

The reduction of the complexes **269** and **272** by KC_8 led to **271** (92%) and **274** (82%) which were characterized ^1H, $^{13}C\{^1H\}$ NMR spectroscopy and X-ray diffraction studies. Variable temperature ^1H NMR experiments with **274** shows significant fluxional behavior (complex may adopts different geometries), contrary to **271**. In the solid state, the complex **271** exhibits dimerization in a "butterfly" fashion. A NHC- and a pyridine- sites from each ligand coordinate the nickel(II) center. The Ni–Ni bond distance is equal to 2.5087(10) Å.

The complex **274** owns a diamond core Ni_2C_2 due to the presence of bridging and chelating modes of coordination for both NHC ligands. The Ni–Ni bond distance (2.5790(6) Å) is longer than that of **271**. The Ni–$C_{carbene}$ bond distances of **271**-**274** fall in the range of 1.865(4)-1.924(3) Å.

The cyclic voltammogram of **271** reveals a quasi-reversible reduction wave at - 0.29 V, which coincides to the irreversible oxidation wave of **269** at - 0.29 V. Therefore, the irreversible oxidation of **269** to **271** is assignable at - 0.29 V. The cyclic voltammograms of **274** and **272** display similar behaviors; the quasi-reversible wave at - 0.8 V for **274** and the irreversible oxidation at - 0.80 V for **272** indicate that the irreversible oxidation wave at - 0.80 V corresponds to the transformation of **272** in **274**. The complexes **269**, **272** and **273** were tested for the catalytic electrochemical reduction of CO_2 to CO.

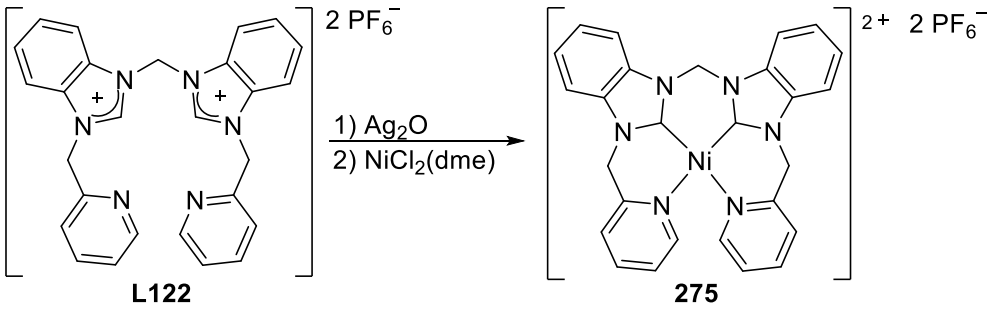

Scheme 74. Tetrapodal bis-NHC complex.[98a]

The reaction of the silver(I) complex, generated *in situ* from the imidazolium salt **L122** and Ag_2O, with $NiCl_2(dme)_2$ led to the nickel(II) complex **275** in good yield (62%).[93a] The complex was characterized by ^{1}H, $^{13}C\{^{1}H\}$ NMR spectroscopy and X-ray diffraction studies. The nickel bound carbene signal is visible at 159.0 ppm. The nickel(II) center owns a square planar environment. The coordination sphere is completed by the tetradendate bis-NHC ligand. The two NHC sites are in *cis*-position as well as the two pyridine rings. The Ni–$C_{carbene}$ bond distances (1.836(8) and 1.848(9) Å) are in the range of those previously reported.[93-94] The pyridine- and NHC- rings are not coplanar due to steric hindrance. As for **268**, the complex **269** was tested for of Kumada and Negishi[97] reactions, and reduction of CO_2 to CO.[99]

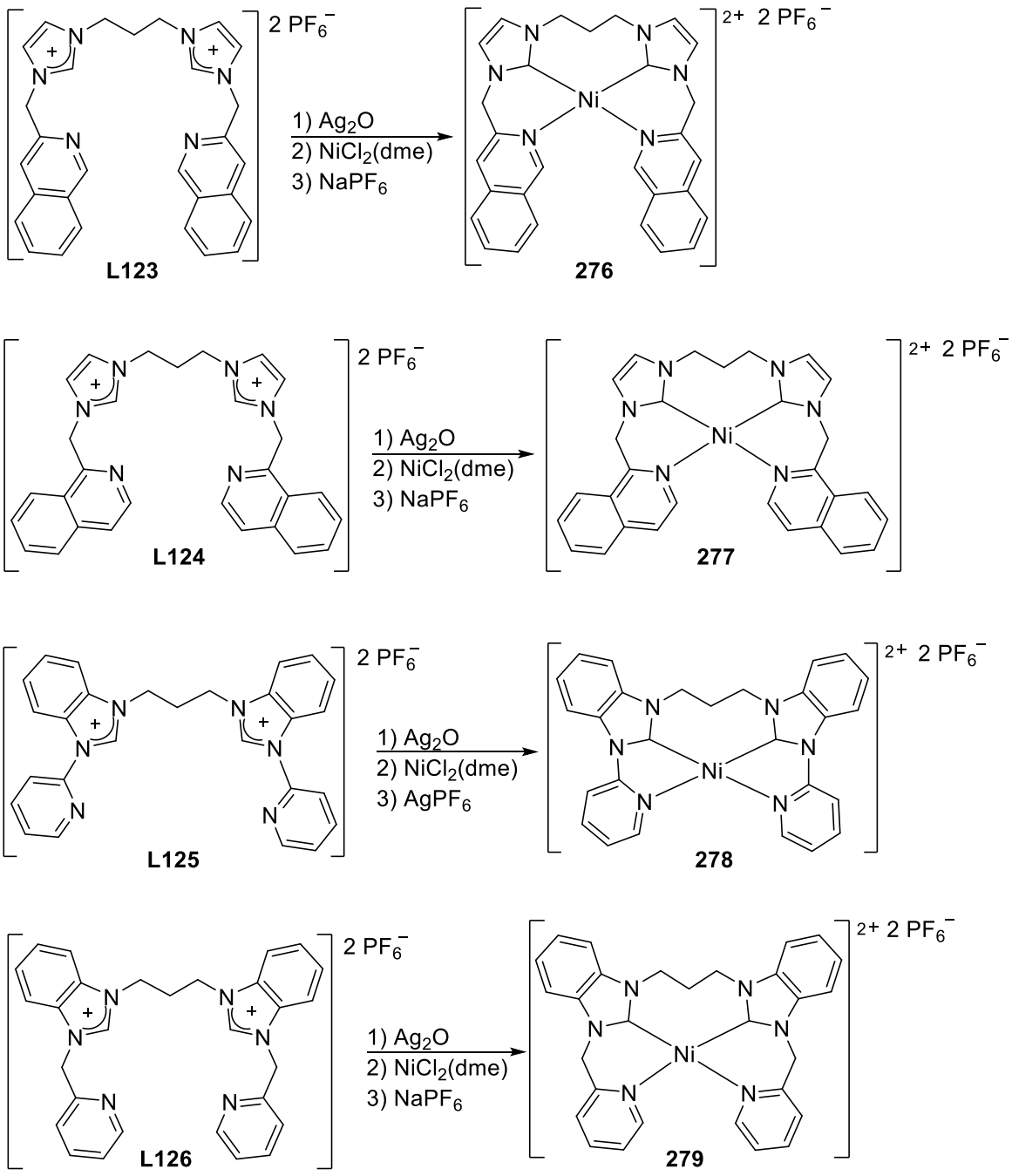

Scheme 75. Tetrapodal bis-NHC complexes.[99]

The reaction between **L123-L126** and silver oxide followed by transmetalation with $NiCl_2$(dme) and treatment with $NaPF_6$ or $AgPF_6$ led to **276-279** in good yields (> 70%). The nickel(II) complexes were characterized by ^1H, $^{13}C\{^1H\}$ NMR spectroscopy and X-ray diffraction studies, even though the $^{13}C\{^1H\}$ NMR spectra signals were not assigned. For **276-279**, the nickel centers exhibit a distorted square planar geometry. The Ni–$C_{carbene}$ bond distances fall in the range 1.843(4)-1.904(4) Å, in agreement with the literature.[97-98] The propyl spacer permits a large degree of flexibility. The torsion angles formed by $N_{pyridine}$–Ni–

$N_{pyridine}$–C_{ortho} in complexes **275-279** are in the range 24.7-57.2°. The complexes **275-279** were tested for CO_2 electrocatalytic reduction.[99]

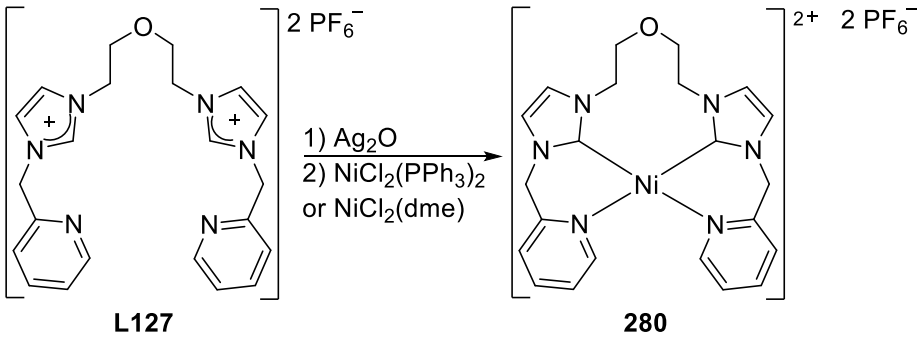

Scheme 76. Tetrapodal bis-NHC complex.[97a]

The carbene transfer reaction with the silver(I) complex, generated *in situ* from **L127** and Ag_2O, led to the nickel(II) complexes **280** in moderate yield (53%).[97a] It was characterized by ^1H, $^{13}C\{^1H\}$ NMR spectroscopy and X-ray diffraction studies, even though the $^{13}C\{^1H\}$ NMR spectrum signals were not assigned. The nickel(II) center owns a square planar geometry. The tetradentate bis-NHC ligand completes the coordination sphere. The Ni–$C_{carbene}$ bond distances (1.885(7) and 1.900(7) Å) are in agreement with the literature.[96a,98-99] The complex **280** was tested for Negishi and Kumada reactions.[97]

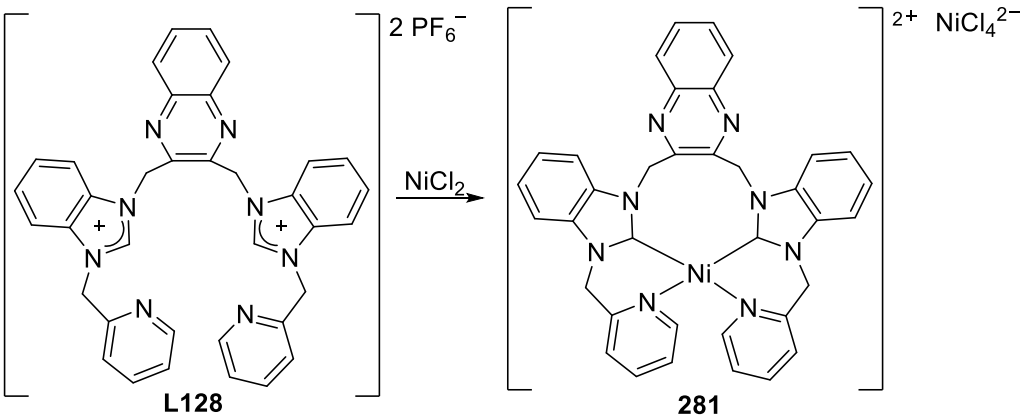

Scheme 77. Tetrapodal bis-NHC complex.[100]

The reaction between the imidazolium hexafluorophosphate salt **L128** and $NiCl_2$ led to the nickel(II) complex **281** (32%).[100] It was characterized by ^1H, $^{13}C\{^1H\}$ NMR spectroscopy and X-ray diffraction studies. The nickel bound carbene signal is visible at 154.5 ppm. The nickel(II) center owns a square planar geometry. The tetradentate bis-NHC ligand completes the coordination sphere. The Ni–$C_{carbene}$ bond distances are equal to 1.883(3) Å.

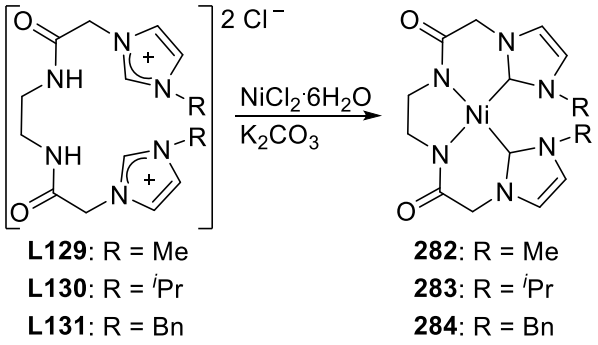

Scheme 78. Bis-NHC amido Ni(II) complex.[101]

The reaction of the imidazolium chloride salts **L129-L131** with $NiCl_2$•$6H_2O$ in presence of K_2CO_3 led to the complexes **282-284** in good yield (64-66%).[101] In the ^1H NMR spectra, the amido-NH protons are absent indicating the formation of a Ni-amide bond. In the $^{13}C\{^1H\}$ NMR spectra, the nickel bound carbene signals are visible at 116.7 (**282**), 166.2 (**283**) and 166.0 ppm (**284**). The ^1H NMR spectra obtained in D_2O and DMSO-d_6 are similar, proving that the complexes are soluble and stable in water, in the view of further biomedical applications. In the solid state, the complexes **282-284** own a nickel center with a distorted square planar environment. The tetradentate bis-NHC ligand completes the coordination sphere. The Ni–$C_{carbene}$ bond distances are equal to 1.8670(19) and 1.8590(18) Å in **282**, 1.870(3) Å in **283** and 1.8644(15) and 1.8637(16) Å in **284**. The complexes **282-284** exhibited significantly subdued cytotoxic activities towards two human cancer HeLa and MCF-7 cells and a non-tumorigenic HCO cell, compared to $NiCL_2$•$6H_2O$ alone. Moreover, morphological studies revealed that **284** caused minimum surface abnormality on cancer cells in agreement with its reduced cytotoxic activity.

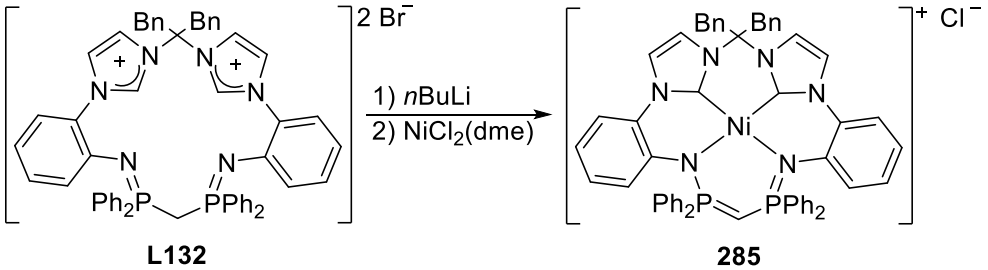

Scheme 79. Tetrapodal bis-NHC complex.[102]

Zhang and Wang reported the synthesis of **285** in good yield (82%) by reaction of the imidazolium bromide salt **L132** with *n*BuLi followed by the addition of $NiCl_2$(dme). Its ^1H NMR spectrum features a triplet for the PC*H*P proton and a unique set of signals per $PhCH_2$ group or NHC moieties. The $^{13}C\{^1H\}$ NMR spectrum also gave a unique set signals per

$PhCH_2$ or NHC moieties. The nickel bound carbene signal is visible at 161.2 ppm. The $^{31}P\{^1H\}$ NMR spectrum displays a signal at 26.0 ppm. The NMR data suggest symmetrical coordination geometry and the formation of a methanide (PCHP) group. The structure of **285** was solved by X-ray diffraction studies even though the quality data was poor. The nickel center owns a square planar environment. The tetradentate NHC ligand completes the sphere of coordination with the NHC sites in *trans* arrangement due to steric repulsion. The phenylene groups of the pincer ligands lie on a side of the plane containing the nickel center and the carbene sites. The complex **285** was tested for Kumada and Negishi reactions.[102]

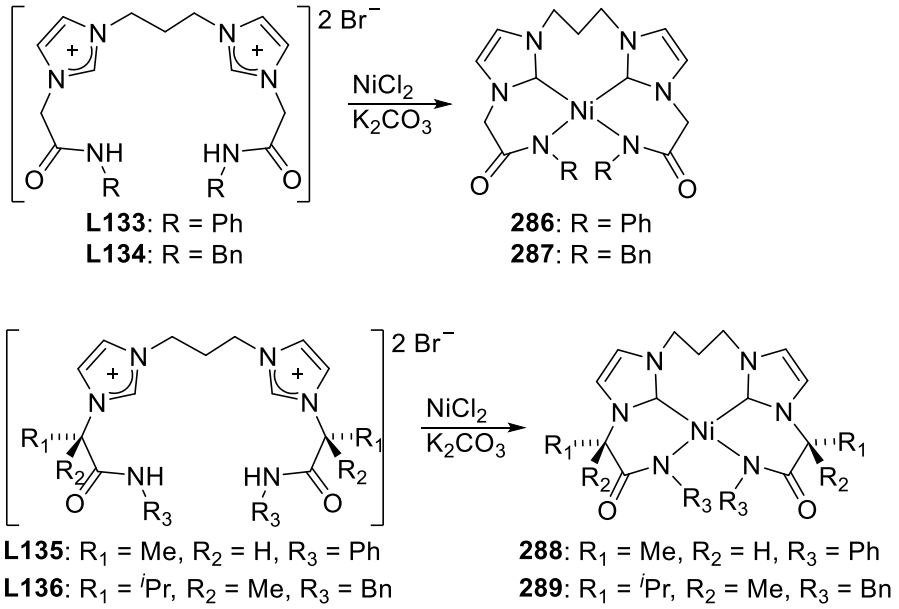

Scheme 80. Tetrapodal bis-NHC complex.[103]

Gornitzka *et al.* reported the complexes **286**-**289** using the procedure established by Lee *et al.*[103] for the formation of bis(amino-NHC) nickel(II) complexes. The reaction between the imidazolium bromide salts **L133**-**L136**, $NiCl_2$ and K_2CO_3 led to the complexes **286**-**289** in good yields (52-87%). Their ^1H NMR spectra feature some scaffolds with symmetry elements. The absence of the amide- and azolium signals suggests the formation of tetradentate bis-NHC nickel complexes. The $^{13}C\{^1H\}$ NMR spectra of **286** and **287** exhibit nickel bound carbene signals at 161.8 and 161.2 ppm. Elemental analysis and mass spectroscopy suggest neutral monomeric species. X-ray diffraction studies corroborate all these assumptions. The complexes exhibit a nickel center with a square planar environment. The $Ni–C_{carbene}$ bond distances are in the range 1.867(3)-1.886(2) ppm, in agreement with **282**-**284** previously described.

The ^{1}H and $^{13}C\{^{1}H\}$ NMR spectra of complex **288** suggest the presence of a racemic mixture of two enantiomers, each or them having also two types of conformers. The $[\alpha]_D$ in solution is equal to +8.5°. A NMR ROESY analysis confirms the presence of the four diastereoisomers. The racemization of the two chiral centers is surely due to the mobility of the hydrogen atom bore by asymmetric carbon under the conditions of complexation. In the solid state, the nickel(II) center owns a distorted square planar environment. The tetradendate bis-NHC ligand completes the coordination sphere. The Ni–$C_{carbene}$ bond distances (1.886(2) Å) are similar of those in complexes **286**-**287**.

Finally, the complex **289** was synthesized to obtain an enantiopure sample. A methyl group replaced the labile proton born by the chiral carbon. The ^{1}H and $^{13}C\{^{1}H\}$ NMR data are similar to those of **286**-**287**. The complex **289** was indeed enantiopure. It has a high $[\alpha]_D$ value of + 85.5°. Its molecular structure exhibits a nickel(II) center with a distorted square planar geometry. It was the first structurally characterized complex with a chiral tetradentate bis-NHC ligand. The Ni–$C_{carbene}$ bond distances (1.887(4) and 1.888(4)) are similar to those of **286**-**288**.

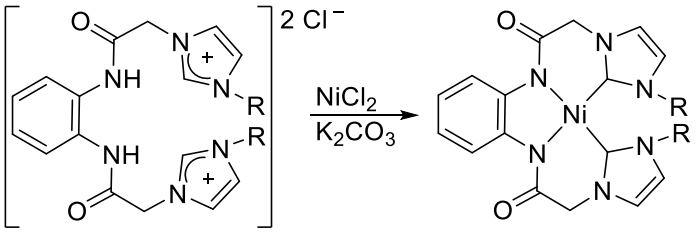

Scheme 81. Bis-NHC amido Ni(II) complex.[104]

The complexes **290** and **291** were obtained by reaction between the imidazolium chloride salts **L137**-**L138** and $NiCl_2$ in presence of K_2CO_3 in low yields (21-23%).[104] Their ^{1}H NMR spectra display some methylene protons with AX pattern for **290** and AB pattern for **291** characteristic of specific stereoisomers, not interconverting on the NMR time scale. The $^{13}C\{^{1}H\}$ NMR spectra, display the nickel bound carbene signals at 162.7 and 164.1 ppm for **290** and **291**. The nickel(II) exhibits a distorted square planar environment due to the steric repulsion between the N-methyl- or N-phenyl- groups born by the imidazole rings. The tetradendate bis-NHC ligand completes the coordination sphere. The Ni–$C_{carbene}$ bond distances (1.857(3), 1.851(3) and 1.860(2), 1.865(2) Å) in **290**-**291** are in agreement with the literature.[102] Finally, DFT calculations and comparison with organopalladium chemistry

demonstrate that NHC abnormal binding mode results in higher energy structure with nickel (kinetic product in this case).

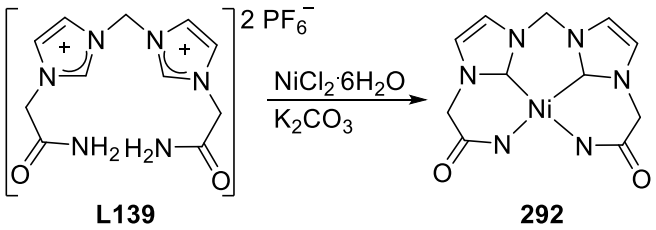

Scheme 82. Bis-NHC amido Ni(II) complex.[50]

The reaction between $NiCl_2$•$6H_2O$ and the imidazolium hexafluorophosphate salt **L139** in presence of K_2CO_3 led to the nickel(II) complex **292** in good yield (71%).[50] The complex **292** was characterized by ^1H and $^{13}C\{^1H\}$ NMR spectroscopy, with the resonance of the nickel bound carbene at 157.4 ppm. In the solid state, the nickel(II) center owns a square planar environment. The tetradentate bis-NHC ligand completes the coordination sphere. The $Ni–C_{carbene}$ bond distances are equal to 1.8530(19) and 1.8514(18) Å in the range of similar complexes (e.g. **282**-**284** or **290**-**291**). Cyclic voltammetry studies evidenced a quasi-reversible one-electron process observed at + 0.89 V for the couple $[Ni(II)/Ni(III)]^+$. EPR spectroscopy in solution at 140K gave rise to an axial spectrum with rhombic distortion. Such signature is typical for d^7 nickel(III) with an unpaired electron in the d_{z2} orbital. It confirms that **292** underwent metal-centered oxidations with the ligand remaining innocent.

2.9 Copper

In the literature, only a few reports deal with the synthesis of chelating bis-NHC copper complexes.

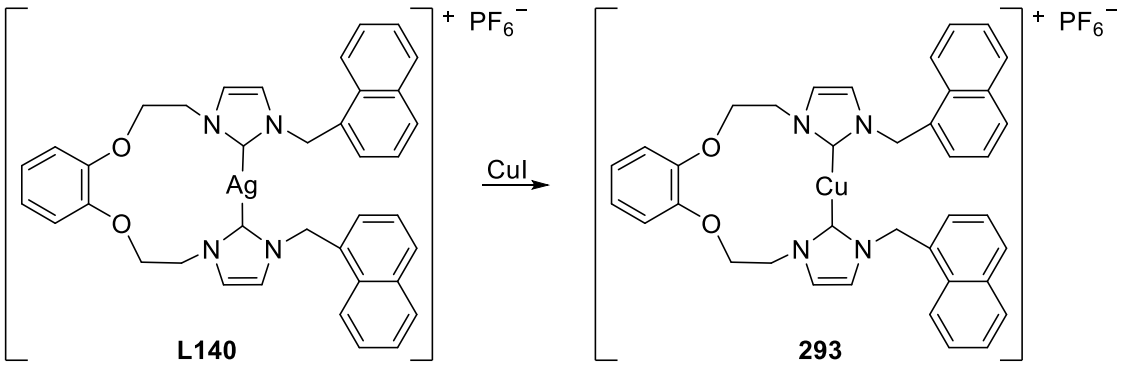

Scheme 83. Bis-NHC Cu(I) complex.[105]

The reaction between the silver(I) complex **L140** and CuI led to the copper(I) complex **293**, by transmetalation, in very good yield (83%).[105] The complex **293** is relatively air stable and slightly light sensitive. It was characterized by ^{1}H NMR spectroscopy and single crystal X-ray diffraction. The geometry around the copper(I) center is linear with an angle $C_{carbene}$–Cu–$C_{carbene}$ of 174.2(2)°. The Cu–$C_{carbene}$ bond distances are equal to 1.960(6) and 1.940(6) Å.

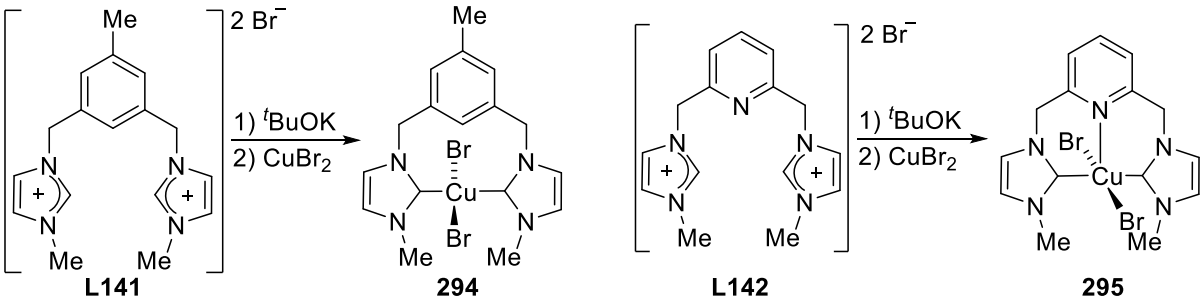

Scheme 84. NHC Cu(II) complexes.[106]

Scholz *et al.* reported the synthesis of **294**-**295** and their investigation on copper-catalyzed monoarylation of aniline (see section 7).[106] The imidazolium bromide salts **L141**-**L142** reacted with ^{t}BuOK and $CuBr_2$ to form the copper(II) complexes **294** and **295** (no yield provided). The complexes were not characterized. The crude reaction mixtures were dried and used straight for catalysis.

2.10 Zinc

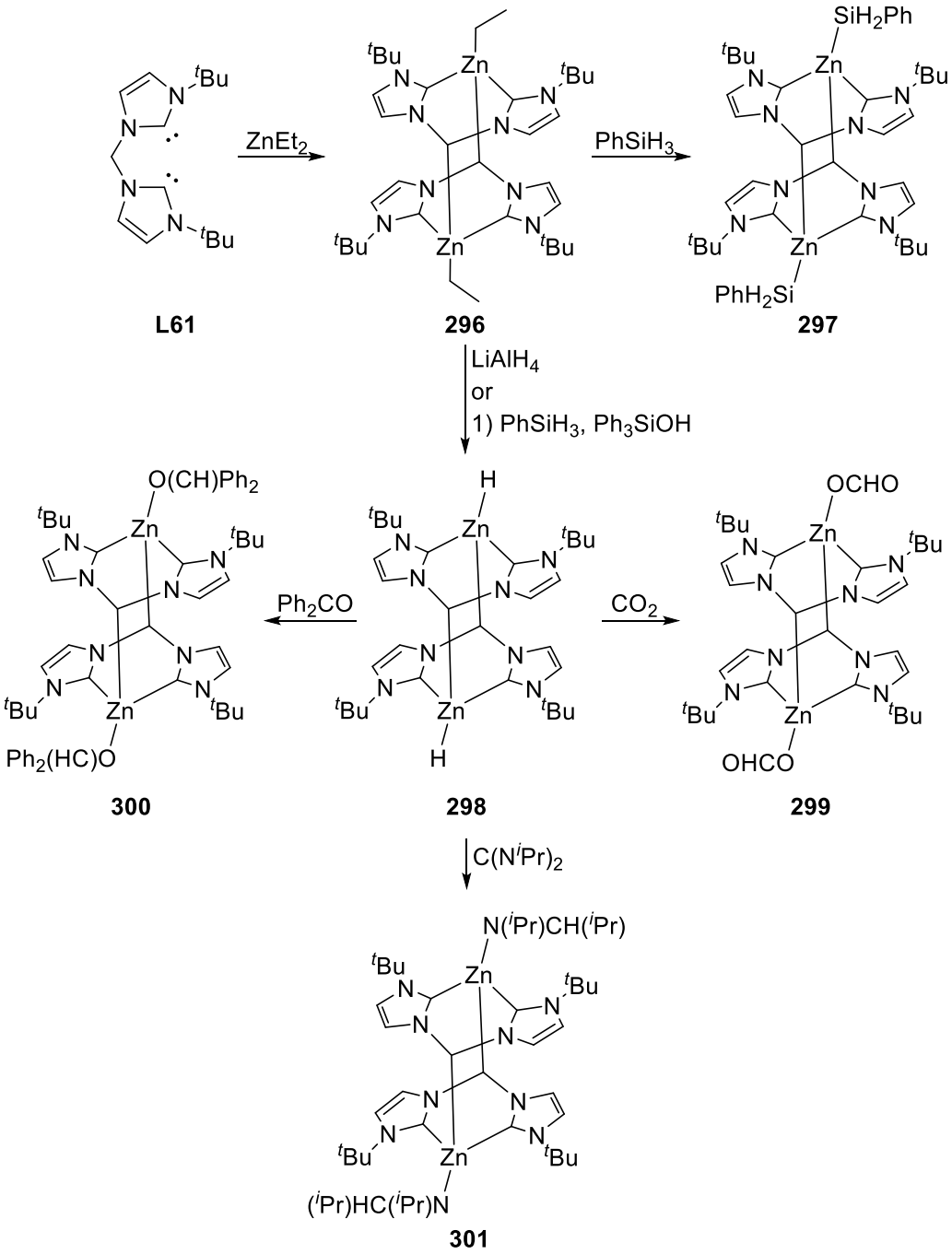

Scheme 85. Bis-NHC methylidyne Zn(II) complexes.[107]

The reaction of the free bis-NHC **L61** with $ZnEt_2$ led to the zinc(II) complex **296** in high yield (88%).[107] The sp^3 C–H activation similar to that producing analogues of **258** with other alkyl metal precursors led to mixtures of inseparable products.[18] The ^1H NMR spectrum reveals the deprotonation of the methylene bridge, and a unique set of signals hinting at a scaffold with symmetry elements. The $^{13}C\{^1H\}$ NMR spectrum displays the zinc bound

carbene signal at 186.4 ppm, in agreement with the literature.[108] The complex **296** did not react with dihydrogen.

The treatment of **296** by $PhSiH_3$ gave the zinc(II) complex **297** in low yield (38%) instead of the desired hydride complex. The ^1H NMR spectrum displays a set of signals with a ratio 1:1 for the bis-NHC- and SiH_2Ph- ligands. The resonance of the silyl ligands is at 4.0 ppm. The $^{29}Si\{^1H\}$ NMR spectrum displays silyl-groups signal at -57.3 ppm. The resonance of the carbene appears at 183.6 ppm in the $^{13}C\{^1H\}$ NMR spectrum.

The reaction of **296** with $LiAlH_4$ allowed the formation of the hydride zinc(II) complex **298** in moderate yield (52%). Reaction between **296** and Ph_3SiOH, followed by the addition of $PhSiH_3$ led to the same complex in better yield (71%). The ^1H NMR spectrum reveals a broad signal at 4.1 ppm assignable to the hydride. The resonance of the methylidyne bridges appear as a doublet due to the coupling with the hydride. On the $^{13}C\{^1H\}$ NMR spectrum, the signal of the carbene is visible at 187.5 ppm. The infrared spectrum displays a vibrational band at 1458 cm^{-1} corresponding to the Zn–H bond. The treatment of **296** with alcohols (i.e. MeOH, Me_3SiOH) led to complicated mixtures of products. The complex **298** was tested for methanolysis and hydrosilylation reactions.

The reaction of **298** with CO_2 led to the complex **299** by double insertion into the Zn–H bond (85%). The signals at 8.68 and 167.9 ppm on the ^1H and $^{13}C\{^1H\}$ NMR spectra confirm the presence of the formate ligand.[109] The resonance of the zinc bound carbene is visible at 180.4 ppm. The CO bands on the infrared spectrum come out at 1621 and 1319 cm^{-1}, indicating a κ^1 coordination.

Treatment of **298** by benzophenone and (^{i}PrN$_2$)C gave **300** and **301** in good yields (79 and 78%). ^1H NMR monitoring experiments indicate the complete consummation of the hydride complex within 1 h. The presence of the alkoxy and formamidinato ligand was confirmed by signals at 6.17 and 6.74 ppm in the ^1H NMR spectra and at 83.0 and 161.4 ppm on the $^{13}C\{^1H\}$ NMR spectra.[110]

The complexes **298-301** were characterized by single crystal X-ray diffraction and present some similitudes. The zinc(II) centers exhibit a distorted tetrahedral environment. The two NHC sites from the same ligand and the methylidyne from the second ligand coordinate a zinc cation. Two atoms of zinc and two methylidyne bridges from two bis-NHC ligands form a central core. Ethyl-, silyl-, hydride-, formate-, alkoxy- or formamidinato- ligands complete

the sphere of coordination. The Zn–$C_{carbene}$ bond distances fall in the range 2.095(2)-2.130(3) Å.

3 Syntheses and reactivity of bridging bis-NHC ligands

3.1 Chromium

In the literature, there are only three example of bridging bid-NHC chromium complexes reported.

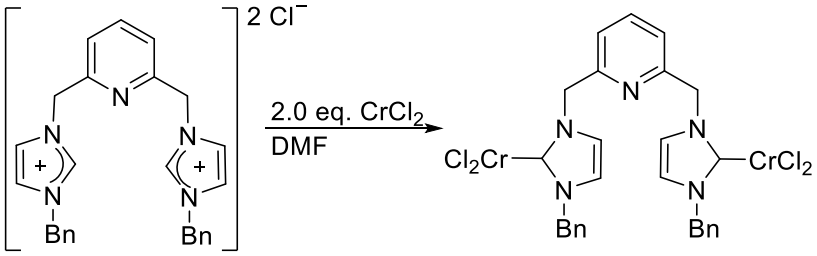

Scheme 86. Bridging bis-NHC Cr(II) complex.[17]

The imidazolium chloride salt **L14** was mixed with ^{t}BuOK and $CrCl_2$ in DMF. The crude reaction mixture was directly used to catalyze the transformation of sugars in HMF (see section 7).[17] The complex **302** was not charaterized.

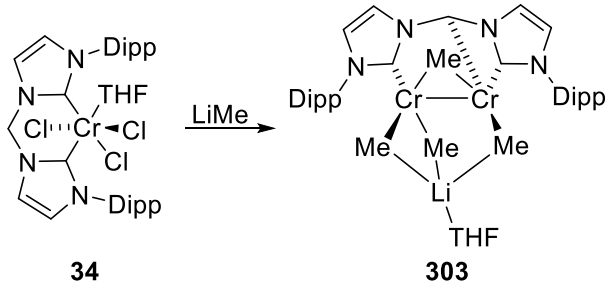

Scheme 87. Trinuclear lithium-chromium bis-NHC complex.[18]

Attempts to obtain an alkyl complex from **34** with LiR or RMgX (R = Me, CH_2SiMe, Ph, Tolyl CH_2CMe_3, X = Cl, Br) led to a mixture of intractable products. However, crystallization from the reaction mixture of **34** and MeLi allowed the collection of crystalline material (no yield value given).[18] Single crystal X-ray diffraction revealed the bimetallic complex **303.** The chromium(II) centers own a distorted square pyramidal with the second chromium center occupying the apical position. The methyl groups and NHC sites occupy the equatorial positions. The chromium(II) centers are bound to the same bis-NHC ligand. Three

terminal methyl- and a bridging methyl- groups complete the coordination spheres. The methylene bridge in **L16** was deprotonated leaving the THF-Li^+ cation balancing the anionic bis-NHC ligand. The lithium cation coordinated to a molecule of THF interacts strongly with the three terminal methyl groups likely due to their carbanionic character.

The $Cr–C_{carbene}$ bond distances (2.186(9) and 2.125(8) Å) are slightly shorter than the $Cr–C_{Me}$ bond distances (2.155(9), 2.172(9), 2.205(9), 2.158(9), 2.174(9) and 2.337(9) Å). The short Cr–Cr bond distance (1.897(2) Å) confirms that the presence of chromium(II) species.

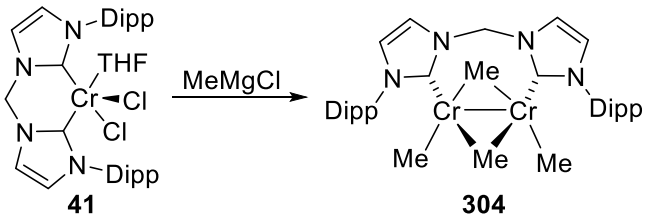

41 **304**

Scheme 88. Bi-NHC dinuclear chromium complex.[35]

Theopold *et al.* reported the synthesis, in moderate yield (57%), of the bimetallic bis-NHC chromium(II) complex **304** by treatment of **41** with MeMgCl.[35] The ^1H NMR spectrum displays sharp signals between 9.0 and 0.5 ppm and very broad signals of the methyl ligands at 0.1 and -0.1 ppm. The three resonances for the ^{i}Pr groups are present with a ratio of 6:6:12, their multiplicity and the protons of the methylene spacer suggest that **L16** has a rigid structure in solution. Variable temperature experiments between -30 and 50 °C confirms this statement. Moreover, the broad signals of the methyl groups are due to slow exchanges between terminal and bridging positions. No $^{13}C\{^1H\}$ NMR data are available. The formation of the bimetallic complex **304** and the loss of **L16** suggest that the chromium(II) center is too electron-rich to support the coordination of two strong donating NHC moieties and two methyl ligands under the addition of MeMgCl. The free bis-NHC **L16** released must had reacted with $MgCl_2$ present in the system and gave the precipitate (**L16**)$MgCl_2$. According to the authors, the mechanism may go through lengthening of the Cr–Cr bond, rearrangement of the methyl ligands and contraction of the Cr–Cr bond.[111] In the solid state, the complex **304** exhibit two chromium(II) centers with a square planar geometry and being bound to the same bis-NHC ligand. A terminal methyl- and two bridging methyl- ligands complete the coordination sphere. The $Cr–C_{carbene}$ bond distances (2.127(2) and 2.123(2) Å) are in the range of those reported in the section 2.4.[6a,b,12-13,16,17b,18]

3.2 Iron

The complex **305** was made, in good yield (68%), by reaction of the free bis-NHC, generated *in situ* from **L40** and *n*BuLi, with $CpFeI(CO)_2$ and subsequent irradiation in CH_2Cl_2.[112] The reaction was performed at low ligand concentration and temperature to avoid the formation of the chelate complex **75**.

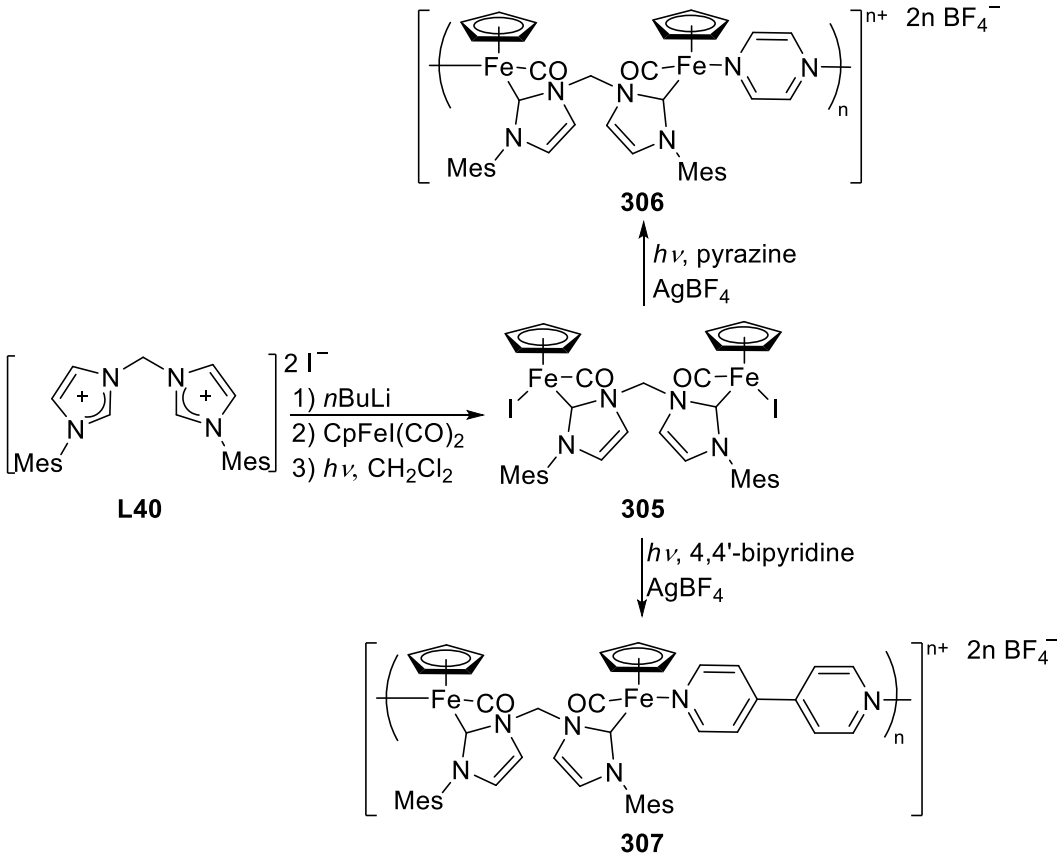

Scheme 89. Bis-NHC dinuclear Fe complexes.[112]

The ^{1}H NMR spectrum of **305** reveals the presence of diastereoisomers *rac* and *meso*. Integration of the Cp- and imidazole- signals confirms the bridging coordination mode of **L40**. The signal of the methylene protons appears as singlet for the major product and as AB doublet for the minor product. Thus, the major product is the *rac* isomer with identical iron chirality centers. The predominance of a diastereoisomer in bimetallic rhodium complexes containing similar bridging bis-NHCs is known.[113] The $^{13}C\{^1H\}$ NMR spectrum displays iron bound carbene signal at 192.1 ppm. The presence of the rac-isomer was confirmed by single crystal X-ray diffraction The iron(II) centers owns an octahedral environment being bound to the same bis-NHC ligand. The Cp- (η^5-coordination – 3 sites), iodide-, CO- and bis-NHC- (1 site per iron) ligands complete the coordination spheres. The Fe–$C_{carbene}$ bond distances

(1.955(5) and 1.977(6) Å.) are similar to those in complex **101** reported by the same group.[32b] The iron(II) centers are separated by 6.812(1) Å ruling out any direct electronic communication. Electrochemical studies reveal a reversible oxidation potential at +0.58 V, confirming this lack of metal-metal communication.

The treatment of **305** with pyrazine or 4,4'-bipyridine in presence of $AgBF_4$ led to the **306** and **307 (**No yield value indicated). ^1H NMR spectroscopy reveals various broad resonances and the UV-visible spectra are similar to the one of **305** with λ_{max} = 419 (**306**), 537 (**307**) and 444 (**307**) nm**.** Electrochemical analyses confirm the polymer formation of **305** and **306** with $E_{1/2}$ = + 1.26 V (**306**) and + 1.09 V (**307**).

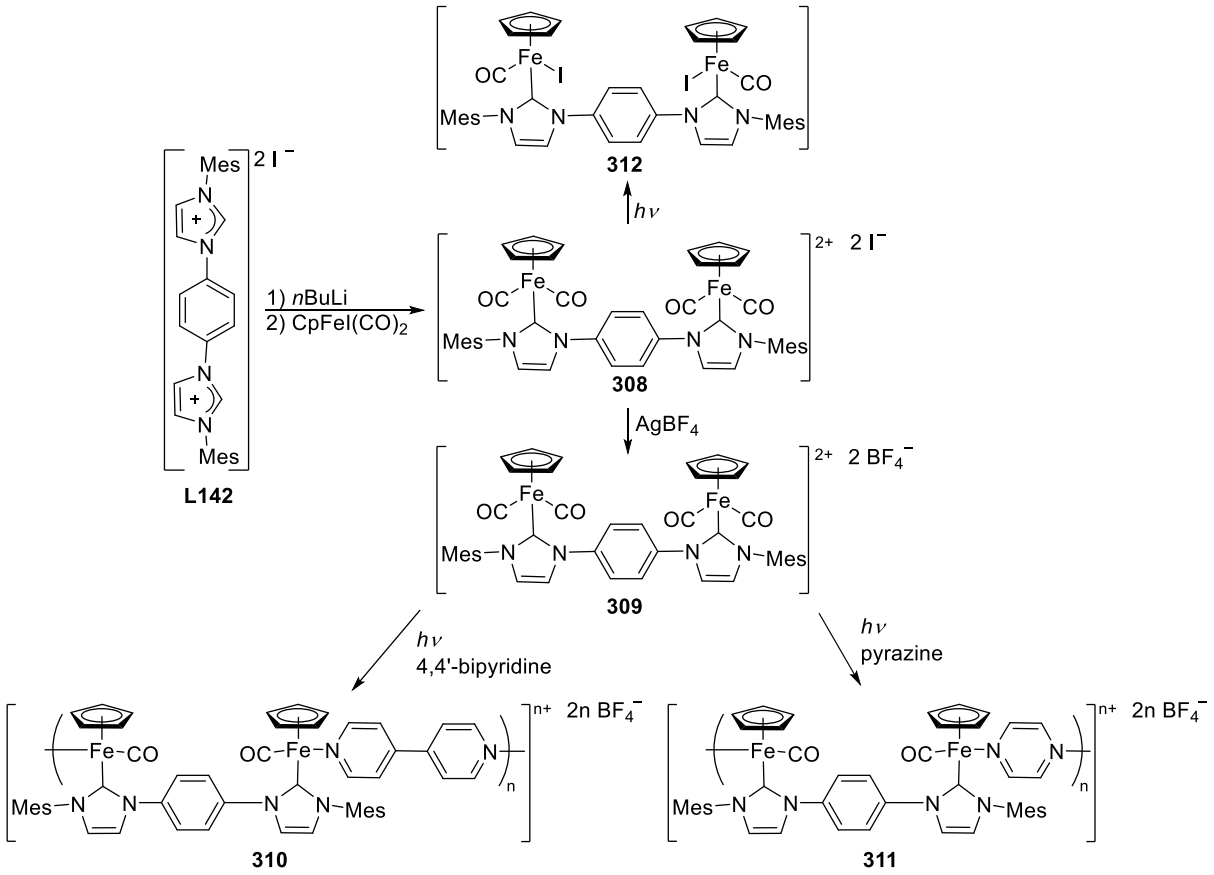

Scheme 90. Dinuclear bis-NHC Fe complexes.[112]

The deprotonation of the imidazolium iodide salt **L142** with *n*BuLi, followed by the addition of $CpFeI(CO)_2$ led to the iron(II) complex **308** in good yield (67%).[112] Similarly, to **305**, the reaction was carried out at low temperature even though **L142** cannot adopt a chelating coordination mode. The complex **308** was characterized by ^1H, $^{13}C\{^1H\}$ NMR spectroscopy and X-ray diffraction studies. The iron bound carbene signal is observed at 165.8 ppm. The bis-NHC ligand bridges the two iron(II) centers with an octahedral

environment. Three sites from the Cp ligand, a NHC site (from **L142**) and two CO complete both coordination spheres. The Fe–$C_{carbene}$ (1.983(6) Å) bond distance are similar to those of **305**. The phenylene ring plane is nearly orthogonal to the plane of the NHC moieties.

The reaction of $AgBF_4$ with **308** in CH_2Cl_2 led to the iron(II) complex **309** in excellent yield (96%). Its ^1H NMR spectrum exhibits a diastereoisomer mixture as for **305**. The $^{13}C\{^1H\}$ NMR spectrum feature two iron bound carbene signals visible at 189.1 and 188.8 ppm. Voltammetry studies evidenced two oxidation waves separated by 0.080 V around a potential of +0.47 V.[32b] The irradiation of **309** in presence of pirazine or 4,4'-bipyridine gave the iron(II) complexes **311**-**312** in a similar fashion to **307**-**306**. For **311**-**312**, the ^1H NMR spectra reveal broad signals. The UV–visible spectra suggest the presence of bound iron diimines, with two peaks at 420 and 540 nm for the pyrazine complexes **312** and 460 nm for bipyridine complexes **311**. The comparison between infrared spectra reveals the formation of polymeric species while some starting material remains.

Unusually broad signals in the voltammogram of complexes **306** and **311** and really low maxima can be explained by multiple metal-metal interactions or by the fact that the electron transfer is not diffusion-controlled. The last one is expected in polymer due to the limited rotational flexibility of the polymers compare to the monomers in solution. For complexes **307** and **310**, the signals are sharp which indicates the formation of oligomers only. The polymers have a better stability towards air and moisture compare to bimetallic complexes. This increasing stability can be useful to process these polymers. Increasing the stability of the imine bonding is useful for molecular electronic applications. This may be done by chelating.

The irradiation of **308** in CH_2Cl_2 led to the iron(II) complex **312** by dissociation of the carbon monoxide in high yield (80%). It was characterized by ^1H, NMR spectroscopy, infrared (ν_{CO} = 1941 cm^{-1}) and elemental analysis. Its ^1H NMR spectrum exhibits a diastereoisomer mixture as for **305**. The $^{13}C\{^1H\}$ NMR spectrum feature two iron bound carbene signals visible at 189.1 and 188.8 ppm. Voltammetry studies evidenced two oxidation waves separated by 0.080 V around a potential of +0.47 V.[32b]

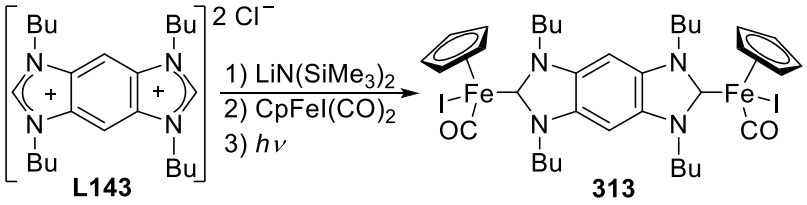

Scheme 91. Half-sandwich bis-NHC complex.[114]

The deprotonation of the imidazolium chloride salt **L143** by $LiN(SiMe_3)_2$ followed by the addition of $CpFeI(CO)_2$ allowed, after irradiation, the formation of the complex **313** in low yield (28%).[114] The complex **313** is moderately air-stable. The ^1H NMR spectrum reveals 4 different signals for the n-butyl substituents implyin a molecular structure with low symmetry and the presence of rac- and the *meso* isomers (two chiral iron centers). The $^{13}C\{^1H\}$ NMR spectrum features a unique iron bound carbene signal visible at 205.2 ppm. X-ray diffraction studies reveal two iron(II) centers with an octahedral environment. The iodide-, CO-, η^3-Cp- and NHC- ligands complete the coordination spheres. The Fe–$C_{carbene}$ bond distances (1.969(3) Å) are in the range of those of iron(II) Cp NHC complexes reported by the same group.[32b,112] The separation distance between iron(II) cations is equal to 10.591(1) Å. Cyclic and differential pulse voltammetry measurements indicate that **313** undergoes two reversible oxidation waves at $E_{1/2}$ = +0.50 and +0.58 V. The small difference between the potentials reflects some weak intermetallic interactions, in solution.

According to Robin and Day classification,[115] the complex **313** corresponds to a class II system, a molecular switch with two mutually dependent redox sites. The right choice of metal and ligand can provide an access to new materials for molecular electronics applications.

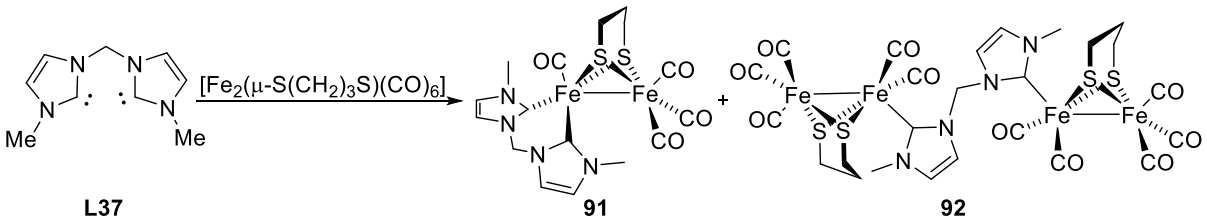

Scheme 92. Dinuclear bis-NHC Fe complexes.[39]

A solution of free carbene **L39** freshly prepared reacted with [Fe_2(μ-$S(CH_2)_3S)(CO)_6$] to afford a mixture of tetranuclear iron(I) complexes **91** (26%) and **92 (**15%**)** (see section 2.6).[39] The complexes **91** and **92** were separated by flash chromatography. The complex **92** was characterized by elemental analysis, X-ray diffraction studies, ^1H NMR and

IR spectroscopy. Its IR spectrum reveals three strong bands in the carbonyl region at 2039, 1974 and 1913 cm^{-1}. This spectrum suggests that 92 is a monosubstituted NHC complex.[116] Two different environments with octahedral geometry are present. Three CO ligands, two bridging thioether functions and a Fe-Fe bond complete two metal coordination spheres. Two CO ligands, two bridging thioether functions, a carbene site and a Fe-Fe bond complete two other metal coordination spheres. The NHC sites occupy the apical positions. The Fe–$C_{carbene}$ bond distances (1.983(3) and 1.966(3) Å) are shorter than those of **71**. The Fe–Fe distances are equal to 2.5162(7) and 2.5228(6) Å).

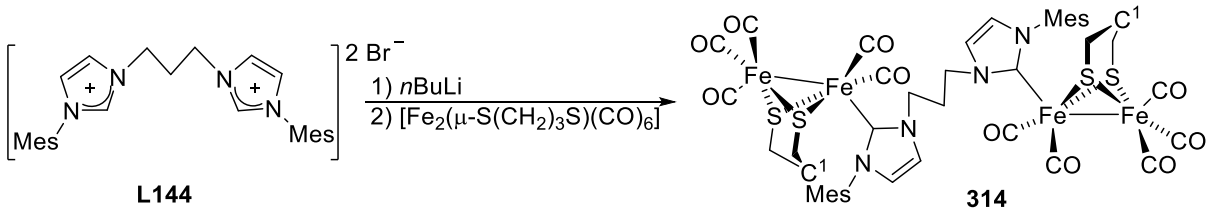

Scheme 93. Dinuclear bis-NHC Fe complexes.[117]

The reaction between **L144** and *n*BuLi, followed by the addition of [Fe_2(μ-$S(CH_2)_3S)(CO)_6$] to the mixture, led to the iron(I) complex **314** in moderate yield (52%).[117] However, the reaction of **L144** with [Fe_2(μ-$SCH_2NHCH_2S)(CO)_6$] led to a mono-NHC iron complex with a dandling imidazolium salt moiety. On the ^{1}H NMR spectrum, the signal of the characteristic imidazolium proton disappeared. The $^{13}C\{^1H\}$ NMR spectrum of **314** displays two resonances for the carbenic carbon signals at 188.7 and 188.89 ppm.

In the solid state, the coordination mode of each iron(I) center is the same as those in complexes **91**-**92** and **94**-**98**.[39] Two different environments with octahedral geometry are present. Two CO ligands, two bridging thioether functions and a Fe-Fe bond complete two metal coordination spheres. The NHC sites occupy the apical positions. The Fe–$C_{carbene}$ (2.003(5) Å) and Fe–Fe (2.5390(16) Å) bond distances are similar to those reported for **91** and **92** by Capon *et al.*[39]

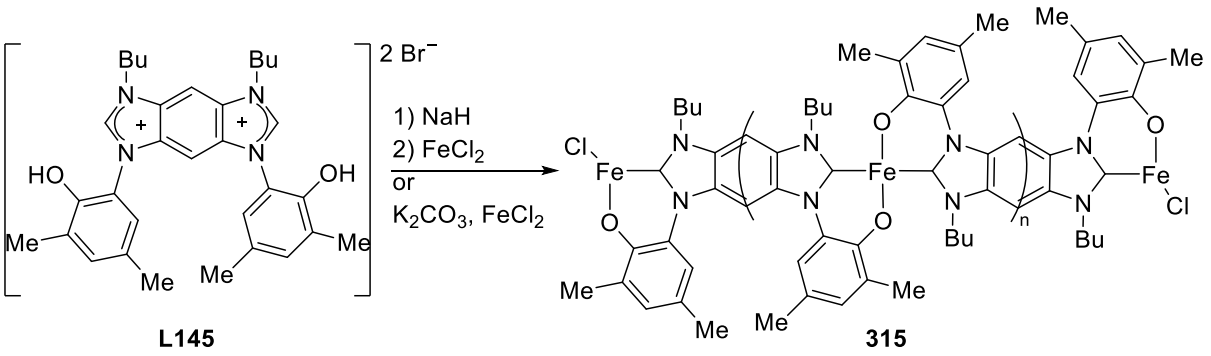

Scheme 94. Bis-NHC Fe polymer.[118]

Boydston and Bielawski reported also the complex **315**.[118] The synthesis, via either stepwise addition of $NiCl_2$ to the free bis-NHC generated from **L145** and NaH (or one-pot with **L145**, K_2CO_3 and $NiCl_2$) led to the polymer **315** in very good to excellent yields (88-97%) with a M_n ranging from 0.84 to 1.05 × 10^5 Da. The inclusion of chain transfer agents during the polymerization permitted to control the longer of the polymers and the end-group. No analysis data are available for the complex **315**.

3.3 Nickel

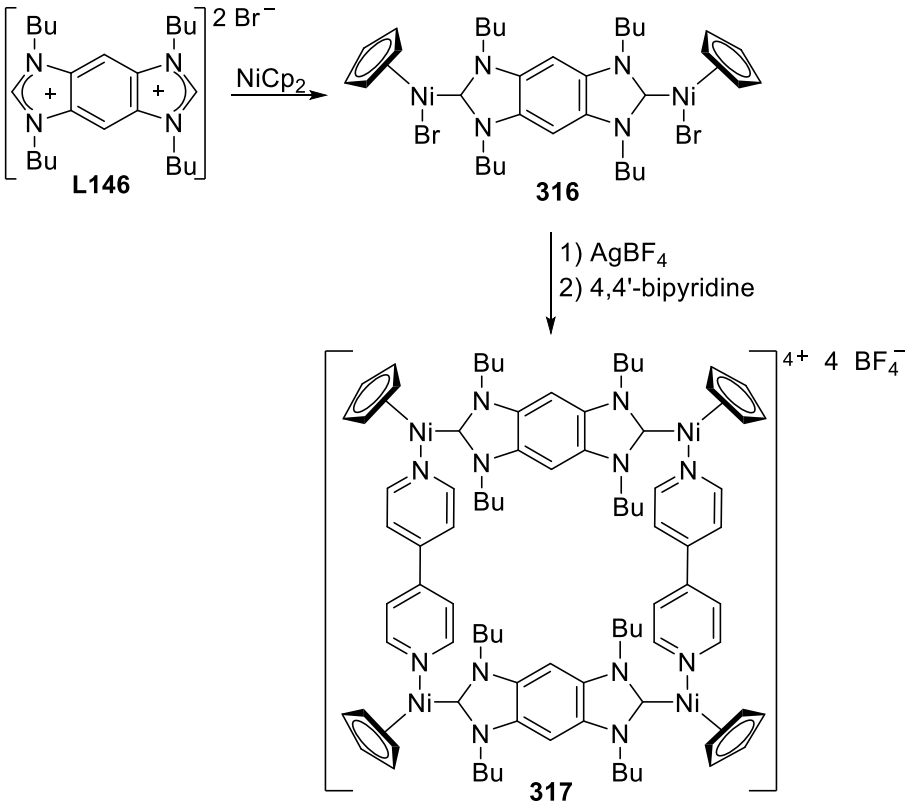

Scheme 95. Ni(II) NHC cage.[119]

The reaction of the imidazolium bromide salt **L146** with nickelocene led to the dinickel(II) complex **316** in good yield (70%).[119a] In the ^{1}H NMR spectrum, the observation of magnetically non-equivalent methylene protons for the N-butyl-chains implies a restricted rotation about the Ni–$C_{carbene}$ bonds. The $^{13}C\{^{1}H\}$ NMR spectrum displays a nickel bound carbene signal visible at 178.2 ppm. In the solid state, **316** exhibits a nickel(II) centers with a pentagonal environments. A NHC site and a bromide ligand occupy two sites while the Cp ligand occupies the three sites. The Br–Ni–$C_{carbene}$ angles are equal to 93.6(4)°. At room temperature, the restricted rotation about the Ni–$C_{carbene}$ bond blocks the Ni–Br bond in parallel orientations. For the construction of a molecular square or rectangle, this parallel pre-orientation will avoid the formation of oligomeric side products. Thus, the reaction involving the complex **316** should be done at room temperature.

Abstraction of the bromide ligand from **316** by $AgBF_4$ followed by the addition of 4,4'-bipyridine led to the complex **317** in moderate yield (43%). The nickel(II) complex is air- and water-stable. The complex was characterized by ^{1}H NMR spectroscopy. On the $^{13}C\{^{1}H\}$ NMR spectrum, the resonance signal of the carbenes (178.1 ppm) is similar to that of **316**. Single crystal X-ray diffraction studies unveil a rectangular structure with a lack of rotation around Ni–$C_{carbene}$ bonds. Four Ni-Cp fragments bound two bis-NHC- and bipy- ligands define the vertexes of the rectangle. The single crystal X-ray diffraction study reveals that the cation in **317** is on a crystallographic inversion center. The Bis-NHC ligands are almost coplanar. The Ni···Ni distances through the bis-NHC (10.380(2) Å) are slightly shorter than one through the bipyridine (10.910(2) Å). In this molecular rectangle the N–Ni–$C_{carbene}$ angles (94.6(3) and 95.4(3) °), similar to Br–Ni–$C_{carbene}$ angle in **316**, indicate that the cation is strain-free. The Ni–$C_{carbene}$ bond distances (1.876(7) and 1.892(7) Å) are in the range of those reported in the section 2.8.

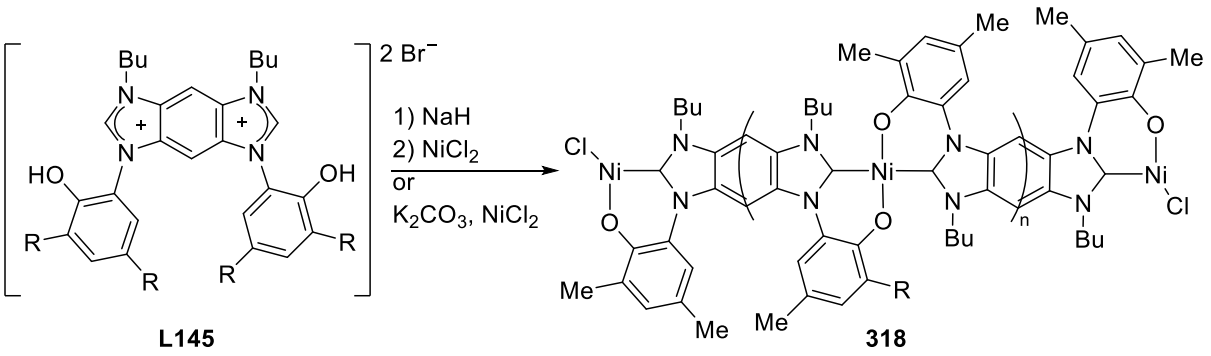

Scheme 96. Bis-NHC Ni polymer.[118]

Similarly to complex **315**, Boydston and Bielawski reported also the complex **318**.[118] The synthesis, via either stepwise addition of $NiCl_2$ to the free bis-NHC generated from **L145** and NaH (or one-pot with **L145**, K_2CO_3 and $NiCl_2$) led to the polymer **318** in very good to excellent yields (88-97%) with a M_n ranging from 0.84 to 1.05 × 10^5 Da. The inclusion of chain transfer agents during the polymerization permitted to control the longer of the polymers and the end-group. No analysis data are available for the complex **318**.

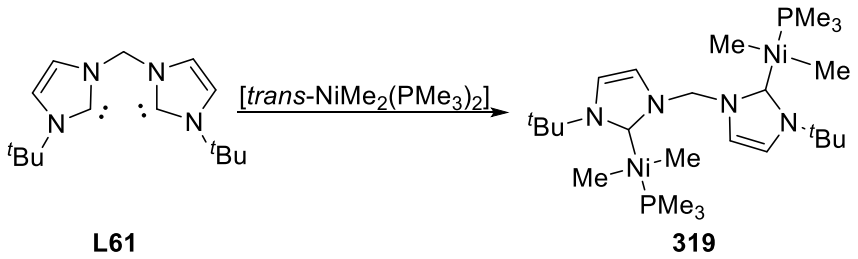

Scheme 97. Bis-NHC methyl Ni(II) complex.[22c]

Initially, due to the unsuccessful attempts on preparing Ni(**L131**)(halide)$_2$ by reaction between **L131** and various nickel halide precursors, Green *et al.* used [*trans*-$NiMe_2(PMe_3)_2$][22c] and **L61** generating the dinuclear complex **319** in low yield (30%). It was characterized by ^1H, $^{13}C\{^1H\}$ NMR spectroscopy, and X-ray diffractions analysis. The nickel bound carbene signal is visible at 200.2 ppm. The metal centers own a distorted square planar environment. The NHC- and phosphine- ligands in *trans* configuration as well as two methyl-groups complete the coordination spheres. The Ni–$C_{carbene}$ (1.879(3) Å) bond distance are comparable to those reported in the section 2.8, including **178** and **181**.[63] The conformation of the complex **319** is probably due to the minimization of the nonbonding interactions between $NiMe_2(PMe_3)$ moieties.

3.4 Copper

Similarly to complex **315**, Boydston and Bielawski reported also the complex **320**.[118]

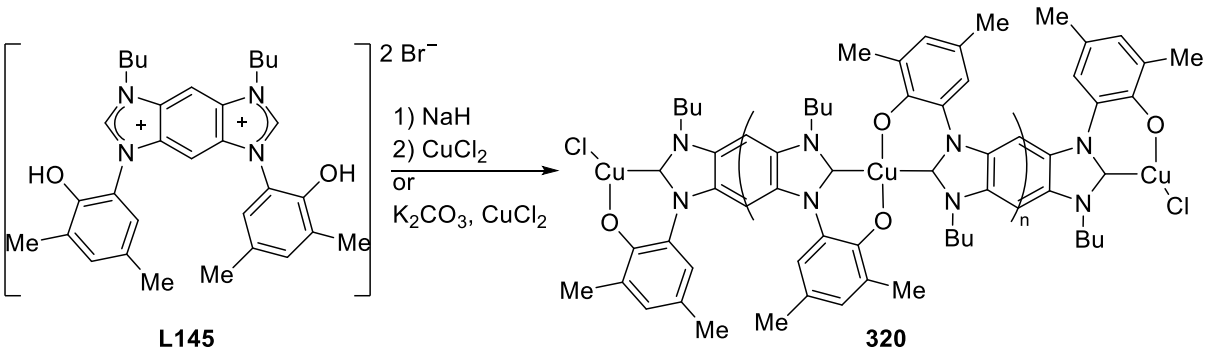

Scheme 98. Bis-NHC Cu polymer.[118]

The synthesis, via stepwise addition of $CuCl_2$ to the free bis-NHC generated from **L145** and NaH or one-pot reaction with **L145**, K_2CO_3 and $CuCl_2$ led to the polymer **320** in very good to excellent yields (88-97%) with molecular weights (Mn) ranging from 0.84 to 1.05×10^5 Da. The inclusion of chain transfer agents during the polymerization permitted to control the lenghts of the polymer chains and the nature of end-groups. No analysis data are available for the complex **320**.

4 Syntheses and reactivity of chelating/bridging bis-NHC ligands

4.1 Nickel

Zi *et al.* reported synthesis of **321**, in moderate yield (52%), by mixing the imidazolium bromide salt **L147** with $Ni(OAc)_2$ in presence of K_2CO_3 and $NaBPh_4$.[120]

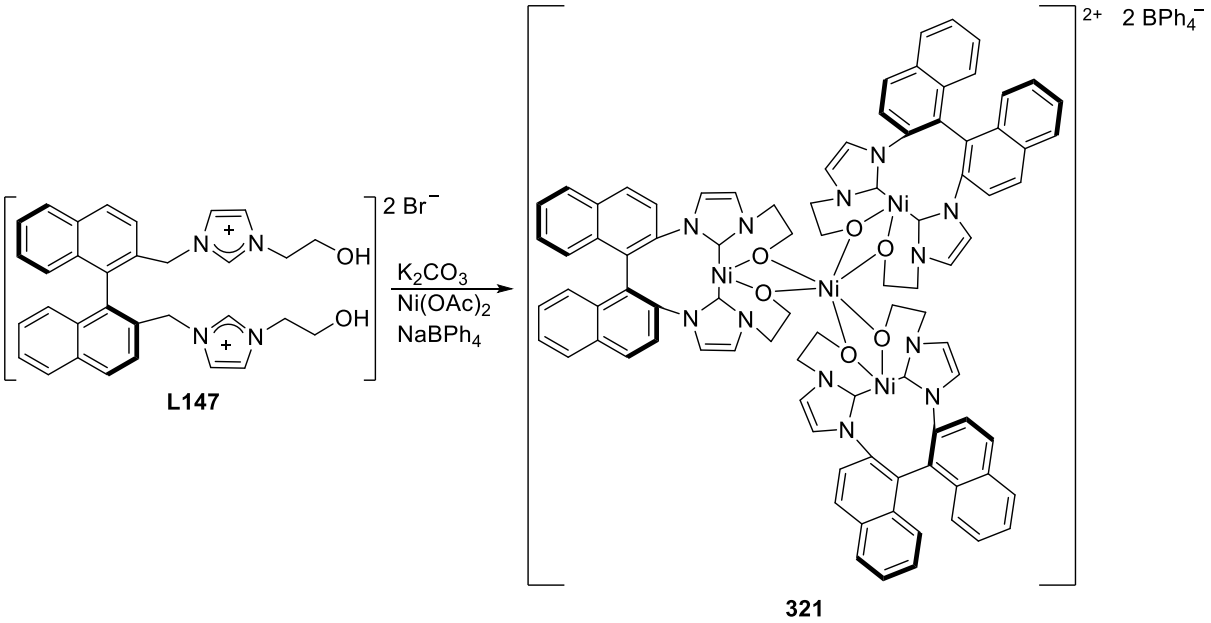

Scheme 99. Tetranuclear Ni(II) complex.[120]

The complex **321** was characterized by ^{1}H NMR and infrared spectroscopy. ^{1}H NMR analysis reveals a slow proton exchange between the alcohol and the alcoholate groups. X-ray diffraction studies unveil a tetranuclear complex with a wheel-type structure. The central nickel(II) cation owns a distorted octahedral environment. Six alcoholate functions from three bis-NHC ligands complete its coordination. Three nickel(II) cation owns similar square planar environments. Two carbene sites from the same ligand, and two alcoholate functions (also bound to the central Ni cation) complete the thee coordination spheres. The Ni–$C_{carbene}$ bond distances (1.882(9), 1.894(10), 1.855(8), 1.879(9), 1.842(9) and 1.876(8) Å) are similar to those found for bis(aryloxide-NHC)Ni complexes.[121] The complex was **321** tested for norbornene polymerization.

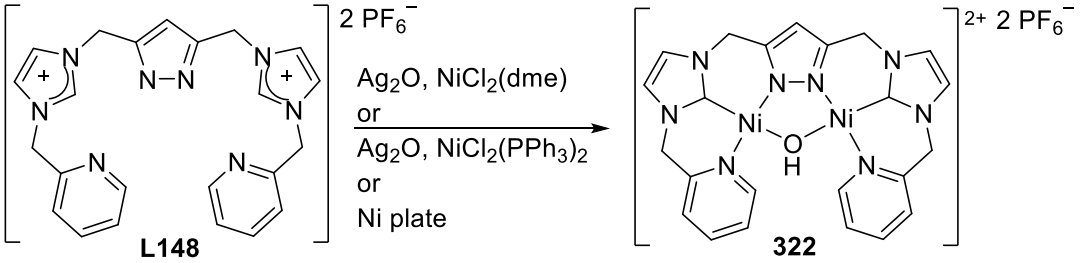

Scheme 100. Bis-NHC oxo-Ni(II) complex.[68,122]

The reaction of silver(I) complex, generated *in situ* from **L148** and silver oxide, with NiCl2$(PPh_3)_2$ (or $NiCl_2$(dme)) led to the nickel(II) complex **322** in good yield (62%).[116] The electrolysis of a nickel plate by a solution of **L148** gave also the complex **322** in lower yield (37%).[63] On the ^{1}H NMR spectrum, the signals of the imidazolylidene are downfield shifted by 0.2 ppm compared to **L148**. The signal at 1.9 ppm indicates the presence of a hydroxide group. On the $^{13}C\{^{1}H\}$ NMR spectrum, the resonance of the carbenic carbon is at 153.5 ppm. The infrared spectrum shows broad absorptions at 3441 cm^{-1} assignable to the hydroxide group. In the solid state, the complex **322** is bimetallic. The geometry around each nickel(II) center is square planar. The two nickel(II) centers are bridged by a pyrazolate and a hydroxide. Each NHC moiety completes the coordination sphere of one nickel(II) center. The cation exhibits a saddle-shaped conformation. The Ni–$C_{carbene}$ bond distances (1.832(7) and 1.822(8) Å) are comparable to those of other nickel NHC pyridine-functionalized complexes.[97a,98a] The Ni–Ni bond distance (3.255 Å) is shorter than the sum of Van der Waals radii of nickel atom. Thus, there is an interaction between the nickel centers. **322** was tested as catalyst for the reaction of Kumada, Negishi and Suzuki.

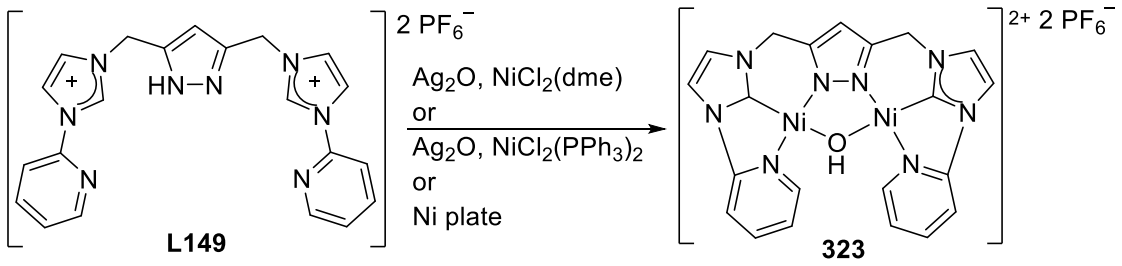

Scheme 101. Bis-NHC oxo-Ni(II) complex.[68,122]

Similarly to complex **322**, The reaction of a silver(I) complex generated *in situ* from **L149** and silver oxide, with NiCl2(PPh_3)$_2$ (or $NiCl_2$(dme)) allowed the formation of the nickel(II) complex **323** in moderate yield (56%).[116] The electrolysis of a nickel plate in presence of **L149** gave also **323** in lower yield (32%).[63] The ^{1}H NMR spectrum displays a singlet at 1.67 ppm assigned for a hydroxyl group, also visible by IR spectroscopy with a band at 3450 cm^{-1}. The ^{13}C{^{1}H} NMR spectrum features a nickel bound carbene signal at 157.9 ppm. The solid-state structure of **323**, determined by X-ray diffraction studies, is similar to that of **322**. Both nickels centers own square planar environments. The carbene-, pyridine-sites and the bridging hydroxyl- and pyrazole- moieties complete the coordination spheres. The Ni–$C_{carbene}$ bond distances (1.807(5) and 1.810(5) Å) are comparable to those of **322**. Moreover, the Ni–Ni distance is short enough (3.216 Å) to allow an intra-molecular electronic communication between cations. The complex **323** was tested for Kumada, Negishi and Suzuki reactions.

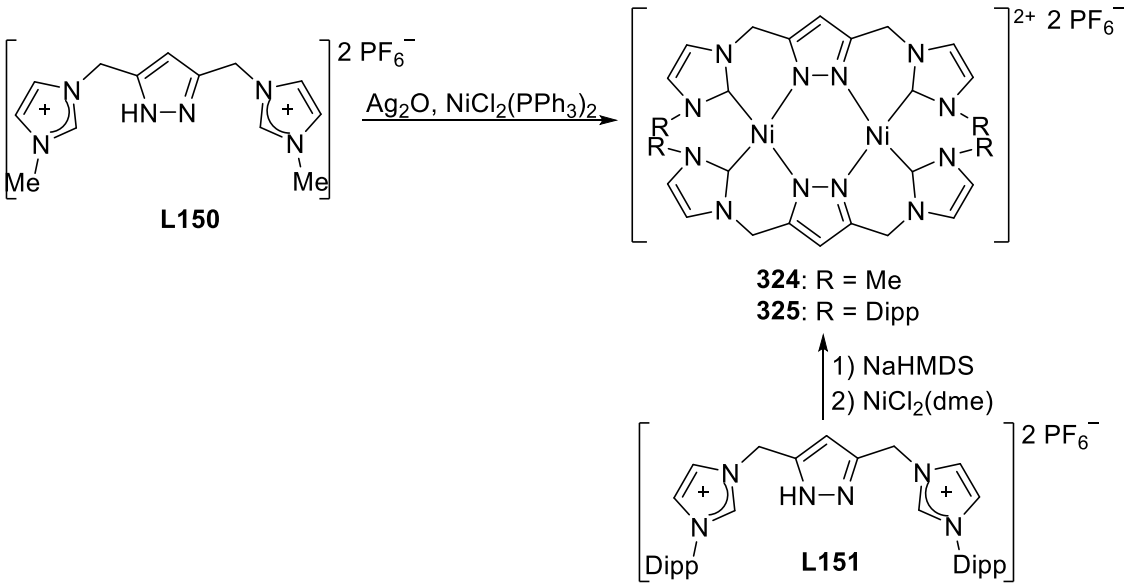

Scheme 102. Bis-NHC Ni(II) complex.[122b,123]

The reaction of the silver(I) complex generated *in situ* from **L150** and Ag_2O, with $NiCl2(PPh_3)_2$ gave the complex **324** in moderate yield (43%).[122b] Regardless the ratio Ni: Ag employed, the reaction always led to the complex **324**. Attempts on making **324** by reacting **L150** with $Ni(OAc)_2$ failed. The methylene groups from the linker displays two magnetically non-equivalent protons, with AB pattern evidenced by ^1H NMR, characteristic of a blocked rotation around the Ni-$C_{carbene}$ bonds. This hypothesis was further confirmed by X-ray diffraction analysis. The complex **324** features two nickel(II) center with a square planar environment. Two carbene sites and two bridging pyrazole moieties from two different pincer ligands completes the coordination spheres. The complex framework appears rigid and flat. The Ni–Ni distance is too long (3.873 Å) to observe any intra-molecular electronic communication between cations. The Ni–$C_{carbene}$ bond distances (1.874(3) and 1.875(3) Å) are in agreement with those reported above.

The reaction of the free bis-NHC, generated *in situ* from **L151** and NaHMDS, with $NiCl_2$(dme) led to **325** in good yield (74%).[123] Similarly to **324**, ^1H NMR experiment indicates a non-planar framework with a spectrum featuring AB patterns for the protons from the methylene bridges, and four distinct doublets (instead of two as initially anticipated) for the methyl-protons from the Dipp fragments. The $^{13}C\{^1H\}$ NMR spectrum exhibits a single nickel bound carbene resonance at 153.2 ppm. The molecular structure of **325**, determined by X-ray diffraction is similar to that of **324** regardless the N-arms born the imidazole-rings. The Ni–$C_{carbene}$ bond distances (1.851(2) Å) are comparable to those of NHC pyridine complexes such as **229**, **230** or **233**-**234**.[96a] The distance between the two nickel(II) cations (3.712 Å) does not allow any intra-molecular electronic communication.

4.2 Copper

The reaction between the silver(I) complex **L152** and CuI led to the copper(I) complex **326** in very good yield (85%).[124]

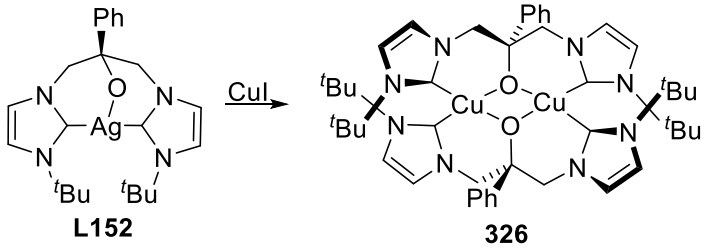

Scheme 103. Bis-NHC alcoholate Cu(I) complex.[124]

It was characterized by ^{1}H, $^{13}C\{^{1}H\}$ NMR spectroscopy. The copper bound carbene signal is visible at 177.0 ppm. X-ray diffraction studies unveil a structure with two copper(I) cations with a very uncommon square planar environment. Two bridging alcoholate functions and two carbene sites from different ligands complete the coordination spheres.

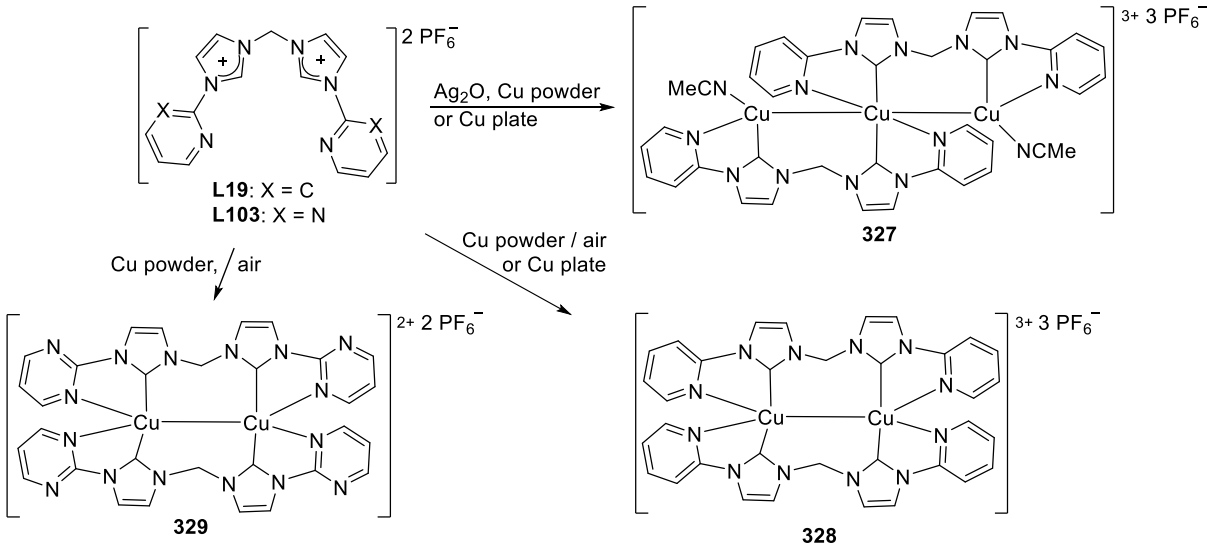

Scheme 104. Di- and tri-NHC Cu(I) complexes.[29,38,68]

The reaction of the silver(I) complex, generated from **L19** with Ag_2O, with Cu(0) powder or Cu(I) cations generated by electrochemical oxidation of copper(0) plates led to the copper(I) complex **327** in excellent yields (99% and 94%).[29,38,68] It was characterized by ^{1}H, $^{13}C\{^{1}H\}$ NMR spectroscopy. The copper bound carbene signal is visible at 181.6 ppm. X-ray diffraction studies unveil a trinuclear structure. The central copper(I) centers exhibits a square planar environment. Two NHC sites in cis-position and two N-bound pyridines from two ligands complete its coordination sphere. The two other copper(I) centers exhibit a trigonal environment. An acetonitrile molecule, a NHC site and a pyridine from the same ligand complete the coordination spheres. The short Cu-Cu distances (2.85 and 2.72 Å), as well as the quasi-straight Cu-Cu-Cu angle (86.12(3) °) indicates the presence of weak cuprophilic interactions. The $Cu–C_{carbene}$ bond distances fall in the range 1.902(5)-1.935(4) Å.

The oxidation of **327** under aerobic conditions, or the reaction between **L19** and Cu powder led to the complex **328** in excellent yields (>95%). Broad resonances or no resonances at all, were obtained during ^{1}H, $^{13}C\{^{1}H\}$ NMR studies, due to the paramagnetic nature of 285. X-ray diffraction studies unveiled two copper center with a distorted tetrahedral environment. Two NHC sites and two N-bound pyridines from two ligands complete the coordination spheres. The presence of three non-coordinating PF_6^- anions implies a total

charge of +3 shared by two copper centers, and consequently the presence of a mixed Cu(I)/(II) complex. The Cu–Cu bond distance (2.587 Å) being shorter than the sum of two covalent radii copper atoms cation (2.64 Å), the unpaired electron is delocalized over the Cu_2^{3+} core. The $Cu–C_{carbene}$ bond distances (1.932 (9) and 1.920(8) Å) are similar to those in complex **327.**

The reaction between **L103** and copper powder, or between **L103** (or its silver(I) complex derivative) and copper(I) cations generated by electrochemical oxidation of copper(0) plates led to the complex **329** in excellent yields (95% or 90 %). It was characterized by ^{1}H, $^{13}C\{^{1}H\}$ NMR spectroscopy. The copper bound carbene signal is visible at 183.9 ppm. The complex **328** exhibits a solid-state structure, determined by X-ray studies, similar to that of **328**. The main difference arises from the Cu-Cu distance equal to 3.370 Å and ruling out any cuprophilic interactions. The $Cu–C_{carbene}$ bond distances are similar to those in complex **327**. Finally, attempts on oxidizing **329** to obtain a Cu_2^{3+} core identical to **328** failed.

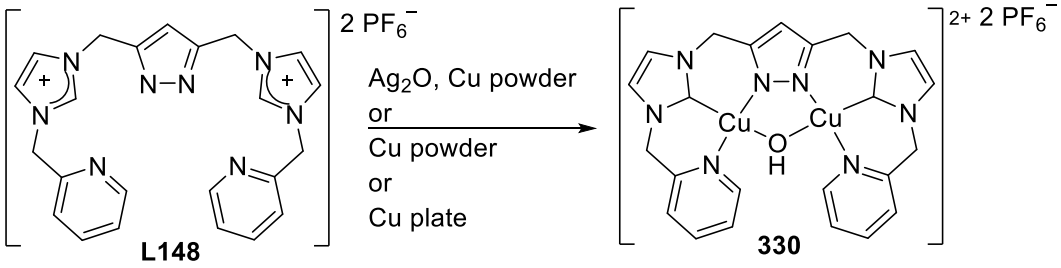

Scheme 105. Bis-NHC alcoholate Cu(II) complex.[68,125]

The reaction of **L148** or it silver(I) complex derivative, with copper(0) powder under aerobic conditions gave the copper(II) complex **330** in moderate yields (34% and 41%).[125] The reaction of **L148** with copper(II) cation generated by electrochemical oxidation of copper plate was more efficient producing **330** with 69% yield.[63] The paramagnetic nature of **330** precluded any NMR investigations. IR spectroscopy features a band at 3446 cm^{-1} characterizing a hydroxyl-group due to moisture traces. X-ray diffraction studies unveiled two copper(II) cations with a distorted square planar environment. Two NHC sites, a bridging pyrazole ring from the same ligand, and a bridging hydroxyl ligand complete the coordination spheres. The $Cu–C_{carbene}$ bond distances are longer than those of copper(I) complexes with similar geometry.[126] The Cu-Cu distance (3.350 Å) excludes any metal-metal interaction.

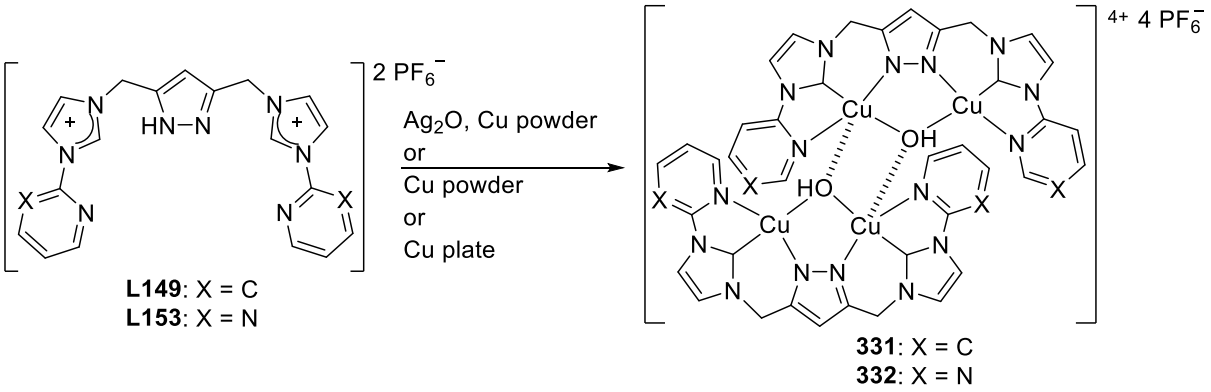

Scheme 106. Bis-NHC alcoholate Cu(II) complex.[68,125]

Three different pathways, similar to those employed to generate **330**, allowed the formation of **331**. I) Reaction of the silver(I) complex, generated *in situ* from **L133** and Ag_2O, with copper powder (73%). II) Reaction of **L149** with copper powder (64%).[117] III) Electrochemical oxidation of a copper plates in presence of **L149** (60%).[63] Moreover, still following pathways I & II, **332** was made from **L153** in lower yields (57 and 51%). The complexes were not characterized by NMR spectroscopy. Their infrared spectra reveal an absorption band at 3442 cm^{-1} corresponding to a hydroxide group.

X-ray diffraction studies of **331** and **332** unveil two quasi-identical tetranuclear structures made by assembly of two dinuclear complexes held by hydroxyl bridges, the difference lying in the presence of pyridine or pyrimidine rings. Two copper(II) centers exhibit a square planar environment. Two carbene sites, two pyridine or pyrimidine rings, a bridging pyrazole, all from the same ligand and a bridging hydroxyl complete the coordination spheres of the cations for both dinuclear sub-units. Two other copper(II) centers exhibits a distorted square pyramidal environment due to the presence of an extra Cu-O bond anchoring the di-nuclear sub-units. The $Cu–C_{carbene}$ bond distances are similar to those of other NHC copper(II) complexes.[127]

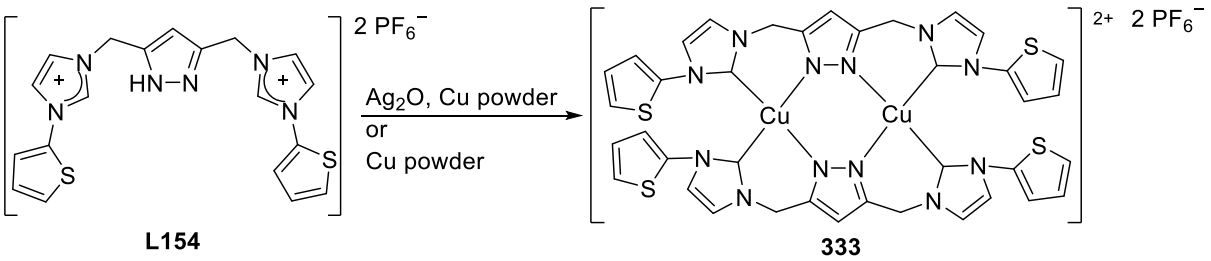

Scheme 107. Dinuclear bis-NHC Cu(II) complex.[125]

The reaction of the silver(I) complex, generated *in situ* from **L154** and Ag_2O, with copper powder or the direct reaction of **L154** with copper powder gave the copper(II) complex **333** in 45 and 47% respectively. These pathways are similar to those employed to generate **333**.[125] X-ray diffraction studies unveil two copper(II) centers with severely distorted square planar environments. The deviation (from ideal geometry) comes from the steric repulsion between both ligands, and the sp^3 geometry of the carbon atom forming the methylene bridges. Two carbene sites and two bridging pyrazole rings from different ligands complete the coordination spheres. The $Cu–C_{carbene}$ bond distances (1.980(6) and 1.989(5) Å) are in agreement with the literature.[127]

5 Conclusion

During the last 20 years, more and more research was made on multidentate NHC complexes with transition metals from the fourth period. Iron, nickel and copper metals well recognized for their potential in catalysis are very popular while the others tend to be forsaken. Multidentate NHC ligands provide a privileged access to polynuclear-, high oxidation-, mixed valence-, metals with saturated coordination sphere- complexes. Generally, the constrained geometry compelled by the ligands forces the metal centers to dwell in a close neighborhood, yielding to complexes with atypical and often appealing chemical or physical properties.

This dissertation introduction will be submitted as a review. Two extra-parts will be incorporated: a first one describing the chemistry of tripodal and tetrapodal NHC based complexes; a second one illustrating the numerous applications of these multidentate NHC complexes in homogeneous catalysis.

References:

(1) (a) Wanzlick, H. W.; Schönherr, H. J. *Angew. Chem. Int. Ed.* **1968**, *7*, 141 (b) Öfele, K. *J. Organomet. Chem.* **1968**, *12*, P42.

(2) (a) Cadenbach, T.; Gemel, C.; Bollermann, T.; Fischer, R. A. *Inorg. Chem.* **2009**, *48*, 5021 (b) Braunschweig, H.; Brenner, P.; Cogswell, P.; Kraft, K.; Schwab, K. *Chem. Commun.* **2010**, *46*, 7894.

(3) Lv, K.; Cui, D. *Organometallics* **2008**, *27*, 5438.

(4) (a) Cui, D.; Lu, K.; Liu, D.; Wang, B.; Wang, L.; Gao, W. **2009**, 101367825A, China (b) Maron, L.; Bourissou, D. *Organometallics* **2009**, *28*, 3686.

(5) Weiss, A.; Pritzkow, H.; Siebert, W. *Eur. J. Inorg. Chem.* **2002**, 1607.

(6) (a) McGuinness, D. S.; Gibson, V. C.; Steed, J. W. *Organometallics* **2004**, *23*, 6288 (b) Pugh, D.; Wright, J. A.; Freeman, S.; Danopoulos, A. A. *Dalton Trans.* **2006**, 775 (c) Edworthy, I. S.; Blake, A. J.; Wilson, C.; Arnold, P. L. *Organometallics* **2007**, *26*, 3684.

(7) Öfele, K.; Herrmann, W. A.; Mihalios, D.; Elison, M.; Herdtweck, E.; Priermeier, T.; Kiprof, P. *J. Organomet. Chem.* **1995**, *498*, 1.

(8) Helgert, T. R.; Hollis, T. K.; Valente, E. J. *Organometallics* **2012**, *31*, 3002.

(9) Abernethy, C. D.; Codd, G. M.; Spicer, M. D.; Taylor, M. K. *J. Am. Chem. Soc.* **2003**, *125*, 1128.

(10) Nugent, W. A.; Mayer, J. M. *Metal-Ligand Multiple Bonds*: N. Y., 1988.

(11) Öfele, K.; Herrmann, W. A.; Mihalios, D.; Elison, M.; Herdtweck, E.; Scherer, W.; Mink, J. *J. Organomet. Chem.* **1993**, *459*, 177.

(12) McGuinness, D. S.; Gibson, V. C.; Wass, D. F.; Steed, J. W. *J. Am. Chem. Soc.* **2003**, *125*, 12716.

(13) (a) McGuinness, D. S. *Organometallics* **2009**, *28*, 244 (b) McGuinness, D. S.; Suttil, J. A.; Gardiner, M. G.; Davies, N. W. *Organometallics* **2008**, *27*, 4238.

(14) (a) Abernethy, C. D.; Clyburne, J. A. C.; Cowley, A. H.; Jones, R. A. *J. Am. Chem. Soc.* **1999**, *121*, 2329 (b) Voges, M. H.; Rømming, C.; Tilset, M. *Organometallics* **1999**, *18*, 529.

(15) Esteruelas, M. A.; López, A. M.; Méndez, L.; Oliván, M.; Oñate, E. *Organometallics* **2003**, *22*, 395.

(16) Ogata, K.; Yamaguchi, Y.; Kurihara, Y.; Ueda, K.; Nagao, H.; Ito, T. *Inorg. Chim. Acta* **2012**, *390*, 199.

(17) (a) Yong, G.; Zhang, Y.; Ying, J. Y. *Angew. Chem. Int. Ed.* **2008**, *47*, 9345 (b) Zhang, Y.; Ying, J. Y.; Yong, G. **2009**, WO2009154566A1,

(18) Kreisel, K. A.; Yap, G. P. A.; Theopold, K. H. *Organometallics* **2006**, *25*, 4670.

(19) Allen, F. *Acta Crystallogr. Sect. B: Struct. Sci.* **2002**, *58*, 380.

(20) (a) Cotton, F. A.; Czuchajowska, J.; Falvello, L. R.; Feng, X. *Inorg. Chim. Acta* **1990**, *172*, 135 (b) Fryzuk, M. D.; Leznoff, D. B.; Rettig, S. *J. Organometallics* **1997**, *16*, 5116 (c) Greene, P. T.; Russ, B. J.; Wood, J. S. *J. Chem. Soc. A* **1971**, 3636 (d) Heintz, R. A.; Leelasubcharoen, S.; Liable-Sands, L. M.; Rheingold, A. L.; Theopold, K. H. *Organometallics* **1998**, *17*, 5477 (e) Liang, Y.; Yap, G. P. A.; Rheingold, A. L.; Theopold, K. H. *Organometallics* **1996**, *15*, 5284 (f) Müller, E.; Krause, J.; Schmiedeknecht, K. *J. Organomet. Chem.* **1972**, *44*, 127.

(21) Cotton, F. A. W., G.; Murillo, C. A.; Bochmann, M. *Advanced Inorganic Chemistry*; 6th ed.: New York, 1999.

(22) (a) Spencer, L. P.; Winston, S.; Fryzuk, M. D. *Organometallics* **2004**, *23*, 3372 (b) Danopoulos, A. A.; Tsoureas, N.; Wright, J. A.; Light, M. E. *Organometallics* **2004**,

23, 166 (c) Douthwaite, R. E.; Green, M. L. H.; Silcock, P. J.; Gomes, P. T. *Organometallics* **2001**, *20*, 2611.
(23) (a) Chai, J.; Zhu, H.; Most, K.; Roesky, Herbert W.; Vidovic, D.; Schmidt, H.-G.; Noltemeyer, M. *Eur. J. Inorg. Chem.* **2003**, *2003*, 4332 (b) Chai, J.; Zhu, H.; Peng, Y.; Roesky, Herbert W.; Singh, S.; Schmidt, H.-G.; Noltemeyer, M. *Eur. J. Inorg. Chem.* **2004**, *2004*, 2673.
(24) (a) Gallo, E.; Solari, E.; Floriani, C.; Chiesi-Villa, A.; Rizzoli, C. *Inorg. Chem.* **1997**, *36*, 2178 (b) Howard, C. G.; Girolami, G. S.; Wilkinson, G.; Thornton-Pett, M.; Hursthouse, M. B. *J. Chem. Soc., Dalton Trans.* **1983**, 2631.
(25) Yagyu, T.; Yano, K.; Kimata, T.; Jitsukawa, K. *Organometallics* **2009**, *28*, 2342.
(26) (a) Abernethy, C. D.; Cowley, A. H.; Jones, R. A.; Macdonald, C. L. B.; Shukla, P.; Thompson, L. K. *Organometallics* **2001**, *20*, 3629 (b) Ruiz, J.; Perandones, B. F.; García, G.; Mosquera, M. E. G. *Organometallics* **2007**, *26*, 5687 (c) Forshaw, A. P.; Bontchev, R. P.; Smith, J. M. *Inorg. Chem.* **2007**, *46*, 3792.
(27) (a) Kaess, M.; Hohenberger, J.; Adelhardt, M.; Zolnhofer, E. M.; Mossin, S.; Heinemann, F. W.; Sutter, J.; Meyer, K. *Inorg. Chem.* **2014**, *53*, 1465 (b) Haetzelt, A.; Kropf, C.; Meyer, K.; Kaess, M. **2013**, WO2013167602A1, Germany.
(28) Flassbeck, C.; Wieghardt, K. *Z. Anorg. Allg. Chem.* **1992**, *608*, 60.
(29) Chen, W.; Liu, B. **2009**, CN101402644A, China.
(30) Meyer, S.; Orben, C. M.; Demeshko, S.; Dechert, S.; Meyer, F. *Organometallics* **2011**, *30*, 6692.
(31) Zlatogorsky, S.; Muryn, C. A.; Tuna, F.; Evans, D. J.; Ingleson, M. J. *Organometallics* **2011**, *30*, 4974.
(32) (a) Hitchcock, P. B.; Lappert, M. F.; Thomas, S. A.; Thorne, A. J.; Carty, A. J.; Taylor, N. J. *J. Organomet. Chem.* **1986**, *315*, 27 (b) Mercs, L.; Labat, G.; Neels, A.; Ehlers, A.; Albrecht, M. *Organometallics* **2006**, *25*, 5648.
(33) (a) Barclay, J. E.; Leigh, G. J.; Houlton, A.; Silver, J. *J. Chem. Soc., Dalton Trans.* **1988**, 2865 (b) Hawrelak, E. J.; Bernskoetter, W. H.; Lobkovsky, E.; Yee, G. T.; Bill, E.; Chirik, P. J. *Inorg. Chem.* **2005**, *44*, 3103.
(34) Zlatogorsky, S.; Ingleson, M. J. *Dalton Trans.* **2012**, *41*, 2685.
(35) Kreisel, K. A.; Yap, G. P. A.; Theopold, K. H. *Chem. Commun.* **2007**, 1510.
(36) Ittel, S. D.; Tolman, C. A.; Krusic, P. J.; English, A. D.; Jesson, J. P. *Inorg. Chem.* **1978**, *17*, 3432.
(37) Blom, B.; Tan, G.; Enthaler, S.; Inoue, S.; Epping, J. D.; Driess, M. *J. Am. Chem. Soc.* **2013**, *135*, 18108.
(38) Liu, B.; Xia, Q.; Chen, W. *Angew. Chem., Int. Ed.* **2009**, *48*, 5513.
(39) Morvan, D.; Capon, J.-F.; Gloaguen, F.; Le Goff, A.; Marchivie, M.; Michaud, F.; Schollhammer, P.; Talarmin, J.; Yaouanc, J.-J.; Pichon, R.; Kervarec, N. *Organometallics* **2007**, *26*, 2042.
(40) Buchgraber, P.; Toupet, L.; Guerchais, V. *Organometallics* **2003**, *22*, 5144.
(41) Lyon, E. J.; Georgakaki, I. P.; Reibenspies, J. H.; Darensbourg, M. Y. *Angew. Chem. Int. Ed.* **1999**, *38*, 3178.
(42) Chouffai, D.; Zampella, G.; Capon, J.-F.; De Gioia, L.; Le Goff, A.; Petillon, F. Y.; Schollhammer, P.; Talarmin, J. *Organometallics* **2012**, *31*, 1082.
(43) Kumar, M.; DePasquale, J.; Zeller, M.; Papish, E. T. *Inorg. Chem. Commun.* **2013**, *32*, 55.
(44) Wu, J.; Dai, W.; Farnaby, J. H.; Hazari, N.; Le Roy, J. J.; Mereacre, V.; Murugesu, M.; Powell, A. K.; Takase, M. K. *Dalton Trans.* **2013**, *42*, 7404.
(45) Grohmann, C.; Hashimoto, T.; Froehlich, R.; Ohki, Y.; Tatsumi, K.; Glorius, F. *Organometallics* **2012**, *31*, 8047.

(46) Danopoulos, A. A.; Pugh, D.; Smith, H.; Sassmannshausen, J. *Chem. - Eur. J.* **2009**, *15*, 5491.
(47) (a) Chen, M.-Z.; Sun, H.-M.; Li, W.-F.; Wang, Z.-G.; Shen, Q.; Zhang, Y. *J. Organomet. Chem.* **2006**, *691*, 2489 (b) Louie, J.; Grubbs, R. H. *Chem. Commun.* **2000**, 1479 (c) Vogel, C.; Heinemann, F. W.; Sutter, J.; Anthon, C.; Meyer, K. *Angew. Chem. Int. Ed.* **2008**, *47*, 2681.
(48) Raba, A.; Cokoja, M.; Ewald, S.; Riener, K.; Herdtweck, E.; Poethig, A.; Herrmann, W. A.; Kuehn, F. E. *Organometallics* **2012**, *31*, 2793.
(49) Kaufhold, O.; Hahn, F. E.; Pape, T.; Hepp, A. *J. Organomet. Chem.* **2008**, *693*, 3435.
(50) Klawitter, I.; Meyer, S.; Demeshko, S.; Meyer, F. *Z. Naturforsch., B: J. Chem. Sci.* **2013**, *68*, 458.
(51) Bedford, R. B.; Betham, M.; Bruce, D. W.; Danopoulos, A. A.; Frost, R. M.; Hird, M. *J. Org. Chem.* **2006**, *71*, 1104.
(52) Yu, R. P.; Darmon, J. M.; Hoyt, J. M.; Margulieux, G. W.; Turner, Z. R.; Chirik, P. J. *ACS Catal.* **2012**, *2*, 1760.
(53) Liu, Y.; Harlang, T.; Canton, S. E.; Chabera, P.; Suarez-Alcantara, K.; Fleckhaus, A.; Vithanage, D. A.; Goeransson, E.; Corani, A.; Lomoth, R.; Sundstroem, V.; Waernmark, K. *Chem. Commun.* **2013**, *49*, 6412.
(54) (a) Danopoulos, A. A.; Wright, J. A.; Motherwell, W. B. *Chem. Commun.* **2005**, 784 (b) Zhang, X. *Int. J. Quantum Chem.* **2010**, *110*, 1880 (c) Obligacion, J. V.; Chirik, P. J. *Org. Lett.* **2013**, *15*, 2680 (d) Liu, H.; Liu, S.; Zhang, X. *J. Mol. Model.* **2013**, *19*, 2625.
(55) Jones, W. D.; Foster, G. P.; Putinas, J. M. *Inorg. Chem.* **1987**, *26*, 2120.
(56) Pugh, D.; Wells, N. J.; Evans, D. J.; Danopoulos, A. A. *Dalton Trans.* **2009**, 7189.
(57) (a) Bart, S. C.; Lobkovsky, E.; Chirik, P. J. *J. Am. Chem. Soc.* **2004**, *126*, 13794 (b) Trovitch, R. J.; Lobkovsky, E.; Chirik, P. J. *Inorg. Chem.* **2006**, *45*, 7252 (c) Kubas, G. J. *Metal Dihydrogen and s-Bond Complexes-Structure, Theory and Reactivity*; Kluwer Academic: NY, USA, 2001.
(58) Sun, H.-Y.; Park, J.-W.; Lee, D.-Y.; Son, S.-U. **2011**, US20110195283A1,
(59) Danopoulos, A. A.; Wright, J. A.; Motherwell, W. B.; Ellwood, S. *Organometallics* **2004**, *23*, 4807.
(60) Mizoguchi, T. J.; Kuzelka, J.; Spingler, B.; DuBois, J. L.; Davydov, R. M.; Hedman, B.; Hodgson, K. O.; Lippard, S. J. *Inorg. Chem.* **2001**, *40*, 4662.
(61) Xi, Z.; Liu, B.; Lu, C.; Chen, W. *Dalton Trans.* **2009**, 7008.
(62) Yu, R. P.; Darmon, J. M.; Milsmann, C.; Margulieux, G. W.; Stieber, S. C. E.; DeBeer, S.; Chirik, P. J. *J. Am. Chem. Soc.* **2013**, *135*, 13168.
(63) Douthwaite, R. E.; Haüssinger, D.; Green, M. L. H.; Silcock, P. J.; Gomes, P. T.; Martins, A. M.; Danopoulos, A. A. *Organometallics* **1999**, *18*, 4584.
(64) (a) Herrmann, W. A.; Elison, M.; Fischer, J.; Köcher, C.; Artus, G. R. J. *Chem. - Eur. J.* **1996**, *2*, 772 (b) Herrmann, W. A.; Schwarz, J.; Gardiner, M. G.; Spiegler, M. *J. Organomet. Chem.* **1999**, *575*, 80.
(65) Allen, F. H.; Davies, J. E.; Galloy, J. J.; Johnson, O.; Kennard, O.; Macrae, C. F.; Mitchell, E. M.; Mitchell, G. F.; Smith, J. M.; Watson, D. G. *J. Chem. Inf. Comput. Sci.* **1991**, *31*, 187.
(66) Sheldrick, G. M. *SHELXL-93: Program for Crystal Structure Refinement*: Univeristy of Göttingen, Göttingen, Germany, 1993.
(67) Olivier-Bourbigou, H.; Commereuc, D.; Harry, S. **2001**, EP1136124A1, France.
(68) (a) Chen, W.; Liu, B. **2010**, CN101787542A, China (b) Liu, B.; Zhang, Y.; Xu, D.; Chen, W. *Chem. Commun.* **2011**, *47*, 2883.

(69) Paulose, T. A. P.; Wu, S.-C.; Olson, J. A.; Chau, T.; Theaker, N.; Hassler, M.; Quail, J. W.; Foley, S. R. *Dalton Trans.* **2012**, *41*, 251.
(70) Guo, J.; Lv, L.; Wang, X.; Cao, C.; Pang, G.; Shi, Y. *Inorg. Chem. Commun.* **2013**, *31*, 74.
(71) Huffer, A.; Jeffery, B.; Waller, B. J.; Danopoulos, A. A. *C. R. Chim.* **2013**, *16*, 557.
(72) Harrold, N. D.; Hillhouse, G. L. *Chem. Sci.* **2013**, *4*, 4011.
(73) Waterman, R.; Hillhouse, G. L. *J. Am. Chem. Soc.* **2008**, *130*, 12628.
(74) Iluc, V. M.; Hillhouse, G. L. *J. Am. Chem. Soc.* **2010**, *132*, 15148.
(75) Brendel, M.; Braun, C.; Rominger, F.; Hofmann, P. *Angew. Chem. Int. Ed.* **2014**, n/a.
(76) (a) Berding, J.; Lutz, M.; Spek, A. L.; Bouwman, E. *Organometallics* **2009**, *28*, 1845 (b) Vinh Huynh, H.; Jothibasu, R. *Eur. J. Inorg. Chem.* **2009**, 1926 (c) Berding, J.; Lutz, M.; Spek, A. L.; Bouwman, E. *Appl. Organomet. Chem.* **2011**, *25*, 76.
(77) Clyne, D. S.; Jin, J.; Genest, E.; Gallucci, J. C.; RajanBabu, T. V. *Org. Lett.* **2000**, *2*, 1125.
(78) Baker, M. V.; Skelton, B. W.; White, A. H.; Williams, C. C. *J. Chem. Soc., Dalton Trans.* **2001**, 111.
(79) Nieto, I.; Bontchev, R. P.; Smith, J. M. *Eur. J. Inorg. Chem.* **2008**, 2476.
(80) (a) Inamoto, K.; Kuroda, J.-i.; Sakamoto, T.; Hiroya, K. *Synthesis* **2007**, 2853 (b) Inamoto, K.; Kuroda, J.-i.; Hiroya, K.; Noda, Y.; Watanabe, M.; Sakamoto, T. *Organometallics* **2006**, *25*, 3095 (c) Xu, M.; Li, X.; Sun, Z.; Tu, T. *Chem. Commun.* **2013**, *49*, 11539 (d) Kuroda, J.-i.; Inamoto, K.; Hiroya, K.; Doi, T. *Eur. J. Org. Chem.* **2009**, 2251.
(81) (a) Mrutu, A.; Dickie, D. A.; Goldberg, K. I.; Kemp, R. A. *Inorg. Chem.* **2011**, *50*, 2729 (b) Pugh, D.; Boyle, A.; Danopoulos, A. A. *Dalton Trans.* **2008**, 1087.
(82) Inamoto, K.; Kuroda, J.-i.; Kwon, E.; Hiroya, K.; Doi, T. *J. Organomet. Chem.* **2009**, *694*, 389.
(83) Mrutu, A.; Goldberg, K. I.; Kemp, R. A. *Inorg. Chim. Acta* **2010**, *364*, 115.
(84) (a) Becker, E.; Stingl, V.; Dazinger, G.; Mereiter, K.; Kirchner, K. *Organometallics* **2007**, *26*, 1531 (b) Waltman, A. W.; Ritter, T.; Grubbs, R. H. *Organometallics* **2006**, *25*, 4238.
(85) Danopoulos, A. A.; Tsoureas, N.; Green, J. C.; Hursthouse, M. B. *Chem. Commun.* **2003**, 756.
(86) (a) Yoshida, K.; Horiuchi, S.; Takeichi, T.; Shida, H.; Hayashi, K.; Imamoto, T.; Yanagisawa, A. **2011**, JP2011178709A, (b) Yoshida, K.; Horiuchi, S.; Takeichi, T.; Shida, H.; Imamoto, T.; Yanagisawa, A. *Org. Lett.* **2010**, *12*, 1764.
(87) Liu, A.; Zhang, X.; Chen, W. *Organometallics* **2009**, *28*, 4868.
(88) (a) Consorti, C. S.; Ebeling, G.; Flores, F. R.; Rominger, F.; Dupont, J. *Adv. Synth. Catal.* **2004**, *346*, 617 (b) Ebeling, G.; Meneghetti, M. R.; Rominger, F.; Dupont, J. *Organometallics* **2002**, *21*, 3221.
(89) Hollis, T. K.; Zhang, X. **2011**, WO 2011050003 (A2) USA.
(90) Mueller, S.; Burgfels, G.; Fischer, R.; Scherg, T. **2009**, DE102008022788A1, Germany.
(91) Tu, T.; Mao, H.; Herbert, C.; Xu, M.; Doetz, K. H. *Chem. Commun.* **2010**, *46*, 7796.
(92) (a) Gu, S.; Chen, W. *Organometallics* **2009**, *28*, 909 (b) Huynh, H. V.; Wong, L. R.; Ng, P. S. *Organometallics* **2008**, *27*, 2231.
(93) Brown, D. H.; Skelton, B. W. *Dalton Trans.* **2011**, *40*, 8849.
(94) MaGee, K. D. M.; Travers, G.; Skelton, B. W.; Massi, M.; Payne, A. D.; Brown, D. H. *Aust. J. Chem.* **2012**, *65*, 823.
(95) Baker, M. V.; Skelton, B. W.; White, A. H.; Williams, C. C. *Organometallics* **2002**, *21*, 2674.

(96) (a) Chiu, P. L.; Lai, C.-L.; Chang, C.-F.; Hu, C.-H.; Lee, H. M. *Organometallics* **2005**, *24*, 6169 (b) Chen, W.; Liu, B. **2012**, CN102351907A, China (c) Liu, B.; Liu, X.; Chen, C.; Chen, C.; Chen, W. *Organometallics* **2012**, *31*, 282.
(97) (a) Xi, Z.; Liu, B.; Chen, W. *J. Org. Chem.* **2008**, *73*, 3954 (b) Xi, Z.; Zhou, Y.; Chen, W. *J. Org. Chem.* **2008**, *73*, 8497.
(98) (a) Xi, Z.; Zhang, X.; Chen, W.; Fu, S.; Wang, D. *Organometallics* **2007**, *26*, 6636 (b) Thoi, V. S.; Chang, C. J. *Chem. Commun.* **2011**, *47*, 6578.
(99) Thoi, V. S.; Kornienko, N.; Margarit, C. G.; Yang, P.; Chang, C. J. *J. Am. Chem. Soc.* **2013**, *135*, 14413.
(100) Liu, Q.-X.; Yao, Z.-Q.; Zhao, X.-J.; Zhao, Z.-X.; Wang, X.-G. *Organometallics* **2013**, *32*, 3493.
(101) Ray, S.; Asthana, J.; Tanski, J. M.; Shaikh, M. M.; Panda, D.; Ghosh, P. *J. Organomet. Chem.* **2009**, *694*, 2328.
(102) Zhang, C.; Wang, Z.-X. *Organometallics* **2009**, *28*, 6507.
(103) Jean-Baptiste dit Dominique, F.; Gornitzka, H.; Hemmert, C. *Organometallics* **2010**, *29*, 2868.
(104) Tan, K. V.; Dutton, J. L.; Skelton, B. W.; Wilson, D. J. D.; Barnard, P. J. *Organometallics* **2013**, *32*, 1913.
(105) Wan, X.-J.; Xu, F.-B.; Li, Q.-S.; Song, H.-B.; Zhang, Z.-Z. *Inorg. Chem. Commun.* **2005**, *8*, 1053.
(106) (a) Haider, J.; Kunz, K.; Scholz, U. *Adv. Synth. Catal.* **2004**, *346*, 717 (b) Kunz, K.; Haider, J.; Ganzer, D.; Scholz, U.; Sicheneder, A. **2004**, EP1437341A1,
(107) Rit, A.; Spaniol, T. P.; Okuda, J. *Chem. - Asian J.* **2014**, *9*, 612.
(108) (a) Wang, D.; Wurst, K.; Buchmeiser, M. R. *J. Organomet. Chem.* **2004**, *689*, 2123 (b) Jensen, T. R.; Schaller, C. P.; Hillmyer, M. A.; Tolman, W. B. *J. Organomet. Chem.* **2005**, *690*, 5881 (c) Jensen, T. R.; Breyfogle, L. E.; Hillmyer, M. A.; Tolman, W. B. *Chem. Commun.* **2004**, 2504 (d) Arduengo Iii, A. J.; Dias, H. V. R.; Davidson, F.; Harlow, R. L. *J. Organomet. Chem.* **1993**, *462*, 13.
(109) Rit, A.; Spaniol, T. P.; Maron, L.; Okuda, J. *Angew. Chem.* **2013**, *125*, 4762.
(110) Schulz, S.; Eisenmann, T.; Schmidt, S.; Blaser, D.; Westphal, U.; Boese, R. *Chem. Commun.* **2010**, *46*, 7226.
(111) (a) Abel, E. W.; Bhargava, S. K.; Kite, K.; Orrell, K. G.; Sik, V.; Williams, B. L. *J. Chem. Soc., Dalton Trans.* **1982**, 583 (b) Adams, R. D.; Brice, M.; Cotton, F. A. *J. Am. Chem. Soc.* **1973**, *95*, 6594 (c) Besançon, K.; Laurenczy, G.; Lumini, T.; Roulet, R.; Bruyndonckx, R.; Daul, C. *Inorg. Chem.* **1998**, *37*, 5634.
(112) Mercs, L.; Neels, A.; Stoeckli-Evans, H.; Albrecht, M. *Dalton Trans.* **2009**, 7168.
(113) Mata, J. A.; Chianese, A. R.; Miecznikowski, J. R.; Poyatos, M.; Peris, E.; Faller, J. W.; Crabtree, R. H. *Organometallics* **2004**, *23*, 1253.
(114) Mercs, L.; Neels, A.; Albrecht, M. *Dalton Trans.* **2008**, 5570.
(115) Robin, M. B.; Day, P. In *Adv. Inorg. Chem. Radiochem.*, 1967; Vol. 10.
(116) Capon, J.-F.; El Hassnaoui, S.; Gloaguen, F.; Schollhammer, P.; Talarmin, J. *Organometallics* **2005**, *24*, 2020.
(117) Song, L.-C.; Luo, X.; Wang, Y.-Z.; Gai, B.; Hu, Q.-M. *J. Organomet. Chem.* **2009**, *694*, 103.
(118) Boydston, A. J.; Bielawski, C. W. *Polym. Prepr. (Am. Chem. Soc., Div. Polym. Chem.)* **2006**, *47*, 177.
(119) (a) Radloff, C.; Hahn, F. E.; Pape, T.; Froehlich, R. *Dalton Trans.* **2009**, 7215 (b) Hahn, F. E.; Radloff, C.; Pape, T.; Hepp, A. *Organometallics* **2008**, *27*, 6408.
(120) Song, H.; Fan, D.; Liu, Y.; Hou, G.; Zi, G. *J. Organomet. Chem.* **2013**, *729*, 40.

(121) Kong, Y.; Cheng, M.; Ren, H.; Xu, S.; Song, H.; Yang, M.; Liu, B.; Wang, B. *Organometallics* **2011**, *30*, 1677.
(122) (a) Chen, W.; Xi, Z.; Zhou, Y. **2008**, CN101284247A, China (b) Zhou, Y.; Xi, Z.; Chen, W.; Wang, D. *Organometallics* **2008**, *27*, 5911.
(123) Jeon, S.-J.; Waymouth, R. M. *Dalton Trans.* **2008**, 437.
(124) Arnold, P. L.; Scarisbrick, A. C.; Blake, A. J.; Wilson, C. *Chem. Commun.* **2001**, 2340.
(125) Liu, B.; Liu, B.; Zhou, Y.; Chen, W. *Organometallics* **2010**, *29*, 1457.
(126) Hu, X.; Castro-Rodriguez, I.; Meyer, K. *Organometallics* **2003**, *22*, 3016.
(127) (a) Arnold, P. L.; Rodden, M.; Davis, K. M.; Scarisbrick, A. C.; Blake, A. J.; Wilson, C. *Chem. Commun.* **2004**, 1612 (b) Van Veldhuizen, J. J.; Campbell, J. E.; Giudici, R. E.; Hoveyda, A. H. *J. Am. Chem. Soc.* **2005**, *127*, 6877 (c) Yun, J.; Kim, D.; Yun, H. *Chem. Commun.* **2005**, 5181.

Chapitre 2

Synthesis and Characterization of Bis-NHC Silver(I) and Copper(I) Complexes

1 Introduction

Since the first stable free carbene was isolated by Arduengo in 1991,[1] N-heterocyclic carbenes (NHCs) have found numerous applications in organometallic chemistry as ligands to prepare new metal-based catalysts.[2] The first *N*-heterocyclic carbene silver(I) complex was prepared by Arduengo *et al.* two decades ago, by reaction between a free carbene and silver(I) triflate.[3] Today, the reaction of imidazol(in)ium salts precursors with a broad variety of silver(I) sources such as Ag_2O,[4] Ag(OAc),[5] Ag_2CO_3[6] or AgCl[7] (with K_2CO_3 or Na_2CO_3 as external base) allows for the formation of Ag(I)-NHC complexes in high yields. Ag(I)-NHC complexes are stable towards air and water conditions. The reaction of Ag_2O with halide imidazol(in)ium salts, first described in 1998 by Lin, is particularly efficient to synthesize halide Ag(I)-NHC complexes under mild conditions, without having to handle free NHCs.[4] The second product formed during Lin's protocol being water, non-distilled solvents can be employed, which renders this approach very convenient and popular.[4] Ag(I)-NHC complexes are potent catalysts for e.g. the cycloaddition of CO_2 to terminal epoxides,[8] and C–N coupling reactions.[9] During pharmacological studies, they proved to release *in vivo* slowly and steadily free silver cations acting as tumour cells killers or suppressants of infections.[10] To date, Ag(I)-NHCs are mostly employed as transmetalating agents to access late transition metal NHC complexes, without the need to handle unwieldy free carbenes. They are indeed known to transmetalate efficiently the NHC ligand to Cu,[11] Ni,[12] Pd,[12-13] Pt[13] and Au[14] precursors. The coordination geometry around the Ag(I) centre tends to be linear. When the associated anion (X^-) is a halide, the formation of polynuclear complexes or clusters with X–Ag–X bridge(s) can lead to a broad structural diversity in the solid state. In silver(I)-NHC cluster complexes, d^{10}-d^{10} interactions between silver(I) cations are often encountered,[15] while the silver(I) cations coordination geometry may deviate from linear to trigonal or even tetrahedral. Tetranuclear silver(I) complexes do not always form cubanes but can lead to planar structures.[16]

Copper is the cheapest coinage metal used in organometallic chemistry, and despite the spectacular recent achievements in organogold chemistry,[17] the development of organocopper chemistry appears most desirable from an economic point of view. The first reported copper(I)-NHC complex was also prepared by Arduengo, by reaction of a free carbene with copper triflate.[3] Owing to the strong σ-donating properties of NHCs in association with copper(I), the resulting complexes are often robust against air and moisture. Several methods are known to access copper(I)-NHC complexes, such as the use of Ag(I)-

Références p. 162

NHCs as transmetalating reagents, the reaction of free carbenes with copper(I) halides, or of imidazolium salts with copper(I) oxide.[2d,18] Recently, copper(I) bis- or multidentate-NHC complexes have attracted much attention[19] because of their luminescence properties,[20] their ability to transmetalate their NHC ligand in presence of Ru,[21] Rh,[22] Pd,[23] Ag,[24] and Ni[25] precursors, or their catalytic properties (Sonogashira reaction,[26] nitrene and carbene transfer reactions).[27] Moreover, the nature of the metal-carbene bond in copper(I)-NHC complexes has been the subject of theoretical studies[28] while copper belongs to the very few metals able to form clusters with bridging imidazolydenes.[25] The coordination geometry around the copper(I) centre tends to be linear but in the presence of bidentate ligands and halide anions, "T-shaped", trigonal planar or tetrahedral coordination geometries readily arise.[16b,29] By contrast with the case of silver, polymeric copper(I)-NHC complexes are scarce. Thus, to the best of our knowledge, only three coordination polymers of copper(I) bromide complexes have been reported: two with pyridine- or oxazoline-functionalized NHC ligands and one with a bis-(NHC) ligands.

In this paper, we report the synthesis and the characterisation of a series of bis-NHC silver(I) and copper(I) complexes, which display various structural features in the solid state.

2 Syntheses of the imidazolium salts

The imidazolium salts **L102**, **L103** and **L155** were prepared in two steps: i) copper-catalyzed imidazole mono-alkylation with alkyl halides, ii) subsequent second alkylation with alkyl halides via N-quaternization (Scheme 1).

The synthesis of the 1,3-bis(imidazolyl)benzene was achieved by a Cu(II)-catalyzed aryl amination.[30] The literature work-up was modified to avoid purification by flash chromatography on silica. A simple filtration of a dichloromethane solution through Celite®, followed by precipitation with pentane, led to a clean product.

Références p. 162

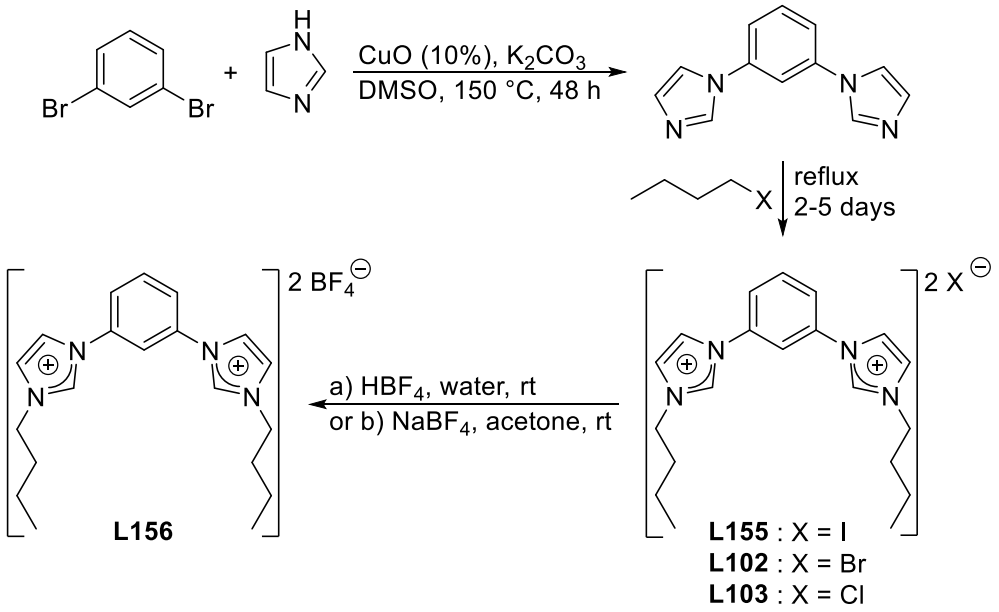

Scheme 1. Synthesis of the imidazolium salts **L102-L103** and **L155-L156**

Two protocols for the synthesis of the imidazolium salt 1,1'-(1,3-phenylene)bis(3-butyl-1H-imidazol-3-ium) iodide (ImidBuI, **L155**) by quaternization of 1,3-bis(imidazolyl)benzene with alkyl iodide were reported in the literature (Scheme 1). In one case, the synthesis was carried out in toluene in a sealed tube at 150 °C for 8 h; then the content was washed with THF to afford a yellow powder in good yield (77%).[31] In the other case, the reagents were mixed and refluxed for two days, then THF was used to wash the crude solid and recrystallization from a MeOH/Et_2O mixture afforded the clean product in moderate yield (66%).[32] For the synthesis of the imidazolium salt **L155**, the second protocol was preferred due to its convenience, despite its lower yield. Precipitation rather than recrystallization was used to purify the crude reaction product, yielding **L155** in 68% yield. The ^{1}H and $^{13}C\{^{1}H\}$ NMR data were in agreement with those in the literature.[31-32]

The reaction conditions for the synthesis of the salts 1,1'-(1,3-phenylene)bis(3-butyl-1H-imidazol-3-ium) bromide (ImidBuBr, **L102**) and 1,1'-(1,3-phenylene)bis(3-butyl-1H-imidazol-3-ium) chloride (ImidBuCl, **L103**) were initially set identical to those employed for **L155**. In presence of 1-bromobutane, 1,3-bis(imidazolyl)benzene was bis-alkylated (**L102**) after 48 h and some mono-alkylated product was also present. Eventually, **L102** was obtained in moderate yield (63%) (no trace of mono-alkylated species) when the reaction time was increased to 72 h. In presence of butyl chloride, 1,3-bis(imidazolyl)benzene was converted to **L103** after three days at 100 °C in low yield (5%). Thus, **L103** was finally obtained in moderate yield (65%) by increasing the temperature to 140 °C in chlorobenzene. The ^{1}H

NMR spectra of the salts **L102-L103** and **L155** in CD_2Cl_2 display the characteristic resonances of the NC*H*N proton between 11.2 and 11.7 ppm.

The salt 1,1'-(1,3-phenylene)bis(3-butyl-1H-imidazol-3-ium) tetrafluoroborate (ImidBuBF$_4$, **L156**) was first obtained in low yield (15%) by anion metathesis using ImidBuBr (**L102**) and tetrafluoroboric acid in distilled water. A second attempt, with sodium tetrafluoroborate in acetone, afforded **L156** as an off-white powder in excellent yield (98%). The metathesis was confirmed by ^{1}H NMR, with a significant shift from 11.5 to 9.7 ppm for the imidazolium NC*H*N signal of **L102** and **L156**; the latter being sensitive to the nature of the associated anion.

3 Syntheses of the silver(I) complexes

During the course of our work with the pro-ligands **L102-L103** and **L155-L156**, Hollis *et al.* reported the silver(I)-NHC complex bis(*μ*-1,3-bis(3'-butylimidazol-2'-ylidene)benzene)-*κ*-C)tetra-μ_3-iodotetrasilver(I) (ImidBu$_2$Ag$_4$I$_4$, **334**), as a white powder**,** obtained by reaction of the pro-ligand ImidBuI (**L155**) with silver(I) oxide in moderate yield (67%).[33] We used the same approach with Ag_2O and a slightly modified purification step for **334**: Hollis reported the filtration of a CH_2Cl_2 solution of **334** and its direct precipitation/washing with diethyl ether. Prior to precipitation, we added an additional step, without any loss of yield (75%), by extracting with water most of the impurities present, including possible traces of unreacted **L155**. Following the same procedure as for **334**, the imidazolium salts **L102-L103** were reacted with 1.5 equivalent of silver(I) oxide, which afforded **335-336** in good yield (75% and 65%, respectively). The disappearance of the characteristic signal of the imidazolium salts in ^{1}H NMR spectroscopy and the appearance in the ^{13}C{^{1}H} NMR spectra of typical downfield signals for the carbenic carbons at 182.6 ppm and 179.2 ppm confirmed the formation of **335** and **336**. The butyl chain signals remain unchanged, in both ^{1}H and ^{13}C{^{1}H} NMR spectra, between the imidazolium salts **L102-L103** and the silver complexes **335-336**. In the ^{1}H NMR spectra, the C*H*^{imidazole} and C*H*^{aryl} signals of **335** in the aromatic region are shifted by 1.30 ppm and 1.16 ppm. Moreover, the signals of the aryl groups and of the imidazole backbones of **335-336** are located between 7.00 and 8.00 ppm.

There is often an ambiguity concerning the structures of silver NHC halide complexes, between neutral mono-NHC complexes of the type [(NHC)AgX] or cationic bis-NHC complexes of the type [(NHC)Ag(NHC)]$^+$ X$^-$ and also in the latter case concerning the nature

of the counterion, a simple halide anion (X^-), or more complicated anionic clusters of the $Ag_nX_m^{n-m-}$-type. Further characterisations were consequently performed. The ESI mass spectrum of complex **335** displays signals for *m/z* (L = ligand) = $[2L+4Ag+4Br+H]^+$ = 1395.98, $[2L+4Ag+3Br]^+$ = 1314.18, $[2L+3Ag+3Br+H]^+$ = 1208.88, $[2L+3Ag+2Br]^+$ = 1126.96, $[2L+2Ag+2Br+H]^+$ = 1015.05, $[2L+2Ag+Br]^+$ = 939.15, $[L+2Ag+2Br+H]^+$ = 698.87, $[L+2Ag+Br]^+$ = 616.94, $[L+Ag+Br+H]^+$ = 511.06; $[2L+2Ag]^{2+}$ = 430.12. It is reasonable to assume that complex **335** is partially unstable under the mass spectrum analysis conditions and slowly reconverted to the imidazolium salt **L102**. Interestingly, the peak at *m/*z = 1395.98 might originate from a cubane-type complex similar to that reported by Hollis *et al.*[33] To have an unambiguous characterisation of **335**, colourless single crystals suitable for X-ray diffraction were grown by slow evaporation of solutions mixture of **335** with THF and octane. The formation of a silver(I)-NHC complex was therefore confirmed. The complex bis(μ-1,3-bis(3'-butylimidazol-2'-ylidene)benzene)-κ-C)tetra-μ_3-bromotetrasilver(I) ($ImidBu_2Ag_4Br_4$, **335**) crystallizes in the monoclinic system with the $P2_1/c$ space group and has a cubane type structure (Figure 1). There is one carbene functionality per metal and halogen. Two of the Ag–Ag bond distances (Ag1–Ag2 = 3.137(1) Å and Ag3–Ag4 = 3.159(1) Å) are shorter than the sum of the van der Waals radii of a silver atom (3.44 Å), so they might be diagnostic of d^{10}-d^{10} "argentophilic" interactions.[15,34] The other two Ag–Ag separations are much longer (Ag2–Ag3 = 3.94 Å; Ag1–Ag4 = 3.54 Å). The ratio between the average Ag–Ag distances (3.44 Å) and the average Br–Br distances (3.31 Å) is 0.799; it is intermediate between the ratios for an ideal cubane (1.00) and stella quadrangular (0.667) geometries.[35] Hence, $ImidBu_2Ag_4Br_4$ (**335**) forms a distorted cubane, mimicking the structure of the very similar bis(μ-1,3-bis(4'-butyltriazol-2'-ylidene)benzene)-κ-C)tetra-μ_3-bromotetrasilver(I) complex reported recently by Hollis *et al.*[46] NHC (or phosphine)-Ag(I) complexes with cubane structures are well documented in the literature.[36] The Ag–C and Ag–Br bond lengths fall in the range between 2.140(4) - 2.161(4) Å and 2.6850(5) - 2.8567(6) Å, respectively. These values are in agreement with those found in other silver halide cubane complexes.[33]

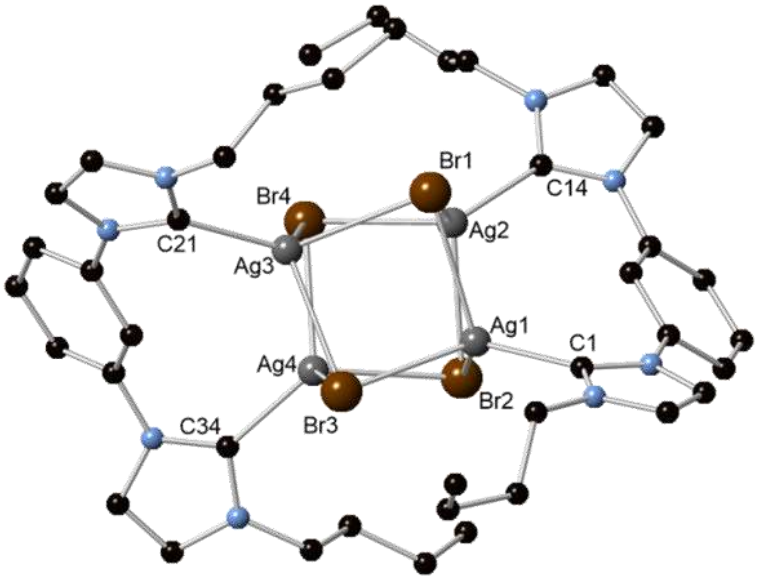

Figure 1. Ball and stick representation of the structure of [ImidBu$_2$Ag$_4$Br$_4$] (**335**). Hydrogen atoms have been omitted for clarity.

The ESI mass spectrum of complex **336** displays signals for *m/z* (L = ligand) = $[L+2Ag+2Cl+H]^+$ = 608.97, $[L+2Ag+Cl]^+$ = 572.99, $[L+Ag+Cl+H]^+$ = 467.10 and $[L+H]^+$ = 323.22, plus a few unassignable signals. Like ImidBu$_2$Ag$_4$Br$_4$ (**335**), the complex **336** is sensitive toward the conditions of the mass spectrometry analysis. The fragmentation patterns found in the mass spectra of **335** and **336** appear totally different. It is interesting to note that there is no signal corresponding to a tetranuclear structure, but rather a peak at *m/*z = 608.97 consistent with a dinuclear NHC complex. In order to unambiguously characterize **336**, colourless single crystals were grown by slow evaporation of solutions of **336** in a mixture of dichloromethane and octane. The complex μ-1,3-bis(3'-butylimidazol-2'-ylidene)benzene)dichlorodisilver(I) (ImidBuAg$_2$Cl$_2$, **336**) is an organometallic coordination polymer, which crystallizes in the monoclinic system and the $P2_1/c$ space group (Figure 2). Monomeric units [ImidBuAg$_2$Cl$_2$] are held together by a bridging chloride anion. There is one carbene centre per metal and halogen. The bond distances Ag1–C1 and Ag2–C14 are equal to 2.081(6) and 2.102(6) Å, and the bond distances Ag1–Cl1, Ag2–Cl2 and Ag2–Cl1 to 2.3340(16), 2.3802(15) and 2.8878(15) Å, respectively. These values are similar to those found in other NHC-silver(I) complexes.[37] The silver cation Ag1 has a distorted linear coordination geometry with a C1–Ag1–Cl1 angle of 169.3(2)°, whereas the second silver cation Ag2 is in a distorted trigonal planar coordination environment with Cl2–Ag2–Cl1, C14–Ag2–Cl1 and C14–Ag2–Cl2 angles of 97.97(5), 108.2(2) and 152.6(2)°, respectively. Each imidazole ring from the same ligand is oriented head to tail with a torsion angle of

173.3°. It is noteworthy that changing the anion from bromide to chloride transformed the structure from cubane- to polymer-type. Finally the reactivity of **336** was assessed toward metathesis of anions in presence of AgBr or LiBr, in dry acetone. ^{1}H NMR spectroscopy and elemental analysis of the crude reaction evidenced the quantitative conversion of **336** into **335** within 16 h. Surprisingly, in wet acetone no conversion was monitored after 24 h. The depolymerisation of **336** to rebuild a cubane-structure is a clear illustration of the great affinity of group 11 metals toward soft halide ligands (I>Br>Cl), as well as the propensity of soft halides to form higher order bridges in polynuclear complexes with late transition metals.

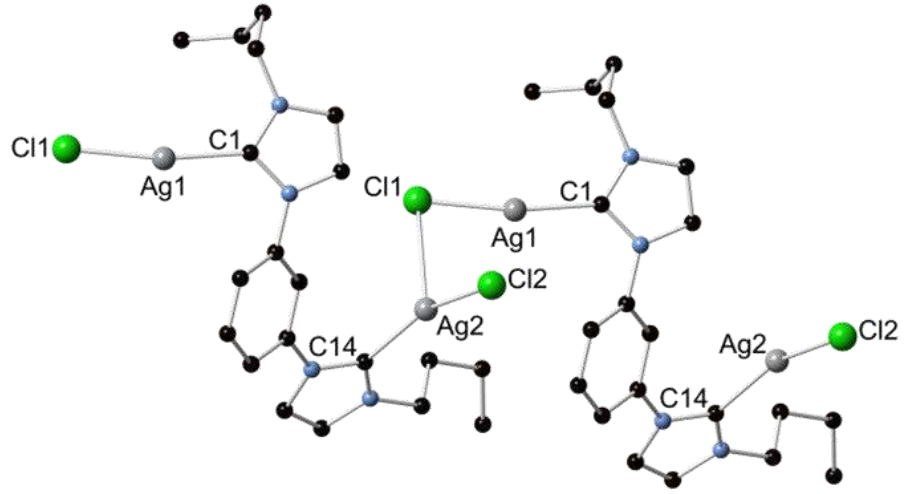

Figure 2. Molecular structure of two monomers [ImidBuAg$_2$Cl$_2$] forming the polymer chains of **336** in the solid state. Hydrogen atoms have been omitted for clarity.

The replacement of the halogen bound to silver by BF_4^-, a non-coordinating anion, should have a strong impact on the complex structure due to the loss of halide bridges. The reaction of **L156** with silver(I) oxide, similarly to the protocols described for **234**-**236**, failed to give the complex **337**. This is probably due to the insufficient difference of relative acid-base strengths between **L156** and Ag_2O (The difference of pK_a between ([NHC–H$^+$][BF_4^-]/[NHC]) and ([Ag_2OH^+]/[Ag_2O]) is the driving force to initiate the reaction when Ag_2O is used as the silver(I) source).[38] An anion metathesis was attempted using **334** or **335** as reagent with 2.0 equivalents of $AgBF_4$ in dichloromethane, at room temperature, for 18 h. The complete formation of the complex **337** versus **334**/**335** was supported by the shift of the aromatic signals in the ^{1}H NMR spectra and the shift of the characteristic signal of the carbenic carbons from 184.80 ppm (**334**) or 182.6 ppm (**335**) to 179.6 ppm. The ESI mass spectrum of the complex **337** displays signals for *m/z* = [2L+2Ag+BF_4]$^+$ = 945.25,

Références p. 162

$[2L+2Ag]^{2+}$ = 430.12 and $[LH]^{+}$ = 322.22. Once again, **337** appears partially stable under the mass spectrometry analysis conditions. To clearly characterise **337**, colourless single crystals suitable for X-ray diffraction analysis were obtained by stratification with pentane of a solution of **337** in dichloromethane. The complex bis-(*μ*-1,3-bis(3'-butylimidazol-2'-ylidene)benzene)disilver(I) ditetrafluoroborate ($\{[ImidBuAg]BF_4\}_2$, **337**) has a dinuclear structure with Ag(I) ions bridged by two NHC ligands binding in a *C*,*C*' mode. It crystallizes with two molecules of dichloromethane, in the triclinic system and the *P*-1 space group (Figure 3). The structure of **337** is typical for bis-(NHC)-dimetallic complexes of the type $\{[(NHC)Ag(NHC)^{+}]_2, 2[X^{-}]\}$ where X^{-} represents a non-coordinating anion.[39] There are two carbene donors and one tetrafluoroborate anion per silver. The C1–Ag1 and C14–Ag1 bond distances are equal to 2.083(3) and 2.085(3) Å, respectively. The Ag(I) cations adopt a quasi-linear coordination geometry in **337** with C1–Ag–C14 angles of 174.28(1)°. Bonds distances and angles are similar to those reported for other cationic bis(NHC)Ag(I) complexes.[40] The planes of the NHC rings bound to a silver ion are tilted by of 45.6(1)°. The planes of the NHC rings belonging to the same ligand form an angle of -138.7(3) and 133.5(3)° with the aryl ring. The planes of the bridging-phenylene spacers are parallel and mutually distant from 4.4 Å, which rules out any π-π stacking (usually observed between 3.3 and 3.8 Å) in the solid state.[41] There is no interaction between the Ag(I) centres and the BF_4^{-} anions. The complexes **334**-**337** are stable towards moisture in ambient day light (Scheme 2).

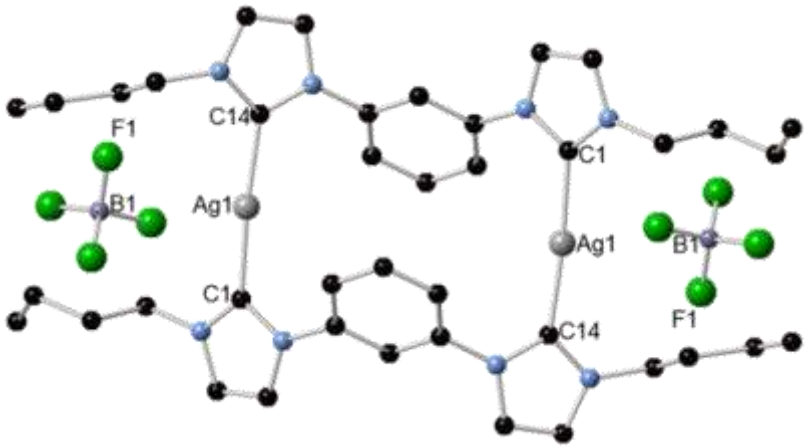

Figure 3. Ball and stick representations of the structure of $[\{(ImidBu)Ag\}BF_4]_2$ (**337**). Hydrogen atoms have been omitted for clarity.

Références p. 162

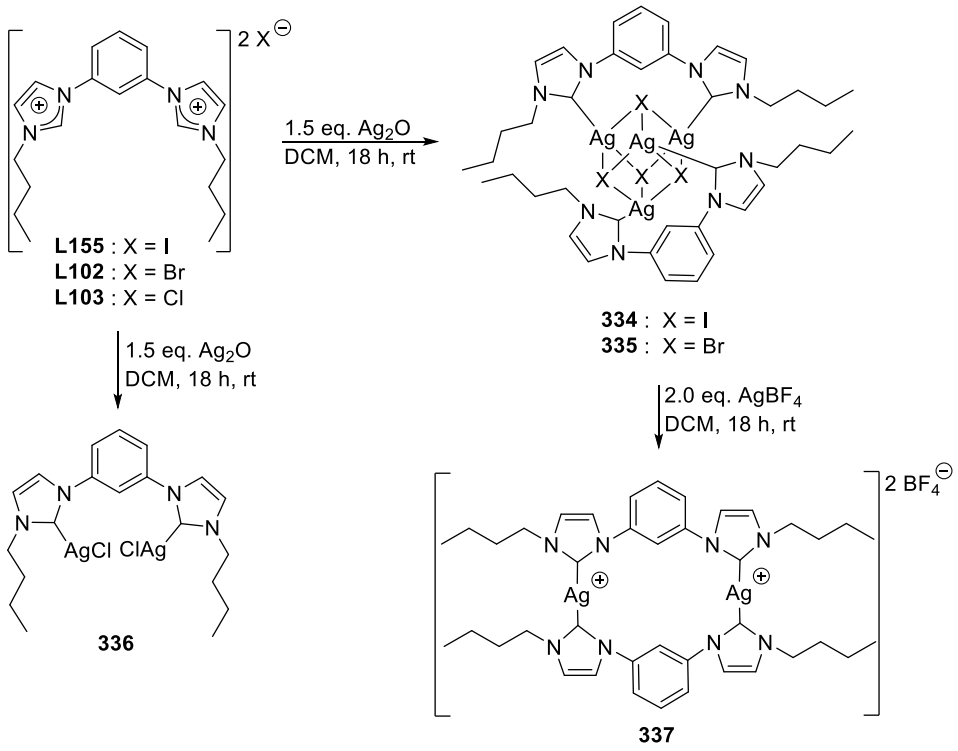

Scheme 2. The diverse solid-state structures encountered in **334**-**337**

4 Synthesis of the copper(I) complexes

In order to identify the most efficient synthesis, four known protocols were tested. First, the imidazolium salt **L155** was reacted with 1.3 eq. of copper(I) oxide in distilled and degassed water or in toluene under reflux.[42] After 24 h no reaction had occurred. Second, **L155** and 1.3 eq. of copper oxide were heated in THF at 110 °C in a sealed tube, under microwave irradiation. After 1 h, the starting materials were recovered.[43] Third, **L155** was reacted in THF for 18 h with 1.0 eq. of copper(I) hexadimethylsilylazide (copper source with an internal base),[44] which led to a 90% conversion into the complex **338**. Ag(I)-NHC complexes being efficient at transmetalating their carbene ligand to copper(I), a fourth approach was tested by dissolving **334** in dichloromethane in the presence of CuI, at room temperature for 18 h.[20a,45] The ^{1}H NMR analysis of the crude mixture showed that the transmetalation only partially occurred. However, increasing the temperature to the boiling point of dichloromethane resulted in the quantitative formation of **338**.

Hence, two pathways were found to produce **338** in good yields. The use of $CuN(SiMe_3)_2$ might become a valuable and promising synthetic approach with ligands not compatible with the silver transmetalation route.[44]

Références p. 162

The formation of **338** was further confirmed by ^{1}H NMR spectroscopy with the disappearance of the characteristic signal of the imidazolium salt **L155** and by $^{13}C\{^{1}H\}$ NMR spectroscopy with the appearance of the characteristic resonance of an N-heterocyclic carbene bound to copper at 184.2 ppm. Converting **L155** to **338** does not affect the chemical shifts of the butyl chains signals in either the ^{1}H or $^{13}C\{^{1}H\}$ NMR spectra. The aryl signals are slightly affected, with variations smaller than 1.0 and 4.5 ppm in the ^{1}H NMR or $^{13}C\{^{1}H\}$ NMR spectra, respectively. The ESI mass spectrum of complex **338** displays signals for *m/z* (L = ligand): $[2L+5Cu+4I]^{+}$ = 1468.70, $[2L+4Cu+4I+H]^{+}$ = 1406.77, $[2L+4Cu+3I]^{+}$ = 1278.86, $[2L+3Cu+3I+H]^{+}$ = 1216.94, $[2L+3Cu+2I]^{+}$ = 1089.03, $[2L+2Cu+2I+H]^{+}$ = 1025.10, $[2L+2Cu+I+H_2O]^{+}$ = 913.19, $[2L+2Cu+I]^{+}$ = 897.19, $[L+2Cu+I+H]^{+}$ = 702.89, $[L+2Cu+I]^{+}$ = 574.98 and $[L+Cu+I+H]^{+}$ = 513.06, and a few unassigned signals of low intensities. Complex **338** undergoes significant fragmentation under the conditions of the analysis. The signal found at 1468.7 *m/z* ($[2L+5Cu+4I]^{+}$) is probably due to the formation of aggregates taking place during the analysis (high concentration effects are well-known during the ESI process).[46] The decomposition patterns of **338** by loss of halogen and/or silver are similar to those encountered for **334** and **335**, hinting at a possible cubane structure. Numerous crystallisation attempts (stratification, slow evaporation and vapour diffusion) were set with diverse couples of solvents/non-solvents (THF-pentane, THF-Et_2O, THF-octane, CH_2Cl_2-pentane and CH_2Cl_2-octane) at different temperatures (room temperature, 4 °C and -20 °C). Unfortunately, none of them was successful at generating single crystals suitable for X-ray diffraction analysis.

Following the protocol employed for **338**, the salts **L102**-**L103** were reacted with $CuN(SiMe_3)_2$ and the desired complexes **339** and **340** were obtained as white powders in excellent yields (>98%). The formation of these new complexes was further confirmed in ^{1}H NMR spectroscopy by the disappearance of the characteristic signal of the imidazolium salts, and in $^{13}C\{^{1}H\}$ NMR spectroscopy by the appearance of typical downfield signals for the copper-bound carbenes at 177.8 and 176.5 ppm. Similarly to **338**, converting **L102**-**L103** to **339**-**340** does not induce any visible change for the butyl chains signals in the ^{1}H and $^{13}C\{^{1}H\}$ NMR spectra. The aromatic ^{1}H NMR signals for **339** and **340** are slightly shifted downfield when compared to those of **L102** and **L103**.

The ESI mass spectrum of complex **339** displays signals for *m/z* (L = ligand) $[L+2Cu+2Br+H]^{+}$ = 610.92, $[L+2Cu+Br]^{+}$ = 528.99, $[L+Cu+Br+H]^{+}$ = 467.07 and $[L+H]^{+}$ = 323.22 and a few unassigned signals. The decomposition pattern of **339** is similar to that encountered for **336** hinting at a possible polymeric structure. To validate this hypothesis,

Références p. 162

colourless single crystals suitable for X-ray diffraction analysis were grown by stratification with pentane of a THF solution of **339**. The complex μ-1,3-bis(3'-butylimidazol-2'-ylidene)benzene)dibromodicopper(I) ($ImidBuCu_2Br_2$, **339**) is an organometallic coordination polymer, which crystallizes in the monoclinic system and the $P2_1/c$ space group (Figure 4). There is one carbene donor per copper and bromide, the bis-carbene ligand acting as a bridge between two Cu centres. Two neutral dinuclear units [$ImidBuCu_2Br_2$] constitute a monomeric entity and are held together by a bridging bromide anion. The Cu2–C14, Cu2–Br2, Cu1–C1, Cu1–Br1 and Cu1–Br2 bond distances are equal to 1.893(7), 2.245(1), 1.904(6), 2.330(1) and 2.647(1) Å, respectively. The copper centre Cu2 exhibits a slightly distorted linear coordination geometry, with an C14–Cu2–Br2 angle equal to 171.3(2)°, whereas Cu1 is in a quasi-trigonal planar environment with C1–Cu1–Br1, C1–Cu1–Br2 and Br2–Cu1–Br1 angles of 147.3(2)°, 113.3(2)° and 98.79(5)°, respectively. The bridging bromide Br2 is bound to Cu1 via a long-range interaction (2.647(1) Å) and to Cu2 via a shorter (covalent) bond (2.245 (1) Å). The imidazole rings from the same ligand are oriented in almost opposite directions, which make the ligand an excellent bridge for coordination polymers, and the angle between their planes is 168°.

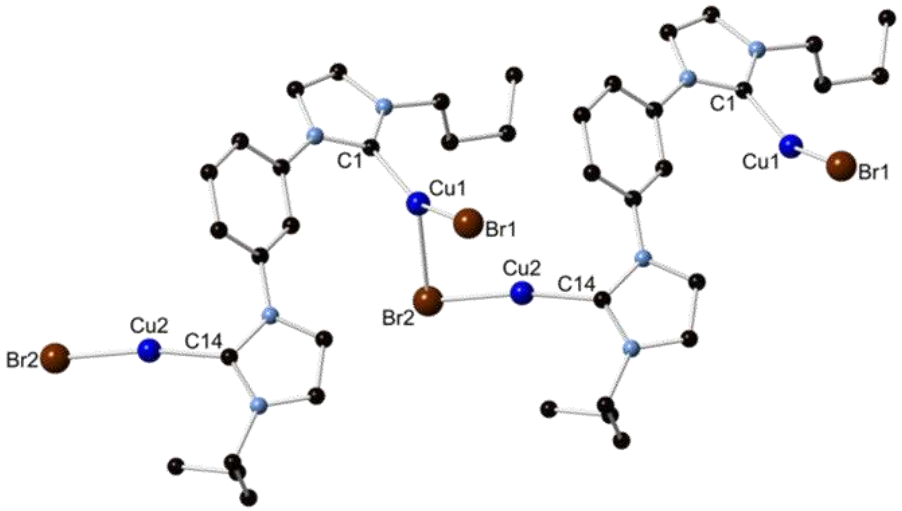

Figure 4. Ball and stick representations of two dinuclear, monomeric units [$ImidBuCu_2Br_2$] which are held together by Br2 and form the polymer chain of **339** in the solid-state. Hydrogen atoms have been omitted for clarity.

The ESI mass spectrum of complex **340** displays signals for *m/z* (L = ligand) $[L+2Cu+2Cl+H]^+$ = 519.02, $[L+2Cu+Cl]^+$ = 483.04, $[L+Cu+Cl+H]^+$ = 421.12 and $[L+H]^+$ = 323.22 and a few unassigned signals. We notice that the fragmentation pattern is similar to those encountered with **336** and **339.** Single crystals suitable for X-ray diffraction were grown

Références p. 162

by stratification with pentane of a THF solution of **340**. The complex μ-1,3-bis(3'-butylimidazol-2'-ylidene)benzene)dichlorodicopper(I) (ImidBuCu$_2$Cl$_2$, **340**) is also an organometallic coordination polymer, which crystallizes in the monoclinic system and the $P2_1/c$ space group (Figure 5). Its structure is very similar to that **339**, with chlorides replacing bromide ions. There is one carbene donor group per copper and chloride. The neutral dinuclear, monomeric units [ImidBuCu$_2$Cl$_2$] are held together by a bridging chloride anion to form a coordination polymer. The Cu1–C1, Cu1–Cl1, Cu2–C14, Cu2–Cl2 and Cu2–Cl4 bond distances are equal to 1.882(5), 2.115(1), 1.901(5), 2.1835(13) and 2.607(1) Å, respectively. The copper centre Cu1 exhibits a slightly distorted linear coordination geometry, with a C1–Cu1–Cl1 angle of 169.5(2)° whereas Cu2 is in a quasi-trigonal planar environment with C14–Cu1–Cl1, C14–Cu2–Cl2 and Cl1–Cu1–Cl2 angles of 142.2(2)°, 116.4(2)° and 101.05(4)°, respectively. The bridging Cl1 anion is bound to Cu2 via a long-range interaction (2.607(1) Å) and to Cu1 via a shorter (covalent) bond (2.115(1) Å). Like in **339**, the imidazole rings from the same ligand are oriented in almost opposite directions and the angle between their planes is equal to 171.5°.

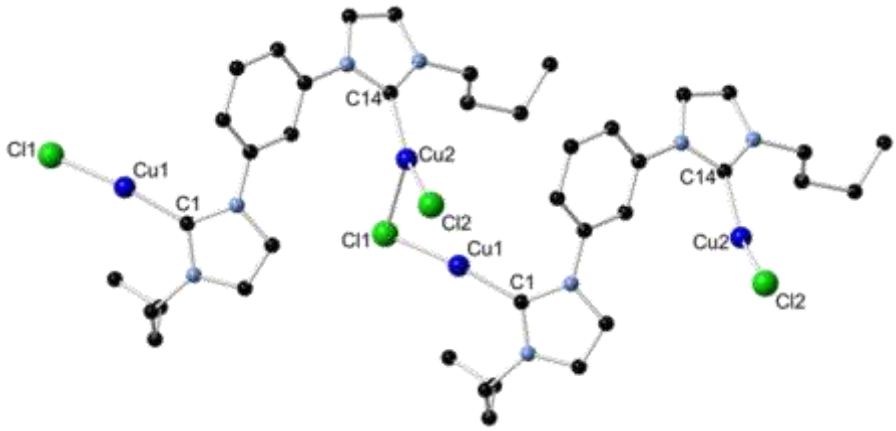

Figure 5. Ball and stick representations of two dinuclear, monomeric units [ImidBuCu$_2$Cl$_2$] which are held together by Cl1 and form the polymer chain of **340** in the solid-state. Hydrogen atoms have been omitted for clarity.

The Cu–C bond distances in the complexes **339**-**340** are comparable to those reported for other neutral copper(I) NHC complexes.[27,47] The bis-NHC ligand act as a bidentate ligand and its assembling role favours the formation of 1D-polymers over mono- or dinuclear-species. Furthermore, long-range halogen-copper interactions also play a key role in the formation of coordination polymers in preference to cubanes. To the best of our knowledge, only three copper(I)-NHC organometallic coordination polymers have been characterized in

Références p. 162

the solid-state.[47a,47c,d] Two of them feature pyridine- or oxazoline-functionalized NHC ligands (acting as bidentate donors) and are of the [–N⌒⌒NHC–(CuBr)–]$_n$ type, in which each copper is ligated by a carbene and a pyridine or oxazoline belonging to different ligands and a bromide anion.[47c,d] The third example contains bis-NHC ligands and is of the (–NHC–Cu–(μ-Br)$_2$–Cu–NHC–)$_n$ type in which each copper is connected by two bridging bromides.[47a] In **339-340**, the connexion between the monomers is different: each copper centre in the monomeric unit is connected to a carbene and a halide to form a neutral complex. These monomers are held together by van der Waals and electrostatic interactions to give a (–NHC–(CuBr)–(μ-Br)–Cu–NHC–)$_n$-type polymer (Scheme 3).

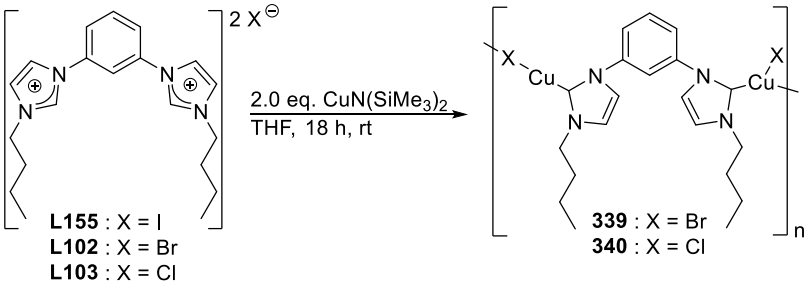

Scheme 3. Syntheses of copper(I) complexes **339** and **340.**

5 Conclusion

We have obtained a series of bis-(NHC) silver(I) or copper(I) complexes in good yields. Their structures strongly depend on the nature of the associated anions, and range from classic di-cationic (**337**), to cubane-type (**335**) or coordination polymers (**336** and **339-340**). The complexes **339-340** constitute new additions to the still rare examples of copper-NHC coordination polymers.

Ag(I)-NHC coordination polymers have found applications in coupling reactions,[9] carbene transfer reactions[37b] and bactericidal activities.[48] The complexes described in this work will be evaluated further for practical applications.

6 Experimental details

Only reactions made copper reagents where carried out under inert atmosphere using standard Schlenk techniques. The compound CuN(SiMe$_3$)$_2$ was synthesized according to a published procedure.[49] All reagents were used as received from commercial suppliers. Solvents were purified and dried under argon by conventional methods. Proton (^{1}H), carbon

Références p. 162

($^{13}C\{^1H\}$) and fluorine ($^{19}F\{^1H\}$) nuclear magnetic resonance (NMR) spectra were recorded on the following instruments: Bruker AVANCE I – 300 MHz spectrometer and Bruker AVANCE I – 500 MHz spectrometer. The chemical shifts are given in part per million (ppm). Data are presented as following: chemical shift, multiplicity (s = singlet, d = doublet, t = triplet, q = quartet, quint = quintet, sept. = septet, m = multiplet, b = broad), coupling constants (J/Hz) and integration. Assignments were determined either on the basis of unambiguous chemical shifts or coupling patterns. The residual solvent proton (^1H) or carbon ($^{13}C\{^1H\}$) resonance, or the BF_4^- anion signals (^{19}F) were used as reference values. For ^1H NMR: $CDCl_3$ = δ 7.26 ppm, CD_2Cl_2 = δ 5.32 ppm and DMSO-d_6 = δ 2.50. For $^{13}C\{^1H\}$ NMR: $CDCl_3$ = δ 77.1 ppm, CD_2Cl_2 = δ 53.8 and DMSO-d_6 = δ 39.5 ppm. For ^{19}F NMR: BF_4^- = δ -150.63 ppm. IR and FIR spectra were recorded in the region 4000-200 cm^{-1} on a Nicolet 6700 FT-IR spectrometer (ATR mode, diamond crystal). Elemental analyses were performed by the "Service de Microanalyses", Université de Strasbourg. Mass spectrometry analyses (ESI-MS) were performed by the "Service de Spectrométrie de Masse", Université de Strasbourg. For X-ray diffraction studies, the intensity data were collected at 173(2) K on a Kappa CCD diffractometer 88 (graphite-monochromated Mo-K_α radiation, λ = 0.71073 Å). The structures were solved by direct methods (SHELXS-97) and refined by full-matrix least-squares procedures (based on F^2, SHELXL-97) with anisotropic thermal parameters for all the non-hydrogen atoms.[50] The hydrogen atoms were introduced into the geometrically calculated positions (SHELXL-97 procedures) and refined riding on the corresponding parent atoms. Crystallographic and experimental details for all structures are summarized below as well as their ORTEP representations.

1,3-di(imidazol-1-yl)benzene. To a solution of 1,3-dibromobenzene (25.00 mL, 0.21 mol) in DMSO (200 mL) were added 1H-imidazole (35.00 g, 0.51 mol), potassium carbonate (72 g, 0.52 mol) and copper(II) oxide (2.00 g, 25.20 mmol). After 48 h at 150°C, the solvent was removed by distillation. The crude solid was solubilized in dichloromethane (inorganic salts were insoluble) and filtered through Celite®. The solution was concentrated. The product was precipitated in pentane. A pale yellow powder was obtained (38.30 g, 0.18 mol). Yield: 88 %. ^1H NMR (300 MHz, $CDCl_3$) δ 7.95 (s, 2H, NCHN), 7.63 (m, 1H, CH^{aryl}), 7.51 (t, J = 2.0 Hz, 1H, CH^{aryl}), 7.45 (d, J = 2.1 Hz, 1H, CH^{aryl}), 7.42 (d, J = 1.8 Hz, 1H, CH^{aryl}), 7.39 (t, J = 1.3 Hz, 2H, $CH^{imidazole}$), 7.25 (s, 1H, $CH^{imidazole}$). $^{13}C\{^1H\}$ NMR (75 MHz, $CDCl_3$) δ 138.5 (NCHN), 135.4 (C^{aryl}), 131.3 ($CH^{imidazole}$), 130.8 ($CH^{imidazole}$), 119.8 (CH^{aryl}), 117.9 (CH^{aryl}), 114.2 (CH^{aryl}).

1,1'-(1,3-phenylene)bis(3-butyl-1H-imidazol-3-ium) iodide (L155). 1,3-di(imidazol-1-yl)benzene (4.00 g, 19.04 mmol) was added in butyl iodide (10.00 mL, 87.87 mmol). The mixture was stirred under reflux for 48 h. The solvent was removed under vacuum and the crude solid dissolved in dichloromethane with few drops of methanol. Off white powder was obtained after precipitation in Et_2O (7.48 g, 12.93 mmol). Yield: 68%. ^{1}H NMR (300 MHz, CD_2Cl_2) δ 11.25 (t, *J* = 1.7 Hz, 2H, NCHN), 8.97 (t, *J* = 2.1 Hz, 1H, CH^{aryl}), 8.48 (t, *J* = 1.9 Hz, 2H, $CH^{imidazole}$), 8.14 (dd, *J* = 8.1, 2.2 Hz, 2H, $CH^{aryl)}$, 7.91 – 7.84 (m, 1H, CH^{aryl}), 7.51 (s, 2H, $CH^{imidazole}$), 4.46 (t, *J* = 7.4 Hz, 4H, NCH_2^{Bu}), 2.11 – 2.00 (m, 4H, CH_2^{Bu}), 1.52–1.42 (m, 4H, CH_2^{Bu}), 1.02 (t, *J* = 7.3 Hz, 6H, CH_3^{Bu}). $^{13}C\{^1H\}$ NMR (75 MHz, CD_2Cl_2) δ 136 .6 (NCHN), 136.3 (C^{aryl}), 133.3 (CH^{aryl}), 123.5 ($CH^{imidazole}$), 123.4 (CH^{aryl}), 122.3 ($CH^{imidazole}$), 116.5 (CH^{aryl}), 51.1 (NCH_2^{Bu}), 32.4 (CH_2^{Bu}), 20.0 (CH_2^{Bu}), 13.7 (CH_3^{Bu}).

1,1'-(1,3-phenylene)bis(3-butyl-1H-imidazol-3-ium) bromide (L102). A procedure similar to that used for compounds **L155** with 1,3-di(imidazol-1-yl)benzene (4.00 g, 19.04 mmol) and butyl bromide (9.70 mL, 87.61 mmol) gave **L102** after 72 h, as an off white powder (5.78 g, 12.00 mmol). Yield: 63%. ^{1}H NMR (300 MHz, CD_2Cl_2) δ 11.56 (s, 2H, NCHN), 9.04 (t, *J* = 2.0 Hz, 1H, $CH^{imidazole}$), 8.91 (t, *J* = 1.7 Hz, 2H), 8.24 (dd, *J* = 8.3, 2.1 Hz, 2H), 7.72 (t, *J* = 8.3 Hz, 1H), 7.60 (s, 2H, $CH^{imidazole}$), 4.45 (t, *J* = 7.3 Hz, 4H, NCH_2^{Bu}), 2.08–1.98 (m, 4H, CH_2^{Bu}), 1.50–1.38 (m, 4H, CH_2^{Bu}), 1.00 (t, *J* = 7.3 Hz, 6H, CH_3^{Bu}). $^{13}C\{^1H\}$ NMR (126 MHz, CD_2Cl_2) δ 137.0 (C^{aryl}), 136.5 (NCHN), 133.0 (CH^{aryl}), 123.4 ($CH^{imidazole}$), 122.8 (CH^{aryl}), 122.4 ($CH^{imidazole}$), 115.5 (CH^{aryl}), 51.0 (NCH_2^{Bu}), 32.4 (CH_2^{Bu}), 20.1 (CH_2^{Bu}), 13.8 (CH_3^{Bu}).

1,1'-(1,3-phenylene)bis(3-butyl-1H-imidazol-3-ium) chloride (L103). A procedure similar to that used for compounds **L155** with 1,3-di(imidazol-1-yl)benzene (4.00 g, 19.04 mmol) and butyl chloride (10.20 mL, 98.07 mmol) gave **L103** in chlorobenzene, at 140 °C, as an off white powder (4.89 g, 12.38 mmol). Yield: 65%. ^{1}H NMR (500 MHz, CD_2Cl_2) δ 11.76 (s, 2H, NCHN), 9.27 (s, 2H, $CH^{imidazole}$), 9.11 (s, 1H, CH^{aryl}), 8.27 (dd, *J* = 8.2, 1.9 Hz, 2H, CH^{aryl}), 7.80 (s, 2H, $CH^{imidazole}$), 7.54 (t, *J* = 8.3 Hz, 1H, CH^{aryl}), 4.43 (t, *J* = 7.3 Hz, 4H, NCH_2^{Bu}), 2.04 – 1.92 (m, 4H, CH_2^{Bu}), 1.44 – 1.32 (m, 4H, CH_2^{Bu}), 0.93 (t, *J* = 7.4 Hz, 6H, CH_3^{Bu}). $^{13}C\{^1H\}$ NMR (126 MHz, CD_2Cl_2) δ 137.0 (C^{aryl}), 136.4 (NCHN), 132.5 (CH^{aryl}), 123.5 ($CH^{imidazole}$), 122.3 (CH^{aryl}), 122.0 ($CH^{imidazole}$), 114.7 (CH^{aryl}), 50.6 (NCH_2^{Bu}), 32.3 (CH_2^{Bu}), 19.9 (CH_2^{Bu}), 13.7 (CH_3^{Bu}).

1,1'-(1,3-phenylene)bis(3-butyl-1H-imidazol-3-ium) tetrafluoroborate (L156). To a solution of 1,3-bis(3'-butylimidazol-l-yl)benzene dibromide (100.0 mg, 0.24 mmol) in acetone was added an excess of $NaBF_4$ (263.5 mg, 2.40 mmol). The mixture was stirred at room temperature overnight. NaBr was filtered through Celite® and the filtrate was washed with pentane yielding to a clean product (117.15 mg, 0.23 mmol). Yield: 98%. ^{1}H NMR (500 MHz, CD_2Cl_2) δ 9.69 (s, 2H, NCHN), 8.26 (t, *J* = 2.1 Hz, 1H, CH^{aryl}), 8.09 (t, *J* = 1.9 Hz, 2H, $CH^{imidazole}$), 7.88 (dd, *J* = 8.2, 2.0 Hz, 2H, CH^{aryl}), 7.78 – 7.71 (m, 1H, CH^{aryl}), 7.59 – 7.54 (m, 2H, $CH^{imidazole}$), 4.32 (t, *J* = 7.4 Hz, 4H, NCH_2^{Bu}), 1.98 – 1.91 (m, 4H, CH_2^{Bu}), 1.40 (dt, *J* = 14.8, 7.4 Hz, 4H, CH_2^{Bu}), 0.96 (t, *J* = 7.4 Hz, 6H, CH_3^{Bu}). ^{13}C{^{1}H} NMR (126 MHz, CD_2Cl_2) δ 136.4 (NCHN), 135.5 (C^{aryl}), 133.2 (CH^{aryl}), 123.9 ($CH^{imidazole}$), 123.6 (CH^{aryl}), 122.2 ($CH^{imidazole}$), 116.5 (CH^{aryl}), 51.1 (NCH_2^{Bu}), 32.2 (CH_2^{Bu}), 19.9 (CH_2^{Bu}), 13.6 (CH_3^{Bu}). ^{19}F NMR (282 MHz, CD_2Cl_2) δ - 149.3 (s, BF_4^-).

Bis(μ-1,3-bis(3′-butylimidazol-2′-ylidene)benzene-*κ*-C)tetra-μ^3-iodotetrasilver(I) (334). 1,3-bis(3'-butylimidazol-l'-yl)benzene diiodide (1.00 g, 1.73 mmol), Ag_2O (0.60 g, 2.59 mmol), molecular sieves (3 Å beads), and CH_2Cl_2 were combined, protected from light and stirred for 18h under argon at room temperature. The solution was filtered through Celite®, concentrated under reduced pressure, and washed three times with distilled water. The organic phase was dried over $MgSO_4$ and filtered. Upon precipitation with pentane, the complex was cleanly recovered (2.05 g, 1.29 mmol). Yield: 75%. Crystals suitable for X-ray analysis were grown by slow evaporation from a solution mixture of **334**/CH_2Cl_2/octane. ^{1}H NMR (300 MHz, CD_2Cl_2) δ 8.38 (t, *J* = 1.8 Hz, 1H, CH^{aryl}), 7.58 – 7.47 (m, 2H, CH^{aryl}), 7.47 – 7.36 (m, 3H, CH^{aryl} + $CH^{imidazole}$), 7.17 (d, *J* = 1.5 Hz, 2H, $CH^{imidazole}$), 4.26 (t, *J* = 7.1 Hz, 4H, NCH_2^{Bu}), 1.89–1.79 (m, 4H, CH_2^{Bu}), 1.42–1.30 (m, 4H, CH_2^{Bu}), 0.90 (t, *J* = 7.3 Hz, 6H, CH_3^{Bu}). ^{13}C{^{1}H} NMR (75 MHz, CD_2Cl_2) δ 184.8 ($C^{carbene}$), 141.0 (C^{aryl}), 130.4 (CH^{aryl}), 123.2 ($CH^{imidazole}$), 121.9 (CH^{aryl}), 121.5 (CH^{aryl}), 121.0 ($CH^{imidazole}$), 52.0 (NCH_2^{Bu}), 33.5 (CH_2^{Bu}), 19.9 (CH_2^{Bu}), 13.7 (CH_3^{Bu}). Anal. Calc. for $C_{40}H_{52}N_8Ag_4I_4$: C, 30.33; H, 3.31; N, 7.07. Found: C, 30.01; H, 3.38; N, 6.88. ESI MS (m/z) (L = Ligand): 1584.68 $[2L+4Ag+4I+H]^+$; 1456.76 $[2L+4Ag+3I]^+$; 1348.86 $[2L+3Ag+3I+H]^+$; 1222.94 $[2L+3Ag+2I]^+$; 1115.05 $[2L+2Ag+2I+H]^+$; 987.14 $[2L+2Ag+I]^+$; 664.92 $[L+2Ag+I]^+$; 559.03 $[L+Ag+I+H]^+$; 430.12 $[2L+2Ag]^+$. IR: ν_{max}(solid)/cm^{-1}: 3158w, 3104w, 3050w, 2954w, 2928w, 2869w, 1604w, 1541w, 1491m, 1463m, 1404m, 1378w, 1343w, 1266w, 1251w, 1221w, 1192w, 1097m, 1072w, 1001w, 946w, 883w, 850w, 821w, 792m, 763w, 721s, 696m, 631w, 505m, 452m, 379w, 307w, 238w, 156w.

Bis(μ-1,3-bis(3′-butylimidazol-2′-ylidene)benzene-κ-C)tetra-μ^3-bromotetrasilver(I) (335). A procedure similar to that used for compounds **334** with **L102** (1.66 g, 3.44 mmol) and Ag_2O (1.19 g, 5.16 mmol) gave **335**, as a white powder (1.47 g, 1.05 mmol). Yield: 61%. Crystals suitable for X-ray analysis were grown by slow evaporation from a solution mixture of **335**/THF/octane. ^{1}H NMR (300 MHz, CD_2Cl_2) δ 7.88 (s, 1H, CH^{aryl}), 7.62 (t, *J* = 1.7 Hz, 2H, $CH^{imidazole}$), 7.59 (d, *J* = 2.0 Hz, 2H, CH^{aryl}), 7.45 (dd, *J* = 8.6, 7.4 Hz, 1H, CH^{aryl}), 7.26 (d, *J* = 1.9 Hz, 2H, $CH^{imidazole}$), 4.22 (t, *J* = 7.3 Hz, 4H, NCH_2^{Bu}), 1.96 – 1.84 (m, 4H, CH_2^{Bu}), 1.45–1.35 (m, 4H, CH_2^{Bu}), 0.99 (t, *J* = 7.3 Hz, 6H, CH_3^{Bu}). $^{13}C\{^1H\}$ NMR (126 MHz, CD_2Cl_2) δ 182.7 ($C^{carbene}$), 141.5 (C^{aryl}), 131.4 (CH^{aryl}), 124.1 (CH^{aryl}), 122.6 ($C^{imidazole}$), 122.4 ($C^{imidazole}$), 120.5 (CH^{aryl}), 52.7 (NCH_2^{Bu}), 33.9 (CH_2^{Bu}), 20.3 (CH_2^{Bu}), 14.0 (CH_3^{Bu}). ESI MS (m/z) (L = Ligand): 1395.98 $[2L+4Ag+4Br+H]^+$; 1314.18 $[2L+4Ag+3Br]^+$; 1208.88 $[2L+3Ag+3Br+H]^+$; 1126.96 $[2L+3Ag+2Br]^+$; 1015.05 $[2L+2Ag+2Br+H]^+$; 939.15 $[2L+2Ag+Br]^+$; 698.87 $[L+2Ag+2Br+H]^+$; 616.94 $[L+2Ag+Br]^+$; 511.06 $[L+Ag+Br+H]^+$; 430.12 $[L+2Ag]^{2+}$. IR: ν_{max}(solid)/cm^{-1}: 3088w br, 2928m br, 2867w, 1604m, 1561m, 1497m, 1460m, 1411m, 1369m, 1257m, 1227m, 1196m, 1108m, 1059m, 1001w, 948w, 872m, 729s, 692s, 507w, 435w, 303w, 280w, 247w, 150w, 118w.

(1,3-bis(3′-butylimidazol-2′-ylidene)benzene)disilver(I) dichloride (336). A procedure similar to that used for compounds **334** with **L103** (0.68 g, 1.72 mmol) and Ag_2O (0.60 g, 2.58 mmol) gave **336**, as a white powder (0.69 g, 1.12 mmol). Yield: 65 %. Crystals suitable for X-ray analysis were grown by slow evaporation from a solution mixture of **336**/CH_2Cl_2/octane. ^{1}H NMR (300 MHz, CD_2Cl_2) δ 7.98 (s, 1H, CH^{aryl}), 7.71 (d, *J* = 1.6 Hz, 3H, CH^{aryl}), 7.66 (d, *J* = 1.9 Hz, 2H, $CH^{imidazole}$), 7.23 (d, *J* = 1.9 Hz, 2H, $CH^{imidazole}$), 4.22 (t, *J* = 7.3 Hz, 4H, NCH_2^{Bu}), 1.94 – 1.83 (m, 4H, CH_2^{Bu}), 1.48–1.35 (m, 4H, CH_2^{Bu}), 0.99 (t, *J* = 7.3 Hz, 6H, CH_3^{Bu}). $^{13}C\{^1H\}$ NMR (126 MHz, $CDCl_3$) δ 179.2 ($C^{carbene}$), 141.0 (C^{aryl}), 131.8 (CH^{aryl}), 124.4 (CH^{aryl}), 122.4 ($CH^{imidazole}$), 122.3 ($CH^{imidazole}$), 120.2 (CH^{aryl}), 52.6 (NCH_2^{Bu}), 33.5 (CH_2^{Bu}), 19.9 (CH_2^{Bu}), 13.8 (CH_3^{Bu}). Anal. Calc. for $C_{20}H_{26}N_4Ag_2Cl_2$: C, 39.44; H, 4.30; N, 9.20. Found: C, 39.35; H, 4.48; N, 9.01. ESI MS (m/z) (L = Ligand): 608.97 $[L+2Ag+2Cl+H]^+$; 572.99 $[L+2Ag+Cl]^+$; 467.10 $[L+Ag+Cl+H]^+$; 323.22 $[L+H]^+$. IR: ν_{max}(solid)/cm^{-1}: 3087w, 2984w, 2929w, 2867w, 1605m, 1560w, 1497m, 1458m, 1412m, 1369m, 1258m, 1228m, 1196, 1110m, 1002w, 948w, 871w, 732s, 692s, 511w, 434w, 409w, 294w, 259w, 236w, 218w, 162w, 154w.

Bis(1,3-bis(3′-butylimidazol-2′-ylidene)benzene)disilver(I) tetrafluoroborate (337). Bis(μ-1,3-bis(3′-butylimidazol-2′-ylidene)benzene-κ-C)tetra-μ^3-bromotetrasilver(I) (0.53 g, 0.45 mmol), $AgBF_4$ (0.18 g, 0.90 mmol) and CH_2Cl_2 were combined and stirred for 18 h. The solution was filtered through Celite®, concentrated under reduced pressure. Upon precipitation with pentane, the complex was recovered (0.46 g, 0.44 mmol). Yield: 98%. Crystals suitable for X-ray analysis were grown by slow evaporation from a solution mixture of **337**/CH_2Cl_2/octane. ^{1}H NMR (300 MHz, CD_2Cl_2) δ 7.64 (s, 2H, $CH^{imidazole}$), 7.56 (dd, *J* = 8.0, 2.0 Hz, 2H, CH^{aryl}), 7.50 (s, 1H, CH^{aryl}), 7.35–7.30 (m, 3H, $CH^{aryl+imidazole}$), 4.26 (t, *J* = 7.2 Hz, 4H, NCH_2^{Bu}), 2.01–1.89 (m, 4H, CH_2^{Bu}), 1.49–1.42 (m, 4H, CH_2^{Bu}), 1.02 (t, *J* = 7.4 Hz, 6H, CH_3^{Bu}). ^{13}C{^{1}H} NMR (126 MHz, CD_2Cl_2) δ 179.6 (d, $^1J(^{13}C\text{-}^{107}Ag)$ = 184 Hz, $^1J(^{13}C\text{-}^{109}Ag)$ = 213 Hz, $C^{carbene}$), 141.6 (C^{aryl}), 131.2 (CH^{aryl}), 124.8 (CH^{aryl}), 124.6 ($CH^{imidazole}$), 123.1 ($CH^{imidazole}$), 120.3 (CH^{aryl}), 52.8 (NCH_2^{Bu}), 34.0 (CH_2^{Bu}), 20.4 (CH_2^{Bu}), 13.9 (CH_3^{Bu}). ^{19}F{^{1}H} NMR (282 MHz, CD_2Cl_2) δ - 150.6 (s, BF_4^-). ESI MS (m/z) (L = Ligand): 947.25 $[2L+2Ag+BF_4]^+$; 430.12 $[2L+2Ag]^{2+}$; 323.22 $[L+H]^+$. IR: ν_{max}(solid)/cm^{-1}: 3134w, 2956w, 2162w, 1606w, 1497m, 1463w, 1415m, 1369w, 1281w, 1261w, 1229w, 1048s br, 950w, 874w, 735m br, 693m, 519m, 419w, 397w, 375w, 352w, 303w, 290w, 279w, 247w, 227w, 202w, 195w, 170w, 151w, 121w.

(1,3-bis(3′-butylimidazol-2′-ylidene)benzene)copper(I) iodide (338). 1,3-bis(3'-butylimidazol-l'-yl)benzene diiodide (0.50 g, 0.86 mmol), $CuN(SiMe_3)_2$ (0.38 g, 1.73 mmol), and THF were combined and stirred for 18h under argon. The solution was filtered through Celite®. Upon precipitation with pentane, the complex was cleanly obtained (1.04 g, 0.74 mmol). Yield: 86 %. ^{1}H NMR (500 MHz, CD_2Cl_2) δ 8.77 (t, *J* = 2.1 Hz, 1H, CH^{aryl}), 7.62 (t, *J* = 8.0 Hz, 1H, CH^{aryl}), 7.44 (dd, *J* = 8.0, 2.1 Hz, 2H, CH^{aryl}), 7.39 (d, *J* = 1.9 Hz, 2H, $CH^{imidazole}$), 7.10 (d, *J* = 1.9 Hz, 2H, $CH^{imidazole}$), 4.21 (t, *J* = 7.3 Hz, 4H, NCH_2^{Bu}), 1.96–1.88 (m, 4H, CH_2^{Bu}), 1.47–1.39 (m, 4H, CH_2^{Bu}), 0.99 (t, *J* = 7.4 Hz, 6H, CH_3^{Bu}). ^{13}C{^{1}H} NMR (126 MHz, CD_2Cl_2) δ 184.2 ($C^{carbene}$), 141.1 (C^{aryl}), 131.0 (CH^{aryl}), 121.8 ($CH^{imidazole}$), 121.4 ($CH^{imidazole}$), 119.9 (CH^{aryl}), 118.5 (CH^{aryl}), 52.1 (NCH_2^{Bu}), 33.6 (CH_2^{Bu}), 20.4 (CH_2^{Bu}), 14.1 (CH_3^{Bu}). ESI MS (m/z) (L = Ligand): 1406.78 $[2L+4CuI+H]^+$; 1278.86 $[2L+4Cu+3I]^+$; 1215.95 $[2L+3Cu+3I+H]^+$; 1089.03 $[2L+3Cu+2I]^+$; 1025.12 $[2L+2Cu+2I+H]^+$; 915.19 $[2L+2Cu+I+H_2O]^+$; 897.19 $[2L+2Cu+I]^+$; 702.91 $[L+2Cu+2I+H]^+$; 574.98 $[L+2Cu+I]^+$; 513.06 $[L+Cu+I+H]^+$. IR: ν_{max}(solid)/cm^{-1}: 3087w, 2984w, 2929w, 2867w, 1605m, 1560w, 1497m, 1458m, 1412m, 1369m, 1258m, 1228m, 1196, 1110m, 1002w, 948w, 871w, 732s, 691s, 511w, 434w, 409w, 294w, 259w, 236w, 218w, 162w, 154w.

(1,3-bis(3′-butylimidazol-2′-ylidene)benzene)dicopper(I) dibromide (339). A procedure similar to that used for compounds **338** with **L102** (0.41 g, 0.86 mmol), $CuN(SiMe_3)_2$ (0.38 g, 1.73 mmol) gave **339**, as a white powder (0.51 g, 0.84 mmol). Yield: 98%. Crystals suitable for X-ray analysis were grown from a solution mixture of **339**/THF/pentane. ^{1}H NMR (300 MHz, CD_2Cl_2) δ 8.24 (s, 1H, CH^{aryl}), 7.78-7.71 (m, 2H, CH^{aryl}), 7.72-7.67 (m, 1H, CH^{aryl}), 7.64 (d, *J* = 1.7 Hz, 2H, $CH^{imidazole}$), 7.16 (d, *J* = 1.7 Hz, 2H, $CH^{imidazole}$), 4.24 (t, *J* = 7.2 Hz, 4H, CH_2^{Bu}), 1.98 – 1.84 (m, 4H, CH_2^{Bu}), 1.48–1.36 (m, 4H, C, 0.99 (t, *J* = 7.3 Hz, 6H, CH_3^{Bu}). $^{13}C\{^1H\}$ NMR (126 MHz, CD_2Cl_2) δ 177.8 ($C^{carbene}$), 141.2 (C^{aryl}), 131.6 (CH^{aryl}), 123.5 (CH^{aryl}), 122.2 ($CH^{imidazole}$), 121.6 ($CH^{imidazole}$), 119.6 (CH^{aryl}), 52.4 (NCH_2^{Bu}), 33.8 (CH_2^{Bu}), 20.2 (CH_2^{Bu}), 14.0 (CH_3^{Bu}). ESI MS (m/z) (L = Ligand): 610.92 $[L+2Cu+2Br+H]^+$, 528.99 $[L+2Cu+Br]^+$, 467.07 $[L+Cu+Br+H]^+$, 323.22 $[L+H]^+$. IR: ν_{max}(solid)/cm^{-1}: 3111w br, 2959w, 2931w br, 2866w br, 1601m, 1492m, 1470w, 1459m, 1412m, 1393w, 1371w, 1343w, 1319w, 1279m, 1256m, 1232m, 1195w, 1164w, 1105w, 1081w, 1029w, 1001w, 945w, 885m, 799m, 773m, 748s, 719s, 696s, 670m, 645m, 635sw, 611w, 513w, 491w, 477w, 458w, 418w, 374w, 315w, 278w, 266w, 249w, 227w, 202w, 189w, 175w, 153w, 148w, 141w, 134w, 128w, 120w, 106w.

(1,3-bis(3′-butylimidazol-2′-ylidene)benzene)dicopper(I) dichloride (340). A procedure similar to that used for compounds **339** with **L103** (0.34 g, 0.86 mmol), $CuN(SiMe_3)_2$ (0.38 g, 1.73 mmol) gave **340**, as a white powder (0.44 g, 0.84 mmol). Yield: 98%. Crystals suitable for X-ray analysis were grown from a solution mixture **340**/THF/pentane. ^{1}H NMR (500 MHz, CD_2Cl_2) δ 8.17 (s, 1H, CH^{aryl}), 7.76 (dd, *J* = 7.2, 1.8 Hz, 2H, CH^{aryl}), 7.70 (t, *J* = 7.2 Hz, 1H, CH^{aryl}), 7.65 (d, *J* = 1.9 Hz, 2H, $CH^{imidazole}$), 7.16 (d, *J* = 1.9 Hz, 2H, $CH^{imisazole}$), 4.24 (t, *J* = 7.2 Hz, 4H, NCH_2^{Bu}), 1.92–1.86 (m, 4H, CH_2^{Bu}), 1.47–1.37 (m, 4H, CH_2^{Bu}), 0.99 (t, *J* = 7.4 Hz, 6H, CH_3^{Bu}). $^{13}C\{^1H\}$ NMR (126 MHz, CD_2Cl_2) δ 176.6 ($C^{carbene}$), 141.2 (C^{aryl}), 131.6 (CH^{aryl}), 123.6 (CH^{aryl}), 122.3 ($CH^{imidazole}$), 121.7 ($CH^{imidazole}$), 119.6 (CH^{aryl}), 52.3 (CH_2^{Bu}), 33.8 (CH_2^{Bu}), 20.2 (CH_2^{Bu}), 13.9 (CH_3^{Bu}). ESI MS (m/z) (L = Ligand): 519.02 $[L+2Cu+2Cl+H]^+$, 483.04 $[L+2Cu+Cl]^+$, 421.12 $[L+2Cu+Cl]^+$, 323.22 $[L+H]^+$. IR: ν_{max}(solid)/cm^{-1}: 2952w, 2865w, 2362w, 2160w, 1978w, 1684w, 1601m, 1559w, 1541w, 191m, 1458m, 1412m, 1371w, 1342w, 1318w, 1278m, 1256m, 1231m, 1194w, 1163w, 1104w, 1081w, 1063w, 884w, 799m, 773m, 748s, 719s, 696s, 670m, 645w, 635w, 513w, 491w, 477w, 457w, 414w, 373w, 317w, 251w, 218w, 205w, 198w, 174w, 144w.

ORTEP of the molecular structures for 335, 336, 337, 339, 340.

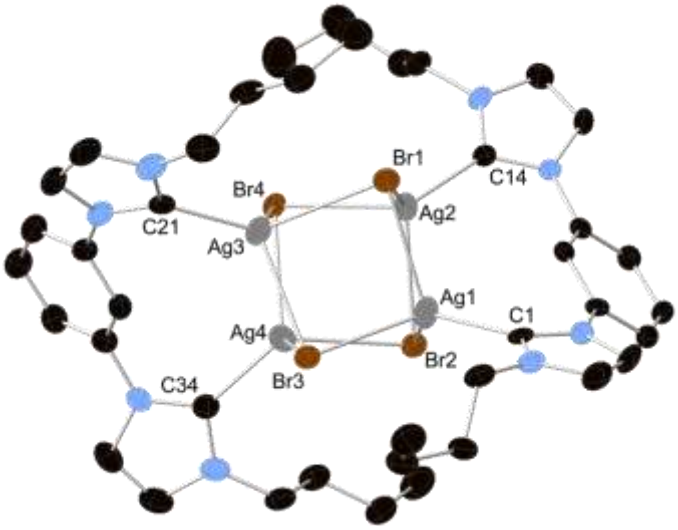

Figure S1. ORTEP of the molecular structure of **335**. Ellipsoids set at 30 % probability level. Hydrogen atoms have been omitted for clarity.

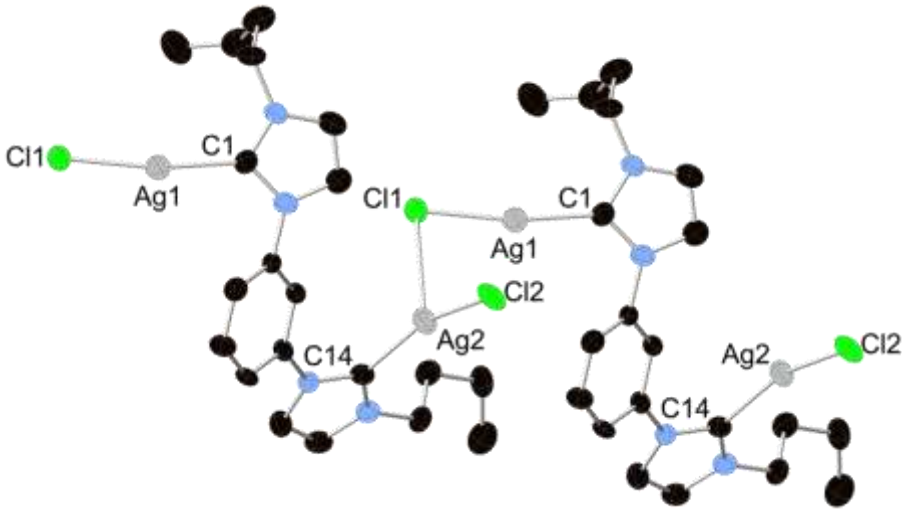

Figure S2. ORTEP of the molecular structure of **336**. Ellipsoids set at 30 % probability level. Hydrogen atoms have been omitted for clarity.

Références p. 162

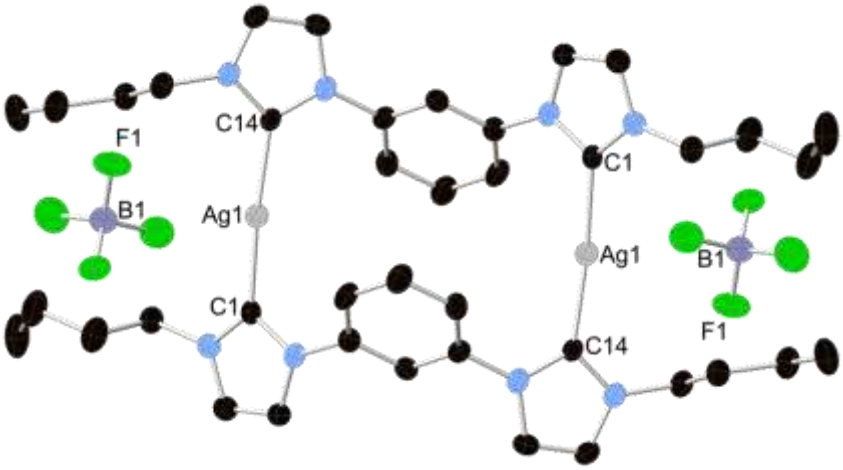

Figure S3. ORTEP of the molecular structure of **337**. Ellipsoids set at 30 % probability level. Hydrogen atoms have been omitted for clarity.

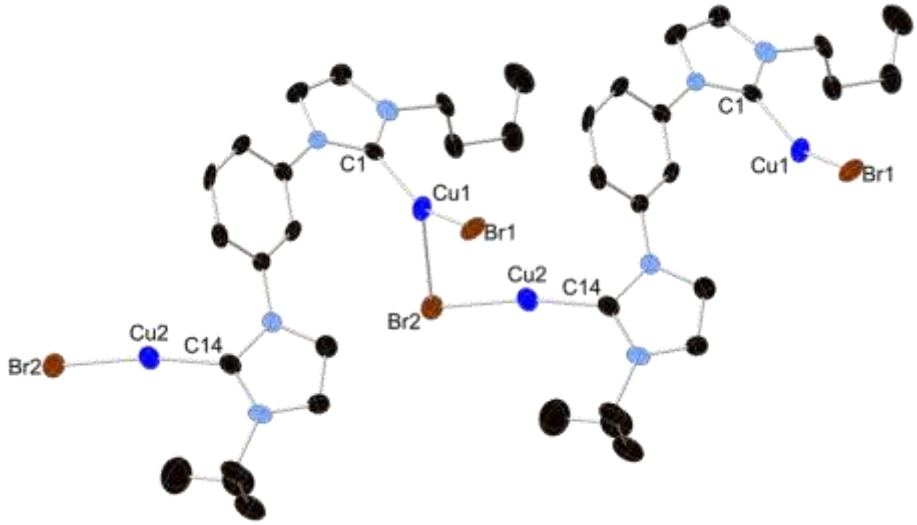

Figure S4. ORTEP of the molecular structure of **339**. Ellipsoids set at 30 % probability level. Hydrogen atoms have been omitted for clarity.

Références p. 162

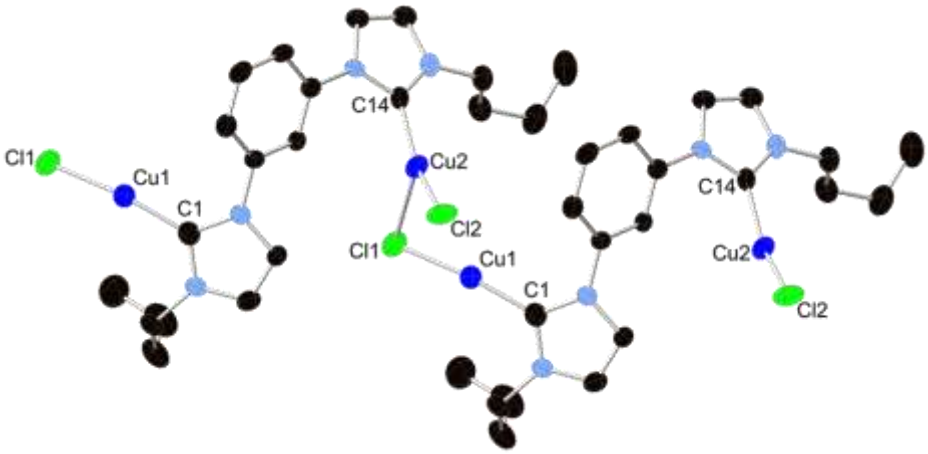

Figure S5. ORTEP of the molecular structure of **340**. Ellipsoids set at 30 % probability level. Hydrogen atoms have been omitted for clarity.

Références p. 162

References :

(1) Arduengo, A. J.; Harlow, R. L.; Kline, M. *J. Am. Chem. Soc.* **1991**, *113*, 361.

(2) (a) Diez-Gonzàlez, S.; Marion, N.; Nolan, S. P. *Chem. Rev.* **2009**, *109*, 3612 (b) de Frémont, P.; Marion, N.; Nolan, S. P. *Coord. Chem. Rev.* **2009**, *253*, 862 (c) Herrmann, W. A. *Angew. Chem. Int. Ed.* **2002**, *41*, 1290 (d) Cazin, C. S. J. *N-Heterocyclic Carbenes in Transition Metal Catalysis and Organocatalysis*; 1st ed.; Springer, 2011 (e) Diebolt, O.; Braunstein, P.; Nolan, S. P.; Cazin, C. S. J. *Chem. Commun.* **2008**, 3190 (f) Diebolt, O.; Jurčík, V. c.; Correa da Costa, R.; Braunstein, P.; Cavallo, L.; Nolan, S. P.; Slawin, A. M. Z.; Cazin, C. S. J. *Organometallics* **2010**, *29*, 1443.

(3) Arduengo, A. J.; Dias, H. V. R.; Calabrese, J. C.; Davidson, F. *Organometallics* **1993**, *12*, 3405.

(4) Wang, H. M. J.; Lin, I. J. B. *Organometallics* **1998**, *17*, 972.

(5) (a) Guerret, O.; Solé, S.; Gornitzka, H.; Trinquier, G.; Bertrand, G. *J. Organomet. Chem.* **2000**, *600*, 112 (b) Guerret, O.; Solé, S.; Gornitzka, H.; Teichert, M.; Trinquier, G.; Bertrand, G. *J. Am. Chem. Soc.* **1997**, *119*, 6668.

(6) Tulloch, A. A. D.; Danopoulos, A. A.; Winston, S.; Kleinhenz, S.; Eastham, G. *J. Chem. Soc., Dalton Trans.* **2000**, 4499.

(7) Zhu, S.; Liang, R.; Jiang, H. *Tetrahedron* **2012**, *68*, 7949.

(8) Taşcı, Z.; Kunduracıoğlu, A.; Kani, İ.; Çetinkaya, B. *ChemCatChem* **2012**, *4*, 831.

(9) Li, Q.; Li, X.; Yang, J.; Song, H.-B.; Tang, L.-F. *Polyhedron* **2013**, *59*, 29.

(10) (a) Kascatan-Nebioglu, A.; Panzner, M. J.; Tessier, C. A.; Cannon, C. L.; Youngs, W. J. *Coord. Chem. Rev.* **2007**, *251*, 884 (b) Budagumpi, S.; Haque, R. A.; Endud, S.; Rehman, G. U.; Salman, A. W. *Eur. J. Inorg. Chem.* **2013**, *2013*, 4367 (c) Teyssot, M.-L.; Jarrousse, A.-S.; Chevry, A.; De Haze, A.; Beaudoin, C.; Manin, M.; Nolan, S. P.; Díez-González, S.; Morel, L.; Gautier, A. *Chem. - Eur. J.* **2009**, *15*, 314 (d) Teyssot, M.-L.; Jarrousse, A.-S.; Manin, M.; Chevry, A.; Roche, S.; Norre, F.; Beaudoin, C.; Morel, L.; Boyer, D.; Mahiou, R.; Gautier, A. *Dalton Trans.* **2009**, 6894.

(11) Cisnetti, F.; Lemoine, P.; El-Ghozzi, M.; Avignant, D.; Gautier, A. *Tetrahedron Lett.* **2010**, *51*, 5226.

(12) Paulose, T. A. P.; Wu, S.-C.; Olson, J. A.; Chau, T.; Theaker, N.; Hassler, M.; Quail, J. W.; Foley, S. R. *Dalton Trans.* **2012**, *41*, 251.

(13) Frøseth, M.; Netland, K. A.; Rømming, C.; Tilset, M. *J. Organomet. Chem.* **2005**, *690*, 6125.

(14) de Frémont, P.; Scott, N. M.; Stevens, E. D.; Nolan, S. P. *Organometallics* **2005**, *24*, 2411.

(15) Sculfort, S.; Braunstein, P. *Chem. Soc. Rev.* **2011**, *40*, 2741.

(16) (a) Fliedel, C.; Braunstein, P. *Organometallics* **2010**, *29*, 5614 (b) Liu, X.; Braunstein, P. *Inorg. Chem.* **2013**, *52*, 7367.

(17) (a) Li, N.; Zhao, P.; Astruc, D. *Angew. Chem., Int. Ed.* **2014**, *53*, 1756 (b) Gu, P.; Xu, Q.; Shi, M. *Tetrahedron Lett.* **2014**, *55*, 577 (c) Bertrand, B.; Casini, A. *Dalton Trans.* **2014**, *43*, 4209 (d) Pereira, S. O.; Barros-Timmons, A.; Trindade, T. *Colloid Polym. Sci.* **2014**, *292*, 33.

(18) Poyatos, M.; Mata, J. A.; Peris, E. *Chem. Rev.* **2009**, *109*, 3677.

(19) Hu, X.; Castro-Rodriguez, I.; Meyer, K. *J. Am. Chem. Soc.* **2003**, *125*, 12237.

(20) (a) Matsumoto, K.; Matsumoto, N.; Ishii, A.; Tsukuda, T.; Hasegawa, M.; Tsubomura, T. *Dalton Trans.* **2009**, 6795 (b) Catalano, V. J.; Munro, L. B.; Strasser, C. E.; Samin, A. F. *Inorg. Chem.* **2011**, *50*, 8465.

(21) Venkatachalam, G.; Heckenroth, M.; Neels, A.; Albrecht, M. *Helv. Chim. Acta* **2009**, *92*, 1034.
(22) Mormul, J.; Steimann, M.; Nagel, U. *Eur. J. Inorg. Chem.* **2014**, *2014*, 1389.
(23) Bullough, E. K.; Little, M. A.; Willans, C. E. *Organometallics* **2013**, *32*, 570.
(24) Liu, X.; Pattacini, R.; Deglmann, P.; Braunstein, P. *Organometallics* **2011**, *30*, 3302.
(25) Chen, C.; Qiu, H.; Chen, W. *J. Organomet. Chem.* **2012**, *696*, 4166.
(26) Ellul, C. E.; Reed, G.; Mahon, M. F.; Pascu, S. I.; Whittlesey, M. K. *Organometallics* **2010**, *29*, 4097.
(27) Tubaro, C.; Biffis, A.; Gava, R.; Scattolin, E.; Volpe, A.; Basato, M.; Díaz-Requejo, M. M.; Perez, P. J. *Eur. J. Org. Chem.* **2012**, *2012*, 1367.
(28) (a) Hu, X.; Castro-Rodriguez, I.; Olsen, K.; Meyer, K. *Organometallics* **2004**, *23*, 755 (b) Nemcsok, D.; Wichmann, K.; Frenking, G. *Organometallics* **2004**, *23*, 3640.
(29) Carvajal, M. A.; Novoa, J. J.; Alvarez, S. *J. Am. Chem. Soc.* **2004**, *126*, 1465.
(30) Vargas, V. C.; Rubio, R. J.; Hollis, T. K.; Salcido, M. E. *Org. Lett.* **2003**, *5*, 4847.
(31) Rubio, R. J.; Andavan, G. T. S.; Bauer, E. B.; Hollis, T. K.; Cho, J.; Tham, F. S.; Donnadieu, B. *J. Organomet. Chem.* **2005**, *690*, 5353.
(32) Raynal, M.; Cazin, C. S. J.; Vallée, C.; Olivier-Bourbigou, H.; Braunstein, P. *Chem. Commun.* **2008**, 3983.
(33) Clark, W. D.; Tyson, G. E.; Hollis, T. K.; Valle, H. U.; Valente, E. J.; Oliver, A. G.; Dukes, M. P. *Dalton Trans.* **2013**, *42*, 7338.
(34) (a) Omary, M. A.; Webb, T. R.; Assefa, Z.; Shankle, G. E.; Patterson, H. H. *Inorg. Chem.* **1998**, *37*, 1380 (b) Wanniarachchi, Y. A.; Khan, M. A.; Slaughter, L. M. *Organometallics* **2004**, *23*, 5881.
(35) Noren, B.; Oskarsson, A. *Acta Chem. Scand. A* **1985**, *39*, 701.
(36) (a) Bowen, R.; Camp, D.; Effend, Y.; Healy, P.; Skelton, B.; White, A. *Aust. J. Chem.* **1994**, *47*, 693 (b) Venter, G. J. S.; Roodt, A.; Meijboom, R. *Inorg. Chim. Acta* **2009**, *362*, 2475 (c) Engelhardt, L.; Gotsis, S.; Healy, P.; Kildea, J.; Skelton, B.; White, A. *Aust. J. Chem.* **1989**, *42*, 149 (d) Olson, S.; Helgesson, G.; Jagner, S. *Inorg. Chim. Acta* **1994**, *217*, 15 (e) Teo, B.-K.; Calabrese, J. C. *Inorg. Chem.* **1976**, *15*, 2474 (f) Churchill, M. R.; DeBoer, B. G. *Inorg. Chem.* **1975**, *14*, 2502 (g) Bowmaker, G. A.; Effendy; Hart, R. D.; Kildea, J. D.; White, A. H. *Aust. J. Chem.* **1997**, *50*, 653 (h) Bowmaker, G. A.; Effendy; Harvey, P. J.; Healy, P. C.; Skelton, B. W.; White, A. H. *J. Chem. Soc., Dalton Trans.* **1996**, 2459 (i) Teo, B.-K.; Calabrese, J. C. *J. Am. Chem. Soc.* **1975**, *97*, 1256 (j) Young, J. F.; Yap, G. P. A. *Acta Crystallogr. Sect. E: Struct. Rep. Online* **2007**, *63*, m2075.
(37) (a) Rubio, M.; Siegler, M. A.; Spek, A. L.; Reek, J. N. H. *Dalton Trans.* **2010**, *39*, 5432 (b) Chiu, P. L.; Chen, C. Y.; Zeng, J. Y.; Lu, C. Y.; Lee, H. M. *J. Organomet. Chem.* **2005**, *690*, 1682.
(38) Hayes, J. M.; Viciano, M.; Peris, E.; Ujaque, G.; Lledós, A. *Organometallics* **2007**, *26*, 6170.
(39) (a) Nielsen, D. J.; Cavell, K. J.; Skelton, B. W.; White, A. H. *Inorg. Chim. Acta* **2002**, *327*, 116 (b) Jean-Baptiste dit Dominique, F.; Gornitzka, H.; Hemmert, C. *J. Organomet. Chem.* **2008**, *693*, 579 (c) Qin, D.; Zeng, X.; Li, Q.; Xu, F.; Song, H.; Zhang, Z.-Z. *Chem. Commun.* **2007**, 147 (d) Willans, C. E.; Anderson, K. M.; Paterson, M. J.; Junk, P. C.; Barbour, L. J.; Steed, J. W. *Eur. J. Inorg. Chem.* **2009**, *2009*, 2835.
(40) Nielsen, D. J.; Cavell, K. J.; Viciu, M. S.; Nolan, S. P.; Skelton, B. W.; White, A. H. *J. Organomet. Chem.* **2005**, *690*, 6133.
(41) Janiak, C. *J. Chem. Soc., Dalton Trans.* **2000**, 3885.

(42) Citadelle, C. A.; Nouy, E. L.; Bisaro, F.; Slawin, A. M. Z.; Cazin, C. S. J. *Dalton Trans.* **2010**, *39*, 4489.
(43) Landers, B.; Navarro, O. *Eur. J. Inorg. Chem.* **2012**, *2012*, 2980.
(44) Ai, P.; Danopoulos, A. A.; Braunstein, P.; Monakhov, K. Y. *Chem. Commun.* **2014**, *50*, 103.
(45) Arnold, P. L.; Scarisbrick, A. C.; Blake, A. J.; Wilson, C. *Chem. Commun.* **2001**, 2340.
(46) de Hoffmann, E. *Spectrométrie de masse*; 3rd ed., 2005.
(47) (a) Shishkov, I. V.; Rominger, F.; Hofmann, P. *Dalton Trans.* **2009**, 1428 (b) Arnold, P. L. *Heteroat. Chem.* **2002**, *13*, 534 (c) Tulloch, A. A. D.; Danopoulos, A. A.; Kleinhenz, S.; Light, M. E.; Hursthouse, M. B.; Eastham, G. *Organometallics* **2001**, *20*, 2027 (d) Schneider, N.; César, V.; Bellemin-Laponnaz, S.; Gade, L. H. *J. Organomet. Chem.* **2005**, *690*, 5556.
(48) Melaiye, A.; Simons, R. S.; Milsted, A.; Pingitore, F.; Wesdemiotis, C.; Tessier, C. A.; Youngs, W. J. *J. Med. Chem.* **2004**, *47*, 973.
(49) Bürger, H.; Wannagat, U. *Monatshefte für Chemie und verwandte Teile anderer Wissenschaften* **1964**, *95*, 1099.
(50) Sheldrick, G. M. *Acta Crystallogr. Sect. A: Found. Crystallogr.* **2008**, *64*, 112.

Références p. 162

Chapter 3

Attempts for the formation of NHC nickel(II) complexes

1 Introduction

N-Heterocyclic carbenes (NHCs) are considered to be neutral ligands with strong σ-donation and weak or inexistent π-back donation ability when coordinated to transition metals. Nevertheless, Radius and Bickelhaupt pointed out that in the case of electron-rich nickel complexes, π-back donation from the nickel center to the NHC ligand should be considered and can account for 10-40% of the total interaction energy depending on the NHC substituents and the electronic structure of the other ligands coordinated to the nickel center.[1] Nowadays, more than 70 articles have reported on bis-NHC chelate nickel complexes (see Chapter 1). Many of these NHC nickel complexes are good catalysts for olefin oligomerization,[2] polymerization,[3] Heck,[4] Suzuki,[4-5] Negishi[6] or Kumada[7] reactions. They also are active for the reduction of CO_2.[8] The NHC nickel chemistry is challenging because the complexes obtained can be very sensitive to moisture or traces of acids. Furthermore, the coordination geometry around the nickel center can be diverse and difficult to predict, giving rise to complexes endowed with very different chemical or physical properties. Paramagnetic species are often encountered, which renders any characterization by NMR spectroscopy impossible or very challenging.

Bidentate bis-NHC ligands associate two donor moieties linked by a spacer. They offer three possible coordination modes: bridging, chelating or monodentate with only one of the two donor groups coordinated to the metal. A chelating ligand is more stabilizing than two monodentate ligands owing to the so-called "chelate effect". The formation of bidentate complexes usually involves a stepwise sequence, the coordination of the first donor group being followed by a suitable orientation of the spacer enabling the coordination of the second donor group. To form a complex with two monodentate ligands, two independent steps are necessary and require more energy.[9] Thus the formation of chelate complexes is more favorable than the formation of monodentate complexes and is entropically favored.[10] Finally, the possibility exists that one of the donors dissociates from the metal center, the second one remaining coordinated. This is the situation encountered in hemilabile systems[11] where the dangling group can re-coordinate by rotation of the spacer, enhancing the overall stability by chelation. With bidentate ligands, it is often possible to finely tune the catalytic activity of the resulting chelates, by playing with the substituents and the electronic nature of the donor sites.

Many routes appear suitable to access nickel(II) NHC chelate complexes including:

- The use of nickel precursors containing an internal base in the presence of bis-imidazolium salts

- The use of nickel precursors in the presence of external bases and bis-imidazolium salts

- The use of metal powder, such as Raney nickel or nickel(0) powder, in the presence of bis-imidazolium salts

- The use of bis-NHC zirconium(IV), silver(I) or copper(I) complexes as carbene transmetalating agents with nickel(II) sources

- The use of isolated free carbenes in the presence of nickel(II) sources

The following chapter covers the different attempts to access a series of nickel(II) bis-NHC pincer chelate complexes, by following these routes.

2 Nickel sources containing an internal base

In the literature, two nickel precursors ($Ni(OAc)_2$ and $Ni(acac)_2$) were reported for the synthesis of bis-NHC or P-NHC nickel(II) complexes in high yield.[12] Bis-NHC or tetra-NHC nickel(II) complexes were obtained depending upon the imidazolium salts employed. In some cases, Bu_4NBr was added to increase the solubility of the reagents.[4,13] The reactions were carried out in hot DMSO or DMF, under air or inert atmosphere, from one to several hours.

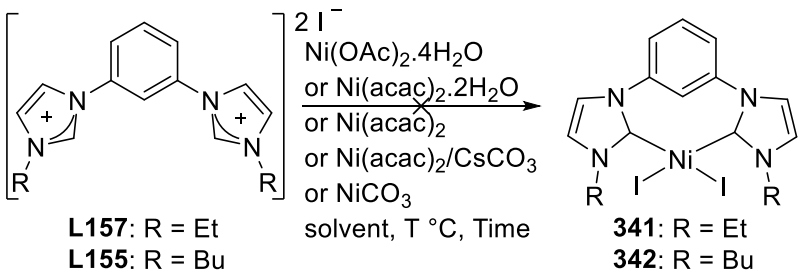

Scheme 1. Attempts to use nickel precursors containing an internal base

The reaction of the imidazolium iodide (**L157**) with 1 equivalent of nickel acetate tetrahydrate ($Ni(OAc)_2•4H_2O$) or of nickel acetylacetonate dihydrate ($Ni(acac)_2•2H_2O$) overnight in boiling THF did not occur (Table 1, Entries 1-2). All reagents were cleanly recovered. The salt **L157** being poorly soluble in THF, it was replaced by the more soluble salt **L155** (Table 1, Entries 3-4). Once again, no reaction occurred. Furthermore, carrying out the reaction under inert atmosphere, with strictly dried reagents, replacing ($Ni(acac)_2•2H_2O$) by $Ni(acac)_2$, did not lead to any improvement (Table 1, Entry 5). The addition of $CsCO_3$ to

Références p. 199

assist nickel chelation by the bis-NHC was unsuccessful (Table 1, Entry 6). Finally, the reaction temperature was increased to 189 °C in DMSO, but once again, the starting materials were recovered (Table 1, Entry 7).

A third nickel precursor, $NiCO_3$, was mixed to the imidazolium iodide salt **L155** for a day in CH_2Cl_2 or DMSO at room temperature (Table 1, Entries 8-9), or at 41 °C and 189 °C (Table 1, Entries 10-11). Once again, no reaction occurred. The ^1H NMR spectra of the crude reaction mixture revealed a set of resonances assignable to clean **L155**.

Table 1. Reactions with various nickel precursors containing an internal base.

Entry	Pro-Ligand	Nickel precursor	Solvent	Temperature	Time	Observation
1	**L157**	$Ni(OAc)_2•4H_2O$	THF	65 °C	16 h	
2	**L157**	$Ni(acac)_2•2H_2O$	THF	65 °C	16 h	
3	**L155**	$Ni(OAc)_2•4H_2O$	THF	65 °C	16 h	
4	**L155**	$Ni(acac)_2•2H_2O$	THF	65 °C	16 h	No reaction
5	**L155**	$Ni(acac)_2$	THF	65 °C	16 h	regardless
6	**L155**	$Ni(acac)_2/CsCO_3$	THF	65 °C	16h	of the reactions
7	**L155**	$Ni(OAc)_2•4H_2O$	DMSO	160 °C	16 h	conditions
8	**L155**	$NiCO_3$	CH_2Cl_2	rt	1 day	
9	**L155**	$NiCO_3$	DMSO	rt	1 day	
10	**L155**	$NiCO_3$	CH_2Cl_2	41 °C	1 day	
11	**L155**	$NiCO_3$	DMSO	189 °C	1 day	

Two phenomena can possibly explain this lack of reactivity: 1/ the limited solubility of imidazolium salts in common solvents; 2/ more likely, the too low basicity of the internal base.

3 Nickel sources with an external base

Several nickel NHC chelates were prepared at room temperature in good yields following this route.[3b,14] KHMDS, LDA or K_2CO_3 were combined with $NiCl_2(dme)$, $NiCl_2$ or $NiBr_2(PPh_3)_2$.

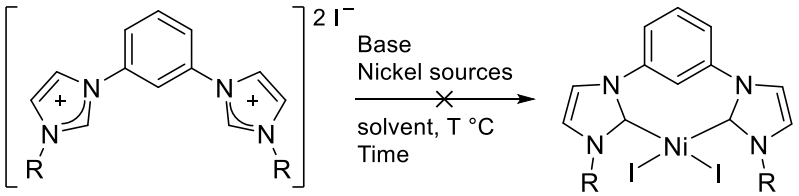

L157: R = Et
L155: R = Bu

341: R = Et
342: R = Bu

Scheme 2. Direct metalation attempts from **L157**-**L155**

Four attempts were made with **L157** using $NiCl_2$(dme) in the presence of NEt_3 or $CsCO_3$ in acetonitrile at room temperature (Table 2, Entries 1-2), or at 82 °C (boiling point of the reaction mixture) (Table 2, Entries 3-4). No reaction occurred. Considering the results obtained previously with the nickel sources containing an internal base, this lack of reactivity was anticipated. The bases NEt_3 and $CsCO_3$ being too weak to assist the deprotonation of **L157**, KHMDS was used in place. Due to the low solubility of the imidazolium iodide salt **L157**, the more soluble compound **L155** was used as starting material.

The addition of $NiCl_2$(dme) to a solution of KHMDS and **L155** led to the free bis-NHC (Table 2, Entry 5). The disappearance of the characteristic signal of the azolium functions was monitored by ^{1}H NMR spectroscopy. However, $^{13}C\{^1H\}$ NMR spectroscopy unveiled a signal at 215.1 ppm strongly suggesting the presence of free carbene (or its potassium adduct) rather than of a Ni-chelate. To note, NHC-Ni(II) complexes are usually characterized by carbene $^{13}C\{^1H\}$ resonances ranging from 153 to 201 ppm.[15] Extending the reaction time up to 3 days led to the same result, emphasizing the good stability of the free (or potassium adduct) carbene solution (Table 2, Entry 6).

In view of some interesting results obtained for the synthesis of mono-NHC Ni(II) complexes,[16] $NiBr_2(PPh_3)_2$ surrogated the non-reactive $NiCl_2$(dme). Unfortunately, ^{1}H NMR analysis of the crude reaction revealed a mixture of paramagnetic products. The resonances were very broad and ill-defined. However, a signal at 11.0 ppm suggested that no reaction had occurred, or the reprotonation of a possibly formed free bis-NHC (early stage of the reaction in this case). Extending the reaction to 32 h did not lead to any improvement (Table 2, Entry 8). The different paramagnetic species could not be separated by classical purification techniques (fractional crystallization / chromatography / sublimation…)

Références p. 199

Table 2. Reaction with various nickel precursors and external bases.

Entry	Base	Nickel precursor	Solvent	Temperature	Time	Observation
1	NEt_3	$NiCl_2(dme)$	CH_3CN	rt	16 h	No reaction
2	NEt_3	$NiCl_2(dme)$	CH_3CN	82 °C	16 h	
3	$CsCO_3$	$NiCl_2(dme)$	CH_3CN	rt	16 h	
4	$CsCO_3$	$NiCl_2(dme)$	CH_3CN	82 °C	16 h	
5	KHMDS	$NiCl_2(dme)$	THF/toluene	rt	16 h	Free bis-NHC
6	KHMDS	$NiCl_2(dme)$	THF/toluene	rt	72 h	Free bis-NHC
7	KHMDS	$NiBr_2(PPh_3)_2$	THF/toluene	rt	16 h	Peak at 11 ppm
8	KHMDS	$NiBr_2(PPh_3)_2$	THF/toluene	rt	32 h	Peak at 11 ppm

Having a free carbene not reacting with a nickel source is very intriguing (almost disturbing). During the deprotonation of the ligand, diverse species including HMDS, dme, PPh_3 or halide are released which might interact with the nickel cation and thus compete against the free NHC, preventing its proper coordination. To suppress these drawbacks, having in hand a stable free NHC in solution, the methodology relying on external bases was abandoned, and the reactivity of the free NHC was tested for the direct metalation of various nickel sources.

4 Complexation of free carbene

4.1 Optimization of the reaction of deprotonation

The free NHC **L158** arising from **L102-L103** and **L155-L156** being stable in solution, the conditions to deprotonate the imidazolium salts were optimized (Scheme 4)

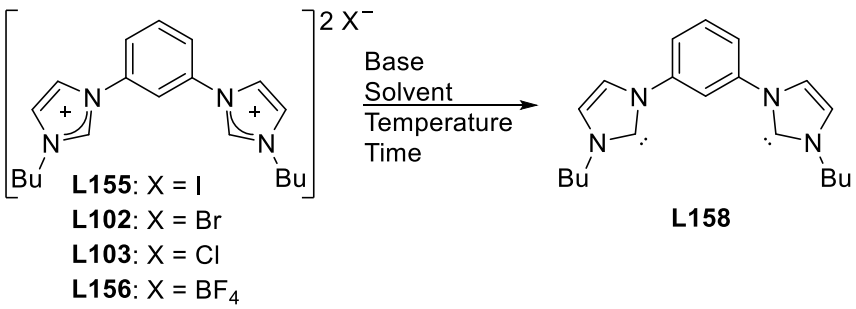

Scheme 3. Parameters affecting the deprotonation

Different parameters were modified (**Table 3**) such as: the temperature, the solvent, the base, and the reaction time. Since **L155** and **L158** are not soluble in the same solvent, no NMR conversion could be used to monitor the reaction of deprotonation.

Table 3. Conditions of deprotonation

Entry	Pro-Ligand	Time	Temperature (°C)	Solvent	Base
1	**L155**	16 h	rt	THF	KHMDS
2	**L155**	16 h	rt (addition at - 78)	THF	KHMDS
3	**L155**	3 h	rt (addition at - 78)	THF	*n*BuLi
4	**L155**	3 h	rt	THF	NaH/^{t}BuOK
5	**L102**	3 h	rt	THF	NaH/^{t}BuOK
6	**L155**	16 h	rt (addition at 0)	THF/Toluene	KHMDS
7	**L155**	16 h	rt (addition at - 78)	THF/Toluene	KHMDS
8	**L155**	16 h	rt (addition at - 78)	Toluene	KHMDS
9	**L155**	3 h	-10 (addition at - 78)	Et_2O	KHMDS
10	**L155**	3 h	rt (addition at - 78)	Toluene	KHMDS

The first attempt using KHMDS with **L155** in THF at room temperature overnight led to the free bis-NHC **L158** (Table 3, Entry 1) (53% isolated yield). The addition of KHMDS at – 78 °C led to **L158** with fewer impurities (Table 3, Entry 2) (60% isolated yield). THF was the first choice due to the insolubility of KI. However, NMR studies revealed that **L158** was not completely pure. The presence of strong bases such as *n*BuLi or NaH with ^{t}BuOK in a THF solution of **L155** or **L156** led to the decomposition of **L158** (Table 3, Entries 3-5) (0%). A brown powder, insoluble in usual solvents, was obtained. The ^{1}H NMR spectra in DMSO-d_6 or C_6D_6 feature no resonances corresponding to the compounds **L158**, **L155** or **L156**. The signals are too broad to allow any specific conclusion. The fact that KHMDS is the weakest among the three bases and non-nucleophilic suggests that soft conditions are required. Therefore, KHMDS was retained for the next optimizations. The reaction between **L155** and KHMDS in a THF/toluene mixture in a ratio 1:1, in toluene or in Et_2O at different temperatures, led to **L158** with impurities (Table 3, Entries 6-9) (37-75% isolated yield). The best conditions were found when toluene was used with the addition of KHMDS at – 78 °C. After 3 hours, the reaction was quantitative (Table 3, Entry 10). The solution was filtered, the solvent and HMDS were removed under vacuum at 50 °C. At this stage **L158** was not yet perfectly pure (impurities < 5%). Sublimation was made under 1.5 x 10^{-5} bar at 150 °C.

Références p. 199

Surprisingly, only the impurities were taken away leaving pristine **L158** with 75% isolated yield. The ^{1}H and $^{13}C\{^{1}H\}$ NMR spectra confirmed this statement (see experimental details). Similarly, the deprotonation of the imidazolium salts **L102** and **L103** using the optimized conditions led to **L158** with similar yields. With the free bis-NHC **L158** isolated in our hand, direct complexation attempts were realized. Scheme 4 presents the optimized conditions to obtain **L158.**

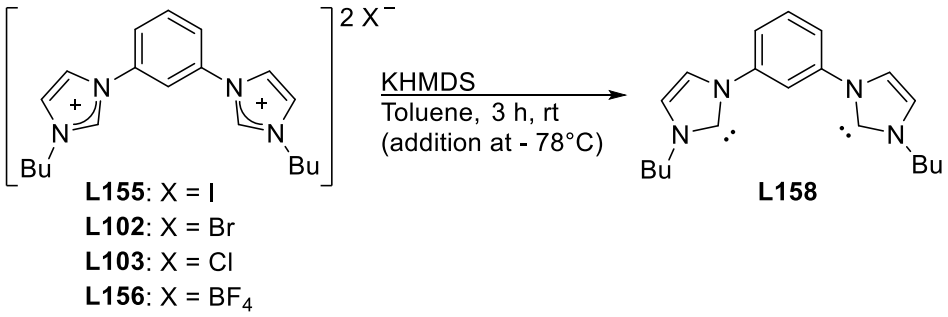

Scheme 4. Optimized synthesis of **L158**

4.2 Complexation attempts

Few groups reported the direct metalation of free bis-NHCs with nickel sources such as $NiCl_2(dme)$, $NiBr_2(dme)$, $NiCl_2(PPh_3)_2$ or $NiCl_2(PMe_3)$.[5b,17]

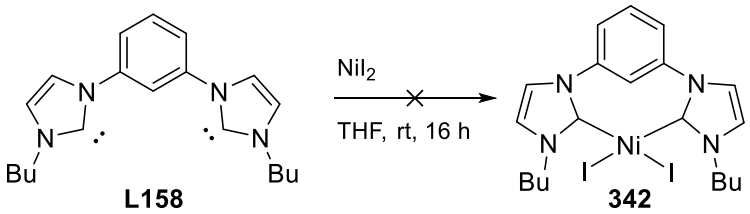

Scheme 5. Direct metalation attempts with **L158**

The addition of **L158** to a suspension of NiI_2 in toluene led to the decomposition of the free carbene (Table 4, Entry 1). After 16 h, the solution turned black. The far infrared spectra of the crude reaction mixture revealed exclusively some unreacted NiI_2 with a single band at 345 cm^{-1}. The ^{1}H NMR spectrum in C_6D_6 was silent. In CD_2Cl_2 various broad signals were present accounting for at least two unidentifiable species. The free-NHC **L158** has decomposed.

The addition of $NiCl_2(dme)$ or $NiBr_2(dme)$ to a solution of **L158** allowed the formation of a dark red precipitate which was only soluble in DMSO and methanol (Table 4, Entries 2-5). ^{1}H NMR analysis revealed the presence of paramagnetic species. The infrared spectra of the powder obtained from different nickel sources were almost identical (see

Références p. 199

experimental part), especially in the far infrared spectral region, with two bands around 397 and 227 cm^{-1}. Interestingly, they pointed out a loss of halide for the nickel cation.[18] We can imagine that two ligands **L158** might have coordinated the same nickel center, leaving the two halides as non-coordinating anions. Unfortunately, elemental analyses were not acceptable to validate this hypothesis. Crystallizations were attempted by slow gas diffusion or stratification at room temperature, 4 or - 20 °C with different couples of solvents but remained unsuccessful.

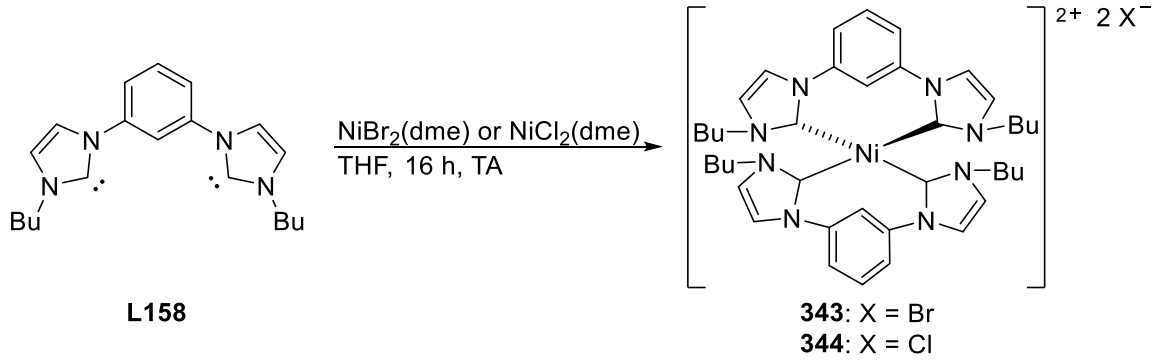

Scheme 6. Direct metalation attempts with **L158**

The addition of **L158** (in solution) to a suspension of $NiBr_2$(dme), at room temperature, in THF or toluene led to a green solution (Table 4, Entries 6-7). After evaporation of the THF, a green paramagnetic powder was obtained, precluding any further NMR studies. This product was also soluble in methanol, acetonitrile and acetone. At -78 °C, the colour of the solution turned from green to yellow. However, the compound remained paramagnetic (VT NMR experiments were made as low as – 100 °C). Attempted crystallizations by slow gas diffusion or stratification with THF/Et_2O or pentane, MeOH/Et_2O, acetone/Et_2O or pentane did not give any result.

The addition of **L158** to a suspension of $NiCl_2$(dme) in toluene or THF gave the same result (Table 4, Entries 8-9). After 16 h, the solution turned black and a yellow or orange powder remained in suspension. Infrared analysis of the powders revealed some unreacted $NiCl_2$(dme) and $NiBr_2$(dme). ^{1}H NMR analysis exhibits a spectrum almost identical to that obtained with NiI_2 (page 8) with two broad signals from 7.75 to 6.17 ppm and 2.00 to 1.10 ppm. Once again, the free bis-NHC **L158** has decomposed.

In 2001, Green *et al.* reported that the reaction between a free bis-NHC (linked by an ethylene spacer) and NiX_2 (X = Cl, Br, I), $NiBr_2$(dme) or $NiBr_2(PPh_3)_2$ led to a mixture of intractable paramagnetic compounds.[15a] They did not push deeper their investigation.

Références p. 199

However, these results tend to emphasize that reactions between free bis-NHC pincers and nickel sources are far from being trivial.

Table 4. Summary of the metalation attempts with **L158**.

Entry	Nickel precursor	Solvent	Observation
1	NiI_2	THF	Decomposition of **L158**
2	$NiCl_2$(dme)	THF	Tetra
3	$NiCl_2$(dme)	Toluene	Tetra
4	$NiBr_2$(dme)	THF	Tetra
5	$NiBr_2$(dme)	Toluene	Tetra
6	$NiBr_2$(dme)	THF	green powder paramagnetic
7	$NiBr_2$(dme)	Toluene	green powder paramagnetic
8	$NiCl_2$(dme)	THF	Decomposition of **L158**
9	$NiCl_2$(dme)	Toluene	Decomposition of **L158**

The addition of a nickel source ($NiCl_2$(dme) or $NiBr_2$(dme)) to **L158** or the reverse, addition of **L158** to a nickel source, did not yield the same compounds. The entries 2-5 describe the addition of a small amount of nickel precursor into a large excess of **L158.** Such conditions should favor the formation of tetra-NHC nickel complexes over bis-NHC nickel complexes. The infrared analysis supported this hypothesis; however, no other conclusive spectroscopic data could be obtained. For the entries 1, 8 and 9 the reactivity of **L158** was not controlled.

Moreover, the entries 6 and 7 display results very different from those obtained by transmetalation using silver(I) complexes (see paragraph **6.2** below) while both methods were expected to yield the same nickel complex.

5 Metal powder

The direct reaction of imidazolium hexafluorophosphate salts with freshly prepared Raney nickel powder was reported in 2012 by Chen *et al.*[19] Several NHC-pyridine, (bis-NHC)-pyrazole or bis-NHC Ni(II) complexes were synthesized, in high yields, by reaction of the parent imidazolium salts with Raney nickel in acetonitrile, under air / moisture conditions, for two days at 70 °C.

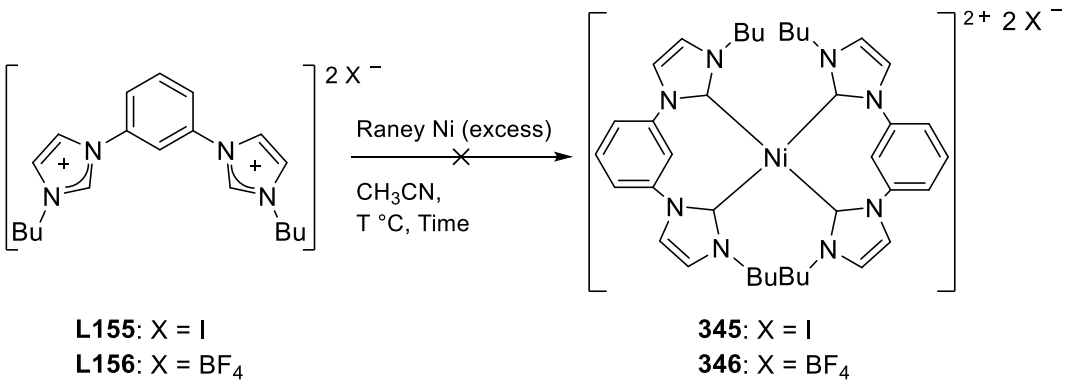

L155: X = I
L156: X = BF_4

345: X = I
346: X = BF_4

Scheme 7. Oxidative addition attempts with Raney Nickel powder.

By precaution, the attempts presented here were made under inert atmosphere, due to the pyrophoric nature of activated Raney nickel.

The imidazolium iodide salt **L155** did not react at all upon addition of activated Raney nickel, at 70 °C (Table 5, Entry 1). Heating up to the solvent boiling point or/and increasing the reactions times to seven days did not help (Table 5, Entry 2). Chen *et al*. used some imidazolium salts with non-coordinating anions. Therefore, the same reactions as described above, were carried out with the imidazolium tetrafluoroborate salt **L156** (Table 5, Entries 3-4). However, once again no reaction occurred.

Table 5. Attempts on using activated Raney nickel.

Entry	Pro-Ligand	Time	Temperature (°C)	Observation
1	**L155**	2 days	70	No reaction
2	**L155**	7 days	82	
3	**L102**	2 days	70	
4	**L102**	7 days	82	

The same group reported the synthesis of NHC nickel(II) complexes, in good yields, using an excess of nickel powder in presence of NHC silver(I) complexes (generated in situ or isolated) under inert atmosphere, at 50 °C.[20] Moreover, the reaction of imidazolium hexafluorophosphate salts with nickel powder allowed the formation of the same nickel(II) complexes in lower yield under air.

Références p. 199

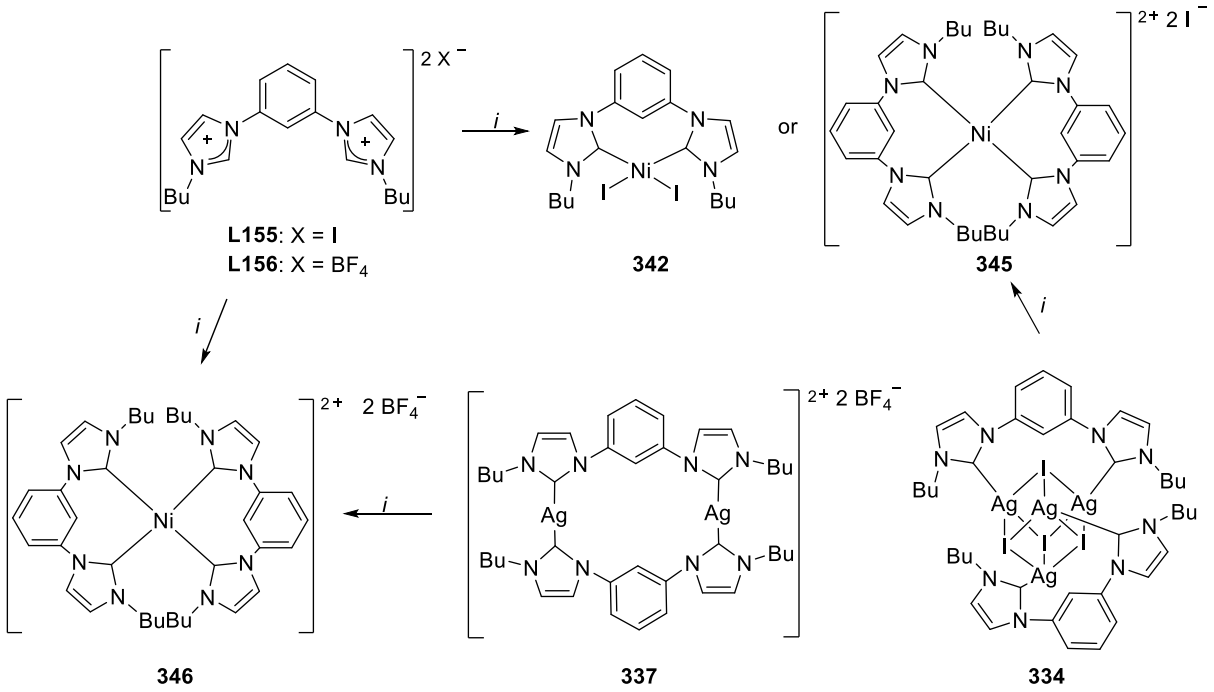

Scheme 8. Attempts on using Ni(0) powder

The salts **L155** and **L102** did not react at all with nickel(0) powder, following Chen's conditions (Table 6, Entries 5-6). The reaction of **L155** with Ag_2O in acetonitrile gave the silver(I) iodide complex **334** in low yield (see chapter 2). **334**, being insoluble in acetonitrile, was isolated before use. The reaction between **334** and nickel(0) powder did not take place at 50 or 82 °C (Table 6, Entries 7-8). An identical behaviour was observed with the silver(I) tetrafluoroborate complex **337** (Table 6, Entries 5-10).

Table 6. Complexation attempts using nickel(0) powder

Entry	Pro-Ligand	Time	Temperature (°C)	Observation
5	**L155**	5 days	82	No reaction
6	**L102**	5 days	82	
7	**334**	5 days	50	
8	**334**	5 days	82	
9	**337**	5 days	50	
10	**337**	5 days	82	

In Chen's work, all mono- and bis- NHCs were *N*-functionalized (e.g pyridine). This functionalization, not present on **L102-L103** and **L155-L157**, might be required to obtain a suitable reactivity with the Ni(0) sources.

Références p. 199

6 Transmetalation

6.1 From zirconium complexes

Hollis *et al.* patented in 2011 a synthetic route from imidazolium salt to nickel(II) complexes involving the generation, *in situ*, of zirconium(IV) complexes (Scheme 9).[21] They used pincer NHC pro-ligands with an aryl linker and obtained zirconium(IV) complexes with the corresponding C,C,C-pincer ligand, displaying $^{13}C\{^{1}H\}$ carbenic resonances at 188.9 and 195.5 ppm.[22]

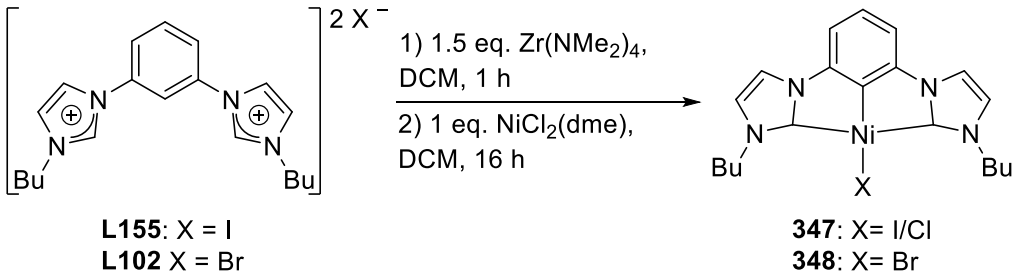

Scheme 9. Transmetalation using zirconium(IV) complexes

Following the protocol reported, several reactions between $Zr(NMe_2)_4$ (commercially available) and **L155** or **L103**, followed by the addition of $NiCl_2$(dme) or NiB_2(dme) were attempted (Table 7, Entries 1-2). The partial disappearance of the characteristic signal of the imidazolium salts and the appearance of typical downfield signals for the carbenic carbons at 174.4 or 172.3 ppm, monitored by ^{1}H and $^{13}C\{^{1}H\}$ NMR spectroscopy, hinted at the formation of nickel(II) complexes **347-348** with 35 and 40% conversion. However, unlike the description in the patent, addition of water produced a precipitate, which turned out to be a mixture of inseparable compounds, including a large quantity of starting material. The purity of the commercial zirconium(IV) sources was incriminated. Its purification by sublimation being extremely cumbersome, it was directly synthesized.[23]

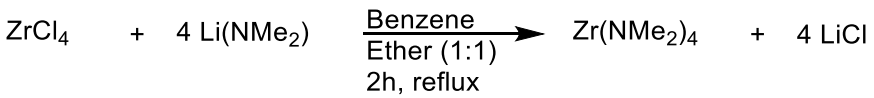

Scheme 10. Synthesis of $Zr(NMe_2)_4$.

The zirconium tetrachloride was purified by sublimation prior reaction with $Li(NMe_2)$. ^{1}H NMR spectroscopy revealed a resonance at 2.89 ppm, confirming the formation of $Zr(NMe_2)_4$, plus a small amount of impurities (less than 10%). Purifications of $Zr(NMe_2)_4$ by distillation or sublimation failed (extensive decomposition).

Table 7. Transmetalation from zirconium complexes

Entry	Pro-Ligand	NMR conversion	Observation
1	**L155**	35%	Formation of nickel complexes in solution
2	**L103**	40%	Similar to entry 1 behavior was observed

As the synthetic conditions described by Hollis *et al.* did not produce in our hands the expected results, silver(I) complexes were used in place as transmetaling agents.

6.2 From silver complexes

In the literature, the transmetalation reactions from bis-, tri- or tetra-NHC silver(I) complexes were achieved using three different nickel sources: $NiCl_2(dme)$,[5a,8,24] $NiBr_2(dme)$[17c,25] or $NiCl_2(PPh_3)_2$.[26] Noteworthy silver(I) complexes are very well known to transfer easily, under air conditions, their NHC ligands to various late transition metals including Au,[27] Cu,[28] Co,[29] Cr,[29] Fe,[29] Pd[25,30] and Pt.[30]

For the first attempts of transmetalation, the cubane-type silver(I) iodide complex **334,** described in chapter 2, was used.

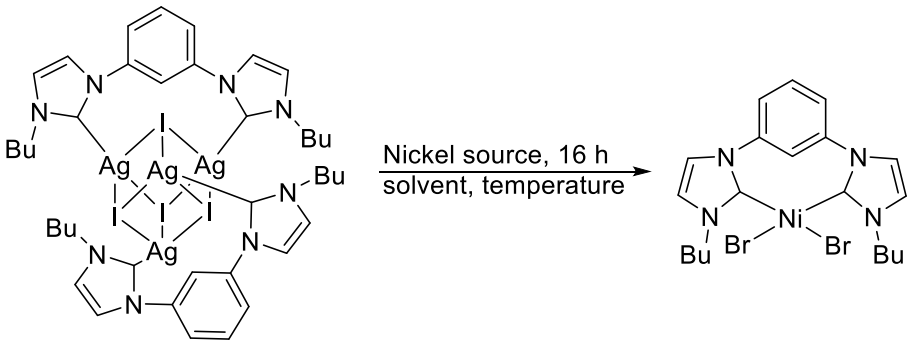

334 **347**

Scheme 11. Transmetalation attempts from **334**

The reaction between the nickel dibromide and the cubane-type complex **334** was attempted in different solvents such as DCM, CH_3CN or THF (Table 8, Entries 3-5) for 16 h, at different temperatures (Table 8, Entries 6-8). Disappointingly, monitoring by ^1H NMR spectroscopy indicated no reaction.

In acetonitrile or DCM, the reaction between **334** and $Ni(CH_3CN)_6(BF_4)_2$ led to the reformation of an imidazolium salt evidenced by ^1H NMR spectroscopy, with a singlet at 9.35

Références p. 199

ppm (Table 8, Entries 9-10). With **337**, no reaction occurred at all (Table 8, Entry 11). Then, **334** was mixed with the three other nickel sources: $NiCl_2$(dme), $NiBr_2$(dme) or $NiCl_2(PPh_3)_2$.

Table 8. Transmetalation attempts from **334** and **337** (PL: Pro-Ligand)

Entry	PL	Nickel sources	Solvent	Temperature	Observation
3	**334**	$NiBr_2$	DCM	rt	No reaction
4	**334**	$NiBr_2$	CH_3CN	Rt	
5	**334**	$NiBr_2$	THF	Rt	
6	**334**	$NiBr_2$	DCM	41 °C	
7	**334**	$NiBr_2$	CH_3CN	82 °C	
8	**334**	$NiBr_2$	THF	66 °C	
9	**334**	$Ni(CH_3CN)_6(BF_4)_2$	DCM	rt	Protonation of the carbene ligand
10	**334**	$Ni(CH_3CN)_6(BF_4)_2$	CH_3CN	rt	No reaction
11	**337**	$Ni(CH_3CN)_6(BF_4)_2$	CH_3CN	rt	No reaction

In the case of $NiCl_2$(dme), the reaction took place overnight in THF or acetonitrile at room temperature or under reflux (Table 9, Entries 12-15). In acetonitrile, the solution remained colorless. No reaction occurred. This can be due to the insolubility of the starting materials.

However in THF, the reaction solution turned orange, and a mixture of new compounds was evidenced by ^{1}H NMR spectroscopy. Two peaks at 10.48 and 10.87 ppm suggested the presence of imidazolium moieties (21%). **334** is present (51%) as well as a new compound (28%) (possibly a nickel NHC complex). In the $^{13}C\{^{1}H\}$ NMR spectrum, a signal at 184.3 corresponds to **334**, four signals at 174.6, 166.8, 159.8 and 159.1 confirmed the presence of different complexes as well as the different peaks assignable to butyl chains. It is important to mention that no $^{1}J(^{13}C\text{-}^{109/107}Ag)$ coupling was visible on the carbene signals for **334** and the new complexes, rendering the discrimination between Ni- or Ag-bound carbene impossible to make by NMR spectroscopy. The far infrared spectrum indicated several bands at 502, 390, 377, 353, 302, 279 and 227 cm^{-1}. Unfortunately, the products were inseparable by precipitation from pentane or Et_2O, partial dissolutions with DCM, toluene or acetonitrile, and crystallizations (see experimental part). Heating to the boiling point of THF did not increase the ratio of the different complexes formed. As the nickel precursor was insoluble, we decided to employ $NiBr_2$(dme) which is soluble in THF.

Table 9. Transmetalation attempts from the silver(I) complex **334** (PL: Pro-Ligand)

Entry	PL	Nickel sources	Solvent	Temperature	Observation
12	**334**	$NiCl_2$(dme)	THF	rt	Orange mixture inseparable
13	**334**	$NiCl_2$(dme)	CH_3CN	rt	No reaction
14	**334**	$NiCl_2$(dme)	THF	66 °C	Orange mixture inseparable
15	**334**	$NiCl_2$(dme)	CH_3CN	82 °C	No reaction

In the case of $NiBr_2(PPh_3)_2$ or $NiBr_2$(dme), the reaction took place in DCM overnight, at room temperature. The solution turned deep red almost instantly (Table 10, Entries 16-17). The ^{1}H NMR spectrum of the reaction mixture using $NiBr_2(PPh_3)_2$ indicated a mixture of products containing some unreacted **334**, protonated carbene and at least a new product (Table 10, Entry 16). The spectrum indicates a ratio **334**/new product/protonated carbene of 38:44:18. The $^{13}C\{^1H\}$ NMR spectrum confirms the presence of **334** with the characteristic signals at 18.8 ppm. Four signals between 174.1 and 168.9 ppm suggested the possible presence of four different nickel- or silver(I)-bound carbene sites. Once again the lack of $^1J(^{13}C\text{-}^{109/107}Ag)$ coupling prevented a clear discrimination between Ni / Ag species.

The ^{1}H NMR spectrum of the reaction mixture with $NiBr_2$(dme) (Table 10, Entry 17) revealed a similar composition as for Entry 16. However the ratio **334**/new product/protonated carbene has changed and is now equal to 69:23:8. On the $^{13}C\{^1H\}$ NMR spectrum, only the carbene signal of **334** is visible. However, the resonances of the butyl chains suggest the presence of four products. Unreacted **334** was removed by treatment with THF. Attempts to extract the protonated carbene with distilled water resulted in a paramagnetic mixture of products from which no NMR studies were possible. The mixture was air-stable but decomposed upon flash chromatography. The different products in solution having similar solubilities, no separation by selective precipitation was possible. Crystallizations from the crude mixture only gave few colorless crystals. ^{1}H NMR analysis of the crystals showed that it was **334**. From these results, $NiBr_2$(dme) was chosen to optimize the reaction of transmetalation.

The effect of the solvents were screened with **334** and $NiBr_2$(dme). In acetonitrile, ^{1}H NMR analysis revealed the formation of an imidazolium salt with a characteristic signature at 10.30 ppm (Table 10, Entry 18). In methanol, a yellow and a green precipitate were formed at the same time. They were insoluble in usual solvents, so no NMR spectrum was recorded.

The infrared spectrum of the combined precipitates exhibits two very broad bands at 451 and 380 cm^{-1} plus some similarities with the NHC scaffold arising from **334** between 1600 and 692 cm^{-1}. No conclusion was possible from these data (Table 10, Entry 19).

In THF, at room temperature or at -78 °C, ^{1}H NMR studies indicated the presence of three new products in a ratio of 71:23:6 while **334** was completely consumed. In the $^{13}C\{^{1}H\}$ NMR spectrum, two carbene signals were visible at 176.0 and 173.5 ppm. In addition to the expected resonances for the bis-NHC ligand scaffolds, three resonances at 21.8, 27.3 and 67.3 ppm were not assignable (Table 10, Entries 20-21). The infrared spectrum confirmed the formation of at least one bis-NHC complex different from **334**. The complexes were air-stable; however they decomposed upon flash chromatography. The mixture of products was not completely soluble in acetone and toluene and was completely soluble in toluene and DCM. Part of the mixture isolated from acetone was analyzed by ^{1}H NMR spectroscopy. However, no trace of nickel complex was present. Trying to precipitate separately the different complexes using pentane, Et_2O, methanol, ethanol or ethyl acetate did not work; they all precipitated simultaneously even at – 20 °C. Filtration of the mixture of complexes in hot THF did not allow any separation.

Table 10. Transmetalation attempts from the silver(I) complex **334** (PL: Pro-Ligand)

Entry	PL	Nickel sources	Solvent	Temperature	Observation
16	**334**	$NiBr_2(PPh_3)_2$	DCM	rt	Red mixture containing nickel complex
17	**334**	$NiBr_2$(dme)	DCM	rt	Same as entry 16
18	**334**	$NiBr_2$(dme)	CH_3CN	rt	No reaction
19	**334**	$NiBr_2$(dme)	MeOH	rt	Two precipitate green and yellow insoluble
20	**334**	$NiBr_2$(dme)	THF	rt	Red nickel complex almost clean by ^{1}H NMR
21	**334**	$NiBr_2$(dme)	THF	rt	Addition at – 78 °C, Same as entry 20

Microwave activation has been used to synthesize palladium[31] or group 11 metals[32] NHC complexes with reduced reaction times. The first attempt was carried out in THF with **334** and $NiBr_2$(dme) at 50 °C, for 5 min, under 50 W. These conditions are really soft. No

reaction occurred. The reaction time was changed from 5 to 10 or 15 min. Once again, no reaction occurred. At 70 °C, the solution turned deep red (Table 11, Entries 22-25) and its ^{1}H NMR spectrum indicated that the reaction was less clean than in THF overnight at room temperature. At 70 °C, the NMR conversion based on **334** is equal to 36% with various impurities. Some of them include mixed halides (bromo/iodo) derivatives. Increasing the temperature to push the reaction was extremely deleterious, so the use of microwaves was dropped. Besides, **334** was replaced by **337** or **335** for the transmetalation trials.

Table 11. Transmetalation attempts from the silver(I) complex **334** under microwaves (PL: Pro-Ligand)

Entry	PL	Nickel sources	Solvent	Temperature	Observation
22	**334**	$NiBr_2$(dme)	THF	50 °C	5 min, 50 W, no reaction
23	**334**	$NiBr_2$(dme)	THF	50 °C	10 min, 50 W, no reaction
24	**334**	$NiBr_2$(dme)	THF	50 °C	15 min, 50 W, no reaction
25	**334**	$NiBr_2$(dme)	THF	70 °C	15 min, 50 W, reaction occurred but less cleanly than in entry 20

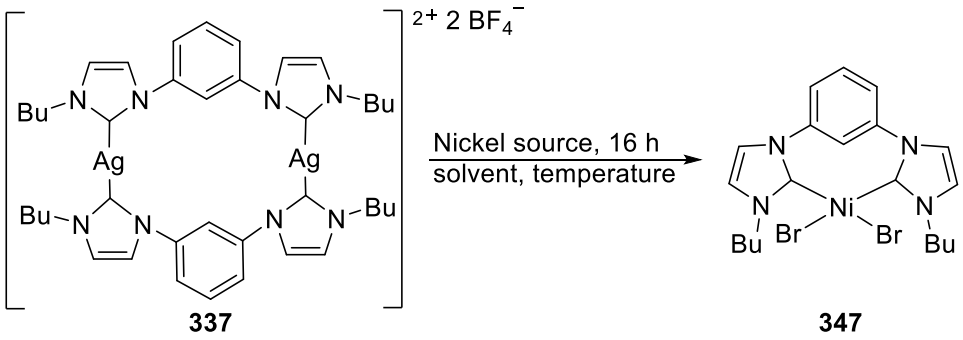

Scheme 12. Transmetalation attempts from the silver(I) complex **337**

The reaction of **337** with $NiBr_2(PPh_3)_2$ in THF led to an orange solution (Table 12, Entry 26). The ^{1}H and $^{13}C\{^{1}H\}$ NMR spectra indicated the formation of a compound different from the red one previously obtained (Table 10, Entry 20). A large quantity of protonated carbene was present according to the ^{1}H NMR spectrum as well as at least three products with a ratio protonated carbene/product 1/product 2/product 3 of 60:14:14:12. The $^{13}C\{^{1}H\}$ NMR spectrum confirmed the presence of several products, however no carbene signal was recorded. Some compounds from the mixture seemed unstable in dichloromethane, resulting in a worse ^{1}H NMR spectrum in CD_2Cl_2. Addition of toluene, pentane or Et_2O as non-

Références p. 199

solvents to a solution of THF triggered the precipitation of all products. Crystallizations using different couple of solvents such as (THF/Et_2O, THF/pentane, acetonitrile/pentane, acetonitrile/Et_2O) of solvents led to orange oils. The transmetalation releasing some silver(I) cation, acetonitrile was also tested as co-solvent to: 1/ form $[Ag(MeCN)_4]^+$ aiming at minimizing the formation of AgBr by bromide stripping from unreacted $NiBr_2(PPh_3)_2$, 2/ stabilize any unsaturated nickel species formed by bromide stripping (if any), by offering a coordinating solvent to fill up the metal coordination sphere (Table 12, Entry 27). Unfortunately, the presence of acetonitrile did not improve the reaction conditions. Finally, changing the metal source for $NiBr_2$(dme), and forcing the reaction conditions under microwave irradiation (50 W), at 70 °C for 15 minutes resulted in the same mixture of compounds than that previously described with $NiBr_2(PPh_3)_2$ (Table 12, Entry 28). The ^1H NMR spectrum revealed various broad and unidentifiable signals. No conclusions were drawn except that the silver(I) complex **337** was absent in the spectrum.

Table 12. Transmetalation attempts from the silver(I) complex **337** (PL: Pro-Ligand)

Entry	PL	Nickel sources	Solvent	Temperature	Observation
26	**337**	$NiBr_2(PPh_3)_2$	THF	rt	Orange mixture inseparable
27	**337**	$NiBr_2(PPh_3)_2$	THF/CH_3CN	rt	Same as entry 26
28	**337**	$NiBr_2$(dme)	THF	70 °C	15 min, 50 W, orange mixture inseparable

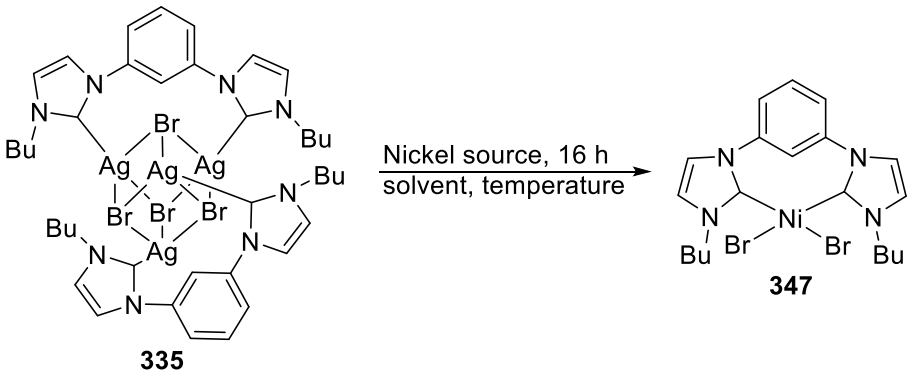

335 347

Scheme 13. Transmetalation attempts from the silver(I) complex **335**

The transmetalation from **337** led to the formation of $AgBF_4$ which is partially soluble in polar solvents, lowering the equilibrium shift toward the formation of nickel complexes. Thus **335** was used in place to have a transmetalation assisted by AgBr precipitation.

The reaction between **335** and $NiBr_2$(dme) in THF at room temperature or at 66 °C led to a deep red solution (Table 13, Entries 29-30). The ^{1}H NMR spectra of the crude mixtures indicated a mixture of products already encountered during the reaction between **334** and $NiBr_2$(dme) (Table 13, Table 29). Three compounds were present with the following ratios 80:17:3. In the $^{13}C\{^1H\}$ NMR spectrum, a signal at 173.6 ppm, without any visible $^1J(^{13}C\text{-}^{109/107}Ag)$ coupling, characterizes a silver or nickel NHC species.

$NiBr_2(PPh_3)_2$ gave a mixture of products similar to those obtained by reaction of **334** or **335** with $NiBr_2$(dme) (Table 10, Entry 20 & Table 13, Entry 31). Once again, no clear discrimination between Ag / Ni species was achieved using NMR spectroscopy. Passing the mixture through flash chromatography column resulted in a complete loss of the complexes.

Fractional precipitations in pentane, Et_2O, methanol, ethanol or ethyl acetate at room temperature or at – 20 °C, partial dissolutions in hot THF or toluene, and finally crystallizations failed, preventing any deeper spectroscopic characterizations.

Table 13. Transmetalation attempts from the silver(I) complex **335** (PL: Pro-Ligand)

Entry	PL	Nickel sources	Solvent	Temperature	Observation
29	**335**	$NiBr_2$(dme)	THF	rt	Red mixture inseparable, similar to 20
30	**335**	$NiBr_2$(dme)	THF	66 °C	reaction occurred but less cleanly than in entry 20
31	**335**	$NiBr_2(PPh_3)_2$	THF	rt	reaction occurred but less cleanly than in entry 20

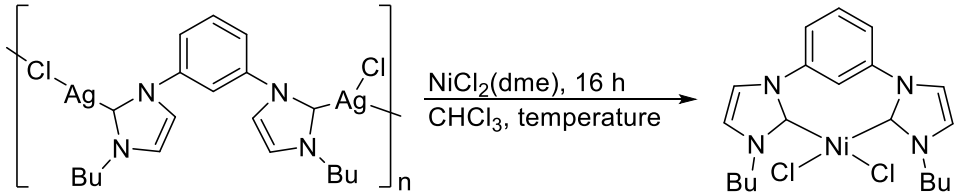

336 **348**

Scheme 7. Transmetalation attempts from the silver(I) complex **336**

A final transmetalation protocol was attempted starting from the silver complex **336** with $NiCl_2$(dme) in chlorinated solvent ($CHCl_3$). The fast precipitation of AgCl, compared to AgBr, was expected to favor the transmetalation.

336 was reacted with 1 equiv. of $NiCl_2$(dme) in chloroform at room temperature or under reflux (Table 14, Entries 32-33). The colourless solution became yellow, the suspension of $NiCl_2$(dme) disappeared with concomitant formation of a white precipitate which turned black under the light. The ^1H and $^{13}C\{^1H\}$ NMR spectra of the crude reaction mixture and **336** are very similar. In the ^1H NMR spectrum, a new set of signals accounting for a unique NHC-based compound was observed with free dme. In the $^{13}C\{^1H\}$ NMR spectrum, a carbene signal is visible at 179.2 ppm, a value identical to that of **336**. The new compound was precipitated with pentane and washed with Et_2O to remove the free dme. Surprisingly, the isotopic profile measured by mass spectroscopy analysis hints at the possible formation of a hetero-dinuclear Ni/Ag complex. This result contradicts the NMR studies, as silver- and nickel-bound carbene sites are expected to feature different chemical shifts. The addition of a second equivalent of $NiCl_2$(dme) to the reaction mixture (Table 14, Entry 34) or the reaction between two equivalents of $NiCl_2$(dme) and one equivalent **336** led to the same new compound (Table 14, Entry 35). This hypothesis was further confirmed with the far infrared spectra of the different crude reaction mixtures (Table 14, Entries 32-35) displaying similar bands at 297, 400 and 459 cm^{-1} (maximum deviation of 3 cm^{-1}).

Crystallization attempts from different couples of solvents (dichloromethane/octane, chloroform/octane) by slow evaporation were unsuccessful.

Table 14. Transmetalation attempts from the silver(I) complex **336** (PL: Pro-Ligand)

Entry	PL	Nickel sources	Solvent	Temperature	Observation
32	**336**	1 equiv. of $NiCl_2$(dme)	$CHCl_3$	rt	Yellow powder
33	**336**	1 equiv. of $NiCl_2$(dme)	$CHCl_3$	61 °C	Yellow powder similar to entry 32
34	**336**	2 equiv. of $NiCl_2$(dme)	$CHCl_3$	61 °C	Yellow powder similar to entry 32
35	**336**	2 equiv. of $NiCl_2$(dme)	$CHCl_3$	61 °C	Yellow powder similar to entry 32

6.3 From copper(I) complexes

An article reported a transmetallation reaction from copper to nickel using $NiCl_2(PPh_3)_2$ as nickel source.[33] Transmetalations from copper(I) complexes **339** and **340** with $NiBr_2(PPh_3)_2$ or $NiCl_2$(dme) as nickel sources were thus attempted.

The reaction between the copper(I) bromide complex **339** (see chapter 2) and $NiBr_2(PPh_3)_2$ in THF at room temperature gave a deep red solution with a black precipitate (Table 15, Entry 36). The ^1H NMR spectrum of the solution was similar to that obtained by transmetalation using the silver(I) bromide complex **335** (Table 15, entry 23) with a ratio protonated carbene/**339**/new product **1**/new product **2**/new product **3** equal to 12:26:25:14:23. The crude reaction mixture was washed three times with toluene to remove the free PPh_3. By comparison with the transmetalation from **337 or 334**, **339** is less effective. In contrast, the reaction in entry 29 was more selective since the ratios between new product **1**/new product **2**/new product **3** were 80:17:3.

Attempts to purify the crude reaction mixture by crystallization, partial dissolution in hot solvents, or partial precipitation at different temperatures failed. Varying the reaction temperatures from – 78 °C to 66 °C did not improve the purity of the crude mixture (Table 15, Entries 37-38).

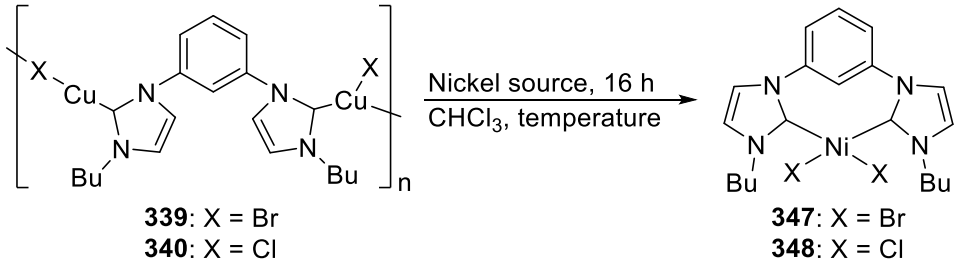

Scheme 15. Transmetalation attempts from the copper(I) complexes **339-340**

The copper(I) chloride complex **340** reacted with $NiCl_2$(dme) at room temperature or at 66 °C. Since **340** decomposes in chloroform, the solvent used was THF (Table 15, Entry 39). The ^1H NMR spectrum of the crude reaction revealed some broad signals. However, two sets of resonances corresponding to **340** and a new complex with a ratio **340**/new complex of 80:20 were clearly visible. A signal at 10.50 ppm hinted at the formation of a protonated carbene (Table 15, Entry 40). Washing a solution of DCM with distilled water removed the protonated carbene. The isolation of a single product failed, by fractional precipitations, or partial dissolution in hot THF or toluene. Crystallization attempts using various couples of solvents such DCM/octane, $CHCl_3$/octane led to the formation of oils. Importantly, this reaction is less clean than with **336.** Overall copper(I) complexes are less effective than silver(I) ones to transfer their NHC to nickel.

Références p. 199

Table 15. Transmetalation attempts from the copper(I) complexes **339-340** (PL: Pro-Ligand)

Entry	PL	Nickel sources	Solvent	Temperature (°C)	Observation
36	**339**	$NiBr_2(dme)$	THF	rt	Red solution with black powder
37	**339**	$NiBr_2(PPh_3)_2$	THF	rt	Behavior similar to entry 34
38	**339**	$NiBr_2(PPh_3)_2$	THF	66	Behavior similar to entry 34
39	**340**	$NiCl_2(dme)$	THF	rt	Mixture of product with protonated carbene
40	**340**	$NiCl_2(dme)$	THF	66	Behavior similar to entry 36

The group of Hoffmann also encountered some difficulties with transmetalation reactions to iridium, palladium or nickel, involving silver(I) clusters.[25,34] The complexes **334-340** being cubanes or polymers, might not be as suitable as classical mono-NHC silver(I) complexes (e.g. IPrAgCl) for transmetalation purposes. The spacer between the two NHCs moieties should be long enough to obtain a chelate nickel complex. If not, the ligand should be able to bridge two metal centers as observed in silver and copper chemistry (**334-340**)

The groups of Danopoulos[17c] and Kemp[35] reported carbene transfers from nickel to silver using $AgNO_3$ or AgOTf. Sometimes, the Ni–$C_{carbene}$ bond is more labile than the Ag–$C_{carbene}$ bond. Therefore, the carbene transfer reactions from silver to nickel might not be that trivial.

In 2012, an unique article reported the transmetalation of NHCs from copper(I) to nickel(II).[33] Overall, the reaction conversions obtained with NHC copper(I) complexes were systematically lower than with silver(I) NHC complexes. Besides, mixtures of untractable compounds were obtained rather than the desired Ni complexes. Clearly, copper(I) NHCs were not suitable transmetalating agents for organonickel chemistry.

7 Conclusion

The aim to synthesize chelating bis-NHC nickel(II) complexes was much more difficult to achieve than initially thought. The five classical routes described in the literature were assessed. The used of nickel sources with an internal base failed, surely due to a lack of basicity. The successive addition of strong bases to nickel sources with various imidazolium salts was not successful, perhaps because the process generated some byproducts which

Références p. 199

competed against the free carbene to coordinate the nickel(II) cation. Direct metalation of free NHC led to paramagnetic untraceable products. Using transmetalating agents such as silver(I) or copper(I) complexes led to diamagnetic mixtures of compounds. Unfortunately, no clean complexes were recovered using the standard separation techniques, such as fractional precipitations or dissolutions, crystallizations, sublimations. However, silver complexes were superior to copper complexes to transfer their NHC fragments. The most convincing results were obtained by transmetalation from the iodide or bromide silver(I) complexes with clear spectroscopic evidences for the formation of nickel complexes.

8 Experimental details

8.1 Internal bases

1) Entry 1: **L157** (100.00 mg, 0.19 mmol), $Ni(OAc)_2.4H_2O$ (47.28 mg, 0.19 mmol) and THF were combined and stirred under reflux. After 16 h, the solvent was removed. The ^1H NMR of the crude mixture reveals the presence of the imidazolium salt **L157**. The nickel source was 100% recovered.

2) Entry 2: A procedure similar to that used before with **L157** (100.00 mg, 0.19 mmol) and $Ni(acac)_2.2H_2O$ (55.66 mg, 0.19 mmol) gave no reaction.

3) Entries 3 and 7: A procedure similar to that used before with **L155** (100.00 mg, 0.17 mmol), $Ni(OAc)_2.4H_2O$ (42.30 mg, 0.17 mmol) in THF or DMSO gave no reaction.

4) Entry 4: A procedure similar to that used before with **L155** (100.00 mg, 0.17 mmol), $Ni(acac)_2.2H_2O$ (49.79 mg, 0.17 mmol) gave no reaction.

5) Entry 5: A procedure similar to that used before with **L155** (100.00 mg, 0.17 mmol), $Ni(acac)_2$ (43.67 mg, 0.17 mmol) gave no reaction.

6) Entry 6: A procedure similar to that used before with **L155** (100.00 mg, 0.17 mmol), $Ni(acac)_2$ (43.67 mg, 0.17 mmol) and $CsCO_3$ (114.04 mg, 0.35 mmol) gave no reaction.

7) Entries 8 to 11: procedure similar to that used before with **L155** (100.00 mg, 0.17 mmol), $NiCO_3$ (20.18 mg, 0.17 mmol) in DMSO or CH_2Cl_2 under reflux or at room temperature gave no reaction.

8.2 External bases

1) Entries 1 and 2: **L157** (180.61 mg, 0.34 mmol), NEt_3 (73.49 mg, 0.73 mmol) and $NiCl_2$(dme) (76.00 mg, 0.34 mmol) were mixed in CH_3CN and stirred overnight at room temperature. The ^1H NMR of the crude mixture reveals the presence of the imidazolium salt **L157**. The nickel source was 100% recovered.

2) Entries 3 and 4: A procedure similar to that used before with **L157** (180.61 mg, 0.34 mmol), $CsCO_3$ (325.82 mg, 0.73 mmol) and $NiCl_2$(dme) (76.00 mg, 0.34 mmol) under reflux gave no reaction.

3) Entries 5 and 6: **L155** (200.00 mg, 0.34 mmol), KHMDS (151.79 mg, 0.76 mmol) and $NiCl_2$(dme) (76.00 mg, 0.34 mmol) were mixed in THF/toluene and stirred overnight at room temperature. The ^1H NMR of the crude mixture reveals the presence of the free bis-NHC **L158**. The nickel source was 100% recovered.

4) Entryies 7 and 8: **L155** (200.00 mg, 0.34 mmol), KHMDS (151.79 mg, 0.76 mmol) and $NiBr_2(PPh_3)_2$ (257.00 mg, 0.34 mmol) were mixed in THF/toluene and stirred overnight or 32 h at room temperature. The ^1H NMR of the crude mixture reveals the presence of protonated bis-NHC.

8.3 Free bis-NHC

Reaction of deprotonation

1) Entry 1: To a THF solution of **L155** (578.3 mg, 1.0 mmol) was added a THF solution of KHMDS (438.9 mg, 2.2 mmol). The mixture was stirred overnight. The solution was filtered and the solvent removed yielding a deep red powder. The ^1H and $^{13}C\{^1H\}$ NMR spectra reveal the disappearance of the characteristic signals of **L155** and the appearance of a typical downfield carbene signal at 215.1 ppm. ^1H NMR (300 MHz, C_6D_6) δ 8.67 (t, J = 2.0 Hz, 1H, CH^{aryl}), 7.74 (d, J = 2.0 Hz, 2H, CH^{aryl}), 7.13 (s, 1H, CH^{aryl}), 7.10 (d, J = 1.6 Hz, 2H, $CH^{imidazole}$), 6.48 (d, J = 1.6 Hz, 2H, $CH^{imidazole}$), 3.85 (t, J = 7.2 Hz, 4H, $NCH_2{}^{Bu}$), 1.66–1.56 (m, 4H, $CH_2{}^{Bu}$), 1.27–1.12 (m, 4H, $CH_2{}^{Bu}$), 0.77 (t, J = 7.3 Hz, 6H, $CH_3{}^{Bu}$). $^{13}C\{^1H\}$ NMR (75 MHz, C_6D_6) δ 215.09 ($C^{carbene}$), 143.65 (C^{aryl}), 130.04 (CH^{aryl}), 120.12 (2 × CH^{aryl}), 117.89 ($CH^{imidazole}$), 117.19 ($CH^{imidazole}$), 113.17 (CH^{aryl}), 51.19 ($NCH_2{}^{Bu}$), 33.83 ($CH_2{}^{Bu}$), 20.03 ($CH_2{}^{Bu}$), 13.88 ($CH_3{}^{Bu}$).

2) Entry 2: A procedure similar to 1) with the addition of KHMDS at - 78 °C led to **L158**. The ^1H NMR spectrum displays fewer impurities than in 1).

3) Entry 3: To a THF solution of **L155** (241.7 mg, 0.4 mmol) was added at – 78 °C a THF solution of *n*BuLi (0.1 ml, 0.8 mmol). The mixture was stirred overnight. A brown powder was filtered. The brown powder was insoluble in usual solvent (THF, toluene or benzene). The ^{1}H NMR spectrum of the solution is silent.

4) Entry 4: Following a procedure similar to 1) **L155** (289.1 mg, 0.5 mmol), NaH (28.8 mmol, 1.2 mmol) and a small amount of *t*BuOK were mixed. After 3 h, the solution was filtered and the solvent removed. Red oil was obtained. No sign of **L158** or **L155** appears on the ^{1}H NMR spectra.

5) Entry 5: A procedure similar to 3) with **L102** (145.0 mg, 0.29 mmol) and NaH (16.8 mg, 0.7 mmol) gave the same result.

6) Entries 6 and 7: A similar procedure to 1) in THF/toluene with addition of KHMDS at 0 or -78 °C gave **L158**, but in lower yield.

7) Entry 9: A similar procedure to 1) in ether with addition of KHMDS at -78 °C and reaction at -10 °C gave **L158**.

8) Entries 8 and 10: A similar procedure to 1) with addition of KHMDS in toluene at -78 °C and stirring overnight or 3 h gave **L158**. The sublimation of the red powder obtained at 150 °C under 1.5x10^{-5} bar led to pure bis-NHC **L158** (75%). ^{1}H NMR (300 MHz, C_6D_6) δ 8.67 (t, *J* = 2.0 Hz, 1H, CH^{aryl}), 7.74 (d, *J* = 2.0 Hz, 2H, CH^{aryl}), 7.13 (s, 1H, CH^{aryl}), 7.10 (d, *J* = 1.6 Hz, 2H, $CH^{imidazole}$), 6.48 (d, *J* = 1.6 Hz, 2H, $CH^{imidazole}$), 3.85 (t, *J* = 7.2 Hz, 4H, $NCH_2{}^{Bu}$), 1.66–1.56 (m, 4H, $CH_2{}^{Bu}$), 1.27–1.12 (m, 4H, $CH_2{}^{Bu}$), 0.77 (t, *J* = 7.3 Hz, 6H, $CH_3{}^{Bu}$). ^{13}C{^{1}H} NMR (75 MHz, C_6D_6) δ 215.09 ($C^{carbene}$), 143.65 (C^{aryl}), 130.04 (CH^{aryl}), 120.12 (2 × CH^{aryl}), 117.89 ($CH^{imidazole}$), 117.19 ($CH^{imidazole}$), 113.17 (CH^{aryl}), 51.19 ($NCH_2{}^{Bu}$), 33.83 ($CH_2{}^{Bu}$), 20.03 ($CH_2{}^{Bu}$), 13.88 ($CH_3{}^{Bu}$).

Direct complexation attempts of **L158**

1) Entry 1: To a suspension of NiI_2 (black) (290.7 mg, 0.9 mmol) in THF, a THF solution of **L158** (300.0 mg, 0.9 mmol) was added and the mixture stirred. After 16 h, the solution has turned black and the black precipitate was still present. The solution was filtered and the solvent removed. The ^{1}H NMR spectrum featured no sign of **L158** or nickel complex. IR of the black precipitate: ν_{max}(solid)/cm^{-1}: 345.

2) Entries 2 and 3: To a THF or toluene solution of **L158** (300.0 mg, 0.9 mmol) was added a THF or toluene suspension of $NiCl_2$(dme) (204.4 mg, 0.9 mmol). The reaction was stirred overnight. A dark red precipitate was formed. The solvent was removed. The ^{1}H NMR spectrum of the solution is silent. The dark powder was only soluble in DMSO and methanol. The ^{1}H NMR analysis of the powder indicates a paramagnetic material. IR: ν_{max}(solid)/cm^{-1}: 3103w, 2956m, 2930m, 2869m, 2161m, 1601s, 1496s, 1460s, 1367m, 1197m, 1094m, 1064s, 867m, 731s, 689s, 397w, 228s. Different couples of solvents were used for the crystallization attempts at room temperature, 4 °C or – 20 °C:

- by gas diffusion with MeOH/Et_2O.
- by stratification with DMSO/THF, DMSO/H_2O, DMSO/Et_2O, MeOH/H_2O, MeOH/pentane.

3) Entries 4 and 5: A similar procedure to 9) with **L158** (300.0 mg, 0.9 mmol) and $NiBr_2$(dme) (287.1 mg, 0.9 mmol) gave the same results. IR: ν_{max}(solid)/cm^{-1}: 3097w, 2955w, 2868w, 2113w, 1600m, 1496m, 1457m, 1417m,1367m, 1257m, 1060m, 869m, 729m, 688m, 402w, 229s.

4) Entries 6 and 7: To a THF or toluene solution of $NiBr_2$(dme) (287.1 mg, 0.9 mmol) was added a THF or toluene solution of **L158** (300.0 mg, 0.9 mmol) at room temperature or at -78 °C. The mixture was stirred overnight at room temperature. The green solution was filtered through Celite®. A green paramagnetic powder was obtained by precipitation from pentane and was soluble in MeOH, THF, acetonitrile and acetone. At – 78 °C the green solution turned yellow. ^{1}H NMR analyses at – 80 °C and – 100 °C in acetone revealed some paramagnetic materials. Crystallization attempts at room temperature, 4 or - 20 °C:

- by gas diffusion with Et_2O/THF, pentane/THF or Et_2O/MeOH
- by stratification with Et_2O/THF, pentane/THF, Et_2O/MeOH or pentane/MeOH

5) Entry 8: A similar procedure to 11) with **L158** (300.0 mg, 0.9 mmol) and $NiCl_2$(dme) (204.4 mg, 0.9 mmol) in THF a room temperature did not work. After 16 h, the solution was filtered and the solvent removed. The ^{1}H NMR analysis of the solution reveals only **L158**. The precipitate was the unreacted nickel source. IR: ν_{max}(solid)/cm^{-1}: 2942w, 2831w, 1463m, 1442w,1359w, 1273w, 1236w, 1192w, 1113w, 1096m, 1062s, 1022m, 868s, 834m, 559w, 381w, 344w, 218s, 162s, 122w.

6) Entry 9: A similar procedure to 12) in toluene gave a black solution and orange precipitate after 16 h. The solution was filtered and the solvent removed. The ^{1}H NMR

spectrum features no sign of **L158** or nickel complex. The precipitate was insoluble in usual solvents.

8.4 Metal powder

1) Entries 1 and 2: **L155** (300.0 mg, 0.5 mmol) and Raney nickel (222.2 mg, 2.6 mmol) combined in CH_3CN and stirred for 2 or 7 days at 70 °C or under reflux, gave no reaction. The ^1H NMR spectrum of the crude reaction mixture displays only one set of signals assignable to **L155**. ^1H NMR (300 MHz, CD_2Cl_2) δ 11.25 (t, *J* = 1.7 Hz, 2H, NCHN), 8.97 (t, *J* = 2.1 Hz, 1H, CH^{aryl}), 8.48 (t, *J* = 1.9 Hz, 2H, $CH^{imidazole}$), 8.14 (dd, *J* = 8.1, 2.2 Hz, 2H, $CH^{aryl)}$, 7.91 – 7.84 (m, 1H, CH^{aryl}), 7.51 (t, 2H, $CH^{imidazole}$), 4.46 (t, *J* = 7.4 Hz, 4H, $NCH_2{}^{Bu}$), 2.11–2.00 (m, 4H, $CH_2{}^{Bu}$), 1.52–1.42 (m, 4H, $CH_2{}^{Bu}$), 1.02 (t, *J* = 7.3 Hz, 6H, $CH_3{}^{Bu}$). $^{13}C\{^1H\}$ NMR (75 MHz, CD_2Cl_2) δ 136 .6 (NCHN), 136.3 (C^{aryl}), 133.3 (CH^{aryl}), 123.5 ($CH^{imidazole}$), 123.4 (2 × CH^{aryl}), 122.3 ($CH^{imidazole}$), 116.5 (CH^{aryl}), 51.1 ($NCH_2{}^{Bu}$), 32.4 ($CH_2{}^{Bu}$), 20.0 ($CH_2{}^{Bu}$), 13.7 ($CH_3{}^{Bu}$).

2) Entries 3 and 4: Following a procedure similar to that above, **L102** (300.0 mg, 0.6 mmol) and Raney nickel (258.0 mg, 3.0 mmol) gave no reaction.

3) Entry 5: **L155** (300.0 mg, 0.5 mmol) and the nickel powder (258.8 mg, 4.4 mmol) were combined in acetonitrile. The mixture was stirred for 5 days at 50 °C. No reaction occurred.

4) Entry 6: A procedure similar to that used for 3) with **L102** (300.0 mg, 0.6 mmol) and the nickel powder (300.5 mg, 5.1 mmol) gave no reaction.

3) Entries 7 and 8: To a solution of **334** (300.0 mg, 0.2 mmol) in acetonitrile, nickel powder (189.0 mg, 3.2 mmol) was added. The mixture was stirred for 5 days at 50 °C or under reflux. The solution was filtered and the solvent removed to afford an off-white powder. The ^1H NMR spectrum of the powder in DCM revealed the sole presence of the silver(I) complex **334**. ^1H NMR (300 MHz, CD_2Cl_2): δ 8.38 (t, *J* = 1.8 Hz, 1H, CH^{aryl}), 7.58 – 7.47 (m, 2H, CH^{aryl}), 7.47 – 7.36 (m, 3H, CH^{aryl} + $CH^{imidazole}$), 7.17 (d, *J* = 1.5 Hz, 2H, $CH^{imidazole}$), 4.25 (t, *J* = 7.1 Hz, 4H, $NCH_2{}^{Bu}$), 1.89–1.79 (m, 4H, $CH_2{}^{Bu}$), 1.42–1.30 (m, 4H, $CH_2{}^{Bu}$), 0.90 (t, *J* = 7.3 Hz, 6H, $CH_3{}^{Bu}$).$^{13}C\{^1H\}$ NMR (75 MHz, CD_2Cl_2) δ 184.80 ($C^{carbene}$), 141.00 (C^{aryl}), 130.39 (CH^{aryl}), 123.20 ($CH^{imidazole}$), 121.88 (CH^{aryl}), 121.46 (CH^{aryl}), 120.96 ($CH^{imidazole}$), 52.00 ($NCH_2{}^{Bu}$), 33.50 ($CH_2{}^{Bu}$), 19.87 ($CH_2{}^{Bu}$), 13.69 ($CH_3{}^{Bu}$).

4) Entries 9 and 10: A similar reaction to 3) with **337** (300.0 mg, 0.3 mmol) and nickel powder (289.4 mg, 4.9 mmol) at 50 °C or under reflux gave no reaction.

8.5 Transmetalation

1) Entry 1: **L155** (394.1 mg, 0.7 mmol) and $Zr(NMe_2)_4$ (272.5 mg, 1.0 mmol) were combined in DCM and stirred for 1 h. $NiCl_2$(dme) (163.7 mg, 0.7 mmol) was added and the mixture stirred for 16 h. Then, H_2O (0.5 ml, 0.03 mmol) was added and the mixture stirred vigorously for 5 min. A green precipitate appeared. The solution was filtered; the precipitate washed three times with 10 mL of DCM. Evaporation of the filtrate led to an orange-brown powder. The ^{1}H NMR spectrum reveals the presence of an imidazolium salt and some nickel complex among various other products. The solution of DCM was washed three times with distilled water (to remove the remaining imidazolium and inorganic salts). All the products in the mixture have a similar solubility in DCM and THF. **L155**: ^{1}H NMR (300 MHz, CD_2Cl_2) δ 11.25 (t, *J* = 1.7 Hz, 2H, NCHN), 8.97 (t, *J* = 2.1 Hz, 1H, CH^{aryl}), 8.48 (t, *J* = 1.9 Hz, 2H, $CH^{imidazole}$), 8.14 (dd, *J* = 8.1, 2.2 Hz, 2H, $CH^{aryl)}$, 7.91 – 7.84 (m, 1H, CH^{aryl}), 7.51 (t, 2H, $CH^{imidazole}$), 4.46 (t, *J* = 7.4 Hz, 4H, $NCH_2{}^{Bu}$), 2.11–2.00 (m, 4H, $CH_2{}^{Bu}$), 1.52–1.42 (m, 4H, $CH_2{}^{Bu}$), 1.02 (t, *J* = 7.3 Hz, 6H, $CH_3{}^{Bu}$). $^{13}C\{^1H\}$ NMR (75 MHz, CD_2Cl_2) δ 136 .6 (NCHN), 136.3 (C^{aryl}), 133.3 (CH^{aryl}), 123.5 ($CH^{imidazole}$), 123.4 (2 × CH^{aryl}), 122.3 ($CH^{imidazole}$), 116.5 (CH^{aryl}), 51.1 ($NCH_2{}^{Bu}$), 32.4 ($CH_2{}^{Bu}$), 20.0 ($CH_2{}^{Bu}$), 13.7 ($CH_3{}^{Bu}$). **7**: ^{1}H NMR (300 MHz, CD_2Cl_2): δ 8.88 (d, *J* = 13.8 Hz, 2H), 8.32 (s, 1H), 7.55 (d, *J* = 6.6 Hz, 2H), 7.04 (d, *J* = 6.4 Hz, 2H), 4.46 – 4.22 (m, 4H), 1.83–1.77 (m, 4H), 1.38 – 1.29 (m, 4H), 0.84 (t, *J* = 7.2 Hz, 6H). $^{13}C\{^1H\}$ NMR (75 MHz, CD_2Cl_2) δ 174.42 ($C^{carbene}$), 147.70 (CH^{aryl}), 147.62 (CH^{aryl}), 123.63 ($CH^{imidazole}$), 121.20 ($CH^{imidazole}$), 114.27 (CH^{aryl}), 108.27 (CH^{aryl}), 49.99 ($CH_2{}^{Bu}$), 33.65 ($CH_2{}^{Bu}$), 20.02 ($CH_2{}^{Bu}$), 13.79 ($CH_3{}^{Bu}$).

2) Entry 2: A similar procedure to 1) with **L103** (316.0 mg, 0.6 mmol), $Zr(NMe_2)_4$ (261.1 mg, 1.0 mmol) and $NiBr_2$(dme) (222.0 mg, 0.7 mmol) stirred for 3 h, gave a mixture of products with a large quantity of imidazolium salt. No trace of nickel complex was observed on the ^{1}H and $^{13}C\{^1H\}$ NMR spectra. ^{1}H NMR (500 MHz, CD_2Cl_2) δ 11.76 (s, 2H, NCHN), 9.27 (s, 2H, $CH^{imidazole}$), 9.11 (s, 1H, CH^{aryl}), 8.27 (dd, *J* = 8.2, 1.9 Hz, 2H, CH^{aryl}), 7.80 (s, 2H, $CH^{imidazole}$), 7.54 (t, *J* = 8.3 Hz, 1H, CH^{aryl}), 4.43 (t, *J* = 7.3 Hz, 4H, $NCH_2{}^{Bu}$), 2.04 – 1.92 (m, 4H, $CH_2{}^{Bu}$), 1.44 – 1.32 (m, 4H, $CH_2{}^{Bu}$), 0.93 (t, *J* = 7.4 Hz, 6H, $CH_3{}^{Bu}$). $^{13}C\{^1H\}$ NMR (126 MHz, CD_2Cl_2) δ 137.0 (C^{aryl}), 136.4 (NCHN), 132.5 (CH^{aryl}), 123.5 ($CH^{imidazole}$), 122.3

(CH^{aryl}), 122.0 ($CH^{imidazole}$), 114.7 (CH^{aryl}), 50.6 (NCH_2^{Bu}), 32.3 (CH_2^{Bu}), 19.9 (CH_2^{Bu}), 13.7 (CH_3^{Bu}).

3) Entries 3 to 8: To a solution of **334** (286.0 mg, 0.2 mmol) in acetonitrile, $NiBr_2$ (78.7 mg, 0.4 mmol) was added. The mixture was stirred in DCM, THF or acetonitrile at room temperature, or under reflux. After 16 h, the solution was filtered and the solvent removed affording an off white powder. The ^1H NMR analysis of the powder reveals the sole presence of **334**.

4) Entry 9: To a solution of **334** in DCM (150.0 mg, 0.1 mmol) was added $Ni(CH_3CN)_6(BF_4)_2$ (86.1 mg, 0.2 mmol). The reaction was stirred overnight at room temperature. A yellow solution and a white precipitate were present at the end of the reaction. The white powder is the complex **334**. The ^1H NMR spectrum of the solution indicates a protonation of the NHC sites, with a signal at 9.35 ppm.

5) Entry 10: A procedure similar to 4) with **334** (150.0 mg, 0.1 mmol) and $Ni(CH_3CN)_6(BF_4)_2$ (86.2 mg, 0.2 mmol) in acetonitrile gave no reaction. The silver(I) complex was fully recovered.

6) Entry 11: A procedure similar to 5) with **337** (200.0 mg, 0.2 mmol) and $Ni(MeCN)_6(BF_4)_2$ (181.9 mg, 0.4 mmol) in acetonitrile gave no reaction. The silver(I) complex was fully recovered.

7) Entries 13 and 15: To a solution of **334** (300.0 mg, 0.2 mmol) in acetonitrile was added $NiCl_2$(dme) (82.4 mg, 0.4 mmol). The mixture was stirred overnight at room temperature, or under reflux. The solvent was removed. The ^1H NMR spectrum in DCM indicates the sole presence of **334**.

8) Entries 12 and 14: A procedure similar to 7) in THF gave an orange solution. The solvent was removed and a ^1H NMR spectrum in C_6D_6 reveals the presence of protonated NHC sites with a signal at 10.51 ppm among other unidentified products. The mixture has a low solubility in toluene or benzene, and a better one in DCM or acetonitrile. The whole mixture precipitated from ether or pentane. Crystallization attempts at room temperature, 4 or - 20 °C:

- by gas diffusion with Et_2O/THF, pentane/THF or acetonitrile/Et_2O
- by stratification with Et_2O/THF, pentane/THF or DCM/pentane

Références p. 199

9) Entries 16 and 17: To a solution of **334** (300.0 mg, 0.2 mmol) in DCM was added $NiBr_2(PPh_3)_2$ (282.4 mg, 0.4 mmol) or $NiBr_2$(dme) (117.3 mg, 0.4 mmol). The mixtures were stirred overnight at room temperature and turned red. The solutions were filtered, concentrated and red powders were obtained upon addition of pentane. ^{1}H NMR spectra of the powders in C_6D_6 reveal a mixture of products including a nickel complex.

10) Entry 18: A similar procedure to 9) with **334** (200.0 mg, 0.1 mmol) and $NiBr_2$(dme) (77.2 mg, 0.2 mmol) in acetonitrile gave no reaction. **334** was poorly soluble. The solvent was removed. The ^{1}H NMR spectrum in DCM reveals the sole presence of **334**.

11) Entry 19: A similar procedure to 9) with **334** (200.0 mg, 0.1 mmol) and $NiBr_2$(dme) (77.2 mg, 0.2 mmol) in MeOH gave white and green precipitates. Both powders were insoluble in usual solvents. IR: ν_{max}(solid)/cm^{-1}: 2956w, 1560w, 1530m, 1493m, 1461w, 1412m, 1260m, 1225w, 1091w, 1013s, 946w, 796s, 725m, 693s, 451w, 380m.

12) Entries 20 and 21: A similar procedure to 9) with **334** (200.0 mg, 0.1 mmol) and $NiBr_2$(dme) (77.2 mg, 0.2 mmol) in THF led to a red solution. The solution was filtered and the solvent removed, yielding a red powder. This powder was soluble in DCM and THF; insoluble in pentane, ether, ethyl acetate, MeOH, EtOH and water; partially soluble in acetone and toluene. Passing a THF or DCM solution through a plug of silica resulted in the partial decomposition of the reaction mixture. Precipitations using pentane, Et_2O, methanol, ethanol or ethyl acetate as non-solvents were unsuccessful at room temperature or at – 20 °C. Recrystallization from hot THF or toluene failed. Signals assigned to the nickel complex: ^{1}H NMR (300 MHz, C_6D_6): δ 8.78 (dd, J = 7.96, 1.94 Hz, CH^{aryl}, 1H), 7.59 (m, CH^{aryl}, 1H), 7.07 (s, CH^{aryl}, 2H), 6.34 (s, $CH^{imidazole}$, 2H), 6.19 (s, $CH^{imidazole}$, 2H), 5.28 (m, NCH_2^{Bu}, 4H), 2.18 (m, CH_2^{Bu}, 4H), 1.16 (m, CH_2^{Bu}, 4H), 0.77 (m, CH_3^{Bu}, 6H). ^{13}C{^{1}H} NMR (126 MHz, CD_2Cl_2) δ 171.33 ($C^{carbene}$), 141.43 (C^{aryl}), 131.72 (CH^{aryl}), 128.22 (CH^{aryl}), 125.99(CH^{aryl}), 123.57 ($CH^{imidazole}$), 121.61 ($CH^{imidazole}$), 51.46 (NCH_2^{Bu}), 32.87 (CH_2^{Bu}), 20.99 (CH_2^{Bu}), 14.32 (CH_3^{Bu}). The following couples of solvents were used for crystallization attempts at room temperature, 4 °C or – 20 °C:

- by slow evaporation, DCM/octane, acetone/octane
- by gas diffusion with THF/Et_2O, THF/pentane, toluene/Et_2O, toluene/pentane.
- by stratification with THF/Et_2O, THF/pentane, toluene/Et_2O, toluene/pentane, DCM/pentane.

Références p. 199

13) Entries 22, 23 and 24: **334** (200.0 mg, 0.1 mmol) and $NiBr_2$(dme) (77.2 mg, 0.2 mmol) were combined in THF. The mixture was stirred for 5, 10 or 15 min at 50 °C under 50 W. No reaction occurred. ^{1}H NMR (300 MHz, CD_2Cl_2) δ 8.38 (t, *J* = 1.8 Hz, 1H, CH^{aryl}), 7.58 – 7.47 (m, 2H, CH^{aryl}), 7.47 – 7.36 (m, 3H, CH^{aryl} + $CH^{imidazole}$), 7.17 (d, *J* = 1.5 Hz, 2H, $CH^{imidazole}$), 4.26 (t, *J* = 7.1 Hz, 4H, NCH_2^{Bu}), 1.89–1.79 (m, 4H, CH_2^{Bu}), 1.42–1.30 (m, 4H, CH_2^{Bu}), 0.90 (t, *J* = 7.3 Hz, 6H, CH_3^{Bu}). $^{13}C\{^1H\}$ NMR (75 MHz, CD_2Cl_2) δ 184.8 ($C^{carbene}$), 141.0 (C^{aryl}), 130.4 (CH^{aryl}), 123.2 ($CH^{imidazole}$), 121.9 (CH^{aryl}), 121.5 (CH^{aryl}), 121.0 ($CH^{imidazole}$), 52.0 (NCH_2^{Bu}), 33.5 (CH_2^{Bu}), 19.9 (CH_2^{Bu}), 13.7 (CH_3^{Bu}).

14) Entry 25: **334** (200.0 mg, 0.1 mmol) and $NiBr_2$(dme) (77.2 mg, 0.2 mmol) were combined in THF. The mixture was stirred for 15 min at 70 °C under 50 W and gave a similar mixture to 12).

15) Entryies 26 and 27: To a solution of **337** (200.0 mg, 0.2 mmol) in THF or THF/acetonitrile was added $NiBr_2(PPh_3)_2$ (282.4 mg, 0.4 mmol). The mixture was stirred overnight at room temperature and turned orange. Precipitation with pentane yielded an orange powder. The ^{1}H NMR spectrum of the solution in C_6D_6 indicates a different fingerprint from that in 12). The powder was soluble in THF and acetonitrile; insoluble in pentane, ether, ethyl acetate, MeOH, EtOH or toluene. Precipitations using pentane, Et_2O, methanol, ethanol, ethyl acetate or toluene as non-solvents were unsuccessful, even at – 20 °C. Dissolution in hot THF did not lead to the isolation of a product. IR: ν_{max}(solid)/cm^{-1}: 2323w, 2050w, 1980w, 1603m, 15 46m, 1495s, 1458s, 1414s, 1370m, 1259m, 1227m, 1191m, 1104m, 1071m, 1001w, 948w, 876w, 789m, 728s, 689s, 621s, 419w, 398w, 385w, 353w, 327w, 303w, 289w, 280w, 266w, 254w, 247w, 227w, 202w, 195, 170w, 150w, 139w, 120w. The following couples of solvents were used for the crystallization attempts at room temperature, 4 °C or – 20 °C:

- by slow gas diffusion with THF/Et_2O, THF/pentane, acetonitrile/pentane, acetonitrile/Et_2O.

- by stratification with THF/Et_2O, THF/pentane, acetonitrile/pentane, acetonitrile/Et_2O.

16) Entry 28: A similar procedure to 15) with **337** (165.5 mg, 0.2 mmol) and $NiBr_2$(dme) (200.0 mg, 0.3 mmol) in THF at 70 °C under 50 W for 15 min gave the same result as for 15).

17) Entry 29: A similar procedure to 11) with **335** (300.0 mg, 0.2 mmol) and $NiBr_2$(dme) (132.6 mg, 0.4 mmol) at room temperature or under reflux gave the same result as for 12).

18) Entries 30 and 31: A similar procedure to 11) with **335** (321.1 mg, 0.2 mmol) and $NiBr_2(PPh_3)_2$ (341.8 mg, 0.5 mmol) gave results similar to 12).

19) Entries 32 and 33: To a solution of **336** (400.0 mg, 0.6 mmol) in chloroform was added $NiCl_2$(dme) (131.8 mg, 0.6 mmol). The mixture was stirred overnight at room temperature or under reflux. A yellow solution and a black precipitate appeared. The solution was filtered and the solvent was concentrated. The yellow powder was precipitated with Et_2O. The power was dried under vacuum. Weight: 391.4 mg. Crystallization attempts at room temperature, 4 °C or – 20 °C by slow evaporation or stratification with the couples DCM/octane or CH_3Cl/octane were unsuccessful. ^{1}H NMR (500 MHz, $CDCl_3$): δ 7.97 (s, 1H), 7.75–7.59 (m, 4H), 7.25 (s, 2H), 4.22 (t, *J* = 7.2 Hz, 4H), 1.89–1.83 (m, 4H), 1.44–1.38 (m, 4H), 0.98 (t, *J* = 7.4 Hz, 6H). $^{13}C\{^1H\}$ NMR (126 MHz, $CDCl_3$): δ 179.19 ($C^{carbene}$), 140.83 (C^{aryl}), 131.44 (CH^{aryl}), 124.00 (CH^{aryl}), 122.29 ($CH^{imidazole}$), 122.25 ($CH^{imidazole}$), 119.84 (CH^{aryl}), 71.73 (dme), 59.03 (dme), 52.36 ($NCH_2{}^{Bu}$), 33.36 ($CH_2{}^{Bu}$), 19.72 ($CH_2{}^{Bu}$), 13.64 ($CH_3{}^{Bu}$). IR: ν_{max}(solid)/cm^{-1}: 3080w, 2955w, 2868w, 2162w, 1979w, 1605s, 1570w, 1550w, 1496s, 1458m, 1413s, 1369m, 1260m, 1228s, 1196m, 1110w, 1074w, 735s, 690s, 461w, 405w, 294w, 125w.

20) Entry 34: To a solution of **336** (400.0 mg, 0.6 mmol) in chloroform was added 1.00 equiv. of $NiCl_2$(dme) (131.8 mg, 0.6 mmol). The reaction was stirred under reflux. After 16 h, 1.00 equiv. of $NiCl_2$(dme) (131.8 mg, 0.6 mmol) was added. The reaction was stirred for 16 h and gave a result similar to 19).

21) Entry 35: A similar procedure to 19) with **336** (400.0 mg, 0.6 mmol) and $NiCl_2$(dme) (285.6 mg, 1.3 mmol) gave similar result to 19).

22) Entry 36: A similar procedure to 12) with **339** (243.7 mg, 0.4 mmol) and $NiBr_2$(dme) (123.5 mg, 0.4 mmol) in THF gave the same red powder but less cleanly than for 9).

23) Entries 37 and 38: A similar procedure to 12) with **339** (243.7 mg, 0.4 mmol), the addition of $NiBr_2(PPh_3)_2$ (297.2 mg, 0.4 mmol) at room temperature or – 78 °C in THF followed by reaction at room temperature or under reflux, gave the same result as 19).

Références p. 199

24) Entries 39 and 40: Following a similar procedure to 12), **339** (300.0 mg, 0.6 mmol) in THF was added to $NiCl_2$(dme) (131.8 mg, 0.6 mmol). The mixture was stirred overnight at room temperature or under reflux. A yellow solution and a grey precipitate appeared. The solution was filtered and the solvent removed. The precipitate was washed three times with Et_2O. The nickel complex and **340** precipitated all together using THF or DCM with pentane or Et_2O. Partial dissolution of only a compound (over two) in hot DCM or THF failed. The following couples of solvents were used for the crystallization attempts at room temperature, 4 °C or – 20 °C:

- by slow evaporation of a mixture DCM/octane, $CHCl_3$/octane
- by stratification with couples THF/Et_2O, THF/pentane

^{1}H NMR (300 MHz, CD_2Cl_2): δ 8.17 (s, 1H, CH^{aryl}), 7.81-7.73 (m, *J* = 21.7 Hz, 3H, CH^{aryl}), 7.65 (s, 2H, $CH^{imidazole}$), 7.28 (s, 2H, $CH^{imidazole}$), 4.22 (s, 4H, $NCH_2{}^{Bu}$), 1.90 (s, 5H, $CH_2{}^{Bu}$), 1.44–1.38 (m, 5H, $CH_2{}^{Bu}$), 0.97 (t, *J* = 7.0 Hz, 9H, $CH_3{}^{Bu}$). The integration of the butyl chains signals is higher than expected probably due to the superposition of the signals from different compounds.

Références p. 199

References:

(1) (a) Radius, U.; Bickelhaupt, F. M. *Organometallics* **2008**, *27*, 3410 (b) Radius, U.; Bickelhaupt, F. M. *Coord. Chem. Rev.* **2009**, *253*, 678.

(2) (a) Olivier-Bourbigou, H.; Commereuc, D.; Harry, S. **2001**, EP1136124A1, France (b) Lecocq, V.; Olivier-Bourbigou, H. *Oil & Gas Science and Technology - Rev. IFP* **2007**, *62*, 761 (c) McGuinness, D. S.; Mueller, W.; Wasserscheid, P.; Cavell, K. J.; Skelton, B. W.; White, A. H.; Englert, U. *Organometallics* **2002**, *21*, 175.

(3) (a) Berding, J.; Lutz, M.; Spek, A. L.; Bouwman, E. *Appl. Organomet. Chem.* **2011**, *25*, 76 (b) Song, H.; Fan, D.; Liu, Y.; Hou, G.; Zi, G. *J. Organomet. Chem.* **2013**, *729*, 40.

(4) Inamoto, K.; Kuroda, J.-i.; Hiroya, K.; Noda, Y.; Watanabe, M.; Sakamoto, T. *Organometallics* **2006**, *25*, 3095.

(5) (a) Inamoto, K.; Kuroda, J.-i.; Kwon, E.; Hiroya, K.; Doi, T. *J. Organomet. Chem.* **2009**, *694*, 389 (b) Paulose, T. A. P.; Wu, S.-C.; Olson, J. A.; Chau, T.; Theaker, N.; Hassler, M.; Quail, J. W.; Foley, S. R. *Dalton Trans.* **2012**, *41*, 251.

(6) (a) Xi, Z.; Zhou, Y.; Chen, W. *J. Org. Chem.* **2008**, *73*, 8497 (b) Zhang, C.; Wang, Z.-X. *Organometallics* **2009**, *28*, 6507.

(7) (a) Berding, J.; Lutz, M.; Spek, A. L.; Bouwman, E. *Organometallics* **2009**, *28*, 1845 (b) Guo, J.; Lv, L.; Wang, X.; Cao, C.; Pang, G.; Shi, Y. *Inorg. Chem. Commun.* **2013**, *31*, 74.

(8) (a) Thoi, V. S.; Chang, C. J. *Chem. Commun.* **2011**, *47*, 6578 (b) Thoi, V. S.; Kornienko, N.; Margarit, C. G.; Yang, P.; Chang, C. J. *J. Am. Chem. Soc.* **2013**, *135*, 14413.

(9) Schwarzenbach, G. *Helv. Chim. Acta* **1952**, *35*, 2344.

(10) Adamson, A. W. *J. Am. Chem. Soc.* **1954**, *76*, 1578.

(11) (a) Braunstein, P.; Naud, F. *Angew. Chem. Int. Ed.* **2001**, *40*, 680 (b) Jeffrey, J. C.; Rauchfuss, T. B. *Inorg. Chem.* **1979**, *18*, 2658.

(12) (a) Brown, D. H.; Skelton, B. W. *Dalton Trans.* **2011**, *40*, 8849 (b) Chiu, P. L.; Lai, C.-L.; Chang, C.-F.; Hu, C.-H.; Lee, H. M. *Organometallics* **2005**, *24*, 6169 (c) Clyne, D. S.; Jin, J.; Genest, E.; Gallucci, J. C.; RajanBabu, T. V. *Org. Lett.* **2000**, *2*, 1125 (d) Herrmann, W. A.; Schwarz, J.; Gardiner, M. G.; Spiegler, M. *J. Organomet. Chem.* **1999**, *575*, 80 (e) Lee, C. C.; Ke, W. C.; Chan, K. T.; Lai, C. L.; Hu, C. H.; Lee, H. *Chem. - Eur. J.* **2007**, *13*, 582 (f) MaGee, K. D. M.; Travers, G.; Skelton, B. W.; Massi, M.; Payne, A. D.; Brown, D. H. *Aust. J. Chem.* **2012**, *65*, 823.

(13) (a) Berding, J.; Lutz, M.; Spek, A. L.; Bouwman, E. *Appl. Organomet. Chem.* **2011**, *25*, 76 (b) Mrutu, A.; Goldberg, K. I.; Kemp, R. A. *Inorg. Chim. Acta* **2010**, *364*, 115.

(14) (a) Jean-Baptiste dit Dominique, F.; Gornitzka, H.; Hemmert, C. *Organometallics* **2010**, *29*, 2868 (b) Nieto, I.; Bontchev, R. P.; Ozarowski, A.; Smirnov, D.; Krzystek, J.; Telser, J.; Smith, J. M. *Inorg. Chim. Acta* **2009**, *362*, 4449 (c) Ray, S.; Asthana, J.; Tanski, J. M.; Shaikh, M. M.; Panda, D.; Ghosh, P. *J. Organomet. Chem.* **2009**, *694*, 2328 (d) Tan, K. V.; Dutton, J. L.; Skelton, B. W.; Wilson, D. J. D.; Barnard, P. J. *Organometallics* **2013**, *32*, 1913.

(15) (a) Douthwaite, R. E.; Green, M. L. H.; Silcock, P. J.; Gomes, P. T. *Organometallics* **2001**, *20*, 2611 (b) Jeon, S.-J.; Waymouth, R. M. *Dalton Trans.* **2008**, 437.

(16) (a) Davies, C. J. E.; Page, M. J.; Ellul, C. E.; Mahon, M. F.; Whittlesey, M. K. *Chem. Commun.* **2010**, *46*, 5151 (b) Fischer, P.; Linder, T.; Radius, U. *Z. Anorg. Allg. Chem.* **2012**, *638*, 1491 (c) Matsubara, K.; Ueno, K.; Shibata, Y. *Organometallics* **2006**, *25*, 3422 (d) Page, M. J.; Lu, W. Y.; Poulten, R. C.; Carter, E.; Algarra, A. G.; Kariuki, B.

M.; Macgregor, S. A.; Mahon, M. F.; Cavell, K. J.; Murphy, D. M.; Whittlesey, M. K. *Chem. - Eur. J.* **2013**, *19*, 2158.
(17) (a) Douthwaite, R. E.; Haüssinger, D.; Green, M. L. H.; Silcock, P. J.; Gomes, P. T.; Martins, A. M.; Danopoulos, A. A. *Organometallics* **1999**, *18*, 4584 (b) Huffer, A.; Jeffery, B.; Waller, B. J.; Danopoulos, A. A. *C. R. Chim.* **2013**, *16*, 557 (c) Pugh, D.; Boyle, A.; Danopoulos, A. A. *Dalton Trans.* **2008**, 1087.
(18) Vinh Huynh, H.; Jothibasu, R. *Eur. J. Inorg. Chem.* **2009**, 1926.
(19) Liu, B.; Liu, X.; Chen, C.; Chen, C.; Chen, W. *Organometallics* **2011**, *31*, 282.
(20) Liu, B.; Xia, Q.; Chen, W. *Angew. Chem. Int. Ed.* **2009**, *48*, 5513.
(21) Hollis, T. K. Z., Xiofei **2011**, WO 2011050003 (A2) USA.
(22) Rubio, R. J.; Andavan, G. T. S.; Bauer, E. B.; Hollis, T. K.; Cho, J.; Tham, F. S.; Donnadieu, B. *J. Organomet. Chem.* **2005**, *690*, 5353.
(23) Bradley, D. C.; Thomas, I. M. *J. Chem. Soc.* **1960**, *0*, 3857.
(24) (a) Yoshida, K.; Horiuchi, S.; Takeichi, T.; Shida, H.; Imamoto, T.; Yanagisawa, A. *Org. Lett.* **2010**, *12*, 1764 (b) Kuroda, J.-i.; Inamoto, K.; Hiroya, K.; Doi, T. *Eur. J. Org. Chem.* **2009**, 2251 (c) Liu, B.; Xia, Q.; Chen, W. *Angew. Chem., Int. Ed.* **2009**, *48*, 5513.
(25) Paulose, T. A. P.; Wu, S.-C.; Olson, J. A.; Chau, T.; Theaker, N.; Hassler, M.; Quail, J. W.; Foley, S. R. *Dalton Trans.* **2012**, *41*, 251.
(26) (a) Lu, Z.; Cramer, S. A.; Jenkins, D. M. *Chem. Sci.* **2012**, *3*, 3081 (b) Jenkins, D. M.; Cramer, S. A.; Lu, Z. **2013**, US20130345431A1, USA.
(27) de Frémont, P.; Scott, N. M.; Stevens, E. D.; Nolan, S. P. *Organometallics* **2005**, *24*, 2411.
(28) Cisnetti, F.; Lemoine, P.; El-Ghozzi, M.; Avignant, D.; Gautier, A. *Tetrahedron Lett.* **2010**, *51*, 5226.
(29) Lu, Z.; Cramer, S. A.; Jenkins, D. M. *Chem. Sci.* **2012**, *3*, 3081.
(30) Frøseth, M.; Netland, K. A.; Rømming, C.; Tilset, M. *J. Organomet. Chem.* **2005**, *690*, 6125.
(31) McCarroll, A.; Sandham, D.; Titcomb, L.; Lewis, A. d.; Cloke, F. G.; Davies, B.; Perez de Santana, A.; Hiller, W.; Caddick, S. *Mol. Diversity* **2003**, *7*, 115.
(32) Landers, B.; Navarro, O. *Eur. J. Inorg. Chem.* **2012**, *2012*, 2980.
(33) Chen, C.; Qiu, H.; Chen, W. *J. Organomet. Chem.* **2012**, *696*, 4166.
(34) (a) Fliedel, C.; Braunstein, P. *Organometallics* **2010**, *29*, 5614 (b) Brill, M.; Kuhnel, E.; Scriban, C.; Rominger, F.; Hofmann, P. *Dalton Trans.* **2013**, *42*, 12861.
(35) Mrutu, A.; Dickie, D. A.; Goldberg, K. I.; Kemp, R. A. *Inorg. Chem.* **2011**, *50*, 2729.

Conclusion générale

Conclusion générale

Au cours de cette thèse, la synthèse d'un carbène libre, de complexes d'argent(I), de cuivre(I) et de nickel(II) portant des ligands bis-NHC a été réalisée. Dans ce but, différentes méthodes de synthèse furent explorées.

Nous avons obtenu une série de complexes bis-(NHC) d'argent(I) ou de cuivre(I) avec de bons rendements. Leurs structures dépendent fortement de la nature des anions associés et vont d'une structure classique di-cationique (**2d**) à un cubane (**2b**) ou à des polymères de coordination (**2c** et **3b-c**). Les complexes **3b-c** constituent de nouveaux ajouts aux exemples encore rares de polymères de coordination basés sur des complexes NHC de cuivre(I).

Les polymères de coordination d'argent(I)-NHC ont trouvé des applications dans des réactions de couplage, des réactions de transfert de carbène et sont utilisées comme bactéricide. Les applications des complexes décrites dans ce travail seront évaluées plus tard.

La synthèse des complexes bis-NHC de nickel(II) a été beaucoup plus difficile à réaliser qu'initialement escompté. Les cinq voies de synthèse classiques décrites dans la littérature ont été évaluées :

- L'utilisation des précurseurs de nickel contenant une base interne a échoué, certainement en raison de leur manque de basicité.

- L'addition de bases fortes à des sources de nickel avec divers sels d'imidazolium n'a pas réussi, certainement parce que la réaction génère des sous-produits qui empêchent la coordination du carbène libre sur le nickel.

-La métallation directe du carbène libre a conduit à des produits paramagnétiques qui n'ont pu être caractérisés.

- L'utilisation des agents de transmétallation tels que les complexes d'argent(I) ou de cuivre(I) ont conduit à des mélanges complexes de composés diamagnétiques. Malheureusement, aucun composé propre n'a été obtenu en utilisant les techniques classiques de séparation, telles que la précipitation ou la dissolution sélective, la chromatographie en phase liquide sur colonne de silice, la cristallisation ou la sublimation. Cependant, les complexes d'argent(I) se sont avérés être de meilleurs agents de transmétallation que les complexes de cuivre(I). Les résultats les plus probants ont été obtenus par transmétallation à

partir des complexes d'iodure ou de bromure d'argent(I) avec des preuves spectroscopiques claires pour la formation de complexes de nickel bis-NHC.

Valentine CHARRA

Coordination de ligands multidentes sur le nickel

Application à l'oligomérisation des oléfines

Résumé

Le sujet de cette thèse porte sur la synthèse de ligands de type bis-NHC (carbène *N*-hétérocyclique) et leur réactivité vis-à-vis des complexes d'argent(I), de cuivre(I) et de nickel(II). Après avoir exploré les différentes méthodologies de synthèse des complexes de nickel(II) bis-NHC, le but était de tester leurs activités en catalyse d'oligomérisation de l'éthylène. Une série de nouveaux complexes d'argent(I) et de cuivre(I) fut synthétisée. Cinq voies furent testées pour la formation de complexes de nickel. Les résultats les plus probants furent obtenus par transmétallation à partir des complexes d'iodure ou de bromure d'argent(I).

Mots clés: carbènes N-hétérocycliques, ligands chélate, complexes organométalliques, complexes d'argent(I), de cuivre(I), de nickel(II).

Résumé en anglais

The purpose of this work was the synthesis of bis-NHC (N-heterocyclic carbene) ligands, the formation of the corresponding silver(I), copper(I) and nickel(II) complexes and the assessment of the catalytic activity of the bis-NHC nickel(II) complexes in ethylene oligomerization. A series of new bis-NHC silver(I) and copper(I) complexes was synthesized. Five different synthetic routes were tested for the formation of nickel(II) bis-NHC complexes. The most significant results were obtained by transmetalation from the silver(I) iodide or bromide complexes.

Keywords: N-heterocyclic carbenes, chelate ligands, organometallic complexes, silver(I), copper(I), nickel(II) complexes.